Remote Sensing of wetland tree species in the iSimangaliso Wetland Park, KwaZulu-Natal, South Africa

Heidi van Deventer

Promoter:

Prof. O. Mutanga
Academic Leader (Environmental Science)
School of Agricultural, Earth & Environmental Sciences
University of KwaZulu-Natal
P. Bag X01 Scottsville, 3209
Pietermaritzburg
Tel: 0332605779
Fax: 0332605344
Cell: 0718548022
Email:Mutangao@ukzn.ac.za

Co-promoter:

Dr Moses Azong Cho (Ecological Remote Sensing)
Earth Observation group, Natural Resources and Environment, Council for Scientific and Industrial Research (CSIR)
Building 33 CSIR Pretoria
P.O. Box 395, Pretoria, South Africa
Tel: +27 12 841 3669
Cell:+27(0) 833345626
Fax: +27 12 841 3909

Remote Sensing of wetland tree species in the iSimangaliso Wetland Park, KwaZulu-Natal, South Africa

Heidi van Deventer

Thesis submitted

A thesis submitted to the School of Agricultural, Earth & Environmental Sciences, at the University of KwaZulu-Natal, in fulfilment of the academic requirements for the degree of Doctor of Geography

January 2016

Pietermaritzburg

South Africa

Table of Contents

List of Figures

List of Tables

Abstract

The impact of global change is expected to result in changes in the distribution and composition of species. Coastal swamp and mangrove forests are some of the most threatened forest types in the world. Remote sensing is a suitable tool for monitoring species distribution and varying condition because of its spatial extent and repeatability. The ability of remote sensing to separate between species can be attributed primarily to its capability to quantify the absorption features in the electromagnetic spectrum which relate to plant biochemical and biophysical properties such as pigments, nutrients (proteins and starch), leaf water content, leaf angle distribution, leaf area index and foliage biomass. For some species, these phenological variations are extreme, as in the case of deciduous tree species, thus enhancing the ability to differentiate between species, whereas others are less pronounced, such as with evergreen tree species, making spectral distinction between species much more challenging.

Few studies have assessed the pigment and nutrient phenology of evergreen tree species in subtropical forested wetlands, let alone their spectral differences. This study assesses whether multi-season data across a number of phenological phases of evergreen wetland tree species will improve their classification accuracy when compared to a single season and single phenological event. The objectives were to (i) assess whether tree species had unique seasonal profiles of foliar biochemicals; (ii) ascertain the spectral bands of plant properties which remain important across phenological phases for species classification; (iii) determine whether leaf reflectance spectra from multiple seasons would improve species classification when compared to a single season; and (iv) whether multi-season imagery would improve species discrimination when compared to a single season. Thus, the study made use of leaf level and canopy level spectra collected using a handheld spectrometer and spaceborne RapidEye imagery, respectively.

Six dominant evergreen tree species from forested wetlands in the subtropical region of KwaZulu-Natal, South Africa, were sampled across four seasons (winter, spring, summer and autumn). Differences in foliar biochemical concentration were assessed for two pigments, including carotenoids and chlorophylls, as well as two nutrients, nitrogen and phosphorous. The results showed that the majority of species had no significant changes in foliar pigments across the four seasons. Foliar nitrogen showed a significantly higher variability in the spring, summer and autumn seasons compared to the winter, whereas foliar phosphorus also varied across the seasons but to a lesser degree. The highest percentage of species pairs was separable using foliar nitrogen, compared to the pigments and phosphorus, emphasizing the importance of nutrients such as leaf proteins for species discrimination.

The study found a changing relationship between leaf spectra and foliar nutrient concentration across the four seasons for the six evergreen tree species. Twenty-two spectral bands which are related to known absorption features of plant properties were

identified across the four seasons as important for tree species discrimination. The relationship between leaf spectra and foliar nitrogen was highest during the spring, summer and autumn seasons for narrow bands associated with absorption features of proteins compared to the red-edge region. The spectra band combination 2130 nm and 2240 nm yielded the highest coefficient of determination between leaf spectra and foliar nitrogen across three of the four seasons. Season-specific prediction models were found to be more accurate in predicting foliar nitrogen than prediction models from across all seasons. The twenty-two bands were effective for the data reduction of the hyperspectral data and yielded a similar overall accuracy compared to 421 bands.

Multi-seasonal data improved tree species classification for multispectral sensors with a few bands. The classification, in which multi-season leaf spectra or canopy data from RapidEye imagery was used, resulted in higher overall and user's accuracies when compared to the single-season classifications. In contrast, the use of multi-season data for the classification of leaf spectra with 22 narrow bands, showed no statistical significance of differences compared to the classification results of the single season in which the highest overall accuracy of all single seasons had been obtained. The value of an increased classification accuracy should however be measured against the increase of cost when using images from multiple seasons. The study concludes that although seasonal profiles of foliar biochemicals overlap, multi-season information do improve species discrimination at foliar biochemical, leaf-spectra and canopy-spectra levels.

PREFACE

The research work described in this thesis was carried out in the School of Environmental Sciences, University of KwaZulu-Natal, Pietermaritzburg, from January 2011 to November 2013, under the supervision of Prof. Onisimo Mutanga (School of Environmental Sciences, University of KwaZulu-Natal; South Africa) and Dr. Moses Azong Cho (Council for Scientific and Industrial Research; South Africa and University of KwaZulu-Natal; South Africa).

I would like to declare that the research work reported in this thesis has never been submitted in any form to any other university. It therefore represents my original work except where due acknowledgments are made.

Heidi van Deventer Signed: _____ Date: _____

As the candidate's supervisor, I certify the above statement and have approved this thesis for submission.

Prof. Onisimo Mutanga Signed: _____ Date: _____

Dr. Moses Cho Signed: _____ Date: _____

DECLARATION 1 - PLAGIARISM

I, Heidi van Deventer, declare that:

1. The research reported in this thesis, except where otherwise indicated, is my original research.
2. This thesis has not been submitted for any degree or examination at any other university.
3. This thesis does not contain other persons' data, pictures, graphs, or other information, unless specifically acknowledged as being sourced from other persons.
4. This thesis does not contain other persons' writing, unless specifically acknowledged as being sourced from other researchers. Where other written sources have been quoted, then:
    a. Their words have been re-written, but the general information attributed to them has been referenced.
    b. Where their exact words have been used, then their writing has been placed in italics and inside quotation marks, and referenced.
5. This thesis does not contain text, graphics, or tables copied and pasted from the Internet, unless specifically acknowledged and the source being detailed in the thesis and in the References section.

Signed: _____

DECLARATION 2 - PUBLICATION AND MANUSCRIPTS

Scientific publications

Van Deventer H, Cho MA, Mutanga, O & Ramoelo A. 2015c. Capability of models to predict leaf N and P across four seasons for six subtropical forest evergreen trees. ISPRS Journal of Photogrammetry and Remote Sensing, 101: 209-220.

Van Deventer H, Cho MA, Mutanga O, Naidoo L & Dudeni-Tlhone N. 2015b. Reducing leaf-level hyperspectral data to 22 components of biochemical and biophysical bands optimises tree species discrimination. IEEE-JSTARS, January.

Van Deventer H, Cho MA & Mutanga O. In review. Improving tree species classification across four phenological phases with multi-season: six subtropical evergreen trees as case study. Manuscript submitted for review.

Van Deventer H, Cho MA & Mutanga O. In prep. Mapping vegetation types associated with wetland tree species in the iSimangaliso Wetland Park using multi-season RapidEye imagery.

Conference publications

Van Deventer H, Cho MA, Mutanga O. 2013. Do seasonal profiles of foliar pigments improve species discrimination of evergreen coastal tree species in KwaZulu-Natal, South Africa? in Conference proceedings of the 35th International Symposium on Remote Sensing of Environment (ISRSE). ISRSE, Beijing, China, pp. 1-12.

Van Deventer H, Cho MA, Mutanga O, Naidoo L, Dudeni-Thlone N. 2014. Identifying the best season for mapping evergreen swamp and mangrove species using leaf-level spectra in an estuarine system in KwaZulu-Natal, South Africa. In: Ahmed FA, Mutanga O & Zeil-Fahlbusch E. (Eds.). 10th International Conference of the African Association of Remote Sensing of the Environment (AARSE). Available online at: http://www.aarse2014.co.za/programme.html#programme [14 January 2016], AARSE, University of Johannesburg, South Africa.

Van Deventer H, Cho MA & Mutanga O. 2015a. Using remote sensing for tree species discrimination in the narrow coastal forests of KwaZulu-Natal, South Africa. XIV World Forest Congress. WFC, Durban, South Africa, 7 - 11 September 2015.

Acknowledgements

Family – Francois, Rosa and Albert who have been tremendously supportive on this journey. Francois, thank you for inspiring me, teaching me persistence, your continual motivation, for all the fieldwork you undertook with me, for the detailed in depth discussions until late at night and for all the proof reading you have done. My gratitude is beyond words. To Rosa and Albert, thank you for being part of this journey and helping me pick leaves in the field when you were only eight and five years old! I am glad we have this shared memory. To Juanita and Lisl, thanks for being back-ups and supports at all times.

Funding organisations – enabling research undertaken. The Earth Observation Research Group of the South African Council for Scientific and Industrial Research (CSIR), under the leadership of Dr Renaud Mathieu, has funded a large contribution of the time of my studies. My gratitude is extended to Renaud who were dedicated to improve the qualifications of researchers in this group to international standards. The South African National Department of Science and Technology (DST) funded the biochemical concentration analysis of this study, as well as the satellite imagery through the grant agreement DST/CON 0119/2010, Earth Observation Application Development in Support of SAEOS). The Water Research Commission (WRC) of South Africa contributed to the research through a 3-year project on the 'Understanding estuarine processes in uMfolozi /uMsundazi/St Lucia estuary from Earth Observation data of vegetation composition, distribution and health", project nr K5/2268, which was in the process of finalisation at the time of submission of this thesis. The National Research Foundation (NRF) supported additional running cost between 2012-2013 under Thuthuka funding with topic "Earth Observation for the identification of wetland tree species" which allowed for additional research trips and conference attendance.

Park authorities – the iSimangaliso Wetland Park Authority and Ezemvelo KZN Wildlife for permitting access to the St Lucia and Maphelane nodes of the iSimangaliso Wetland Park for sampling.

Supervisors and mentors - Moses and Oni, thank you for matching my passion of wetlands to a research topic. Jeanne Nel first awakened my interest in freshwater ecosystems and served as an earlier mentor to understanding these ecosystems and scientific writing. Moses has done a tremendous job in teaching critical thinking, superb scientific writing and increasing output beyond my imagination.

Colleagues & friends – many people contributed to this work in direct contributions to indirect support and advice. Where possible, I have thanked people in individual papers that originated from the PhD work, but herewith also acknowledge other intangible input and support. Dr Lorren Haywood, Dr Karin Eatwell and Mr Russell Main proof read sections of the thesis, many thanks.

Coincidentally I have made many turns through St Lucia earlier in my life, more than any other place in the world: as a scholar on a walking hike and camp in 1989; as a lecturer on a student excursion in 2001 and then in 2011-2015 as a researcher/ PhD student. I believe this work is a significant output resulting from the synchronicity of these events, which is beyond my comprehension. As such, I dedicate the work to Nature and Life.

Notes:

i) *The names uMfolozi and uMsunduzi are used interchangeably with Mfolozi and Msunduzi in the text.*

ii) *The use of the terms 'multi-season' and 'combined seasons' were also used interchangeably in the text. Originally 'combined seasons' were used and accepted in the journal paper publications of earlier chapters, although external reviewers of later chapters required an alternative term be used. As such, modifications to 'multi-season' were made as far as possible throughout the text, except for where a Chapter reflect an already-published journal paper.*

CHAPTER 1: GENERAL INTRODUCTION

1.1. Monitoring the impact of global change on forested wetlands at individual tree species level

The impacts of global change, particularly a rise in temperature and sea-levels as well as changes in rainfall patterns, are expected to cause a shift in species distribution, composition and functioning (Kirschbaum, 2000; Sardans and Peñuelas, 2012). Many experts ask whether vegetation will be able to adapt to climate changes or face extinction (Intergovernmental Panel on Climate Change (IPCC), 2007; Booth *et al.*, 2012; Richardson *et al.*, 2013). To detect changes in vegetation distribution and condition, a monitoring system should be able to map species distribution and detect significant deviations from natural variations in plant properties across phenological[1] phases per species (Richardson *et al.*, 2013).

Coastal swamp and mangrove forests are some of the most threatened forest types in the world (Valiela *et al.*, 2001; Posa *et al.*, 2011; Crooks *et al.*, 2011). Losses of mangrove forest over the past 50 years have been estimated at between 25 % and 50 % (Alongi, 2002; Spalding *et al.*, 2010). The losses of swamp forest are less known across the globe, although it is estimated that only 36 % of the original extent of swamp forest remain in Southeast Asia (Posa *et al.*, 2011). The decline in these forested wetlands[2] is primarily attributed to the clearance of forests for aquaculture and agriculture, although the impact of global change through sea-level rise and erosion, nitrification and drought as a result of water extraction within the catchment are also known to cause serious degradation (Alongi, 2002; Mucina and Rutherford, 2006; Posa *et al.*, 2011). Where these forested wetlands are intact, they offer a number of ecosystem services, such as the sequestration of carbon, particularly swamp forest, which occurs on floodplains where peat soils accumulate from the woody plant debris (Posa *et al.*, 2011; Crooks *et al.*, 2011). Forested wetlands also provide flood control and protection against storm surges which minimize coastal erosion. Swamp and mangrove forests are unique habitats which host some rare and endangered species, and are also considered as refugia for a number of fauna (Alongi, 2002; Posa *et al.*, 2011). These forests are also sources of food, construction material, fuel and medicine for communities

[1] Lieth (1974:4) defines phenology as "… the study of the timing of recurring biological events, the causes of their timing with regard to biotic and abiotic forces, and the interrelation among phases of the same or different species" (Lieth, 1974).
[2] Where the South African National Wetland Classification System (Ollis *et al.*, 2013) recognises swamp forests as freshwater ecosystems and mangroves as estuarine ecosystems, for ease of reading these two forest types are referred to as 'forested wetland', and the associated tree species of this work are collectively referred to as 'wetland trees' as per the Ramsar definition of wetlands at https://www.environment.gov.au/water/wetlands/ramsar.

(Alongi, 2002; Mucina and Rutherford, 2006; Crooks *et al.*, 2011). The impacts of global change, however, compromise their functioning and reduce the quality and quantity of ecosystem services offered by these forests. Increased population demands for water and food production increase water extraction leading to drought. Drought and a reduction in precipitation can also lead to the loss of mangrove forests resulting in an increase of coastal erosion (Bate *et al.*, 2010; Van Heerden, 2011). When the peat substrates of swamp forests dry out, it can result in fires that can burn both above and underground biomass, destroy the seed banks and ultimately releases carbon dioxide into the atmosphere (Posa *et al.*, 2011; Crooks *et al.*, 2011). Owing to the multitude of stressors to these already fragmented forests, mangrove and swamp forests, like tropical and subtropical forests, are considered to be some of the most vulnerable ecosystems to climate change (Seppälä *et al.*, 2009).

Mangrove and swamp forests in South Africa are both critically endangered forest types with conservation targets listed as 100 % (Mucina and Rutherford, 2006). The South African swamp and mangrove forests, located at the southern-most extent of the subtropical climate region of Africa, are small and occupy areas of 3 803 and 3 340 ha respectively (Mucina and Rutherford, 2006). A large proportion of the swamp and mangrove forests are located in the iSimangaliso Wetland Park, 66 % and 56 % respectively as estimated from Mucina and Rutherford (2006). Threats to the swamp forests situated on the uMfolozi River floodplain date back to 1911 where land had been cleared for sugarcane farming and commercial forestry (Taylor, 2011). More recently, the continual slash and burn practice to open land for the subsistence farming of bananas and *Colocasia esculenta* (locally known as 'madumbe') contribute to the reduction of the swamp forest and its condition (Mucina and Rutherford, 2006). In many of the South African estuaries where swamp and mangrove forests occur, water extraction in the upper catchments for agricultural and residential purposes, along with droughts, contributed to lower water levels in the estuarine systems and an increase in salinity levels, risking the intactness of both the mangrove and swamp forests (Van Heerden, 2011; Van Niekerk and Turpie, 2012).

Regardless of the small extent of these forested wetland types in South Africa, their value and importance necessitate a better understanding of their distribution and condition in space and time. Such knowledge will assist in the understanding of the impacts of global change on these systems. Mapping the distribution of individual tree species can contribute to the protection of tree species listed under the South African National Forest Act (Act 84 of 1998; RSA, 1998). Six wetland tree species occur in the coastal mangrove and swamp forests which are listed in the South African National Forest Act including four mangrove (*Bruguiera gymnorrhiza, Ceriops tagal, Lumnitzera racemosa* var*. racemosa* and *Rhizophora mucronata*) and two swamp species (*Barringtonia racemosa* and *Ficus trichopoda*) (RSA, 1998; Boon, 2010). Knowing the extent of the swamp and mangrove forests will also improve the implementation of setback lines where no development will be allowed, regulated under the National Environmental Management: Integrated Coastal Management Act (Act No. 24 of 2008, ICM Act) (Republic of South Africa (RSA), 2008).

1.2. Remote sensing of species classification across phenological phases

Remote sensing has been proven to be a suitable tool for vegetation species discrimination based on the premise that plant properties can be quantified. Absorption features in the electromagnetic spectrum between the visible (400 nm) and Shortwave Infrared (SWIR, 2500 nm) showed strong correlation to variation in pigments, nutrients (proteins and starch), leaf water content and foliage biomass, (Elvidge, 1990; Curran *et al.*, 2001; Curran, 2001). Hyperspectral data is effective in the quantification of these plant properties with the use of narrow sequential bands of < 10 nm between the visible and SWIR. Variations in foliar biochemical and biophysical properties occur over phenological phases and remote sensing was able to quantify seasonal changes in plant properties (Garcia-Plazaola *et al.*, 1997; Gond *et al.*, 1999; Cooke and Weih, 2005; Dillen *et al.*, 2012). Various spectral bands associated with a number of plant properties were successfully used in separating wetland tree species, graminoids and macrophytes at leaf-level scale with hyperspectral data (Vaiphasa *et al.*, 2005; Artigas and Yang, 2006; Adam and Mutanga, 2009). Although the hyperspectral studies offer a greater range in representation of plant properties, the properties that are essential for species discrimination vary across climatic regions and seasons. To date no robust selection of spectral bands has been determined (Martin *et al.*, 1998; Fung *et al.*, 2003). In addition, hyperspectral studies remain costly and limited in regional extent compared to space-borne multispectral images, limiting their use thereof in monitoring species distribution over time.

Multispectral sensors such as Landsat, SPOT, IKONOS and Quickbird were considered less suitable for species discrimination, on the one hand owing to the spatial resolution being larger than individual tree canopies (e.g. Landsat missions have a spatial resolution of >15 m), and on the other hand owing to the number and range of bands which can detect only a few of the plant properties (Belluco *et al.*, 2006; Adam *et al.*, 2010). IKONOS and Quickbird images have however been successfully used to discriminate between three species of mangroves in closed-canopy forests in Panama, relying on texture analysis and large window sizes (Wang *et al.*, 2004). The improved spatial resolution of these sensors as well as an increase in a more diverse set of plant properties is expected to further improve the possibility of mapping and monitoring tree species composition.

The past six years witnessed tremendous improvements in the mapping of tree species at regional scale. Space-borne sensors, such as RapidEye (RE) and WorldView-2 (WV2) (both launched in 2009), have an additional band in the red-edge region, which has been shown to benefit the quantification of biophysical and biochemical parameters and enhancing species classification (Mutanga and Skidmore, 2004; Cho *et al.*, 2008; Mutanga *et al.*, 2012; Adelabu *et al.*, 2013). The spatial resolution of these sensors range between 2 and 10 m, in line with individual tree canopy sizes, which offer more spectral bands compared to IKONOS

and Quickbird. The inclusion of bands from the SWIR region, although proven valuable for improved tree species discrimination, remains costly (Martin *et al.*, 1998; Huber *et al.*, 2008; Immitzer *et al.*, 2012). WorldView-2 has particularly advanced the capability of mapping tree species at individual crown level and increasing classification accuracies in comparison to traditional multispectral sensors (Kanniah, 2011), having a spatial resolution of 2 m and 8 bands between the visible and near-infrared (DigitalGlobe Pty Ltd, http://www.digitalglobe.com/). Additional benefits were shown in the past two years when these new multispectral sensors were successfully used in mapping nutrients for broad vegetation groups at regional level (Ramoelo *et al.*, 2012; Ramoelo *et al.*, 2013; Cho *et al.*, 2013). Mapping and monitoring tree species at individual crown level over a broad region has an advantage compared to hyperspectral studies or field assessments. It offers a regional perspective particularly for areas that are inaccessible owing to dense overgrowth, flooding or dangerous animals (United States Department of Energy (US DOE), 2012). Multispectral imagery is also considered comparatively more affordable compared to field and laboratory measurements of plant properties over broad regional levels at regular time intervals (Mumby *et al.*, 1999).

Multispectral space-borne sensors also offer the advantage of regular temporal imagery which is ideal for long-term monitoring of tree species. Time-series data is bound to increase the representation of the natural variation of plant properties across phenological phases, and with better representation, the optimisation of species discrimination is expected. For example, two species may vary more in foliage biomass or nitrogen levels over a longer period of time compared to a single snapshot in time. A number of studies related the optimization of species classification to particular phenological events such as flowering or seeding, although the majority found the spring season optimal for species discrimination (Bartlett and Klemas, 1980; Laba *et al.*, 2005; Sobhan, 2007), yet these events may differ from one region to another based on the different species occurring in such regions. Multiple seasons may therefore offer more phenological events for optimising species discrimination compared to a single season. A study in China showed that the separability between 25 subtropical trees vary over four seasons (winter, spring, summer and autumn) with classification accuracies ranging from the lowest in spring (80 %) to the highest in winter (91 %) using seasonally-important hyperspectral bands (Fung *et al.*, 2003). The study did not however, assess whether the aggregation of the seasons improve the species discrimination when compared to a single season. The classification of deciduous tree species in the United States of America achieved maximum classification accuracy when a number of aerial images between the spring and autumn seasons were used (Key *et al.*, 2001). Similarly, the separability of seven, predominantly grassland habitats in Berlin Germany, showed that RapidEye time-series imagery over 8 seasons achieved an overall classification accuracy of >90 % (Shuster *et al.*, 2015). These studies allude to the potential of using multiple-seasons data for improved species discrimination. The hypothesis is therefore formulated that multi-season data could improve species discrimination when compared to

a single season, since it includes a variety of differences in the variation of plant properties. This hypothesis remains to be tested for evergreen wetland tree species in a subtropical forest.

Although multi-season data can contribute to the optimisation of tree species discrimination, a number of challenges should be addressed in the assessment of the data. First, time-series data normally comprises of a superfluous amount of information which results in unnecessary cost and redundancy. It may be that only a few seasons carry essential information for species classification, and as such, can optimize classification to the essential time-range across a phenological phase. Second, spectral bands are also highly correlated and therefore appropriate methods should be used to remove both redundancy or correlation. Lastly, the classification of forested wetlands also pose some challenges for remote sensing considering the presence and fluctuation of water levels (Schmidt and Skidmore, 2003; Rebelo *et al.*, 2009; Adam and Mutanga, 2009; Adam *et al.*, 2010). Background water and wet soil reduce the reflection from vegetation particularly those with narrow leaves (e.g. sedges) or where background influences the reflectance of a pixel value not fully covered by a closed-canopy tree species. The fluctuation of water levels causes difficulties in classification for change-detection assessments in grassland or water over some seasons (Lück-Vogel *et al.*, Submitted). In such cases, it remains to be assessed whether the classification of species from multi-season data improves the classification accuracy and turns to an advantage for monitoring and change detection.

1.3. Research Objective and Aims

Considering that space-borne multispectral imagery offer time-series data across phenological phases, and that representation of plant properties across phenological phases is expected to improve the representation and uniqueness of species, this study investigated whether multi-season data from leaf to image scales would improve the species discrimination of wetland tree species when compared to a single season's data.

A number of sub hypotheses were made during the investigation:

- The variability of foliar biochemical and biophysical properties within species and between species in one season would be similar.
- Foliar biochemical and biophysical properties of a species may show an increase in variation over a number of seasons compared to a single season and therefore multi-season information may enhance species discrimination.
- Multi-season data can improve representation of biochemical and biophysical properties in a seasonal profile that may be unique to species and enhance differences between species.

A number of research questions were formulated from the literature and assumptions:

- Are tree species unique in foliar chemical concentration over phenological phases?
- If so, which spectral bands would capture the variability of a species across phenological phases?
- Would the leaf spectra of species over multiple seasons improve the separability between species compared to a single season?
- Would multi-season imagery data be used to improve species discrimination when compared to a single season?

The aim of this study was to assess whether multi-seasonal information of plant properties of six evergreen wetland tree species from a subtropical forest in KwaZulu-Natal, South Africa were detectable, unique and effective for optimizing species discrimination. The hypothesis was formulated as follow:

> H0: multi-season information of evergreen wetland tree species is not unique and do not improve species discrimination when compared to a single season's information
>
> Ha: multi-season information of evergreen wetland tree species is unique and improves species discrimination when compared to a single season's information

The four objectives resulting from the research questions include:

- Assess whether tree species are unique in foliar biochemical concentration over multiple seasons.
- Ascertain the most important bands across phenological phases for species discrimination.
- Determine whether leaf reflectance spectra of multiple seasons will improve the species classification compared to a single season.
- Assess whether image stacks of multiple seasons will improve species discrimination when compared to a single season.

1.4. Study area

The iSimangaliso Wetland Park (28°S, 32°30'E) is located on the east coast of South Africa in the KwaZulu-Natal Province (Figure 1.1). The Park extends over ±218 000 ha of land along 190 km of coastline, with vegetation and land cover categories (Figure 1.1; Inset B) comprising mostly of natural thicket and grassland (± 42 %), coastal and dune forests (± 17 %), wetland (± 18 %) and estuarine (± 17 %) systems as well as transformed land (± 6 %) (GeoTerraImage (GTI), 2010; Ezemvelo KZN Wildlife, 2011). The Park is listed as both a Ramsar and World Heritage Site (WHS) on grounds of the high biodiversity in the region and the number of diverse wetland types (Cowan, 1999).

Sub-tropical climatic conditions prevail along a narrow ±6 km wide zone on the east coast of South Africa. The Mean Annual Precipitation (MAP) ranges from 1 000 to 1 500 mm in this coastal corridor, although decreases to below 1 000 mm inland (Middleton and Bailey, 2008). In the Park, mean temperatures during summer range from 23 – 30°C, and can decrease to approximately 10°C and lower during the winter periods (Sokolic, 2006). Coastal swamp and mangrove tree species occur in the coastal forested wetlands along the uMsunduzi, uMfolozi and St Lucia Rivers and estuaries. Owing to the large extent of wetlands and presence of dangerous animals such as hippopotami, crocodiles and the big five (The iSimangaliso Wetland Park, 2014), safe access is limited for monitoring vegetation through fieldwork. Consequently, the Park will benefit greatly in using earth observation for vegetation assessments such as tree species monitoring at regional scale. A section of the Park has been assessed in this study, located between Catalina Bay in the north and the Maphelane node in the south, and from the coast in the east to the DukuDuku Forest in the west (Figure 1.1).

Table 1.1: Number of tree species sampled across four seasons in the iSimangaliso Wetland Park, South Africa*.

Tree species	Common name	Acronym	Trees Winter (*n* =)	Trees Spring (*n* =)	Trees Summer (*n* =)	Trees Autumn (*n* =)	Total number of trees per species (*n* =)
Avicennia marina	White mangrove	AM	23 (21)	23 (21)	22 (21)	22 (21)	90 (84)
Bruguiera gymnorrhiza	Black mangrove	BG	20 (19)	19	20 (19)	20 (19)	79 (76)
Ficus sycomorus	Sycamore fig	FSYC	15	15	15	15	60
Ficus trichopoda	Swamp fig	FT	12 (11)	11	11	11	45 (44)
Hibiscus tilliaceus	Lagoon hibiscus	HT	31 (30)	31 (30)	30	30	122 (120)
Syzygium cordatum	Waterberry	SC	17	17	17	17	68 (68)
Total per season			118 (113)	116 (113)	115 (113)	115 (113)	464 (452)

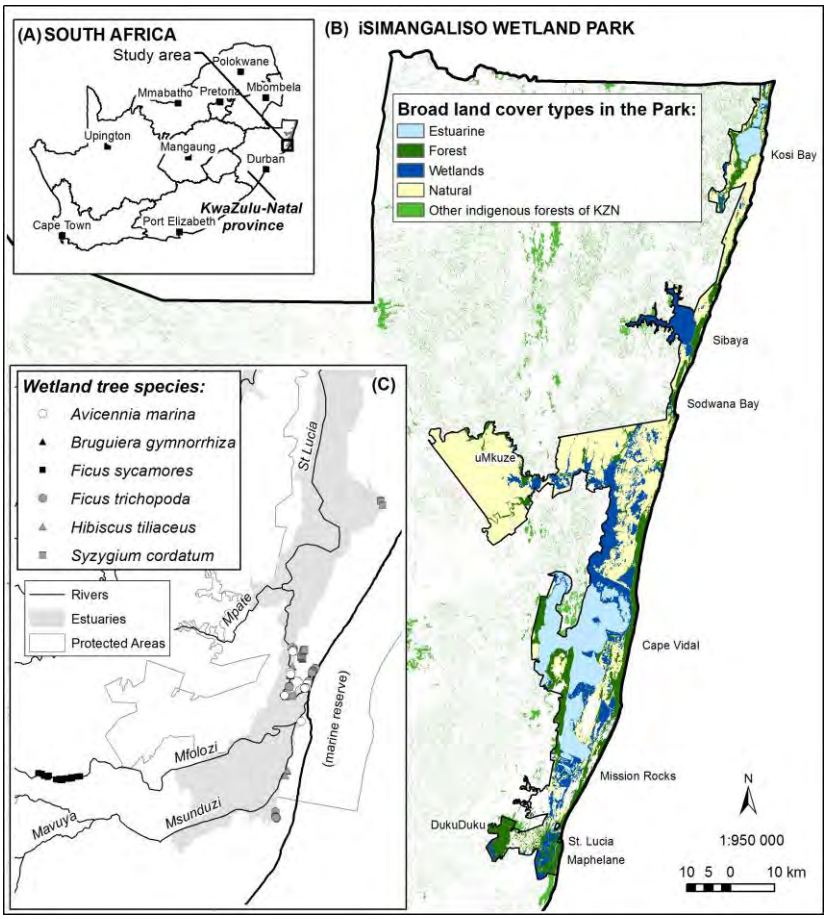

Figure 1. 1: The study area is located in the iSimangaliso Wetland in the KwaZulu-Natal Province of South Africa (Inset A). The Park stretches along the coast with broad vegetation and land cover comprising natural thicket and grassland, forests and wetlands (Inset B). Six tree species were sampled along the Msunduzi, Mfolozi and St Lucia estuarine systems (Inset C).

1.5. Thesis outline

Field surveys were undertaken and images obtained over four seasons (winter, spring, summer and autumn) over two years (2011-2). The hypotheses were tested using a number of plant properties at three structural scales in five Chapters:

(i) At foliar biochemical level, to assess whether differences between the foliar concentration of two pigments (carotenoids and chlorophyll) and two nutrients (nitrogen and phosphorus) are statistically significant across winter, spring, summer and autumn of the six species – **Chapter 2**.

(ii) At leaf-level spectral scale:

First, spectral bands which relate to nutrients (nitrogen and phosphorus) were determined over the four seasons. The relationship between foliar nutrient concentration and leaf reflectance was assessed over the four seasons to determine whether significant changes occur. Bands which were proven to relate to plant properties were selected where high coefficients of determination existed between the nutrient concentration and leaf reflectance across the four seasons – **Chapter 3**.

Second, the effective reduction of redundancy in the leaf-level hyperspectral data was assessed through using selected bands, relating to plant properties, for species classification. In addition, two data transformation methods which reduce correlation between the bands were compared. The Principal Component Analysis (PCA) and the Partial Least Square (PLS) decomposition methods were combined with a Random Forest (RF) classification algorithm for species classification to assess the best method for data transformation and classification – **Chapter 4**.

Third, it was assessed whether the aggregation of all four seasons into a multi-season data set improves the classification of the six tree species when compared to any one of the four seasons (winter, spring, summer and autumn). Multi-season data sets were also created from aggregating every combination of two and three seasons as means of optimising the multi-season classifications – **Chapter 5**.

(iii) At image-level scale, it was assessed whether multi-season imagery would improve the classification accuracies of evergreen tree species, or associated vegetation types, compared to four single seasons (autumn, winter, spring and summer season). Various combinations of seasons were also assessed to ensure optimisation of multi-season data for classification – **Chapter 6**.

In the synthesis chapter, **Chapter 7**, the implications of the results are discussed for the classification of tree species using bands that related to plant properties, the advantage of phenological representation of plant properties for species discrimination and the potential for the newer space-borne sensors to use multi-season data for monitoring species distribution and condition under the threats of global change.

CHAPTER 2: DO TREE SPECIES HAVE UNIQUE SEASONAL PROFILES?

This chapter is based on the findings of two conference publications:

Van Deventer H, Cho MA, Mutanga O, Mutanga O. 2013. Do seasonal profiles of foliar pigments improve species discrimination of evergreen coastal tree species in KwaZulu-Natal, South Africa? In: Conference proceedings of the 35th International Symposium on Remote Sensing of Environment (ISRSE). ISRSE, Beijing, China, pp. 1-12.

Van Deventer H, Cho MA & Mutanga O. 2015. Using remote sensing for tree species discrimination in the narrow coastal forests of KwaZulu-Natal, South Africa. XIV World Forest Congress. WFC, Durban, South Africa, 7 - 11 September 2015.

Abstract

A number of ecophysiological studies has shown the potential of the seasonal profiles of foliar pigments and nutrients for improving species discrimination. Remote sensing vegetation indices have been used to optimise absorption features presented by foliar pigments and nutrients, as well as improve species discrimination. This study investigated the potential of the seasonal profiles of pigments and nutrients in improving species discrimination for trees using leaf spectral data. The aims were to (i) determine whether evergreen tree species show significant changes in foliar pigments or nutrients across four seasons; (ii) assess whether foliar pigments and nutrients can be used to separate between species over four (winter, spring, summer and autumn) seasons; and (iii) whether the aggregation of foliar pigments and nutrients for four seasons could improve the separability of species when compared to a single season. Five sunlit leaves were sampled from the canopies of seven evergreen tree species in a sub-tropical region of South Africa, over four seasons during 2011-12. A one-way ANalysis Of Variance (ANOVA) and post-hoc Tukey Honest Significant Difference (HSD) multiple comparisons test were used to assess whether differences between species over four seasons were statistically significant. Most of the species showed no distinct variation in foliar carotenoids, chlorophyll, nitrogen and phosphorus across the four seasons, except for the water berry (*Syzygium cordatum*). Of the four foliar biochemicals, nitrogen concentration resulted in the highest number of significantly different inter-species pairs across the spring, summer and autumn seasons. The aggregation of the four season's data into a single multi-seasonal data set increased the separability between the six evergreen wetland tree species particularly for foliar carotenoids and phosphorus concentration.

2.1. Introduction

Phytosynthetic pigments (carotenoids and chlorophylls) and nutrients (nitrogen and phosphorus) respond to environmental and climate conditions and hence reflect corresponding phenological changes in vegetation (Garcia-Plazaola *et al.*, 1997; Gond *et al.*, 1999; Asner *et al.*, 2009). In deciduous trees, the leaf expansion phase is marked by the increase in concentrations of leaf pigments, nitrogen, phosphorus and biomass (Sharma, 1983; Gond *et al.*, 1999; Lal *et al.*, 2001; Nakaji *et al.*, 2006; Hilker *et al.*, 2011). A decrease in leaf water content has been noted from spring to summer (Gond *et al.*, 1999). The highest concentration of N and P has been noted in newly matured leaves in deciduous trees (Franco *et al.*, 2005). Following leaf maturity, a gradual decline in leaf pigments and nutrients has been observed, whereas a sharp decline in pigments, nutrients and biomass has been observed prior to abscission (Chapin and Kedrowski, 1983; Gond *et al.*, 1999). During the spring and summer seasons, nutrients are allocated to leaf and woody growth, although prior to leaf abscission, while proteins and starch are produced and translocated for storage in stems and bark of the roots or trunk during the dormant period (Niinements and Tamm, 2005; Millard and Grelet, 2010).

In evergreen trees, similar increases in leaf chlorophyll, nutrients and biomass are noted in spring, however, a more gradual decline towards the dormant season is observed, with leaf drop occurring in both summer and winter (Lewandowska and Jarvis, 1977; Sharma, 1983; Bell and Ward, 1984; Garcia-Plazaola *et al.*, 1997; Gamon and Surfus, 1999; Fife *et al.*, 2008; Cai *et al.*, 2009). Leaf carotenoid concentration, in contrast, showed high concentrations in winter and declined towards spring for evergreen spruce (Lewandowska and Jarvis, 1977). The modelling of carotenoid content of evergreen conifers in Canada from canopy spectra also showed the highest concentration of this pigment in the winter season (Hilker *et al.*, 2011). Contrary to deciduous vegetation, evergreen vegetation show less extreme seasonal variation in pigments, biomass and leaf water content over four seasons (Cai *et al.*, 2009; Flores-de-Santiago *et al.*, 2012). Furthermore, a slight increase in leaf water was observed in spring for evergreen *Quercus* followed by a gradual decline over the growth season (Gond *et al.*, 1999). In a region of Australia with a Mediterranean climate and savannah region of Brazil, evergreen trees generally show lower concentrations of foliar nitrogen and phosphorus compared to deciduous species, measured over a period of one and three years respectively (Bell and Ward, 1984; Franco *et al.*, 2005). Proteins and starches are also stored primarily in older leaves from where translocation to new leaf growth takes place in spring (Cherbuy *et al.*, 2001; Millard and Grelet, 2010). Many studies on seasonal variation of foliar characteristics are species and location specific, and few provide bioregional oversight of the phenology of foliar nutrients (Reich and Oleksyn, 2004; De Weirdt *et al.*, 2012; Richardson *et al.*, 2013). According to De Weirdt *et al.* (2012), the seasonality of evergreen tropical forests is not well understood and highly simplified in global ecosystem models.

While a number of studies have investigated seasonal changes in foliar pigments and nutrients, few have assessed whether multi-season data will improve the separability of species compared to a single season. Understanding the seasonal variation of pigment and nutrient concentrations for each species can contribute to the choice of these foliar biochemicals and season(s) to use in species discrimination, as well as identifying regions of the electromagnetic spectrum to target for sensor development (Blackburn, 1998a). In this chapter the seasonality of foliar pigments and nutrients was investigated, in particular (i) whether species show significant changes in foliar pigments and nutrients across four seasons; (ii) whether foliar pigments and nutrients can be used to separate between species in over four (winter, spring, summer and autumn) seasons; and (iii) whether the aggregation of foliar pigments and nutrients concentrations into a multi-season data set would improve the separability of species when compared to a single season.

2.2. Methods

2.2.1. Study area

The iSimangaliso Wetland Park (28°S, 32°30'E) is a Ramsar and World Heritage Site located on the east coast of South Africa in the KwaZulu-Natal Province (Figure 2.1). The Park is situated in a sub-tropical coastal region with mean annual precipitation ranging from 1000 to 1500 mm on the coast, to below 1000 mm inland (Middleton and Bailey, 2008). Mean temperatures during summer range from 23 – 30°C, and can decrease to approximately 10°C during winter periods (Sokolic, 2006). A section of the park has been assessed in this part of the study, located between Catalina Bay in the north and the Maphelane node in the south, and from the coast in the east to the DukuDuku Forest in the west (Figure 2.1).

The iSimangaliso Wetland Park hosts the highest number of wetland habitat types (thirteen listed for Ramsar) in Southern Africa (Cowan, 1999). Six evergreen wetland tree species were sampled along the uMsunduzi, uMfolozi and St Lucia Rivers over four seasons (winter, spring, summer and autumn) between 2011 and 2012 (Table 2.1). The tree species were associated with a number of freshwater and estuarine ecosystem types including estuarine, swamp, riverine and groundwater-fed depression systems.

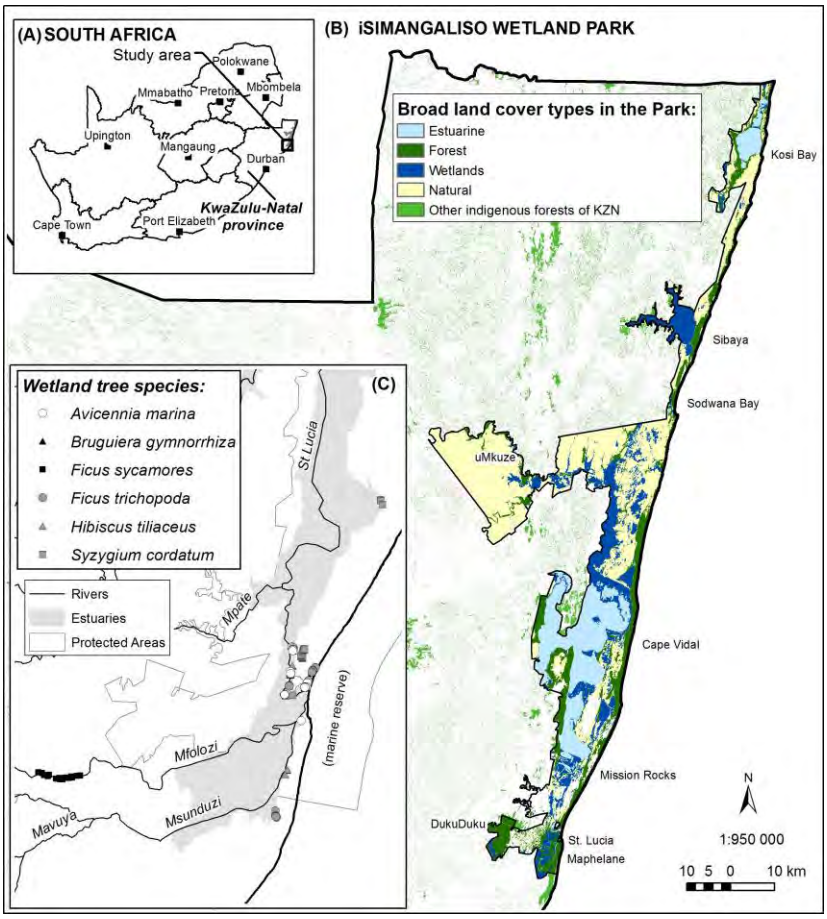

Figure 2.1: The study area is located in the iSimangaliso Wetland in the KwaZulu-Natal Province of South Africa (Inset A). The Park stretches along the coast with broad vegetation and land cover comprising natural thicket and grassland, forests and wetlands (Inset B). Six tree species were sampled along the uMsunduzi, uMfolozi and St Lucia River and estuarine systems (Inset C).

Table 2.1: Number of tree species sampled across four seasons in the iSimangaliso Wetland Park, South Africa*.

Tree species	Common name	Acronym	Trees Winter (*n* =)	Trees Spring (*n* =)	Trees Summer (*n* =)	Trees Autumn (*n* =)	Total number of trees per species (*n* =)
Avicennia marina	White mangrove	AM	23 (21)	23 (21)	22 (21)	22 (21)	90 (84)
Bruguiera gymnorrhiza	Black mangrove	BG	20 (19)	19	20 (19)	20 (19)	79 (76)
Ficus sycomorus	Sycamore fig	FSYC	15	15	15	15	60
Ficus trichopoda	Swamp fig	FT	12 (11)	11	11	11	45 (44)
Hibiscus tilliaceus	Lagoon hibiscus	HT	31 (30)	31 (30)	30	30	122 (120)
Syzygium cordatum	Waterberry	SC	17	17	17	17	68 (68)
Total per season			118 (113)	116 (113)	115 (113)	115 (113)	464 (452)

** Species and number of trees were equalised for regression and classification purposes to the number shown in brackets.*

2.2.2. Sampling protocol and nutrient analysis

Five leaves were sampled from the sun-exposed canopy of 113 mature trees which were more than 2x2 m in size (Table 2.1). Leaf spectral reflectance measurements of the adaxial surface of each leaf were made using the Analytical Spectral Device (ASD) plant probe accessory connected to an ASD spectroradiometer (FieldSpec Pro FR, Analytical Spectral Device, Inc., USA), with the average scan time set at 10 seconds. The ASD covers the spectral range between 350 and 2500 nm with a 1.4 nm sampling interval between 350 and 1050 nm range, and ±2 nm between 1050 and 2500 nm. The plant probe provides a direct-contact probe which limits ambient light. The radiance measurements were converted to reflectance against scans of a white spectralon reference panel. The five leaf specimens per tree were combined for nutrient analysis (N and P). The leaves were oven-dried at 65°C until constant weight was reached. Bemlab Pty Ltd analysed nitrogen concentration using a Leco FP528 nitrogen analyser (Horneck and Miller, 1998) and phosphorus through Inductively Coupled Plasma Optical Emission Spectrometry (ICP-OES) analysis (Isaac and Johnson, 1998).

2.2.3. Predicting pigment concentrations from leaf spectra

Fresh leaves from the canopies of 17 evergreen wetland trees were sampled in the spring season for pigment analysis. Leaves from tree species *Avicennia marina*, *Barringtonia racemosa*, *Bruguiera gymnorrhiza*, *Ficus sur*, *Ficus sycomorus*, *Ficus trichopoda*, *Hibiscus tilliaceus* and *Syzygium cordatum* were sampled for laboratory analysis. For these discussed tree canopies, carotenoids and chlorophylls were extracted using 100 % acetone and absorbance measured at 470 nm for carotenoids, 661.2 nm for chlorophyll *a* and 644.8 nm for chlorophyll *b*. Total chlorophyll content was computed using equations from Lichtenthaler and Buschmann (Lichtenthaler and Buschmann, 2001).

Predictive equations for the carotenoid and chlorophyll concentrations for each tree were derived from laboratory chemical analysis and leaf spectral measurements. Vegetation indices, which have previously been proven to be robust across species (Blackburn, 1998b; Main *et al.*, 2011), were calculated using the collected leaf spectra (Table 2.2). An iterative bootstrap process (1 000 iterations) using R software divided the data randomly into a training (2/3) and test (1/3) data set. A linear model was fit to the training data set between pigment concentration and each vegetation index, and then applied to the test data set as well. The root mean square error (RMSE) was then calculated for both the training and test data set and recorded, before each new reiteration. The vegetation index with the lowest RMSE was considered the best predictive index and was then used to predict the pigment concentrations from the spectral data.

Table 2.2: Vegetation indices used in predicting foliar pigment concentration from leaf spectra (Blackburn, 1998b; Main *et al.*, 2011).

Carotenoid Index	Chlorophyll index
Carotenoid red edge (Gitelson *et al.*, 2002; Gitelson *et al.*, 2003)	Carter4 (Carter, 1994)
Carotenoid Reflectance Index using reflectance at 550 nm (CRI_550) (Gitelson *et al.*, 2002)	$Datt_1$ (Datt, 1999)
Carotenoid Reflectance Index using reflectance at 700 nm (CRI_700) (Gitelson *et al.*, 2002)	Maccioni (Maccioni *et al.*, 2001)
Datt1998U (Datt, 1998)	Modified Normalised Difference Vegetation Index (NDVI) - (mND_{705}) (Sims and Gamon, 2002)
Datt1998SA (Datt, 1998)	
Photochemical Reflectance Index (PRI) (Gamon *et al.*, 1997)	Modified Ref-Edge Inflection Point (mREIP) or Inverted Gaussian fit on reflectance (IG_REP) (Miller *et al.*, 1990)
Photochemical Reflectance Index x Chlorophyll Index (PRI_CI) (Garrity *et al.*, 2011)	
Pigment Specific Simple Ratio using the reflectance at 470 nm (PSSR_470) (Blackburn, 1998b)	MERIS Terrestrial chlorophyll index (MTCI) (Dash and Curran, 2004)
Pigment Specific Simple Ratio using the reflectance at 500 nm (PSSR_500) (Blackburn, 1998b)	
Pigment Specific Normalised Difference using the reflectance at 470 nm (PSND_470) (Blackburn, 1998b)	Normalised Difference Vegetation Index ($NDVI_2$) (Gitelson and Merzlyak, 1994)
Pigment Specific Normalised Difference using the reflectance at 500 nm (PSND_500) (Blackburn, 1998b)	
Reflectance at 470 nm (R_{470}) (Blackburn, 1998a)	Optimised Soil-Adjusted Vegetation Index ($OSAVI_2$) (Wu *et al.*, 2008)
Reflectance at 500 nm, adjusted from Blackburn 1998b (R_{500}) (Blackburn, 1998a) adjusted	Red-edge Inflection Point (REIP) (Collins, 1978)
Ratio analysis of reflectance spectra for carotenoids (RARS_c) (Chappelle *et al.*, 1992)	Red-edge Position Linear Extrapolation (REP_Le1) (Cho and Skidmore, 2006)
Structure Insensitive Pigment Index (SIPI) (Penuelas *et al.*, 1995)	$Vogelman_1$ (Vogelmann *et al.*, 1993)
Yellowness Index (YI) (Adams *et al.*, 1999)	$Vogelman_3$ (Vogelmann *et al.*, 1993)

2.2.4. Analysing seasonal variance of foliar pigments and nutrients per species

The seasonal variation and mean seasonal profile of foliar pigments (carotenoids and chlorophyll) and nutrients (nitrogen and phosphorous) for each tree species were assessed using the predicted pigment and laboratory nutrient results. The statistical significance of differences in the foliar pigment and nutrients between the species as well as for each species across the four seasons was assessed using a one-way ANalysis Of Variance (ANOVA) followed by a post-hoc Tukey Honest Significant Difference (HSD) multiple comparisons test. The alpha level at 95 % confidence interval (p = 0.05) were corrected for the Bonferroni effect by dividing the alpha level by the number of comparable pairs: $p < 0.05 / 6$ comparable pairs = $p < 0.008$. Thereafter the statistical significant of differences between species were assessed for each season and foliar biochemical, with an adjusted alpha level to 15 comparable pairs = $p < 0.003$. Lastly the foliar carotenoids, chlorophyll, nitrogen or phosphorous of all four individual seasons were aggregated into a multiseasonal data set, and the statistical significance of differences between species assessed for each foliar chemical using the ANOVA and Tukey HSD tests.

2.3. Results

2.3.1. Vegetation indices used to predict foliar pigments concentration

The Datt1998 index for untransformed spectra (Datt1998U; Table 2.2) had the lowest RMSE for carotenoids while the Vogelman3 index had the lowest RMSE for chlorophyll (Tables 2.3 and 2.4). These indices were therefore used to predict pigment concentration for the wetland trees used in the study.

2.3.2. General variation of foliar pigment and nutrient across season

In general, carotenoids and chlorophyll showed little variation across the four seasons for the six evergreen subtropical tree species (Table 2.5; Figure 2.2). Chlorophyll showed a slight increase in the coefficient of variation (COV) in spring, compared to the winter, summer and autumn seasons (Table 2.5). Nitrogen, in contrast, showed a higher variability of foliar concentration across the four seasons with the winter season having the highest mean and lowest COV, and the growth seasons (spring, summer and autumn) showing a decrease in the mean foliar nutrient concentration but showed an increase in the COV (Table 2.5; Figure 2.2). Foliar phosphorous concentration showed no variation from winter to spring, but an increase in the variability was noticed for summer and a decrease in the variability in autumn.

Table 2.3: Results of the bootstrap process of the best predictive vegetation index for carotenoids. Values are sorted for the test set by increasing mean RMSE.

Carotenoid vegetation index	Training data set							Test data set						
	Min	1st Qu	Median	Mean	3rd Qu	Max	SD	Min	1st Qu	Median	Mean	3rd Qu	Max	SD
Car_rededge	29.21	34.91	36.55	36.38	38.03	41.92	2.15	10.93	16.51	18.03	18.03	19.57	23.26	2.07
CRI_550	39.80	48.10	50.19	50.00	52.21	56.47	2.90	17.11	22.64	24.80	24.71	26.64	32.82	2.79
CRI_700	41.22	49.48	51.35	51.17	53.21	58.51	2.85	16.31	23.31	25.05	25.10	26.84	33.85	2.77
Datt1998U	29.66	34.07	35.51	35.33	36.61	40.03	1.82	11.75	16.16	17.35	17.41	18.71	22.08	1.79
PRI (Gamon)	40.31	48.20	49.96	49.85	51.63	56.13	2.57	17.14	22.99	24.70	24.61	26.31	32.19	2.55
PRI_CI	34.44	43.64	45.52	45.30	47.09	52.35	2.57	13.54	20.96	22.62	22.66	24.29	31.86	2.56
PSSR_470	43.24	50.18	51.94	51.90	53.81	58.65	2.72	17.86	24.07	25.99	25.82	27.59	33.57	2.65
PSSR_500	40.22	46.81	48.84	48.59	50.46	55.03	2.53	16.07	22.16	23.81	23.81	25.65	30.66	2.48
PSND_470	40.73	49.2	51.31	51.09	52.99	58.34	2.69	17.21	23.46	25.29	25.29	27.08	33.47	2.59
PSND_500	38.65	45.96	47.6	47.52	49.35	53.24	2.51	17.04	21.70	23.39	23.34	24.97	31.22	2.42
R470	40.96	50.4	52.26	52.12	54.05	58.90	2.65	17.27	23.70	25.55	25.51	27.27	33.93	2.59
R500	40	47.38	49.14	49.03	50.82	54.99	2.47	17.33	22.54	24.22	24.17	25.85	32.17	2.41
RARS_c	39.34	47.51	49.14	49.01	50.74	55.80	2.49	15.53	22.38	23.97	23.97	25.55	32.01	2.44
SIPI	37.36	44.65	46.5	46.36	48.18	52.60	2.60	15.19	21.39	23.04	23.10	24.96	31.65	2.68
YI	40.29	47.11	49.05	48.92	50.79	55.00	2.50	16.55	22.27	24.01	23.96	25.69	31.24	2.51

Table 2. 4: Results of the bootstrap process of the best predictive vegetation index for chlorophyll. Values are sorted for the test data set by increasing mean RMSE.

Chlorophyll vegetation index	Training data set							Test data set						
	Min	1st Qu	Median	Mean	3rd Qu	Max	SD	Min	1st Qu	Median	Mean	3rd Qu	Max	SD
Vogelman3	38.41	51.15	54.95	54.19	57.81	63.60	4.76	29.54	48.91	55.49	55.87	62.89	84.18	9.75
REP_Le1	38.77	51.78	56.46	55.35	59.37	64.40	4.94	31.59	48.37	55.10	56.27	64.60	82.43	9.80
Vogelman1	40.81	54.21	57.78	57.17	60.68	66.72	4.67	33.53	52.98	59.62	60.07	67.00	89.62	9.68
NDVI2	38.59	54.96	59.32	58.76	62.67	68.66	5.07	33.28	52.89	60.40	60.31	68.73	88.29	10.23
mND705	42.65	54.91	60.35	59.21	63.69	68.90	5.44	34.57	51.95	59.69	60.65	70.14	87.17	10.80
Carter4	45.56	56.96	61.46	60.85	64.99	71.36	5.13	34.93	55.58	63.77	63.69	72.18	87.42	10.29
Maccioni	48.22	59.94	63.98	63.33	67.18	74.52	4.97	33.44	57.63	64.79	65.09	72.93	90.97	10.08
Datt1	46.70	60.63	64.67	64.00	67.81	75.26	4.93	34.29	58.77	65.94	66.16	73.57	96.36	9.98
mREIP/IG_REP	97.89	133	142.64	141.56	151.93	167.81	13.14	34.94	60.85	70.44	69.89	78.86	99.90	12.42
OSAVI2	49.1	67.45	71.22	70.96	74.92	83.19	5.29	41.03	66.56	74.79	74.27	82.37	107.92	10.90
REIP	113.1	141.8	149.30	148.80	156.50	173.20	10.33	45.80	67.43	74.88	74.42	81.44	102.95	9.92
MTCI	40.46	61.47	66.72	65.42	70.98	78.35	7.25	38.52	62.53	72.28	75.02	82.34	131.30	16.91

Table 2. 5: Descriptive statistics of foliar pigments and nutrient concentrations over four seasons.

Foliar chemical	Statistic	Winter	Spring	Summer	Autumn
Cars	Min	55.13	55.04	55.17	55.96
	Mean	85.58	83.14	82.29	81.38
	Max	137.61	127.32	134.57	127.62
	Stdev	18.38	18.10	15.65	15.99
	COV	21.48	21.78	19.02	19.65
Chl	Min	124.81	102.81	84.24	116.92
	Mean	359.01	362.19	353.87	363.20
	Max	705.03	687.89	684.41	656.11
	Stdev	118.37	140.19	115.01	118.14
	COV	32.97	38.71	32.50	32.53
N	Min	1.47	0.69	0.57	0.55
	Mean	2.16	1.89	1.75	1.71
	Max	2.51	3.33	3.37	3.37
	Stdev	0.17	0.67	0.63	0.67
	COV	8.01	35.45	36.08	38.90
P	Min	0.05	0.05	0.03	0.04
	Mean	0.17	0.17	0.17	0.14
	Max	0.59	0.93	1.14	0.41
	Stdev	0.13	0.14	0.17	0.08
	COV	72.89	77.91	100.71	58.73

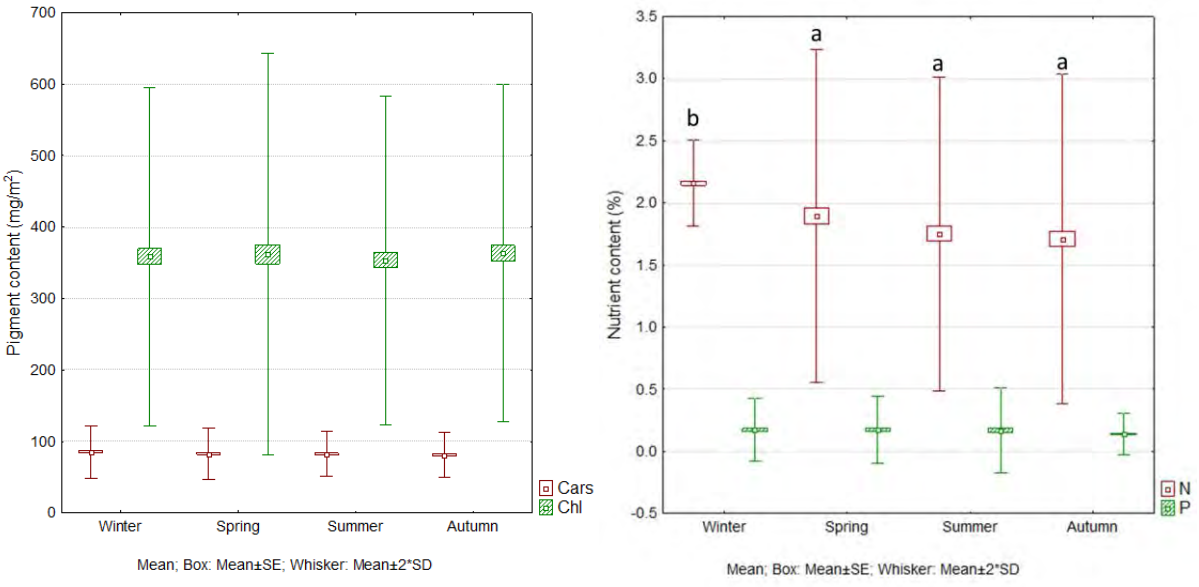

Figure 2. 2: Seasonal variation in foliar concentration per species for foliar (A) pigments and (B) nutrients. Mean foliar N was significantly ($p < 0.008$, Bonferroni corrected for six comparable seasonal pairs) higher in winter compared to spring, summer and autumn.

2.3.3. Variation of foliar pigment and nutrient across seasons per species

The average carotenoids and chlorophyll concentration increased between winter and spring for the two species AM and HT only (Table 2.6; Figure 2.4). For all other species, both carotenoids and chlorophyll decreased over the same time, except for species FSYC, which showed an increase in chlorophyll while carotenoids remained the same. Average carotenoid and chlorophyll values dropped between spring and summer for species AM, FSYC and HT; increased for SC; whereas species BG's carotenoids remained the same while its chlorophyll decreased. For species FT, the average carotenoid values increased between spring and summer while chlorophyll decreased. With the changeover from summer to autumn, average carotenoid levels remained the same for the species, except for an increase in FSYC and decrease in HT. For the same time period, average chlorophyll levels increased for all species, except HT and SC.

Average carotenoid and chlorophyll levels peaked in winter for species BG, FT and SC, while species HT had the highest average carotenoid and chlorophyll levels in spring. Average carotenoid and chlorophyll levels for species AM peaked in spring. For FSYC the average carotenoid levels peaked in winter and chlorophyll peaked in spring. Species BG showed low levels of carotenoids (maximum values for each season was lower than the average of all species) and chlorophyll (average values below the average of all species) compared to all the other species.

The average foliar nitrogen concentration showed an increase from winter to spring for species AM, FSYC and HT, whereas the other species decreased during the same period. All species showed a decrease in average foliar nitrogen concentration with the change over from spring to summer, except for BG which remained the same. The average nitrogen levels also remained the same for BG and HT from summer to autumn, while the other species showed a decrease in this period and FSYC an increase.

The average foliar nitrogen concentration peaked in winter for BG, FT and SC; in spring for AM and HT whereas values remained equally high for FSYC over spring, summer and autumn. AM, and HT showed higher than average values across all four seasons, and FSYC higher than average nitrogen values for spring, summer and autumn. BG showed lower average nitrogen levels in the spring, summer and autumn seasons compared to the average of all species.

The six species showed little variability in the average foliar phosphorus concentration across seasons, particularly BG and HT. AM decreased from summer to autumn in average foliar phosphorus concentration whereas FT and SC peaked in average phosphorus concentration in spring with a decrease from spring to summer and autumn. FSYC showed a decrease in the average phosphorus concentration from winter to spring, and increase from spring to summer and then a decrease from summer to autumn again.

Table 2. 6: Descriptive statistics for foliar biochemical of each species over four seasons.

		Carotenoids (mg/m^2)				Chlorophyll (mg/m^2)				Nitrogen (%)				Phosphorus (%)			
Species	Statistic	Winter	Spring	Summer	Autumn	Winter	Spring	Summer	Autumn	Winter	Spring	Summer	Autumn	Winter	Spring	Summer	Autumn
AM	Min	70.7	69.5	68.8	69.4	254.5	224.2	230.6	259.9	2.08	1.72	1.53	1.67	0.15	0.12	0.03	0.10
	Mean	80.2	85.0	79.1	79.0	351.7	363.7	342.3	361.8	2.29	2.52	2.36	2.23	0.33	0.31	0.32	0.21
	Max	89.8	110.9	94.8	94.2	482.1	510.4	475.2	475.3	2.50	3.33	3.37	3.28	0.59	0.93	1.14	0.41
	Stdev	5.6	10.0	7.3	6.6	60.0	75.8	67.9	64.6	0.10	0.47	0.54	0.42	0.16	0.25	0.34	0.10
	COV	6.9	11.7	9.2	8.3	17.1	20.8	19.8	17.9	4.42	18.62	23.01	18.66	47.01	79.71	107.15	47.25
BG	Min	55.1	55.0	55.2	56.0	124.8	124.3	84.2	116.9	1.91	0.69	0.57	0.55	0.05	0.05	0.06	0.05
	Mean	62.7	60.5	60.1	59.1	237.4	235.7	209.8	228.3	2.06	0.87	0.88	0.87	0.07	0.07	0.08	0.07
	Max	78.5	72.9	67.4	65.7	486.7	378.0	363.6	360.7	2.20	1.24	1.16	1.27	0.09	0.09	0.09	0.08
	Stdev	6.8	4.7	3.3	3.1	95.9	70.5	66.4	69.3	0.07	0.17	0.17	0.21	0.01	0.01	0.01	0.01
	COV	10.8	7.7	5.5	5.2	40.4	29.9	31.6	30.4	3.57	19.79	19.88	23.96	15.63	13.97	9.75	12.94
FSYC	Min	76.5	79.3	76.7	73.8	276.7	306.0	347.7	307.2	1.47	1.87	1.63	1.79	0.10	0.13	0.14	0.09
	Mean	103.8	102.8	92.8	94.5	404.6	480.0	415.2	450.1	1.97	2.31	2.25	2.34	0.22	0.16	0.20	0.16
	Max	123.6	125.2	111.3	127.6	552.0	629.5	526.8	636.1	2.29	2.73	2.68	3.37	0.55	0.23	0.30	0.32
	Stdev	16.4	12.2	9.7	16.1	90.3	89.6	52.1	100.9	0.21	0.22	0.31	0.46	0.13	0.03	0.04	0.06
	COV	15.8	11.8	10.4	17.0	22.3	18.7	12.5	22.4	10.65	9.41	13.71	19.73	58.03	21.17	19.78	38.28
FT	Min	66.8	68.1	69.7	69.9	255.2	298.9	269.5	296.7	1.98	1.40	1.23	1.13	0.05	0.11	0.08	0.07
	Mean	91.9	82.4	85.7	86.9	427.4	420.5	403.1	413.0	2.09	1.67	1.48	1.37	0.12	0.15	0.12	0.09
	Max	116.1	94.4	115.7	110.3	584.0	489.6	615.7	584.7	2.19	1.84	1.80	1.57	0.21	0.27	0.17	0.12
	Stdev	15.3	6.6	11.9	13.5	100.7	54.4	90.7	96.7	0.07	0.14	0.18	0.15	0.05	0.05	0.03	0.02
	COV	16.7	8.0	13.9	15.5	23.6	12.9	22.5	23.4	3.26	8.31	11.87	10.70	37.29	30.15	26.94	17.40
HT	Min	65.1	71.5	70.9	69.4	149.1	278.2	227.4	261.1	1.79	1.62	1.43	1.39	0.07	0.09	0.08	0.08
	Mean	93.4	95.8	92.6	89.6	422.8	464.7	439.3	434.8	2.20	2.27	2.03	2.04	0.18	0.19	0.19	0.19
	Max	137.6	127.3	134.6	123.7	705.0	687.9	684.4	656.1	2.51	3.10	2.76	3.13	0.27	0.34	0.27	0.34
	Stdev	19.1	15.1	16.8	15.5	132.5	115.1	116.5	113.8	0.18	0.37	0.30	0.45	0.05	0.06	0.05	0.06
	COV	20.4	15.8	18.1	17.3	31.3	24.8	26.5	26.2	7.99	16.22	14.97	21.91	26.84	29.61	25.73	32.47
SC	Min	71.9	58.7	73.1	66.7	183.5	102.8	217.1	208.3	1.99	0.98	0.97	0.91	0.05	0.07	0.06	0.04
	Mean	83.9	67.0	81.3	79.6	306.9	179.1	292.4	280.5	2.24	1.38	1.23	1.10	0.07	0.11	0.07	0.06
	Max	118.4	77.0	100.7	90.2	454.9	300.6	395.1	337.3	2.45	1.70	1.54	1.29	0.09	0.16	0.09	0.10
	Stdev	10.9	4.6	6.4	6.1	68.0	47.8	45.5	39.4	0.11	0.21	0.15	0.13	0.01	0.03	0.01	0.02
	COV	12.9	6.9	7.9	7.7	22.2	26.7	15.6	14.1	4.94	15.32	11.86	11.79	20.93	25.32	13.48	25.30

Abbreviations for species: AM = *Avicennia marina*; BG = *Bruguiera gymnorrhiza*; FSYC = *Ficus sycomorus*; FT = *Ficus trichopoda*; HT = *Hibiscus tilliaceus*; SC = *Syzygium cordatum.*

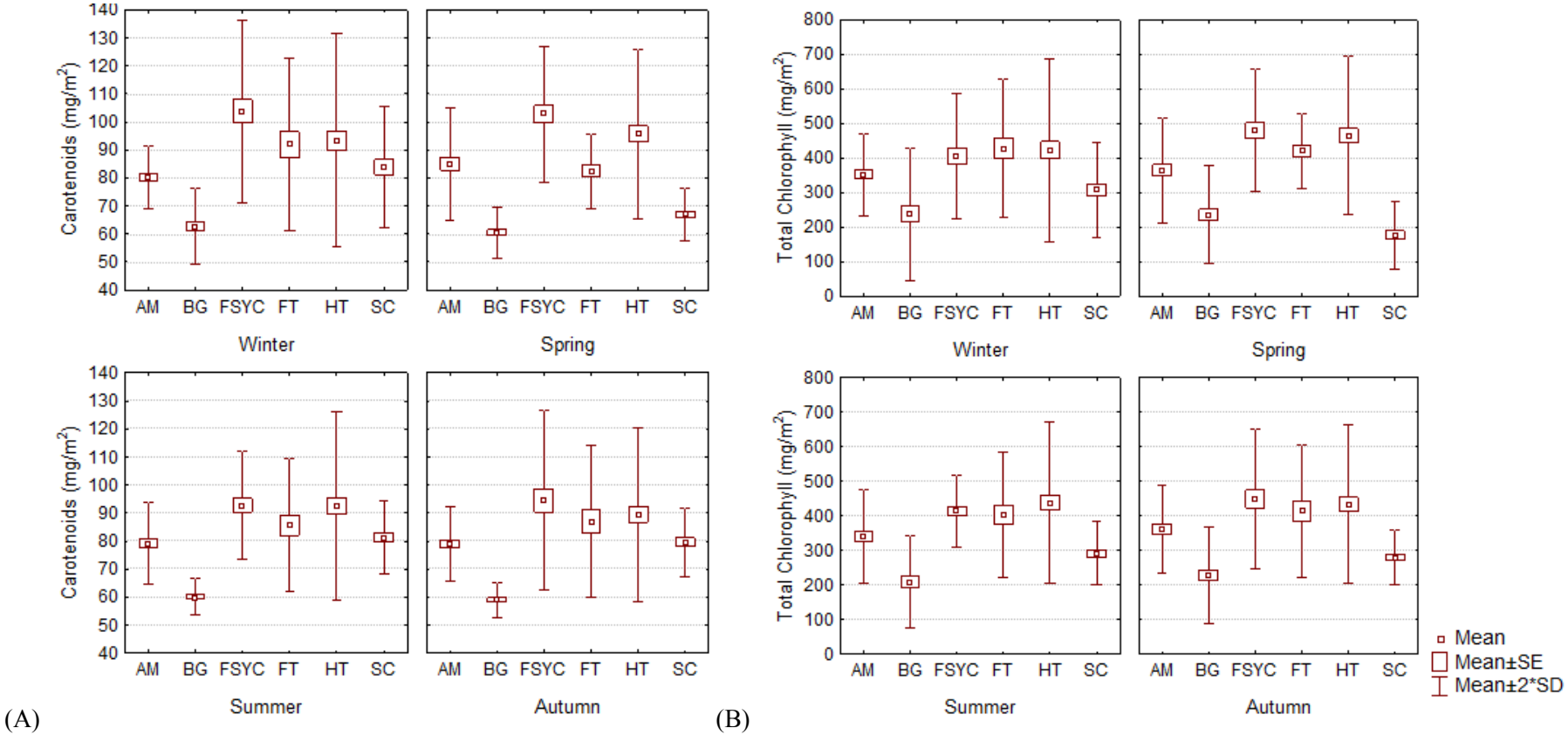
Carotenoids (mg/m2)
Total Chlorophyll (mg/m2)
AM
BG
FSYC
FT
HT
SC
Winter
Spring
Summer
Autumn
Mean
Mean±SE
Mean±2*SD

(A) (B)

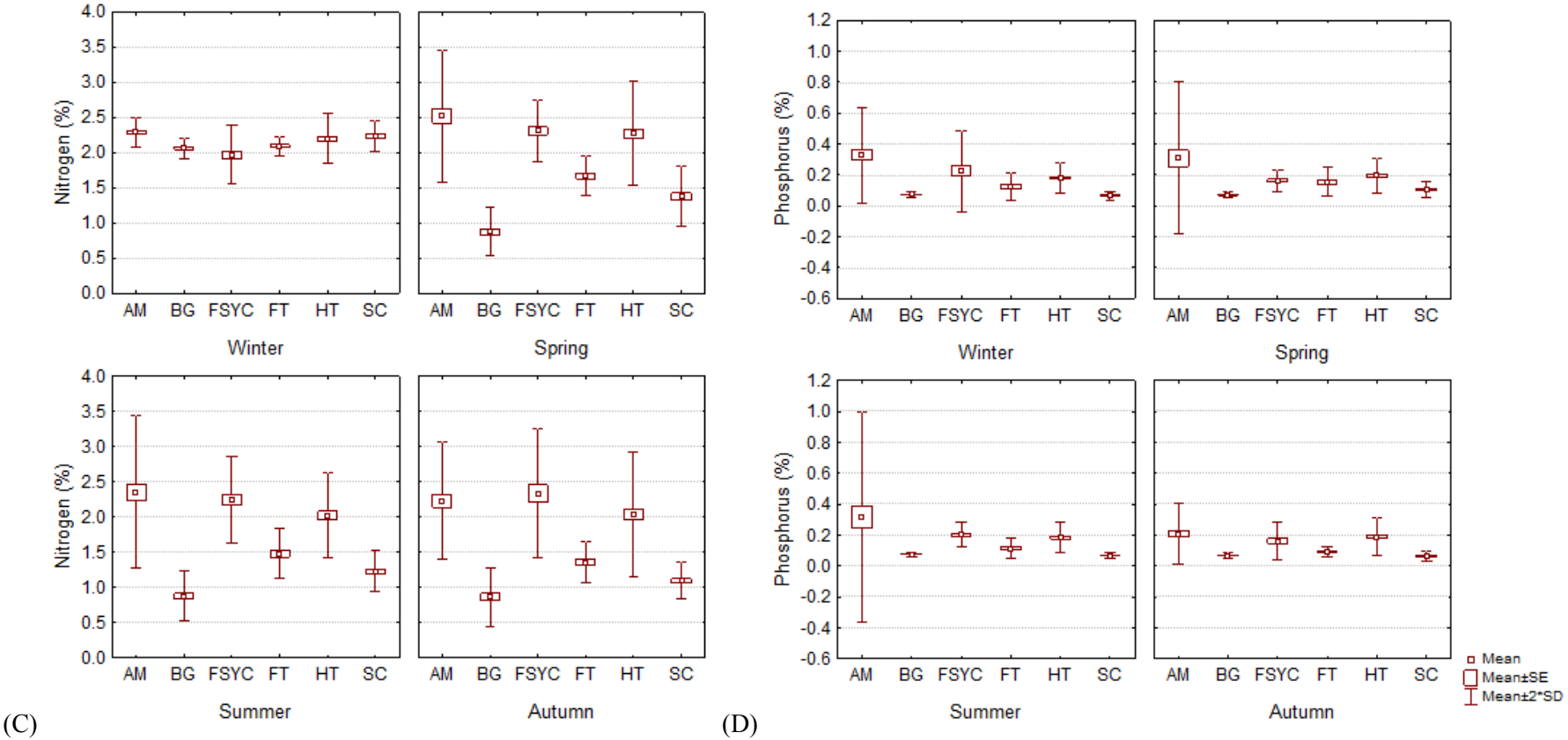

(C) (D)

Figure 2.3: Seasonal variation in foliar concentration per species for foliar (A) carotenoids, (B) chlorophyll, (C) nitrogen and (D) phosphorus.

2.3.4. Seasonal profile analysis: mean profiles, variance and similarity measures

2.3.4.1. *Mean seasonal profiles.*

Mean seasonal profiles for carotenoids and chlorophylls are visually unique seasonal profiles per species (Figure 2.4). Species BG showed a low concentration of pigments over the four seasons compared to the other species. The mean seasonal profiles of other species overlap in variance.

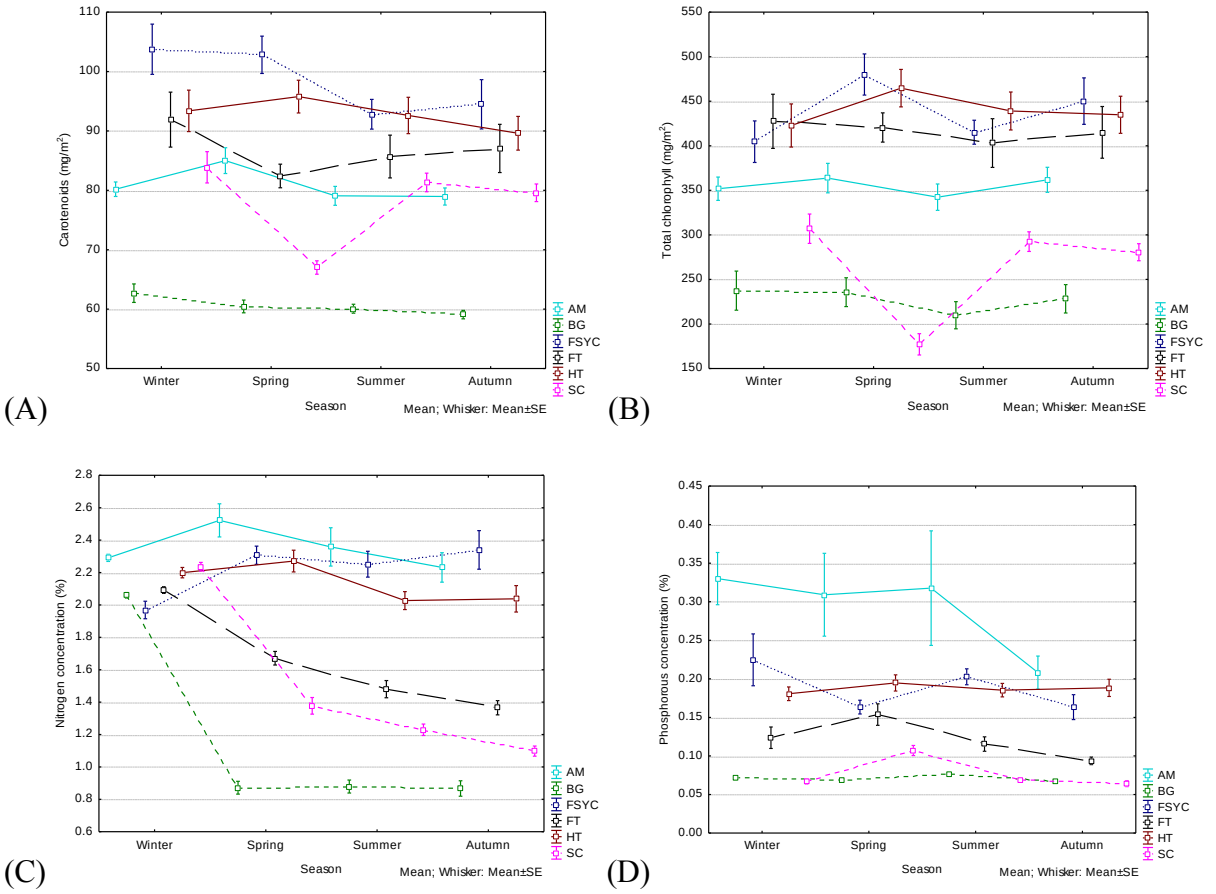

Figure 2.4: Mean seasonal profiles per species over four seasons for (A) carotenoids, (B) chlorophyll, (C) nitrogen and (D) phosphorous. Abbreviations of tree species: AM = *Avicennia marina*; BG = *Bruguiera gymnorrhiza*; FSYC = *Ficus sycomorus*; FT = *Ficus trichopoda*; HT = *Hibiscus tilliaceus*; SC = *Syzygium cordatum*.

2.3.4.2. *Intra-species variation in foliar pigments and nutrients across four seasons*

Intra-species comparisons showed that five of the six species had no significantly different variation in foliar pigments across the four seasons (Tables 2.7, 2.8 and 2.9). SC was the only species which showed significant lower foliar pigment concentration in the spring seasons compared to the winter, summer and autumn seasons. Three species (BG, FT and SC)

showed significantly higher foliar nitrogen concentration in the winter compared to the other three seasons. FT and SC also showed significantly lower nitrogen concentration in autumn compared to spring. The foliar phosphorus concentration of these two species was also significantly lower in autumn compared to spring whereas SC showed significantly high values in spring compared to the other seasons. The other four tree species showed no statistically significant differences in foliar phosphorus between seasons.

SC was therefore the only species which showed significantly variation in foliar biochemicals: lower pigments in spring, higher nitrogen concentration in winter, and low phosphorus concentration in spring. Seasonal profiles in foliar pigments and nutrients were also visible, but less distinct for BG and FT with significantly higher foliar nitrogen in winter, with FT showing additional seasonal differences in nutrients between autumn and spring.

Table 2.7: Differences in foliar pigments for each species over four seasons.

		Carotenoids			Chlorophyll		
Species	**Season**	**Winter**	**Spring**	**Summer**	**Winter**	**Spring**	**Summer**
AM	Spring	0.173			0.939		
	Summer	0.964	0.060		0.968	0.732	
	Autumn	0.952	0.054	1.000	0.963	1.000	0.785
BG	Spring	0.462			1.000		
	Summer	0.322	0.995		0.683	0.725	
	Autumn	0.092	0.804	0.914	0.983	0.991	0.879
FSYC	Spring	0.998			0.085		
	Summer	0.146	0.209		0.986	0.172	
	Autumn	0.269	0.362	0.987	0.467	0.773	0.678
FT	Spring	0.283			0.998		
	Summer	0.638	0.924		0.914	0.966	
	Autumn	0.791	0.813	0.994	0.987	0.999	0.989
HT	Spring	0.945			0.530		
	Summer	0.998	0.882		0.953	0.841	
	Autumn	0.817	0.482	0.898	0.980	0.768	0.999
SC	Spring	0.000[S]			0.000[S]		
	Summer	0.747	0.000[S]		0.847	0.000[S]	
	Autumn	0.336	0.000[S]	0.902	0.450	0.000[S]	0.907

[S] – significant, Bonferroni corrected $p = 0.008$ for 6 comparable pairs; values rounded to 3 decimals.

Table 2.8: Differences in foliar nutrients for each species over four seasons.

		Nitrogen			Phosphorus		
Species	**Season**	**Winter**	**Spring**	**Summer**	**Winter**	**Spring**	**Summer**
AM	Spring	0.284			0.991		
	Summer	0.953	0.585		0.998	0.999	
	Autumn	0.968	0.118	0.760	0.319	0.487	0.414
BG	Spring	0.000[s]			0.900		
	Summer	0.000[s]	0.999		0.316	0.082	
	Autumn	0.000[s]	1.000	0.996	0.513	0.900	0.014
FSYC	Spring	0.025			0.141		
	Summer	0.079	0.963		0.862	0.505	
	Autumn	0.011	0.992	0.871	0.141	1.000	0.505
FT	Spring	0.000[s]			0.246		
	Summer	0.000[s]	0.012		0.954	0.091	
	Autumn	0.000[s]	0.000[s]	0.225	0.246	0.003[s]	0.519
HT	Spring	0.845			0.748		
	Summer	0.204	0.031		0.987	0.909	
	Autumn	0.257	0.043	0.999	0.947	0.969	0.996
SC	Spring	0.000[s]			0.000[s]		
	Summer	0.000[s]	0.033		0.992	0.000[s]	
	Autumn	0.000[s]	0.000[s]	0.070	0.963	0.000[s]	0.869

[s] – significant, Bonferroni corrected $p = 0.008$ for 6 comparable pairs; values rounded to 3 decimals.

Table 2.9: The percentage of seasons (of four) where a species show statistically significant differences ($p < 0.008$ Bonferroni corrected for 6 comparable pairs) in the foliar biochemical concentrations of six tree species.

Season	Carotenoids	Chlorophyll	Nitrogen	Phosphorous
AM	0	0	0	0
BG	0	0	50	0
FSYC	0	0	0	0
FT	0	0	67	17
HT	0	0	0	0
SC	50	50	67	50

2.3.4.3. *Inter-species differences per foliar pigment and nutrient for each single season and multi-season data set*

The inter-species comparisons (Tables 2.10, 2.11, 2.12 and 2.13) showed that species are mostly separable in spring (> 67 % of all 15 comparable pairs) using foliar carotenoids, chlorophyll and nitrogen (Table 2.14). Winter showed the lowest separability of all four seasons of < 53 %. Most species were separable (maximum of 73 %) using nitrogen in spring. Foliar nitrogen showed the highest percentage of separability (> 60 %) of all four foliar biochemicals in the spring, summer and autumn seasons (others < 67 %). The pigments

showed poor separability in winter, summer and spring (< 50 %), whereas phosphorus showed relative separability in winter and autumn (53 %).

Table 2.10: Differences between species for foliar carotenoids over four seasons.

Season	Species	AM	BG	FSYC	FT	HT
Winter	BG	0.001				
	FSYC	0.000[S]	0.000[S]			
	FT	0.203	0.000[S]	0.255		
	HT	0.012	0.000[S]	0.166	1.000	
	SC	0.962	0.000[S]	0.001	0.655	0.208
Spring	BG	0.000[S]				
	FSYC	0.000[S]	0.000[S]			
	FT	0.986	0.000[S]	0.000[S]		
	HT	0.006	0.000[S]	0.287	0.006	
	SC	0.000[S]	0.428	0.000[S]	0.003[S]	0.000[S]
Summer	BG	0.000[S]				
	FSYC	0.004	0.000[S]			
	FT	0.585	0.000[S]	0.575		
	HT	0.000[S]	0.000[S]	1.000	0.475	
	SC	0.988	0.000[S]	0.043	0.907	0.012
Autumn	BG	0.000[S]				
	FSYC	0.002[S]	0.000[S]			
	FT	0.411	0.000[S]	0.579		
	HT	0.018	0.000[S]	0.758	0.988	
	SC	1.000	0.000[S]	0.005	0.546	0.053
Multi-season	BG	0.000[S]				
	FSYC	0.000[S]	0.000[S]			
	FT	0.086	0.000[S]	0.000[S]		
	HT	0.000[S]	0.000[S]	0.039	0.050	
	SC	0.694	0.000[S]	0.000[S]	0.002[S]	0.000[S]

[S] – significant, Bonferroni corrected p = 0.003 for 15 comparable pairs; values rounded to 3 decimals.

Table 2.11: Differences between species for foliar chlorophyll over four seasons.

Season	Species	AM	BG	FSYC	FT	HT
Winter	BG	0.005				
	FSYC	0.608	0.000[S]			
	FT	0.313	0.000[S]	0.992		
	HT	0.123	0.000[S]	0.992	1.000	
	SC	0.728	0.288	0.065	0.024	0.002[S]
Spring	BG	0.000[S]				
	FSYC	0.001[S]	0.000[S]			
	FT	0.470	0.000[S]	0.491		
	HT	0.001[S]	0.000[S]	0.993	0.679	
	SC	0.000[S]	0.312	0.000[S]	0.000[S]	0.000[S]
Summer	BG	0.000[S]				
	FSYC	0.099	0.000[S]			

	FT	0.353	0.000[s]	0.999		
	HT	0.001[s]	0.000[s]	0.940	0.814	
	SC	0.429	0.036	0.001[s]	0.009	0.000[s]
Autumn	BG	0.000[s]				
	FSYC	0.037	0.000[s]			
	FT	0.569	0.000[s]	0.911		
	HT	0.043	0.000[s]	0.993	0.987	
	SC	0.054	0.468	0.000[s]	0.002[s]	0.000[s]
Multi-season	BG	0.000[s]				
	FSYC	0.000[s]	0.000[s]			
	FT	0.004	0.000[s]	0.849		
	HT	0.000[s]	0.000[s]	1.000	0.663	
	SC	0.000[s]	0.149	0.000[s]	0.000[s]	0.000[s]

[s] – significant, Bonferroni corrected $p = 0.003$ for 15 comparable pairs; values rounded to 3 decimals.

Table 2.12: Differences between species for foliar nitrogen over four seasons.

Season	Species	AM	BG	FSYC	FT	HT
Winter	BG	0.000[s]				
	FSYC	0.000[s]	0.409			
	FT	0.003[s]	0.990	0.229		
	HT	0.195	0.011	0.000[s]	0.249	
	SC	0.832	0.003[s]	0.000[s]	0.086	0.951
Spring	BG	0.000[s]				
	FSYC	0.328	0.000[s]			
	FT	0.000[s]	0.000[s]	0.000[s]		
	HT	0.061	0.000[s]	0.999	0.000[s]	
	SC	0.000[s]	0.000[s]	0.000[s]	0.155	0.000[s]
Summer	BG	0.000[s]				
	FSYC	0.923	0.000[s]			
	FT	0.000[s]	0.000[s]	0.000[s]		
	HT	0.006	0.000[s]	0.243	0.000[s]	
	SC	0.000[s]	0.018	0.000[s]	0.343	0.000[s]
Autumn	BG	0.000[s]				
	FSYC	0.946	0.000[s]			
	FT	0.000[s]	0.004	0.000[s]		
	HT	0.397	0.000[s]	0.086	0.000[s]	
	SC	0.000[s]	0.380	0.000[s]	0.378	0.000[s]
Multi-season	BG	0.000[s]				
	FSYC	0.403	0.000[s]			
	FT	0.000[s]	0.000[s]	0.000[s]		
	HT	0.004	0.000[s]	0.807	0.000[s]	
	SC	0.000[s]	0.000[s]	0.000[s]	0.305	0.000[s]

[s] – significant, Bonferroni corrected $p = 0.003$ for 15 comparable pairs; values rounded to 3 decimals.

Table 2.13: Differences between species for foliar phosphorous over four seasons and for multiple seasons.

Season	Species	AM	BG	FSYC	FT	HT
Winter	BG	0.000[S]				
	FSYC	0.007	0.000[S]			
	FT	0.000[S]	0.617	0.048		
	HT	0.000[S]	0.001[S]	0.604	0.436	
	SC	0.000[S]	1.000	0.000[S]	0.550	0.001[S]
Spring	BG	0.000[S]				
	FSYC	0.003[S]	0.162			
	FT	0.004	0.367	1.000		
	HT	0.007	0.003[S]	0.951	0.906	
	SC	0.000[S]	0.918	0.722	0.893	0.117
Summer	BG	0.000[S]				
	FSYC	0.219	0.157			
	FT	0.006	0.984	0.689		
	HT	0.030	0.145	0.999	0.774	
	SC	0.000[S]	1.000	0.129	0.967	0.118
Autumn	BG	0.000[S]				
	FSYC	0.216	0.000[S]			
	FT	0.000[S]	0.842	0.038		
	HT	0.841	0.000[S]	0.754	0.000[S]	
	SC	0.000[S]	1.000	0.000[S]	0.781	0.000[S]
Multi-season	BG	0.000[S]				
	FSYC	0.000[S]	0.000[S]			
	FT	0.000[S]	0.142	0.024		
	HT	0.000[S]	0.000[S]	1.000	0.008	
	SC	0.000[S]	1.000	0.000[S]	0.270	0.000[S]

[S] – significant, Bonferroni corrected $p = 0.003$ for 15 comparable pairs; values rounded to 3 decimals.

When aggregating the data of all four seasons into a single multi-season data set, the percentage of significantly different comparable pairs were highest for carotenoids and nitrogen (73 %), followed by chlorophyll (67 %) and phosphorus (60 %) (Table 2.14).

Table 2.14: Percentage of comparable pairs that are significantly different ($p < 0.003$ Bonferroni corrected for 15 comparable pairs) between the foliar chemical concentrations of six tree species across the single and multi-season data.

Season	Carotenoids	Chlorophyll	Nitrogen	Phosphorous
Winter	33	27	40	53
Spring	67	67	73	27
Summer	40	47	67	13
Autumn	40	47	60	53
Multi-season	73	67	73	60

2.4. Discussion

Seasonal variation in foliar biochemicals of evergreen wetland trees in subtropical regions is not well understood. This study assessed the seasonal variation of foliar carotenoids, chlorophyll, nitrogen and phosphorous across four seasons (winter, spring, summer and autumn) for six evergreen wetland tree species in the iSimangaliso Wetland Park of South Africa. This is the first study reporting seasonal variation in foliar pigments and nutrients for evergreen trees of South Africa.

In general, foliar carotenoids and chlorophyll showed no significant variation across the four seasons. Our results are supported by other studies on evergreen tree species where no significant changes in the mean pigment concentrations were observed over seasons (Lewandowska and Jarvis, 1977; Cai *et al.*, 2009; Flores-de-Santiago *et al.*, 2012). Statistically significant differences in mean foliar pigment concentrations were however reported for evergreen tree species in Northeastern Mexico (Sauceda *et al.*, 2008). The mean foliar nitrogen varied across seasons with a significantly higher mean foliar N concentration (% of dry weight) in winter compared to the spring, summer and autumn seasons. Foliar N was also highest in the winter for evergreen eucalypts in Australia, a mangrove species in China and oak in Spain and Japan (Bell and Ward, 1984; Sabaté *et al.*, 1995; Lin *et al.*, 2010; Yasamura and Ishida, 2011). In evergreen trees, leaves serve as storage of foliar N during winter from where foliar N is translocated to new growth during the spring season (Sabaté *et al.*, 1995; Yasamura and Ishida, 2011). Statistically significant differences between foliar P between four seasons (autumn, winter, spring and summer) were reported for the mangrove species of China (Lin *et al.*, 2010), although no significant changes in mean foliar P were reported for the eucalypts over a five month period between August and December from 1981-2, as well as evergreen tropical trees in Nigeria (Sharma, 1983; Bell and Ward, 1984). Our results showed no significant changes in mean foliar P across the four seasons, but the variability increased in summer and decreased in autumn. A decrease in both mean foliar N and P was noted for evergreen eucalypts, acacias and pine trees in Australia decreased from summer to winter (Fife *et al.*, 2008). Our study was limited to six species and four seasons in a subtropical forest of South Africa. Further research can contribute to assess whether the seasonal trends observed persist for other evergreen tree species in other climatic regions.

Although tree species varied in foliar pigments and nutrients over seasons, few showed significant changes across seasons. Five of the six wetland tree species showed no significant variation in foliar pigments and three of the six species no significant variation in foliar nutrients across the four seasons. The water berry (*Syzygium cordatum*) was the only species which showed significant variation across seasons for all four foliar biochemicals, with significantly lower mean pigments in spring, higher mean foliar N in winter, and low mean foliar P in spring. Other species with significant variation in foliar nitrogen was the black mangrove (*Bruguiera gymnorrhiza*) and the swamp fig (*Ficus trichopoda*). The evergreen

wetland tree species from this subtropical forest was therefore mostly similar in seasonal variation of foliar carotenoid, chlorophyll, nitrogen and phosphorus concentration. Differences in the seasonal variation of foliar biochemicals have also been reported for evergreen trees elsewhere (Sharma, 1983; Lu *et al.*, 2007; Cai *et al.*, 2009).

The separability between the six wetland tree species was highest for foliar nitrogen across the spring, summer and autumn seasons (≥ 60 % of the comparable pairs were separable). Foliar carotenoids and chlorophyll were also able to separate between species during the spring season (67 % of the comparable pairs were separable). Of all the foliar biochemicals, foliar phosphorus showed the lowest capability to discriminate between the species across the four seasons. The spring season showed the highest number of statistically significant differences between species (≥ 67 % comparable pairs were separable) for foliar pigments and nitrogen. Foliar pigments showed a low separability (< 47 % of the comparable pairs were separable), however in winter, summer and autumn. Using multiple season for species discrimination, foliar carotenoids and nitrogen showed the highest number of significant different comparable pairs (73 %), followed by chlorophyll (67 %) and phosphorus (60 %). Foliar nitrogen concentrations from the spring seasons are therefore expected to yield the highest classification results for species discrimination between these six evergreen tree species. In addition, the increasing separability of species with multiple seasons foliar carotenoid concentration, may offer additional increased separability between the evergreen tree species.

2.5. Conclusion

The influence of phenology on tree species classification has thus far been limited. This study assessed how the variation of plant properties across four seasons influenced the classification of six evergreen tree species for a subtropical region in the KwaZulu-Natal Province of South Africa. Most of the species showed no distinct variation in foliar carotenoids, chlorophyll, nitrogen and phosphorus across the four seasons, except for the water berry. Of the four foliar biochemicals, nitrogen concentration resulted in the highest number of significant different inter-species pairs across the spring, summer and autumn seasons. The aggregation of the four season's data into a single multi-season data set increased the separability between species for carotenoids and phosphorus.

The results emphasized the importance of foliar nitrogen concentration for the discrimination of six evergreen tree species in the iSimangaliso Wetland Park of South Africa. At a spectral level, however, foliar nitrogen is associated with a multitude of narrow absorption regions in hyperspectral data. The most important absorption features in leaf spectra that relate to nitrogen across the four seasons remains to be identified in order to assess the separability of the six evergreen wetland trees. In addition the statistically significant differences noted for foliar nitrogen concentration across seasons may indicate

that the relationship between leaf spectra and foliar nitrogen could also differ between seasons.

CHAPTER 3: REMOTE SENSING MODELS FOR PREDICTING LEAF NITROGEN AND PHOSPHOROUS ACROSS FOUR SEASONS FOR SIX SUBTROPICAL FOREST EVERGREEN TREE SPECIES

This chapter is based on the journal publication:

Van Deventer, H, Cho, MA, Mutanga, O & Ramoelo, A. 2015. Capability of models to predict leaf N and P across four seasons for six subtropical forest evergreen trees. ISPRS Journal of Photogrammetry and Remote Sensing, 101: 209-220.

Abstract

Nutrient phenology of evergreen subtropical forests of southern Africa is poorly understood. Foliar nitrogen (N) and phosphorous (P) forms key components of photosynthesis and are vulnerable to global change stressors. Remote sensing techniques can potentially map and monitor nutrient phenology, yet models to predict foliar nutrients across species, seasons and climatic regions are deficient. This study evaluated the capability of various models, developed from leaf spectra of selected spectral regions and seasons, to predict leaf nutrient concentration across seasons and species. Seasonal differences in foliar N and P were assessed using a one-way ANalysis Of VAriance (ANOVA). The relationship between leaf spectra and nutrients was assessed using linear regression between the foliar nutrients and spectral indices. The predictive capability of three models was compared using root mean square error (RMSE) values. Amongst the four seasons, winter leaves showed the highest mean N (2.16 %, $p < 0.01$). However, winter showed the lowest variability of foliar N (coefficient of variation = 8 %) compared to the variability of the other three seasons (coefficient of variance > 35 %). In fact, between winter and spring, the variability in foliar N increased by 294 %. Foliar P did not significantly differ between the four seasons. Predictive models for leaf N concentration developed for each season showed a higher level of accuracy compared to predictive models from across seasons, whereas predictive models for leaf P showed low accuracies. Models developed from a single season showed a slight increase in error for the summer and autumn, however a larger increase in error for the winter season for the evergreen trees. The results suggest that spectral measurements can potentially be used to quantify nutrient phenology at regional scale and monitor the impacts of global change on nutrient phenology and photosynthesis.

3.1. Introduction

Global change has shown significant impacts on the periodic behaviour of plants or phenology since the 1970s (Richardson *et al.*, 2013). Most noticeably, the onset and duration of the active growth season has been affected across climatic zones, but the impact on the autumnal season is not well established (Zhou *et al.*, 2003; Richardson *et al.*, 2013). Several authors have argued that global increase in carbon dioxide and temperature may speed up the rates of photosynthesis and respiration in vegetation, although the increased rates are dependent on water and nutrient availability (Evans, 1989; Penuelas *et al.*, 1995; Drake and Gonzalez-Meler, 1997; Kirschbaum, 2000). Predicting the impact of global change on these processes remains difficult, owing to the limitations of simulating regional scale ecosystem responses either in laboratories or *in situ*, particularly for forests (Seppälä *et al.*, 2009; Lukac *et al.*, 2010; Millard and Grelet, 2010; Booth *et al.*, 2012; United States Department of Energy (US DOE), 2012; FAO and JRC, 2012; Sardans and Peñuelas, 2012; Richardson *et al.*, 2013). It is, however, generally recognised that global change is causing changes to vegetation physiology, condition, composition and distribution, and therefore to vegetation phenology, at local to regional scales (Campoy *et al.*, 2011; Sardans and Peñuelas, 2012). Phenological expression is however unique to species and climate regions, therefore, to address uncertainties in vegetation response to global change, our understanding of the unique phenology of vegetation types needs to be improved (Reich and Oleksyn, 2004; Lukac *et al.*, 2010; Richardson *et al.*, 2013).

Tropical and subtropical forests are considered to be some of the most vulnerable systems to global warming because of their exposure to multiple stressors (Seppälä *et al.*, 2009). Tropical forests are nutrient poor (Reef *et al.*, 2010) and with limited availability of phosphorus (Jordan, 1985), hence may have limitations in adapting to increased temperatures and photosynthesis. In addition, humid subtropical forest areas are highly fragmented and have been extensively converted into commercial plantations (Seppälä *et al.*, 2009). Their resilience and adaptive capacity to global change is therefore considered reduced (Seppälä *et al.*, 2009). Despite the sensitivity of these forests to global change, seasonal variation of leaf chemicals and translocation in evergreen tropical forests are not well understood and often highly simplified in global ecosystem models (De Weirdt *et al.*, 2012). Furthermore, global change impacts on tropical and subtropical forests vary greatly from regional to continental scales (United States Department of Energy (US DOE), 2012).A systematic approach to monitor global changes in a comparable way at regional scale is deficient.

Monitoring foliar nutrients in tropical and subtropical forests using traditional methods of leaf harvesting and transportation to laboratories for analysis implies a number of difficulties. These forests are sometimes inaccessible, because of dense overgrowth or

located in swamp wetlands (United States Department of Energy (US DOE), 2012). Laboratories are often not close enough to the collection site which risks the loss of nutrients from leaves during the transportation period. The cost of human resources and laboratory analysis for a high number of foliar chemicals and repetitive time periods can increase beyond affordability. More cost-effective methods would be required to monitor global change impacts at the physiological leaf level and at the regional scale in the long term. Remote sensing, using air- or spaceborne imagery has been utilised as a cheaper alternative for assessing foliar nutrients of forest canopies at the broad landscape scale. Furthermore, spaceborne sensors offer continuous repetitive coverage of areas across the globe and are ideal for monitoring nutrients across a number of ecosystems. Various regions of the leaf or canopy electromagnetic spectrum have been associated with leaf water, pigments, nutrients and leaf biomass absorption or scattering of electromagnetic energy (Curran, 1989) (Figure 9). High spectral (hyperspectral) resolution sensors on airborne and spaceborne platforms have enabled the mapping of foliar nutrients since the late 1990s (Smith *et al.*, 2002; Townsend *et al.*, 2003; Huang *et al.*, 2004; Mutanga and Kumar, 2007; Huber *et al.*, 2008; Kokaly *et al.*, 2009; Schlerf *et al.*, 2010; Skidmore *et al.*, 2010; Knox *et al.*, 2011). However, the high cost of hyperspectral sensors has restricted their routine utilisation for forest nutrient analysis. New spaceborne multispectral sensors such as WorldView-2 and RapidEye with fewer bands adapted for foliar pigment assessment also offer promise for assessing canopy nutrients such as leaf N. These multispectral sensors have proved successful in mapping foliar nutrients at regional scale (Ramoelo *et al.*, 2012; Ullah *et al.*, 2012; Clevers and Gitelson, 2013; Ramoelo *et al.*, 2013; Cho *et al.*, 2013).

The successful employment of remote sensing in monitoring the impact of global change across phenologically-unique climate regions requires; (a) the ability to detect and characterise the unique patterns of nutrient phenology of various climate regions and (b) capable models that can be used to predict nutrients across species, seasons and regions. Regardless of the advances made in mapping foliar nutrients with remote sensing at small scales, a few challenges remain. First, the relationship between foliar nutrient concentration and spectral reflectance across species, season and ecosystems remains poorly understood. Foliar nutrients are known to vary over seasons, yet it is not well established how the empirical relationship between foliar nutrients and spectral information reflects seasonal variation. Variations in foliar nitrogen, chlorophyll and carotenoids were positively related to seasonal variation of the photochemical reflectance index (PRI) for deciduous Japanese larch over two seasons in Japan (Nakaji *et al.*, 2006). The relationship between foliar chlorophyll *a* and leaf spectral vegetation indices varied between the wet and dry season for evergreen mangrove tree species in Mexico (Flores-de-Santiago *et al.*, 2013). Similarly, a changing relationship between foliar nitrogen and leaf reflectance in the red-edge was also found to vary with carboxylation rates for two deciduous species in the growth season of the United States of America (Dillen *et al.*, 2012). In Canada, the relationship between chlorophyll predicted from vegetation indices and observed chlorophyll for deciduous maple leaves

varied over the spring, summer and autumn seasons (Zhang *et al.*, 2007). The relationship between foliar nutrient and leaf spectral data across different seasons has therefore not been well established for evergreen trees or subtropical forests. Secondly, models for predicting nitrogen and phosphorus remain difficult as they co-vary with related biochemical and biophysical parameters such as chlorophyll, leaf structure, foliage biomass and leaf water content (Elvidge, 1990; Yoder and Pettigrew-Crosby, 1995). The relationship between the nutrients and co-varying parameters are however known to change over seasons and time (Yoder and Pettigrew-Crosby, 1995; Zhang *et al.*, 2007). The chlorophyll red-edge position, for example, has often been used as a reliable co-variant in the mapping of nitrogen (Cho and Skidmore, 2006; Mutanga and Skidmore, 2007; Ramoelo *et al.*, 2012), yet if the varying relationship between chlorophyll and nitrogen across seasons is poorly understood, the mapping and monitoring of nutrient phenology will potentially be erroneous. The ability to use the Near Infrared (NIR) and Shortwave Infrared (SWIR) bands to decouple nutrients from other co-variants across seasons, remains to be tested. A changing relationship between chlorophyll content estimated from leaf spectra and foliar chlorophyll content, for example, was observed for the maple species in Canada, where the relationship was highest in the spring season for the maple species in Canada, but decreased in correlation and accuracy towards summer and autumn (Zhang *et al.*, 2007). The ability of nutrient models developed from single-season data to predict across phenological phases should be evaluated in model development. Currently, models to predict nutrients across species, seasons and climatic zones are deficient (Ferwerda *et al.*, 2005; Ollinger *et al.*, 2008; Knyazikhin *et al.*, 2012; Ollinger *et al.*, 2013).

This study compared the capability of predictive nutrient models, developed from single-season and multiple-seasons leaf spectra, to predict nutrient concentration across seasons and species. Six evergreen tree species, in a subtropical environment in South Africa, were sampled over four seasons (winter, spring, summer and autumn) to assess how the nutrient-spectral relationship changes over seasons. Thereafter, predictive models were developed using the linear regression between leaf spectra and nutrient concentration of the season with the highest coefficient of determination (R^2) as well as those of a combined-seasons data set, and compared to the predictive model of each individual season, to assess the capability of the various models to predict nutrients across the seasons.

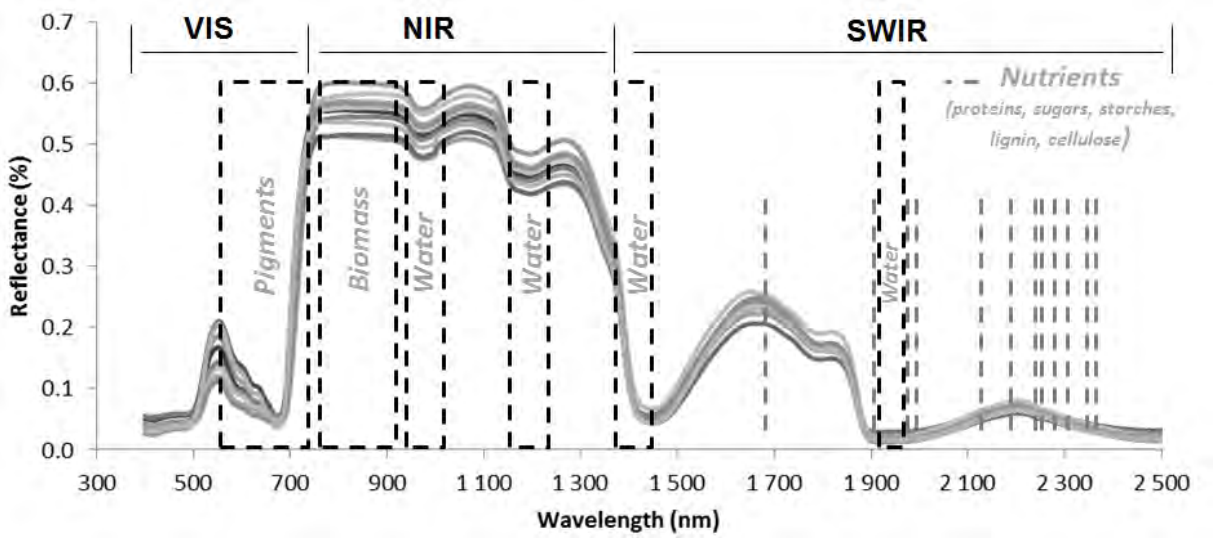

Figure 3.1: Regions of the electromagnetic spectrum known to relate to leaf pigments, foliage biomass, leaf water content, proteins, starches and structural components of leaf reflectance data.

3.2. Methods

3.2.1. Study area

The iSimangaliso Wetland Park (28°S, 32°30'E) is located on the east coast of the KwaZulu-Natal province in South Africa. The area has a humid sub-tropical climate with strong seasonal variation in rainfall and temperature (Figure 3.2). Mean Annual Precipitation (MAP) ranges between 1 000 – 1 500 mm (Middleton and Bailey, 2008) and the mean temperatures in summer ranges from 23 – 30°C, with winter temperatures decreasing to approximately 10°C (Sokolic, 2006). The Park is situated on a coastal plain (Partridge *et al.*, 2010) with sandy undulating hills between 10 m to 20 m above mean sea level (a.m.s.l.). The vegetation types include wooded grassland, dune vegetation and dune forests, to swamp forests and critically endangered mangrove forests (Mucina and Rutherford, 2006). A number of evergreen tree species are found in the St. Lucia and Maphelane nodes of the iSimangaliso Wetland Park (Table 3.2; Figure 3.3).

Table 3.1: Number of trees sampled per species and season in St. Lucia, KwaZulu-Natal, South Africa.

Tree species	Common name	Trees Winter (*n*)	Trees Spring (*n*)	Trees Summer (*n*)	Trees Autumn (*n*)	Total number of trees per species (*n*)
Avicennia marina	White mangrove	21	21	21	21	84
Bruguiera gymnorrhiza	Black mangrove	19	19	19	19	76
Ficus sycomorus	Sycamore fig	15	15	15	15	60
Ficus trichopoda	Swamp fig	11	11	11	11	44
Hibiscus tilliaceus	Lagoon hibiscus	30	30	30	30	120
Syzygium cordatum	Waterberry	17	17	17	17	68
Total per season:		113	113	113	113	***452***

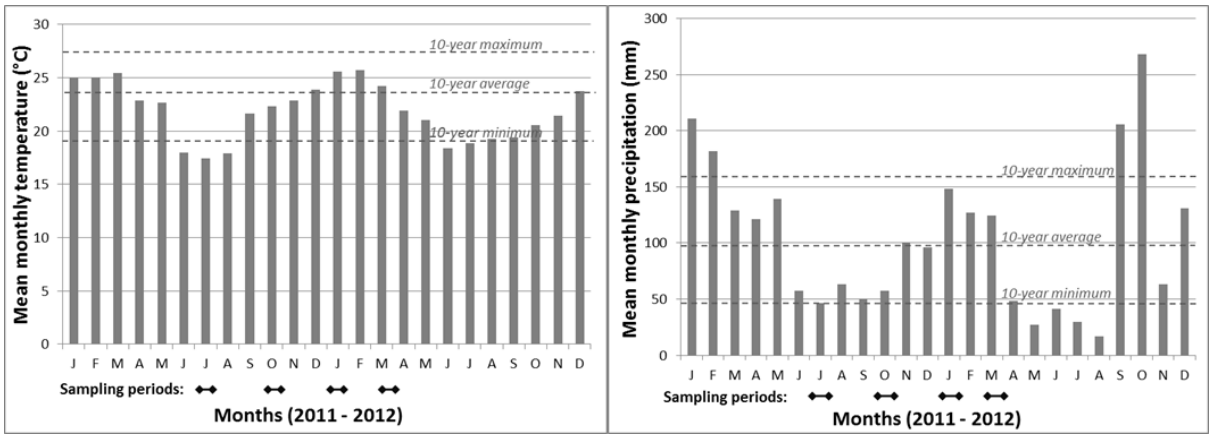

Figure 3.2: Mean monthly temperature and rainfall between January 2011 and December 2012 for the St. Lucia study area, KwaZulu-Natal, South Africa (Harris *et al.*, 2013).

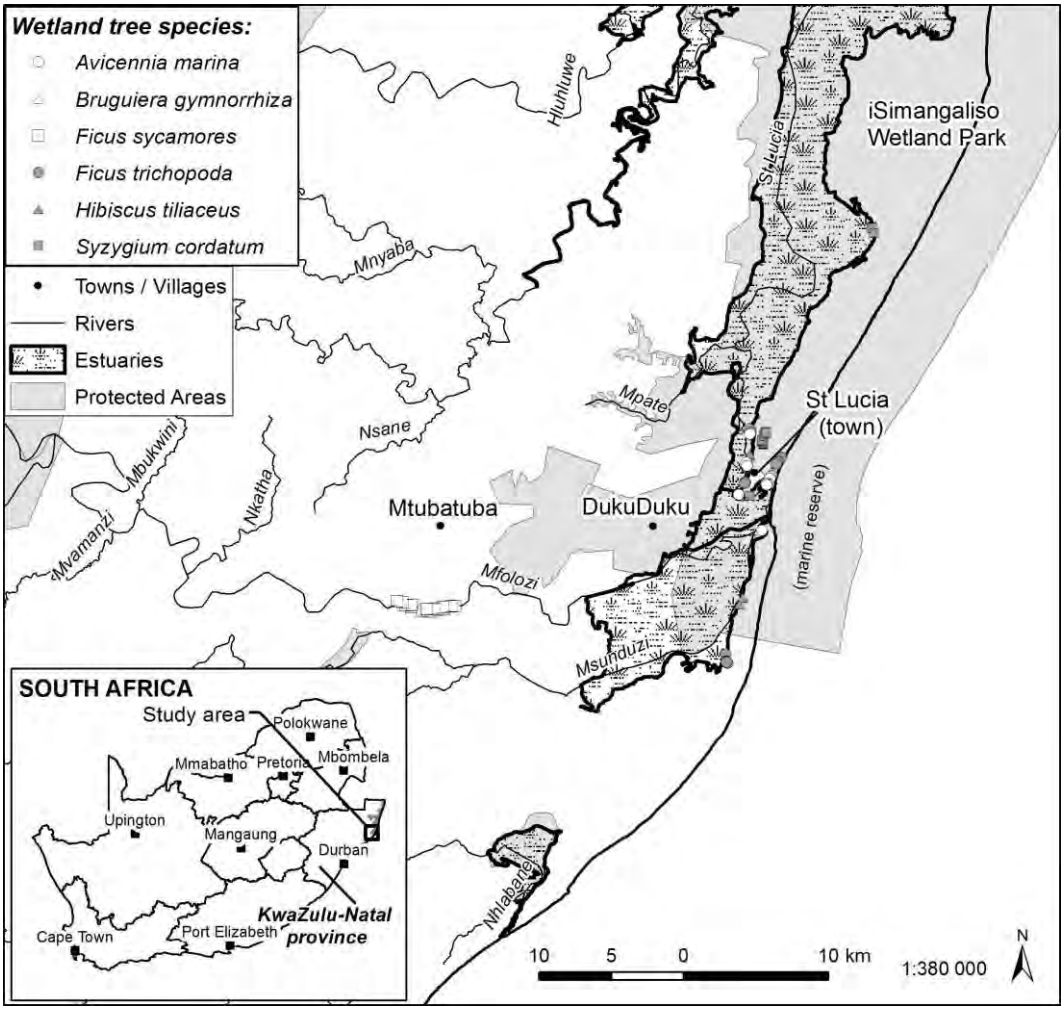

Figure 3.3: The St. Lucia study area is located northeast of the city of Durban in the KwaZulu-Natal Province of South Africa. Six wetland and estuarine tree species were sampled in the study area along the uMfolozi River, as well as the St. Lucia, uMfolozi and uMsunduzi estuaries.

3.2.2. Leaf sampling, spectral measurements and laboratory analysis of foliar N and P

Field campaigns were conducted for four seasons (winter, spring, summer and autumn) across 2011 and 2012. Sample sites were selected along wetlands and estuaries where tree canopies were accessible, mature and sun exposed. Five sunlit leaves were randomly sampled across the canopy of each tree (*n* trees = 452, Table 3.2). Leaf spectral reflectance measurements of the adaxial surface of each leaf were made using the Analytical Spectral Device (ASD) plant probe accessory connected to an ASD spectroradiometer (FieldSpec Pro FR, Analytical Spectral Device, Inc, USA), with the average scan time set at 10. The ASD covers the spectral range between 350 and 2500 nm with a 1.4 nm sampling interval between 350 and 1050 nm range, and ±2 nm between 1050 and 2500 nm. The plant probe provides a direct-contact probe which limits ambient light. The radiance measurements were converted to reflectance against scans of a white spectralon reference panel. The five leaf specimens per tree were combined for nutrient analysis (N and P). The leaves were oven-dried at 65°C until constant weight was reached. Bemlab Pty Ltd analysed nitrogen concentration using a Leco FP528 nitrogen analyser (Horneck and Miller, 1998) and phosphorus through Inductively Coupled Plasma Optical Emission Spectrometry (ICP-OES) analysis (Isaac and Johnson, 1998).

3.2.3. Data analysis

Differences in leaf N or P concentration between seasons were assessed using one-way ANalysis Of VAriance (ANOVA). The alpha levels were corrected for Bonferroni effects to decrease the likelihood of committing type 1 error as a result of multiple comparable pairs (McDonald, 2008). The adjustment is made to ensure that the alpha level ($p = 0.05$) is not merely a reflection of the differences between the dependent (nutrient concentrations) and independent variables (combined seasons), but adjusted downwards to assess the differences between each combination of individual seasons. The comparison of four seasons to one another results in six comparable pairs and therefore the alpha level ($p < 0.05$) is adjusted by dividing 0.05 by the six comparable pairs = $p < 0.01$. Thereafter, the linear relationship between foliar nutrients and leaf spectral reflectance was assessed using a spectral vegetation index (VI), based on the normalised difference vegetation index (NDVI). NDVI is one of the most commonly used vegetation indices where two bands are combined and normalized through their difference (Rouse *et al.*, 1973; Tucker, 1979). One band is traditionally located at the absorption feature of the vegetation parameter in question and the other band is used to normalize the absorption band. VI values were computed for all possible band combinations (Cho *et al.*, 2009) (Eq. 1). First, the 1 nm spectral reflectance ASD data were resampled using a Gaussian model (full-width half-maximum equal to every 10 nm band spacing between 400 and 2 500 nm) in the Environment for Visualizing Images

(ENVI) software (v.4.8, ITT Visual Information Systems, 2012-2014) to reduce complexity and redundancy in the data. Subsequently, the 10 nm data were used to compute VIs for all possible band combinations (210! = 210!/[(210-2)!*2!]) from the visible (400 nm) to the SWIR (2500 nm). This was done to assess the behaviour of the relationship between leaf N or P and VIs for various spectral regions associated with pigments, foliage biomass, leaf water content, proteins, starch as well as lignin across seasons. A simple linear regression was used to determine the strength of the relationship (coefficient of determination (R^2)) between each foliar nutrient and the VIs. For each nutrient, the season which attained the highest R^2 between the VI and nutrient concentration, was selected as one of the predictive models for evaluation.

$$VI_{(i,j,n)} = \frac{(R_{(i,n)} - R_{(j,n)})}{(R_{(i,n)} + R_{(j,n)})} \quad (1)$$

Where $R_{(i,n)}$ and $R_{(j,n)}$ are the reflectance of any two bands for each sample $_n$.

Foliar N or P was predicted from known absorption regions of the electromagnetic spectrum which yielded the highest coefficient of determination (R^2) for each nutrient. Absorption regions were selected for pigments (500, 510, 670, 680, 700 and 760 nm), foliage biomass (740 and 780 nm), leaf water content (860 and 1240 nm), as well as for starch, lignin, tannins, pectin, protein and cellulose (1630, 1690, 1900, 2000, 2050, 2060, 2130, 2180, 2200, 2210, 2240, 2250, 2300 and 2380 nm).

The model with the best predictive capability for each nutrient was selected through comparing the root mean square error (RMSE) and percentage error of prediction or relative RMSE per season. Model comparison was done to assess the capability of models to predict across seasons. RMSE values were calculated for three different predictive models for each nutrient across seasons: (a) a model using predicted values for each season (individual-season model); (b) a model developed from the season providing the highest R^2 for the particular nutrient and applied to all four seasons; and (c) a model developed combining data from all four seasons for each nutrient (multiple- or combined-seasons model). The RMSE (Eq. 2) was calculated for each model, season and nutrient to compare accuracies.

$$RMSE = \sqrt{\frac{1}{n}\sum_{i=1}^{n}(\hat{y}_i - y_i)^2} \quad (2)$$

Where $\hat{y}_i$ is the predicted nutrient concentration, y_i is the observed nutrient concentration, and n is the number of samples.

For the combined-seasons model, a third of the data for each season was retained as an independent data set, whereas the remaining 2/3 of each season was combined into a single data set. An iterative bootstrap process (1 000 iterations) using R software (RStudio v. 0.98.507, © 2009-2013 RStudio, Inc.) divided the combined data set randomly into a training

(2/3) and test (1/3) data set. A linear model was fit to the training data set between the observed nutrient concentration and the vegetation index, and then applied to the test data set. The RMSE was then calculated for both the training and test data set and recorded with the model coefficients, before each new reiteration. The mean coefficients were thereafter applied to the independent data sets of each season and the RMSE calculated and reported per season. The percentage of error was calculated using the mean observed nutrient concentration per season for model comparison. The change in percentage error between the models was compared to evaluate the capability of each model to predict across seasons.

3.3. Results

3.3.1. Foliar nutrient variations per season

Amongst the four seasons, winter leaves showed the highest mean N ($p < 0.01$, Bonferroni corrected $p = 0.008$) (Table 3.2; Table 3.3). However, winter showed the lowest variability of foliar N (standard deviation = 0.17) when compared to the other three seasons (standard deviation > 0.6). In fact, between winter and spring, the variability increased by 294 % whereas the variability over the active growth season showed little difference.

Contrary to what was observed with foliar N, foliar P showed no statistically significant differences between the four seasons. The transition from winter to spring showed a slight increase in variability (8 %) for foliar P compared to 294 % observed for foliar N. The variability of foliar P actually declined by 71.5 % between summer and autumn, whereas the variability of foliar N showed very little change between these two seasons.

Table 3.2: Descriptive statistics for laboratory-analysed foliar nitrogen (N) and phosphorus (P) concentration (%) over four seasons.

Foliar nutrient (%)	Statistic	Winter	Spring	Summer	Autumn
N	Min	1.47	0.69	0.57	0.55
	Mean	2.16	1.89	1.75	1.71
	Max	2.51	3.33	3.37	3.37
	Stdev	0.17	0.67	0.63	0.67
P	Min	0.05	0.05	0.03	0.04
	Mean	0.17	0.17	0.17	0.14
	Max	0.59	0.93	1.14	0.41
	Stdev	0.13	0.14	0.17	0.08

Table 3.3: Intra-season ANalysis Of VAriance (ANOVA) for foliar N and P concentration (%).

Nutrient	Seasons	Winter	Spring	Summer	Autumn
N	Winter				
	Spring	0.003293 *			
	Summer	0.000008 *	0.246426		
	Autumn	0.000008 *	0.075883	0.947032	
P	Winter				
	Spring	0.999999			
	Summer	0.996919	0.996201		
	Autumn	0.244360	0.237694	0.346901	

* –significant ($p < 0.01$), Bonferroni corrected $p = 0.008$

3.3.2. Assessing the seasonal relationship between foliar nutrient concentration and leaf spectra

The relationship between foliar N and leaf spectra varied across seasons (Figure 3.4; Table 3.4). Winter showed the lowest correlations between foliar N and leaf spectra compared to the other three seasons. The highest R^2 for winter was recorded in the SWIR with a two-band combination associated with protein and starch (R^2 = 0.22, $p < 0.01$) (Table 3.4). In contrast, spring showed an increase in correlation between foliar N and leaf spectra across spectral regions associated with foliar pigments, foliage biomass, leaf water content, protein, starches, cellulose and lignin (Figure 3.4; Table 3.4). The region with the highest average R^2 across seasons (0.59) was recorded in the SWIR associated with protein absorption bands (2130, 2240), yielding the highest R^2 in spring (R^2 = 0.80, $p < 0.01$), followed by summer (R^2 = 0.77, $p < 0.01$) and autumn (R^2 = 0.71, $p < 0.01$) (Table 3.4). The second highest region was also located in the SWIR associated with protein and cellulose (2180, 2210), followed by foliage biomass in the red-edge region (740, 780), lignin, tannins, pectin and protein in the SWIR (1630, 1690), and then the chlorophyll bands in the red-edge region (700, 760). The relationship in the carotenoid pigment region remained relatively constant from spring to summer and autumn (R^2 = 0.37, 0.37, 0.34, $p < 0.01$), although the relationship between foliar N and spectra showed a slight increase (30 %) in the bands associated with chlorophyll from spring to autumn, as well as for lignin, waxes, protein and nitrogen (16 %). The relationship showed a decrease from spring to autumn in the region associated with foliage biomass (-21 %), leaf water content (-57 %) and the region of lignin, tannins, pectin and protein (-50 %). Bands associated with protein or protein bond absorption features showed an average decrease from spring to autumn of < 22 %), whereas bands associated with starch showed a decrease by > -90 % from spring to autumn.

Compared to leaf N, the relationship between foliar P and leaf spectra also varied over the four seasons, but with lower R^2 values over all four seasons (Figure 3.4; Table 3.4). High R^2 values ($R^2 > 0.25$) between foliar P and leaf spectra were recorded for all four seasons in the SWIR, compared to the high diversity of regions noted for N. In the winter, the highest

average coefficient of determination (R^2) across the four seasons (R^2 = 0.25, p < 0.01) was recorded in the SWIR region associated with lignin, waxes, protein and nitrogen (2050, 2380), followed by protein, nitrogen and lignin (2060, 2380). Other high average R^2 regions were mainly associated with protein (2130, 2240), protein and cellulose (2180, 2210) and lignin, tannins, pectin and protein (1650, 1690). The SWIR region with the highest average R^2 across all four seasons (2050, 2380), also showed the highest R^2 in autumn (R^2 = 0.38, p < 0.01). The pigment region showed a marked increase from winter to spring and spring to summer (> 110 %). An increase in the relationship was observed from winter to spring (> 150 %), in the regions associated with chlorophyll, foliage biomass and starch, although a decrease was noted from spring to summer (> -66 %) for these regions. The band combinations protein, protein bonds with cellulose, nitrogen and starch, in general, showed a decrease from winter to spring (by > -27 %) and spring to summer (by > 6 %), but increased between summer and autumn between 13 – 93 %.

Spring showed the highest R^2 between foliar N and leaf spectra and winter the lowest. In contrast, the highest relationship between foliar P and leaf spectra was recorded in the winter, summer and autumn, and the lowest in spring. Foliar nitrogen and phosphorus showed higher R^2 values with the SWIR region, except for nitrogen in the red-edge regions associated with chlorophyll and foliar biomass (Table 3.4).

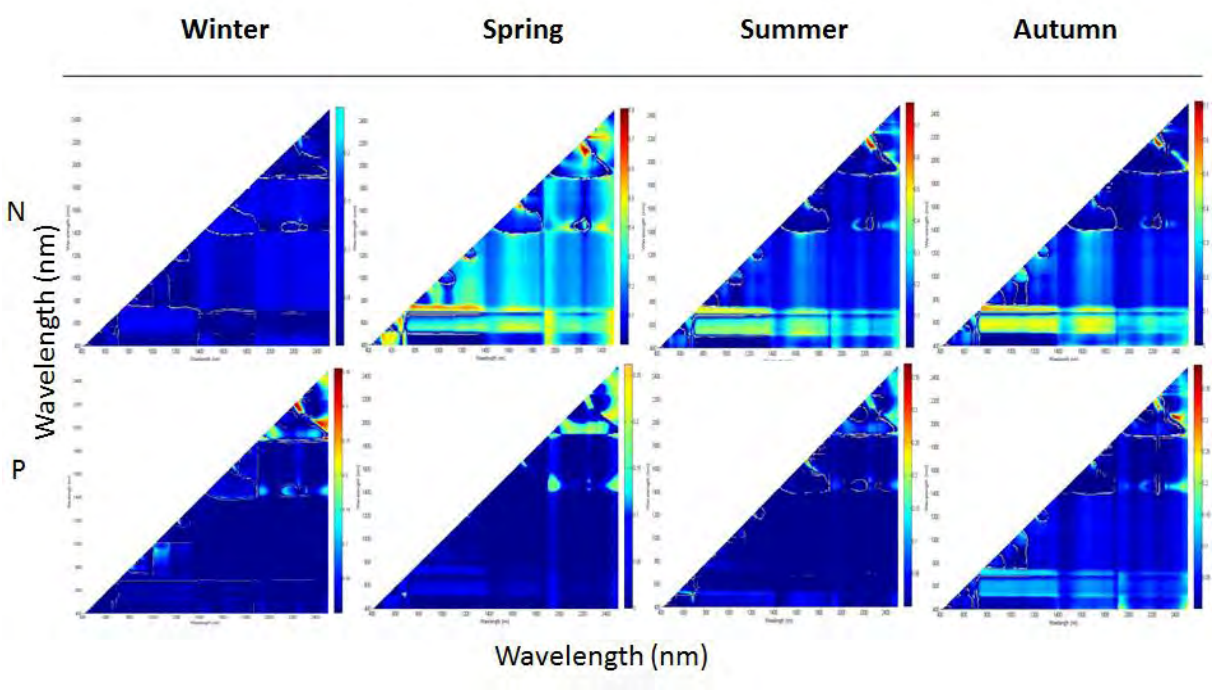

Figure 3.4: Contour plots showing the regression (R^2) between selected vegetation indices calculated from all possible waveband combinations (vertical and horizontal axes) in the 400 – 2500 nm range (at 10 nm intervals) and leaf N or P concentrations (%).

Table 3.4: Maximum linear regression coefficient of determination (R^2), extracted from a matrix showing the relationship between nutrient concentrations and spectra, for band regions known to relate to leaf features, given per season and nutrient.

Foliar nutrient	VI Band combination •	Associated parameter	Winter	Spring	Summer	Autumn	*Average*
N	510, 680	Carotenoids	0.00	0.37*	0.37*	0.34*	*0.27*
	700, 760	Chlorophyll	0.09*	0.40*	0.44*	0.52*	*0.36*
	740, 780	Foliage biomass	0.08*	0.62*	0.49*	0.49*	*0.42*
	860, 1240	Leaf water content	0.00	0.37*	0.15*	0.16*	*0.17*
	1630, 1690	Lignin, tannins, pectin & protein	0.06*	0.66*	0.47*	0.33*	*0.38*
	1900, 2250	Starch	0.01	0.33*	0.13*	0.01	*0.12*
	2000, 2250	Starch	0.01	0.40*	0.13*	0.03	*0.14*
	2050, 2380	Lignin, waxes, protein & nitrogen	0.02	0.38*	0.48*	0.44*	*0.33*
	2060, 2300	Protein & nitrogen	0.02	0.22*	0.00	0.01	*0.06*
	2060, 2380	Protein, nitrogen & lignin	0.00	0.47*	0.47*	0.37*	*0.33*
	2130, 2240	Protein	0.09*	0.80*	0.77*	0.71*	*0.59*
	2180, 2210	Protein & cellulose	0.06*	0.60*	0.63*	0.59*	*0.47*
	2180, 2240	Protein & nitrogen	0.21*	0.42*	0.41*	0.27*	*0.33*
	2200, 2240	Protein & starch	0.22*	0.31*	0.30*	0.18*	*0.25*
P	500, 670	Carotenoids	0.06*	0.17*	0.37*	0.10*	*0.18*
	700, 760	Chlorophyll	0.02*	0.05*	0.00*	0.14*	*0.05*
	740, 780	Foliage biomass	0.02	0.06*	0.02	0.13*	*0.06*
	860, 1240	Leaf water content	0.01	0.01	0.00	0.04	*0.02*
	1650, 1690	Lignin, tannins, pectin & protein	0.17*	0.19*	0.30*	0.19*	*0.21*
	1900, 2250	Starch	0.04*	0.18*	0.06*	0.06*	*0.09*
	2000, 2250	Starch	0.01	0.13*	0.03	0.05	*0.06*
	2050, 2380	Lignin, waxes, protein & nitrogen	0.28*	0.24*	0.09*	0.38*	*0.25*
	2060, 2300	Protein & nitrogen	0.02	0.02	0.00	0.00	*0.01*
	2060, 2380	Protein, nitrogen & lignin	0.20*	0.25*	0.13*	0.36*	*0.24*
	2130, 2240	Protein	0.23*	0.16*	0.15*	0.29*	*0.21*
	2180, 2210	Protein & cellulose	0.29*	0.15*	0.14*	0.25*	*0.21*
	2180, 2240	Protein & nitrogen	0.31*	0.20*	0.17*	0.21*	*0.22*
	2200, 2240	Protein & starch	0.26*	0.19*	0.15*	0.17*	*0.19*

• Two-band combinations yielding high correlations were extracted from regions known to be related to pigments (Gitelson *et al.*, 2002; Gitelson and Merzlyak, 2004; Gitelson *et al.*, 2006); foliage biomass (Mutanga and Skidmore, 2004; Cho *et al.*, 2007); leaf water content (Gao, 1996); proteins & starches (Curran, 1989); waxes & protein/enzyme *D*-ribulose 1-5-diphosphate carboxylase@2050, tannic acid@1660, lignin, pectins & protein/enzyme *D*-ribulose 1-5-diphosphate carboxylase@1680, lignin@2380 (Elvidge, 1990).

* –significant ($p < 0.01$)

3.3.4. Comparison of predictive models across seasons

The individual-seasons model showed the lowest prediction error of leaf N for the winter season for the indices developed in the red-edge (chlorophyll and foliage biomass) and SWIR regions (protein) of the spectrum (Table 3.5). For the spring, summer and autumn seasons, the individual-seasons model of N showed lower error of prediction (%) in the SWIR, compared to the red-edge region. When the spring-season model (the spring season recorded the highest R^2 between the VI and N concentration) was used to predict N for the other three seasons, the error of prediction (%) increased by 1 – 5 % for the summer and autumn seasons for the VIs in both the red-edge and SWIR regions. Applying the spring-season model to the winter leaf spectra resulted in an increase of the error of prediction by 11 – 18 %. The combined-seasons model for N, compared to the individual-seasons model, showed an increase in error of between 4 – 7 % for the three VIs in winter, a slight decrease in error (≤ 4 %) for the spring season, but showed no major changes for the summer and autumn seasons.

The accuracy of the predictive models for leaf P when compared to the leaf N models was very low (Error > 46 %; Table 3.6). The VI for the lignin, waxes, protein and nitrogen bands in the SWIR showed the lowest error of prediction (46 %). The combined-season model, on the other hand, decreased the error in prediction by 12 – 28 %, but for the SWIR region in autumn, only by 3 %.

Table 3.5: Assessing the capability of the three different predictive models for nitrogen across four seasons. The capability of the spring-season model and combined-seasons model is evaluated in the change of percentage error from the individual-seasons model.

		Winter			Spring			Summer			Autumn		
Model:	VI-band combination	700, 760	740, 780	2130, 2240	700, 760	740, 780	2130, 2240	700, 760	740, 780	2130, 2240	700, 760	740, 780	2130, 2240
	Associated parameter	Chlorophyll region	Foliage biomass	Protein	Chlorophyll region	Foliage biomass	Protein	Chlorophyll region	Foliage biomass	Protein	Chlorophyll region	Foliage biomass	Protein
Individual-seasons	Linear regression:	y = 0.6229x +1.7924	y = 3.7848x +2.0208	y = -1.7299x +2.2936	y = 3.9682x -0.41	y = 34.17x +0.7901	y = -19.06x +3.4246	y = 5.0957x -1.2398	y = 39.447x +0.5076	y = -22.107x +3.9439	y = 5.6791x -1.659	y = 40.194x +0.4004	y = -26.185x +4.3275
	RMSE	0.16	0.17	0.17	0.51	0.41	0.30	0.46	0.44	0.30	0.45	0.48	0.35
	% Error	7.61	7.66	7.68	26.94	21.45	15.92	26.45	25.08	16.90	26.25	27.80	20.67
Spring-season model	Linear regression:	y = 3.9682x -0.41	y = 34.17x +0.7901	y = -19.06x +3.4246	y = 3.9682x -0.41	y = 34.17x +0.7901	y = -19.06x +3.4246	y = 3.9682x -0.41	y = 34.17x +0.7901	y = -19.06x +3.4246	y = 3.9682x -0.41	y = 34.17x +0.7901	y = -19.06x +3.4246
	RMSE	0.40	0.44	0.55	0.51	0.41	0.30	0.50	0.46	0.38	0.53	0.52	0.43
	% Error	18.69	20.39	25.42	26.94	21.45	15.92	28.64	26.17	21.41	30.82	30.28	25.39
Combined-seasons	Mean linear regression:	y = 3.767x -0.3291	y = 29.29x +0.9075	y = -16.04x +3.318	y = 3.767x -0.3291	y = 29.29x +0.9075	y = -16.04x +3.318	y = 3.767x -0.3291	y = 29.29x +0.9075	y = -16.04x +3.318	y = 3.767x -0.3291	y = 29.29x +0.9075	y = -16.04x +3.318
	Mean RMSE training data	0.47	0.44	0.39	0.47	0.44	0.39	0.47	0.44	0.39	0.47	0.44	0.39
	Mean SD training data	0.01	0.01	0.01	0.01	0.01	0.01	0.01	0.01	0.01	0.01	0.01	0.01
	Mean SEP	0.48	0.45	0.39	0.48	0.45	0.39	0.48	0.45	0.39	0.48	0.45	0.39
	Mean SD SEP	0.02	0.02	0.02	0.02	0.02	0.02	0.02	0.02	0.02	0.02	0.02	0.02
	Mean SEP Independent dataset	0.26	0.27	0.32	0.43	0.34	0.25	0.47	0.42	0.28	0.49	0.47	0.34
	SD SEP Independent dataset	0.17	0.18	0.23	0.34	0.28	0.18	0.33	0.30	0.23	0.31	0.32	0.27
	Training % error	21.79	20.40	18.08	24.81	23.23	20.59	26.83	25.11	22.26	27.49	25.73	22.81
	Test % error	22.25	20.86	18.08	25.34	23.76	20.59	27.40	25.69	22.26	28.07	26.32	22.81

	Independent % error	12.05	12.52	14.83	22.70	17.95	13.20	26.83	23.97	15.98	28.65	27.49	19.88
Difference in % error between models:	Spring-season model compared to Individual	-11.08	-12.73	-17.74	0.00	0.00	0.00	-2.19	-1.09	-4.51	-4.57	-2.48	-4.72
	Combined compared to Individual	-4.44	-4.86	-7.15	4.24	3.50	2.72	-0.38	1.11	0.92	-2.40	0.31	0.79
	Combined compared to Spring-season model	6.64	7.87	10.59	4.24	3.50	2.72	1.81	2.20	5.43	2.17	2.79	5.51

SD, standard deviation

SEP, standard error of prediction

Table 3.6: Assessing the capability of the three different predictive models for phosphorus across four seasons. The capability of the autumn-season model and combined-seasons model is evaluated in the change of percentage error from the individual-seasons model.

		Winter		Spring		Summer		Autumn	
Model:	VI-band combination	500, 670	1650, 1690	500, 670	1650, 1690	500, 670	1650, 1690	500, 670	1650, 1690
	Associated parameter	Carotenoids	Lignin, waxes, protein & nitrogen	Carotenoids	Lignin, waxes, protein & nitrogen	Carotenoids	Lignin, waxes, protein & nitrogen	Carotenoids	Lignin, waxes, protein & nitrogen
Individual-seasons	Linear regression:	y = 0.9929x +0.1932	y = 3.7752x +0.3748	y = 1.6711x +0.2559	y = 3.726x +0.2359	y = 3.5344x +0.2985	y = 3.701x +0.3398	y = 1.0447x +0.1865	y = 3.0753x +0.2738
	RMSE	0.12	0.11	0.12	0.12	0.13	0.16	0.08	0.06
	% Error	69.90	60.68	68.79	67.80	77.17	94.15	54.37	45.95
Autumn-season model	Linear regression:	y = 1.0447x +0.1865	y = 3.0753x +0.2738	y = 1.0447x +0.1865	y = 3.0753x +0.2738	y = 1.0447x +0.1865	y = 3.0753x +0.2738	y = 1.0447x +0.1865	y = 3.0753x +0.2738
	RMSE	0.12	0.12	0.13	0.14	0.15	0.16	0.08	0.06
	% Error	70.05	71.32	73.53	79.74	90.25	96.85	54.37	45.95
Combined-seasons	Mean linear regression:	y = 1.3777x +0.2077	y = 2.837x +0.3004	y = 1.3777x +0.2077	y = 2.837x +0.3004	y = 1.3777x +0.2077	y = 2.837x +0.3004	y = 1.3777x +0.2077	y = 2.837x +0.3004
	Mean RMSE training data	0.11	0.11	0.11	0.11	0.11	0.11	0.11	0.11
	Mean SD training data	0.01	0.01	0.01	0.01	0.01	0.01	0.01	0.01
	Mean SEP	0.11	0.11	0.11	0.11	0.11	0.11	0.11	0.11
	Mean SD SEP	0.02	0.02	0.02	0.02	0.02	0.02	0.02	0.02
	Mean SEP Independent dataset	0.08	0.08	0.08	0.07	0.09	0.09	0.06	0.06
	SD SEP Independent dataset	0.08	0.08	0.13	0.14	0.15	0.17	0.06	0.04
	Training % error	63.48	63.48	63.39	63.39	64.84	64.84	78.32	78.32
	Test % error	63.48	63.48	63.39	63.39	64.84	64.84	78.32	78.32
	Independent % error	46.17	46.17	46.10	40.34	53.05	53.05	42.72	42.72
Difference in % error between models:	Autumn-season model compared to Individual	-0.15	-10.64	-4.74	-11.94	-13.08	-2.70	0.00	0.00
	Combined compared to Individual	23.73	14.51	22.69	27.46	24.12	41.10	11.65	3.23
	Combined compared to Autumn-season model	23.88	25.15	27.43	39.40	37.20	43.80	11.65	3.23

SD, standard deviation. SEP, standard error of prediction,

3.4. Discussion

3.4.1. Foliar nutrient variation compared to other evergreen subtropical trees

Our results of high foliar nitrogen concentration in winter concurred with other evergreen tropical and subtropical trees (Cai *et al.*, 2009; Lin *et al.*, 2010). Evergreen *Quercus* and spruce trees in other climatic zones showed similar trends (Chapin and Kedrowski, 1983; Sabaté *et al.*, 1995; Yasamura and Ishida, 2011). These findings support the notion that older leaves of evergreen trees are used for N storage during the dormant season, and remobilised in spring for leaf growth (Cherbuy *et al.*, 2001; Millard and Grelet, 2010). Other studies showed, however, a lower concentration and variability of foliar nitrogen in winter, compared to the other seasons, for evergreen tropical dry and savannah forests (Franco *et al.*, 2005; Chaturvedi *et al.*, 2011). Few studies reported detailed observations of variability with mean nitrogen concentrations over four seasons or a full phenological cycle. Contrary to our findings, Bell and Ward (1984) reported low variability and concentration of foliar nitrogen in winter for evergreen trees in a Mediterranean climate, and a high variability and concentration in spring (Bell and Ward, 1984).

In this study, foliar phosphorus showed relatively similar mean concentrations over the four seasons, however the variability was highest in all seasons except autumn. Bell and Ward (1984) also found very little variability in mean foliar phosphorus concentration of mature evergreen leaves of *Eucalyptus wandoo* over the seasons, with a high variability in summer (Bell and Ward, 1984). Other tropical evergreen trees also showed high mean concentration and higher variability of foliar phosphorus for the summer season compared to the other seasons (Cai *et al.*, 2009; Lin *et al.*, 2010). In evergreen savanna trees, however, foliar phosphorus showed a slight decrease from winter to spring, and a significant increase towards summer (Franco *et al.*, 2005). In the study of the two evergreen *Eucalyptus* spp., the lowest variability of foliar phosphorus was recorded for winter (Bell and Ward, 1984), compared to our findings of the lowest variability in autumn. In a tropical forest of Nigeria, foliar phosphorus concentrations showed no seasonal variation (Sharma, 1983).

3.4.2. Seasonally varying nutrient-spectral relationship

The relationship between leaf spectra and foliar nutrients varied over seasons and spectral regions. The highest correlation between leaf N and spectra was recorded in spring and the lowest in winter, whereas the highest correlation between leaf P and spectra was recorded in winter, summer and autumn. Co-variants of foliar N, chlorophyll and foliage biomass did not follow similar patterns of change between spring and autumn, confirming the varying relationship over seasons. The variations recorded in the relationship concur with the variations noted in the seasonal foliar N patterns, associated with the photosynthesis process. Seasonal patterns of N, derived through VIs from leaf spectra, can therefore potentially indicate seasonal changes in photosynthetic activity of subtropical evergreen

trees. All spectral regions used in this study were consistent with other studies for regions associated with foliar N, i.e., the red-edge and SWIR, as well as with foliar P, i.e., the SWIR region (Curran, 1989; Elvidge, 1990; Kokaly and Clark, 1999; Johnson, 2001; Kumar *et al.*, 2001; Kokaly, 2001; Cho and Skidmore, 2006; Cho *et al.*, 2010b; Ramoelo *et al.*, 2011).

The other high correlation (R^2 = 0.37, p < 0.01) between foliar P and leaf spectra was found between the carotenoid spectral region (500 – 520 nm) and the red-edge region (680 – 760 nm) which may be indicative of a possible relationship between foliar carotenoids, foliar chlorophyll and foliar P occurring at peak productivity in summer. The methyl-erythritol phosphate pathway, which is responsible for the production of both carotenoids and foliar abscisic acid, controls stomatal opening which is also associated with foliar P (Barta and Loreto, 2006). The correlation between foliar P and this spectral band combination is, however, only high in summer and not in any of the other three seasons.

To our knowledge, our work is the first study noting the variance in the seasonal relationship between foliar nutrients and related leaf spectral absorption features. Changing relationships between foliar chlorophyll *a* and related leaf spectra was also observed for evergreen mangrove species in a subtropical environment between the wet and dry seasons (Flores-de-Santiago *et al.*, 2013). Zhang et al (2007) also noted a changing relationship between estimated and observed chlorophyll for a deciduous maple species, showing a decline in the correlation and accuracy from spring to summer, and an increase in correlation and accuracy from summer to autumn.

3.4.3. Monitoring foliar nutrient phenology using remote sensing models

A number of models, developed from leaf-level spectra, were assessed for their capability to predict foliar nutrient concentration across species and seasons. The RMSE values and error of prediction (%) of two models were compared to those of the model developed for each individual season: a predictive model of the season in which the highest R^2 values were recorded between a VI and nutrient concentrations, as well as a predictive model combining all the seasons. To minimise the influence of individual species on the development of a regression model, a 1000-times iterative bootstrap procedure was used in the evaluation of the combined-seasons predictive model. The maximum error ranges of the various predictive models for leaf N concentration of the evergreen subtropical trees were below 31 % and offered relative capable models to predict across species and season. The individual-season leaf N model showed the lowest range of error for leaf N with an error range between 7 – 28 %. The combined-season leaf N model increased in the prediction error range of between 12 – 29 %, while the spring-season model for leaf N showed an increase in prediction error of between 15 – 31 %. The predictive models for foliar P were mostly > 40 % and therefore considered inaccurate in predicting P for these evergreen subtropical trees.

The seasons with the lowest error of prediction was mainly the spring, summer and autumn seasons. The error of prediction for these three seasons deviated by < 5.5 % from the error of prediction of the individual-seasons model. However, the error of prediction increased by 4 – 7 % when the combined-seasons model was applied to winter, and by > 10 % when the spring-season model was applied to the winter season. The winter season showed significantly higher (p < 0.08) mean observed N concentration, and lower variance, compared to the other three seasons. The phenology of these evergreen trees therefore had a definite influence on the error of predicting leaf N concentration when a model developed in spring was applied to the leaf spectra collected in winter.

The bands with the lowest error of prediction for leaf N concentration was found in the SWIR region for the spring, summer and autumn seasons, compared to the bands used in the red-edge region (related to chlorophyll and foliage biomass). The reverse was observed for winter, where the error of prediction was lower in the red-edge region, compared to the SWIR region bands.

The various models and bands were assessed as an initial step to assess the potential of remote sensing techniques to monitor nutrient phenology across regions and species. A number of multispectral spaceborne sensors, such as RapidEye (RE) launched in 2008, and WorldView-2 (WV2) launched in 2009, is expected to improve vegetation health and foliar nitrogen monitoring through the incorporation of a band in the red-edge region. A number of multispectral sensors are also planned for deployment, including WorldView-3 (WV3; 2014), and Sentinel-2 (2015), which will improve the spatial resolution of current sensors, and add to the number of red-edge and SWIR bands at higher spectral resolution. These sensors are expected to improve nutrient mapping at the landscape level (Clevers and Gitelson, 2013). The improved spatial resolution of these sensors, will further allow single-canopy species identification and monitoring, overcoming most of the current limitations of multispectral imagery. In support of these developments, further research is required to improve our understanding of whether the relationship between foliar N and P and spectra reflectance features will change annually, under different climatic conditions, at canopy scale or for other species.

3.4.4. Implications for monitoring global change impact on vegetation

The impact of global change on the seasonal dynamics of nutrients can be potentially monitored through the changing relationship of foliar nutrients to spectra, at canopy (satellite image) scale. Seasonal patterns of nutrients are expected to differ across climatic zones. Remote sensing can contribute to the characterization of foliar nutrient phenology at the bioregional scale, and secondly, monitor the impact of global change on these patterns. The quantification of foliar nutrients could potentially provide more information on subtle changes in magnitude of foliar nutrients, in addition to impacts already noted in

phenophases. Considering the low photosynthetic activity currently observed in the dormant season, and that temperature increases may increase photosynthetic activity, an increase in the variability of foliar nutrients, particularly nitrogen, may be expected in future.

3.5. Conclusion

This study found a seasonally changing relationship in foliar nutrients (nitrogen and phosphorus) for evergreen subtropical tree species in St. Lucia, South Africa. The relationships between foliar nutrients and leaf spectra also varied over the seasons and across regions associated with known biochemical and biophysical parameters. The high variability in foliar N in spring for example possibly reflects the high mobilisation of N during the actively growing season, whereas the higher mean concentration of foliar N in winter may indicate storage of N during this dormant season. Predictive models for leaf N concentration developed for each season showed a higher level of accuracy, particularly for winter, whereas predictive models for leaf P showed low accuracies. Models developed from a single season showed a slight increase in error for the summer and autumn, however a larger increase in error for the winter season for the evergreen trees. Global biogeographic patterns of foliar N and P of tropical and subtropical forests are limited. Many studies focus on nutrient dynamics of a few species and locations, yet monitoring the impact of global change at species level may be difficult and time consuming. Remote sensing offers the potential to monitor N and P at canopy level to establish biogeographical patterns at the regional scale. Furthermore, the subtle initial changes of an increased temperature on photosynthetic activity, is possible through the quantification of nutrient variability over seasons. We recommend further studies on the phenology of foliar nutrients at regional scale for a number of species and climatic zones, using remote sensing.

At biochemical level, foliar nitrogen showed the highest potential of discrimination between six evergreen tree species in a subtropical forest, when compared to two foliar pigments and foliar phosphorus. It remains to be established whether the spectral features related to leaf N and other biochemicals could yield accurate results for classification of evergreen tree species.

CHAPTER 4: REDUCING LEAF-LEVEL HYPERSPECTRAL DATA TO 22 COMPONENTS OF BIOCHEMICAL AND BIOPHYSICAL BANDS OPTIMISES TREE SPECIES DISCRIMINATION

This chapter is based on the journal publication:

Van Deventer, H, Cho, MA, Mutanga, O, Naidoo, L & Dudeni-Tlhone, N 2015. Reducing leaf-level hyperspectral data to 22 components of biochemical and biophysical bands optimises tree species discrimination. IEEE-JSTARS, January. DOI: 10.1109/JSTARS.2015.2424594.

Abstract

The high dimensionality of hyperspectral data constitutes a challenge for species classification. This study assessed (i) whether tree species classification can be optimized with the selection of bands related to known plant properties, and (ii) whether a Partial Least Square (PLS) transformation of the spectral bands improves species classification in comparison to Principal Component Analysis (PCA). Leaf spectra between 400 – 2 500 nm were measured for six evergreen tree species in the spring of 2011, in the KwaZulu-Natal Province of South Africa. Twenty-two bands known to be related to pigments, nutrients, foliage biomass, and leaf structural components were selected from the hyperspectral data set. The 2 100 bands of 1 nm were resampled to 421 bands at 5 nm spectral resolution, ensuring the number of variables are less than the number of samples. The Random Forest classification algorithm was used to assess the accuracy for both PCA and PLS transformations on the 421 and 22 bands. The accuracy of individual species classes were calculated as the average of ten iterations, for each data reduction option. The three 22-band models resulted in comparable accuracies to the 421-band classifications (OA of 84±4.9 % for untransformed, 78±5 % for PCA and 84±4 % for PLS) and no statistically significant differences between the 421 and 22-band models ($p > 0.4$). The optimised PLS model (22 bands, 8 components) showed a 6 % ($p < 0.01$) increase in accuracy compared to the optimised PCA model (22 bands, 3 components). Reducing hyperspectral data to bands which relate to plant properties, and the use of PLS for data transformation, optimises species classification.

4.1. Introduction

Vegetation species discrimination is important for understanding and monitoring complex spatial patterns of biodiversity (Heywood and Watson, 1996; Gaston, 2000; Turner *et al.*, 2003; Carlson *et al.*, 2007). Hyperspectral remote sensing has been successfully used for species discrimination compared to multispectral data which are more suitably applied to the mapping of broad vegetation categories or plant functional groups (Asner, 1998; Cochrane, 2000; Van Aardt and Wynne, 2001; Wang *et al.*, 2004; Clark *et al.*, 2005; Sobhan, 2007; Adam and Mutanga, 2009; Adam *et al.*, 2010; Dalponte *et al.*, 2012). Even though the spatial resolution of more recent multispectral sensors have increased, the primary limitation in the use of multispectral sensors for vegetation species mapping, is the low spectral resolution. Multispectral data often have less than 10 spectral bands, recording limited regions of the electromagnetic spectrum with spectral resolutions which are too wide to detect the subtle absorption features related to individual plant properties (Carlson *et al.*, 2007). In contrast, hyperspectral sensors record more than fifty narrow contiguous spectral bands from the visible to shortwave infrared regions (350 to 2 500 nm). The narrow spectral bands allow for the measurement of the depth of absorption features associated with plant biochemical and biophysical parameters, such as pigments, nutrients, biomass, lignin, and cellulose (Elvidge, 1990; Chappelle *et al.*, 1992; Vogelmann *et al.*, 1993; Jacquemoud *et al.*, 1996; Blackburn, 1998b; Kokaly and Clark, 1999; Blackburn, 1999; Lichtenthaler and Buschmann, 2001; Kokaly, 2001; Gitelson *et al.*, 2002; Gitelson and Merzlyak, 2004; Kokaly *et al.*, 2009). As a result, hyperspectral data are capable of not only capturing the complexity of plant properties for species discrimination, but offer a range of additional information on the variation in expression of species across time and space.

Regardless of the abundance of information provided through hyperspectral data, data redundancy remains one of the key problems (Clark *et al.*, 2005; Adam *et al.*, 2010). Of the 2150 bands that could potentially be recorded by current-day spectrometers, less than 50 spectral bands relate to biochemical and biophysical characteristics of plant properties (Elvidge, 1990; Chappelle *et al.*, 1992; Vogelmann *et al.*, 1993; Jacquemoud *et al.*, 1996; Blackburn, 1998b; Kokaly and Clark, 1999; Blackburn, 1999; Lichtenthaler and Buschmann, 2001; Kokaly, 2001; Gitelson *et al.*, 2002; Gitelson and Merzlyak, 2004; Kokaly *et al.*, 2009). Ideally, the optimisation of a classification model should remove redundant information and use only key, relevant components to assess true class separability. Using redundant information in classification modelling results in the overfitting of independent variables and poor classification accuracies (Saeys *et al.*, 2007). Optimised models, on the other hand, are more cost-effective, as fewer variables are required for classification with the benefit of increased performance and a decrease in the number of samples to be collected in the field to ensure true pattern recognition (Hughes, 1968; Landgrebe, 1997). The selection of spectral bands should, however, be followed with decomposition to avoid overfitting the

model with bands which are highly correlated (Tu *et al.*, 2005; Clark *et al.*, 2005; Saeys *et al.*, 2007). Consideration of data dimensionality, relevant components and intra-band correlation is essential in the pre-processing of hyperspectral data prior to the classification of vegetation species.

A number of methods have been developed for feature selection and decorrelation of hyperspectral data. Various selection methods have been developed and used in species classification studies to reduce data dimensionality, including filter and wrapper methods (Saeys *et al.*, 2007). In many instances, filter and wrapper methods are combined, for example the use of the Mann–Whitney U-test or an Analysis Of Variance, which determine the most significant bands from the spectrum relating to the species classes, combined with selection algorithms and discriminant analyses (Van Aardt and Wynne, 2001; Schmidt and Skidmore, 2003; Clark *et al.*, 2005; Artigas and Yang, 2006; Sobhan, 2007; Dudeni *et al.*, 2009; Jones *et al.*, 2010; Manevski *et al.*, 2011; Dalponte *et al.*, 2012). Despite the advantage of these methods (Saeys *et al.*, 2007), the inclusion of spectral bands unrelated to plant properties introduces "noise" into the classification of vegetation species i.e. fitting the classification with irrelevant information. A number of studies have however, considered only bands which relate to plant biochemical and biophysical parameters (Martin *et al.*, 1998; Cho *et al.*, 2010a). One of the earliest studies reporting the importance of selecting plant-related bands, was that of Martin, Newman, Aber, and Congalton (Martin *et al.*, 1998). A number of forest stands in America, with dominant conifer and deciduous species, were found highly separable using AVIRIS sensor bands. The selection of bands was based on the differences in variation in nitrogen and lignin concentrations between species, resulting in an overall classification accuracy of 75 %. In a species classification study in Africa (Cho *et al.*, 2010a), canopy spectra were extracted from an airborne image to compare the classification performance of multiple-endmember spectral angle mapper (SAM) to the traditional SAM approach. A Band-Add on were used for feature selection, followed by the refinement of bands relating to plant properties from the visible to near-infrared regions. It remains to be assessed, however, whether the selection of bands which encompasses a multitude of plant properties such as pigments, leaf foliage biomass, leaf water, nutrients, and leaf structural components such as cellulose and lignin, will optimise species classification when compared to the use of unrelated bands.

Data transformation methods, in addition to feature selection methods, also offer a reduction in data dimensionality, with the additional benefit of transforming highly correlated bands into latent components (Pearson, 1901; Hotelling, 1933). A number of transformation or band decomposition methods have been used in species classification studies, including the Minimum Noise Fraction transformation (Green *et al.*, 1988; Belluco *et al.*, 2006), Partial Least Squares (PLS) method (Peerbhay *et al.*, 2014) and the commonly-used Principal Component Analysis (PCA) (Fung *et al.*, 2003; Thenkabail *et al.*, 2004). Both PCA and PLS are often combined with discriminant analysis or Random Forest (RF) for classification purposes (Boulesteix *et al.*, 2008; Peerbhay *et al.*, 2014).

In the case of PCA, latent variables are modelled from the variability of the whole data set, irrespective of the unique variation of individual classes. The optimum number of latent variables is selected based on the first two to five components which explain up to 95 % of the variability in the full data set. Therefore, while reducing the data by > 90 %, decorrelation and band selection can be achieved (Thenkabail *et al.*, 2004; Sobhan, 2007). As a result, less than five components are usually used in species classification (Thenkabail *et al.*, 2004; Belluco *et al.*, 2006; Sobhan, 2007; Barnard *et al.*, 2010). However, Barnard et al. (Barnard *et al.*, 2010) showed that further PCs which explain only a small percentage of the variability in the data significantly contributed to improving the classification accuracies of savanna tree species, raising the challenge of selecting the appropriate PCs for classifying species. PLS, similar to PCA, transform the data to latent variables, however, contrary to PCA, PLS, considers the variability of the independent variables during the regression phase (Wold, 1966; Wold *et al.*, 2001). As a result, PLS are considered more appropriate in the extraction of features from hyperspectral data, and particularly for vegetation species classification, compared to PCA (Cheriyadat and Bruce, 2003; Tsai *et al.*, 2007). Contrary to PCA, the optimum number of components in a PLS classification is selected where the percentage cross-validation (CV) error reduces the standard error of prediction by > 2 % (Kooistra *et al.*, 2004; Cho *et al.*, 2007).

This study investigated (i) whether tree species classification can be optimised for leaf-level hyperspectral data through selecting bands which relate to plant properties, and (ii) whether a PLS transformation procedure will improve species classification compared to a PCA. A number of bands, which relate to plant biochemical and biophysical properties, was selected followed by data transformation, the selection of the ideal number of latent variables and then species classification. Six evergreen tree species were sampled in the KwaZulu-Natal Province of South Africa in the spring of 2011. The dimensionality of 2 100 bands of leaf-level hyperspectral data was reduced first, through the targeted feature selection of 22 bands which are known to be related to biochemical and biophysical properties of plants. Secondly, a PCA was applied to a large selection of bands (2 100 bands sampled at 1 nm, which were resampled to 421 bands at 5 nm spectral resolution) as well as to the selected 22 spectral bands. The first three components, which described > 95 % of the variation, were used in the species classification using the Random Forest (RF) algorithm. A RF species classification was also done using the full number of principal components of the 22 bands to assess whether smaller components also contributed to improved accuracy. Thereafter a PLS data transformation and RF classification was done using the 421 and 22 bands. Finally, the average overall accuracies of ten iterations of each species classification models and each reduced data set were compared to assess which data reduction option provided the best results.

4.2. Methods

4.2.1. Study area

The study area is located in the iSimangaliso Wetland Park (28°S, 32°30'E) on the east coast of the KwaZulu-Natal province in South Africa (Figure 4.1). The climate is humid and sub-tropical with mean temperatures in summer ranging from 23 to 30°C and winter temperatures decreasing to approximately 10°C (Sokolic, 2006). Mean Annual Precipitation (MAP) ranges from 1 000 to 1 500 mm (Middleton and Bailey, 2008). The vegetation is comprised of wooded grassland, dune vegetation and dune forests, as well as coastal wetlands, swamp and mangrove forests on an undulating coastal plain, elevated 10 to 20 m above mean sea level (Partridge *et al.*, 2010). Six evergreen tree species were sampled in the spring season of 2011, at the St Lucia and Maphelane nodes of the iSimangaliso Wetland Park, as well as along the uMfolozi and uMsunduzi Rivers (Figure 4.1; Table 4.1).

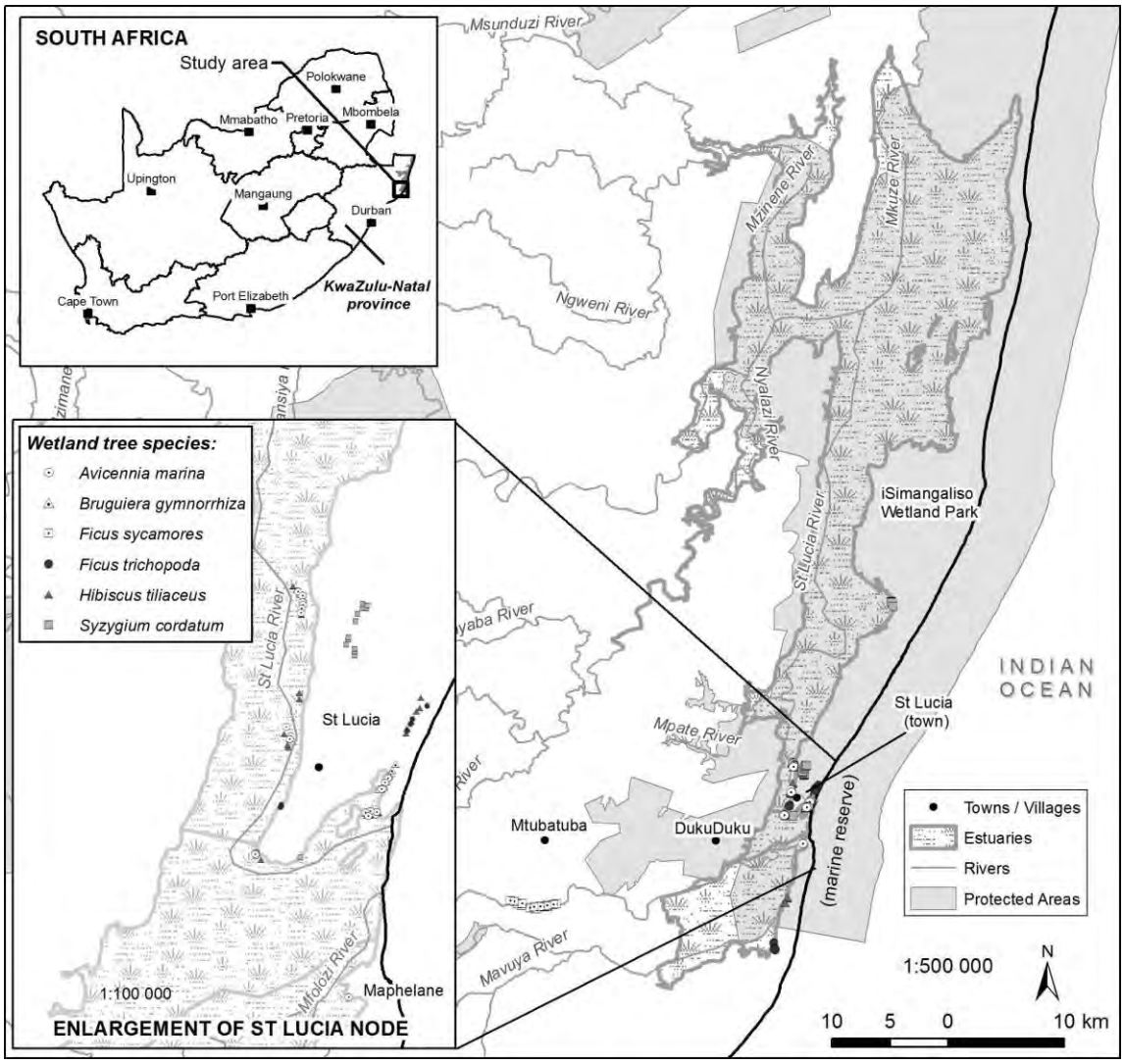

Figure 4.1: Study area showing the locations of the sample sites for six evergreen species in the KwaZulu-Natal province.

Table 4.1: Number of leaves sampled per tree species in the spring season of 2011.

Tree species	Common name	Acronym	*n* trees	*n* leaves
Avicennia marina	White mangrove	AM	21	104*
Bruguiera gymnorrhiza	Black mangrove	BG	19	94*
Ficus sycomorus	Sycamore fig	FSYC	15	75
Ficus trichopoda	Swamp fig	FT	11	55
Hibiscus tilliaceus	Lagoon hibiscus	HT	30	150
Syzygium cordatum	Waterberry	SC	17	85
Total:			113	563

* The reflectance spectra of one leaf were omitted because of low quality.

4.2.2. Leaf spectral measurements

Sample sites were selected where mature and sun-exposed tree canopies were accessible along the wetland and estuarine systems in the spring of 2011. Five sunlit leaves were randomly sampled with a telescopic pruner across the canopy of each tree (n leaves = 563, Table 4.1). Single leaf spectral reflectance measurements on the adaxial surface of each leaf were collected using the leaf-clip device of the Analytical Spectral Device (ASD) spectroradiometer (FieldSpec Pro FR, Analytical Spectral Device, Inc, USA), with the average scan time set at 10 (averaged to reduce scanner noise). The ASD covers the spectral range between 350 and 2 500 nm with a 1.4 nm sampling interval between 350 and 1 050 nm range, and ±2 nm between 1 050 and 2 500 nm. The leaf-clip device provides a direct-contact probe which limits ambient light. The radiance measurements were calibrated using a white spectralon reference panel prior to scanning a set of 5 leaves, and converted to reflectance accordingly. Spectral bands between 400 and 2 500 nm (2 100 bands) were selected for analysis and resampled to 1 nm.

4.2.3. Data analysis

We reduced the high dimensionality of the leaf-level hyperspectral data (2 100 bands), first, through the selection of twenty-two bands (Figure 4.2) which are known to relate to biochemical and biophysical plant properties (Table 4.2). The plant properties considered include pigments, nutrients, water content, biomass and other leaf structure components such as lignin, which ranged from the visible to shortwave infrared regions (Table 4.2). Previously published literature were used in the selection of band centers of carotenoid and chlorophyll absorption regions (Gitelson *et al.*, 2002; Gitelson and Merzlyak, 2004; Gitelson *et al.*, 2006) as well as bands used in vegetation indices for foliage biomass and leaf water content (Gao, 1996; Mutanga and Skidmore, 2004; Cho *et al.*, 2007). Bands of known absorption features relating to leaf structural components were selected from previously published literature (Curran, 1989; Elvidge, 1990) which showed the highest coefficient of determination between leaf spectra and nutrients for the six tree species (Van Deventer *et al.*, 2015b). The selected band centers of leaf structural components included starch, lignin, tannins, pectin, protein and cellulose located in the Shortwave Infrared (SWIR) region. The

correlation between these 22 bands was assessed for intra-band correlation and to determine whether the use of bands will result in overfitting of a species classification model.

Table 4.2: Spectral bands associated with plant biochemical and biophysical parameters selected for species classification.

Spectral bands	Spectral region	Associated plant biochemical or biophysical parameter
510, 680	Visible (VIS)	Carotenoids (Gitelson *et al.*, 2002; Gitelson and Merzlyak, 2004; Gitelson *et al.*, 2006)
700, 760	VIS – chlorophyll red edge (RE)	Chlorophyll (Gitelson *et al.*, 2002; Gitelson and Merzlyak, 2004; Gitelson *et al.*, 2006)
740, 780	RE	Foliage biomass (Mutanga and Skidmore, 2004; Cho *et al.*, 2007)
860, 1240	Mid-Infrared (MIR)	Leaf water content (Gao, 1996)
1630, 1690, 1900, 2000, 2050, 2060, 2130, 2180, 2200, 2210, 2240, 2250, 2300, 2380	Shortwave Infrared (SWIR)	Leaf structure, proteins, starches & nutrients (Elvidge, 1990), (Curran, 1989)

Secondly, a PCA was performed on the original data and feature-selected data in R (RStudio Inc. v. 0.98.507, 2009-2013). The 2 100 spectral bands of 1 nm resolution were resampled to 421 spectral bands of 5 nm using a Gaussian model (full-width half-maximum equal to every 5-nm band spacing between 400 to 2 500 nm) in the Environment for Visualizing Images (ENVI) software (v.4.8, ITT Visual Information Systems, 2012-2014), to ensure that the variables are less than the number of samples (563 leaves) evaluated. In the third step (Figure 4.2), the optimum number of principal components of each data set (421 and 22 bands), which explained the majority of the variability, were selected for species classification. The full number of components of the 22-band data set and the first 100 components (default of *princomp* in R) of the 421-band data set were also assessed to determine if smaller components would increase the accuracy.

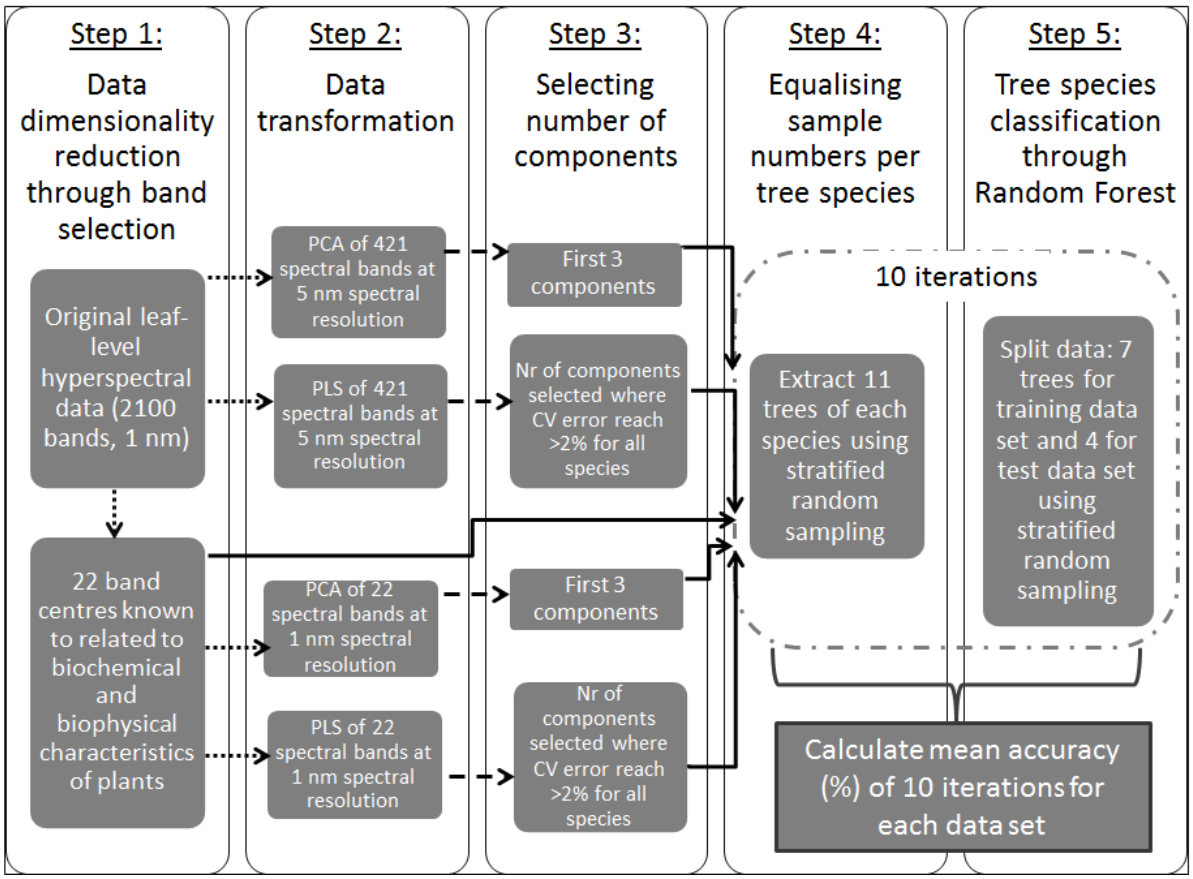

Figure 4.2: Tree species classification workflow to reduce data dimensionality (Step 1), data transformation (Step 2), selecting the optimal number of components (Step 3), equalising samples per species (Step 4) and iteration of the accuracy assessment of the classification models (Step 5).

Sample numbers from the tree species were equalised through extracting 11 trees of each species in a random stratified sampling process (Tillé and Matei, 2014), resulting in a total of 66 trees for the evaluation data set (Step 4 of Figure 4.2). This was done to avoid bias towards species classes with more samples (Chen *et al.*, 2004). Thereafter the 66 trees were repetitively divided into ten evaluation data sets through a random sampling procedure whereby, in each iteration, 7 trees from each species were selected for the training data set (total 42 trees) and 4 trees for the test data set (24 trees). The leaf-level hyperspectral data was divided according to the trees listed in each of the ten training and test data sets.

Tree species classification of the PCA-transformed data was done using the leaf-level spectra in the Random Forest (hereafter PCA-RF) decision tree classifier (Breiman, 2001) (Step 5 of Figure 4.2). Random Forest, similar to machine learning classifiers such as Artificial Neural Networks (ANN) and Support Vector Machine (SVM) algorithms, are capable of processing a large number of predictor variables and has proven to outperform traditional classifiers in statistical performance and accuracy for a number of species classification studies (Strobl *et al.*, 2009; Sluiter and Pebesma, 2010; Dalponte *et al.*, 2012; Naidoo *et al.*, 2012; Adelabu *et al.*, 2013; Adelabu and Dube, 2014). The defaults of the randomForest script in R of 500

trees to be grown, and the square root of the number of variables to be randomly sampled at each split, were maintained (Liaw and Weiner, 2008).

A PLS data transformation, combined with a Random Forest classifier (Boulesteix *et al.*, 2008), was also applied to the 421-band and 22-band data sets in R (hereafter PLS-RF). In this instance the defaults of 200 trees and the square root of the number of variables were maintained. The percentage of the cross-validation (CV) error (or *out-of-bag-error*) was calculated for each species across the sequential increase of the first 22 latent variables. Redundancy was further minimised through the selection of the optimum number of latent variables where the percentage CV error reduces the standard error of prediction by > 2 % for all species (Step 3 of Figure 4.2). The data sets were also equalized per species and divided into training and test data sets similar to the PCA-RF data sets (Steps 4 of Figure 4.2).

Finally, the user, producer and overall accuracy were calculated as the average of the ten iterations for each data reduction option (Step 5, Figure 4.2). Differences in overall accuracy between the 421-band and 22-band data reduction options were assessed through a Welch two sample t-test of the overall accuracies of the 10 iterations.

4.3. Results

4.3.1. Intra-band correlation of 22 bands related to plant properties

Intra-band correlation between the 22 selected bands was highest within various spectral regions, for example within the visible or within the shortwave infrared region (Figure 4.3). The combination of different regions resulted in a reduction in the correlation.

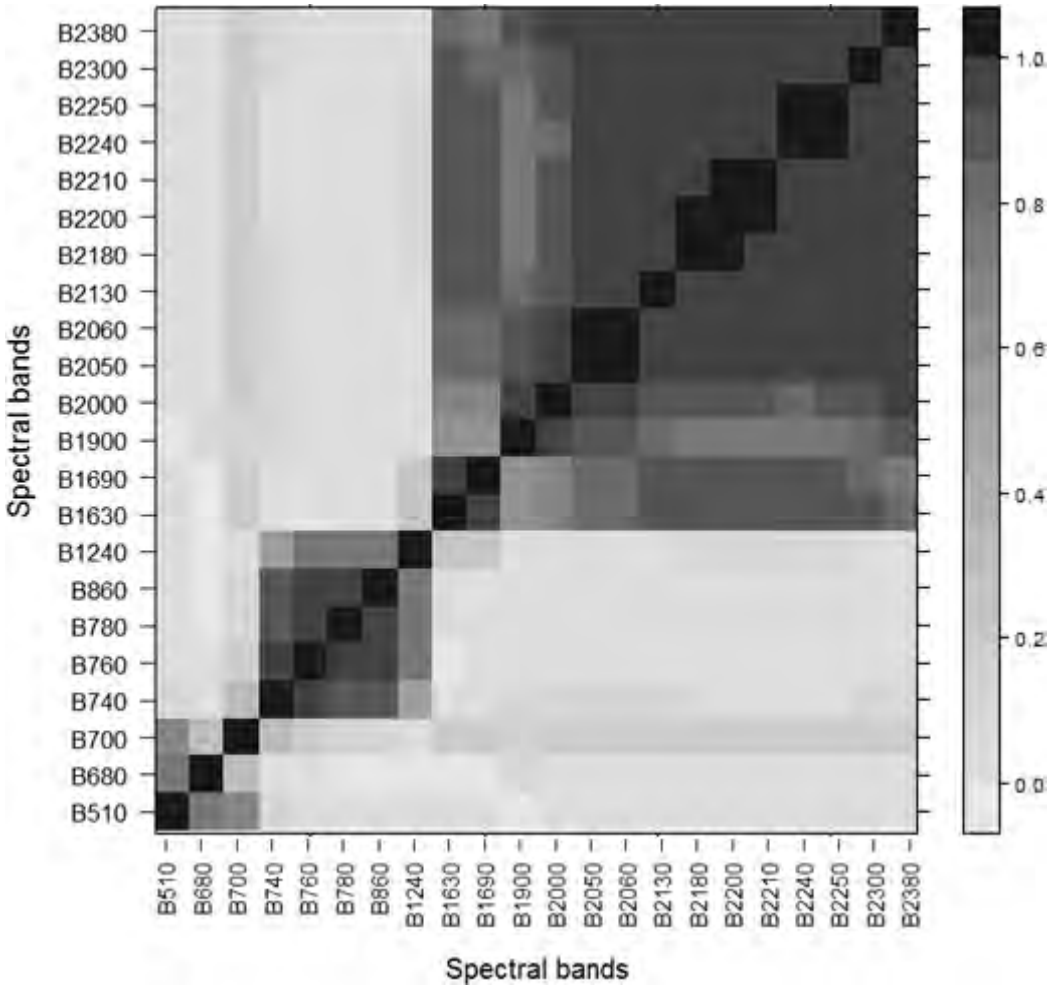

Figure 4.3: Correlation matrix showing the level of correlation between the 22 selected spectral bands (1 nm). The scale bar shows the correlation coefficient values (*R*) between 0 and 1.

4.3.2. Results of the Principal Component Analysis

The PCA of the 421 resampled and 22 selected bands showed that the first three components explained 95 % and 97 % of the variance of the data, respectively (Figure 4.4). The first five components of both data sets explained 99 % of the variance.

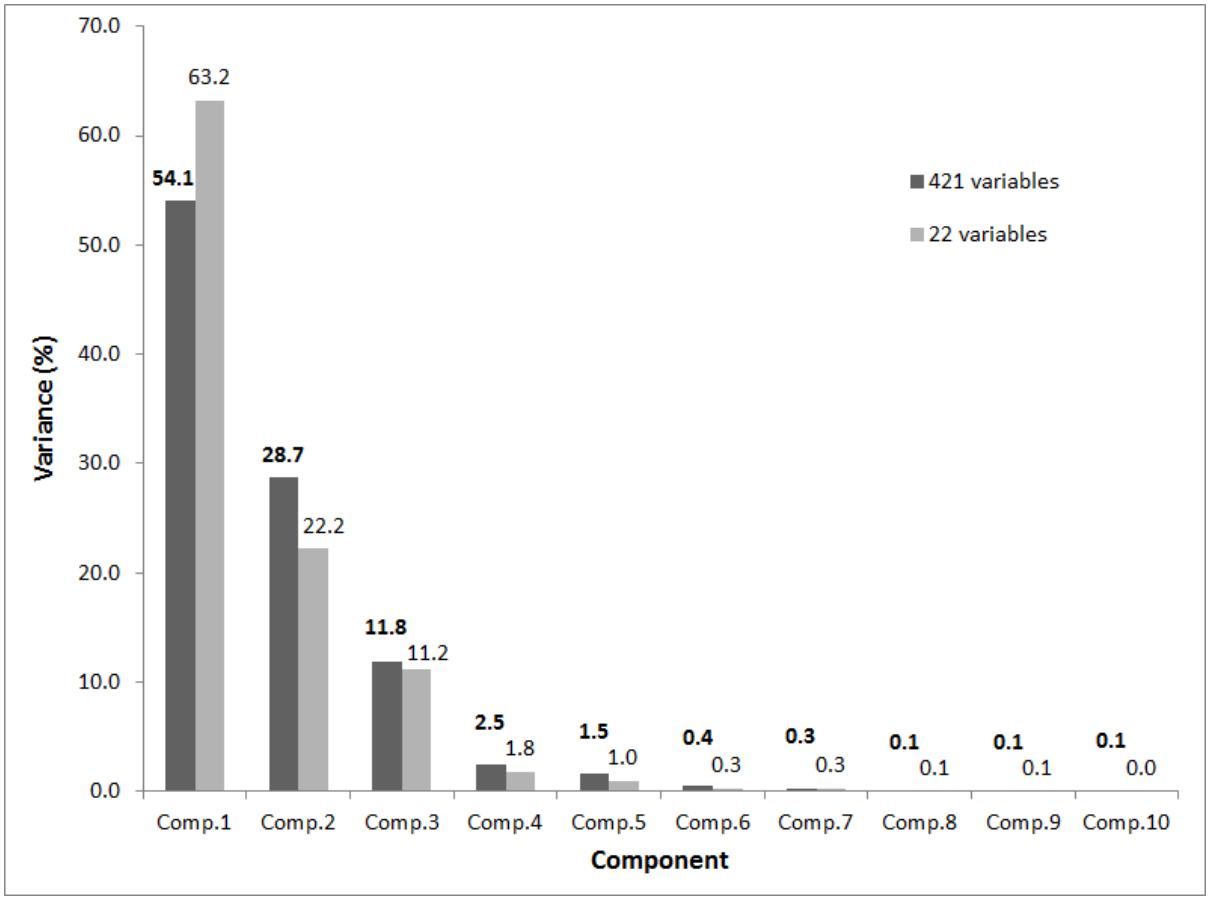

Figure 4.4: Scree plot showing the variance of the first ten components of a PCA of 421 spectral bands (black column with bold labels) and 22 selected spectral bands (grey column with grey labels).

4.3.3. Comparing tree species classification accuracy results

The classification of the untransformed 421 bands showed an overall accuracy of 86±4.7 %, compared to the overall accuracy of 84±4.9 % of the selected 22 bands (Table 4.3). The reduction of the untransformed bands to 22 bands showed no significant difference compared to the 421 resampled bands ($p > 0.44$; Table 4.6).

Table 4.3: Comparison of the prediction accuracies of 421 bands of untransformed leaf-level hyperspectral data and 22 bands relating to plant properties used in species classification (average and standard deviation of 10 iterations).

	Untransformed 421 bands		**Untransformed 22 bands**	
OA (%)	86±4.7		84±4.9	
ACCURACY (%)	**PRODUCER**	**USER**	**PRODUCER**	**USER**
Avicennia marina	85±8.9	87±12.4	86±11.1	87±12.7
Bruguiera gymnorrhiza	93±4.1	90±4.8	93±5.4	92±4.4
Ficus sycomorus	96±4.4	88±6.9	96±5.0	89±6.1
Ficus trichopoda	80±12.0	79±11.0	74±17.8	73±7.4
Hibiscus tilliaceus	71±18.0	87±6.2	69±13.3	83±8.0
Syzygium cordatum	90±6.0	88±10.0	87±6.7	83±8.5

The results of the PCA-RF species classification, where the first three principal components of 421 bands were used, showed an overall classification accuracy (average of ten iterations) of 79±4.2 % (Table 4.4). The classification of the first three components of the PCA-RF of 22 bands was similar, resulted in an overall accuracy of 78±5 % (Table 4.4), and was not significantly different from the 421-band PCA-RF classification where the first three components were used ($p > 0.72$; Table 4.4).

Table 4.4: Comparison of the prediction accuracies of the principal components of 421 bands and 22 bands relating to plant properties used in species classification (average and standard deviation of 10 iterations).

	PCA-RF of 421 bands, 100 components		**PCA-RF of 421 bands, first 3 components of 100 components**		**PCA-RF of 22 bands, 22 components**		**PCA-RF of 22 bands, first 3 components of 22 components**	
OA (%)	92±1.7		79±4.2		91±4.0		78±5.0	
ACCURACY (%)	**PRODUCER**	**USER**	**PRODUCER**	**USER**	**PRODUCER**	**USER**	**PRODUCER**	**USER**
Avicennia marina	95±5.0	93±7.3	62±17.6	66±10.0	96±7.0	93±8.0	73±15.2	71±12.1
Bruguiera gymnorrhiza	96±3.2	95±4.6	91±8.5	94±6.2	98±3.5	97±4.0	92±7.1	92±5.3
Ficus sycomorus	96±3.2	90±6.4	94±4.6	92±6.7	95±5.8	93±5.4	92±8.2	89±2.7
Ficus trichopoda	90±5.3	92±6.2	73±16.5	70±8.7	85±7.1	87±8.8	66±16.1	69±12.2
Hibiscus tilliaceus	81±9.0	95±5.1	71±12.9	82±6.7	79±16.3	91±8.0	69±15.6	79±7.1
Syzygium cordatum	95±3.3	91±3.3	83±8.2	77±9.6	96±4.6	90±8.4	80±12.1	77±9.4

An increase in accuracy of the PCA-RF classifications was observed when a larger number of components were included in the classification (Table 4.4). The 421-band PCA-RF resulted in the highest overall accuracy (92±1.7 %), followed by the use of 22 principal components of the 22-band PCA-RF (91±4 %) (Table 4.4). Using all the components showed a significant increase (t=-9.1, df=11.7, $p < 0.01$ for the 421 bands; t=-6.5, df=17.2, $p < 0.01$ for the 22 bands) of overall accuracy by 13 % compared to using only the first three components of the PCA-RF for both the 421 and 22-band models (Table 4.4).

The CV error of both the 421 and 22 bands reduced by > 2 % for all species when 8 components were used in the PLS-RF classification (Figure 4.5). The PLS-RF classification of 8 components of 421 bands resulted in an overall accuracy of 83±4 %, whereas the PLS-RF classification of the 8 components of 22 bands resulted in an overall accuracy of 84±3.6 % (Table 4.5). No statistically significant differences were noted between the 421-band and 22-band PLS-RF classifications ($p > 0.5$; Table 4.6). The overall accuracy of the PLS-RF classification of 8 components of the 22 bands was significantly higher compared to the PCA-RF of 22 bands where the first three components were used (t=-3.0, df=16.4, $p < 0.01$).

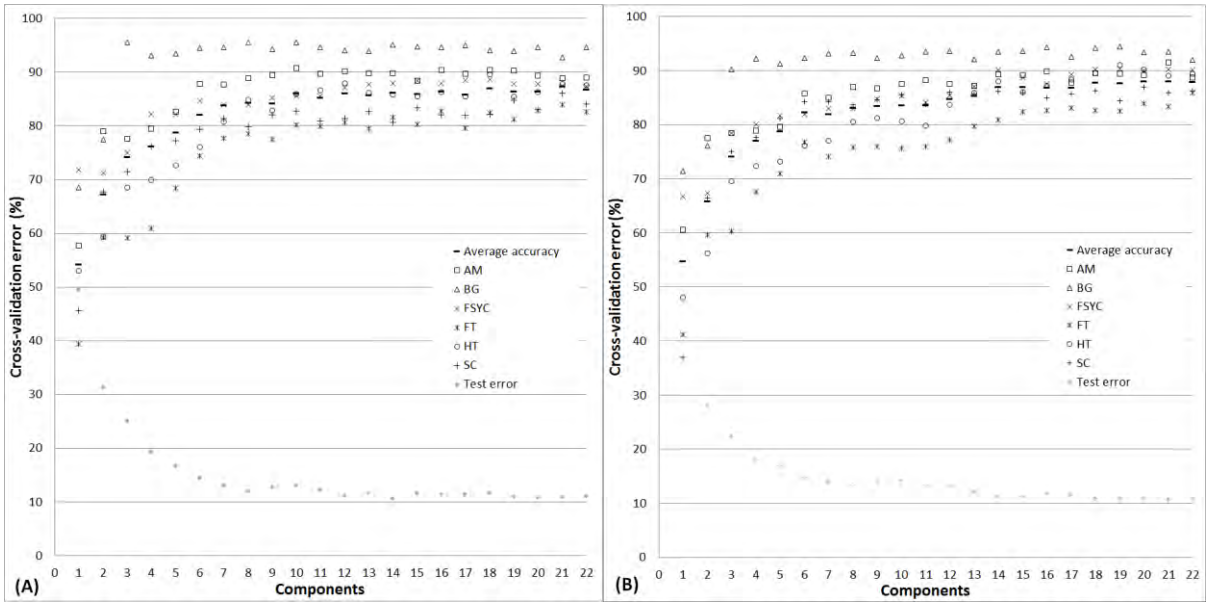

Figure 4.5: Assessing the optimum number of components for species classification using PLS-RF. The average cross-validation error (%) for ten iterations was calculated for each component for the 421 bands (A) and 22 bands (B). The optimal component was selected where the cross-validation error reduced by > 2 % for all species. Species include (AM) *Avicennia marina*, (BG) *Bruguiera gymnorrhiza*, (FS) *Ficus sycomorus*, (FT) *Ficus trichopoda*, (HT) *Hibiscus tilliaceus*, and (SC) *Syzygium cordatum*.

The producer's accuracies of individual tree species for the untransformed 421-band data ranged from 71 % to 96 % whereas the user's accuracies ranged from 79 % to 90 %. When reducing the data to 22 selected bands, the producer's and user's accuracies show a slightly lower minimum, ranging from 69 % to 96 %, and 73 % to 92 %, respectively. The accuracies of individual species of the PCA-RF classification, where only the first 3 components of both the 421 and 22 bands were used, showed comparable ranges in producer's and user's accuracies of approximately 62 % to 94 % for the producer's accuracy and 73 % to 92 %. The accuracies of the individual species of the 421-band PLS-RF models, where 8 components were used for classification, showed similar ranges in producer's accuracy compared to the PCA-RF classifications (producer's = 61 % to 93 %; user's = 76 % to 93 %). The accuracies of the PLS-RF using the 22 selected bands were comparable to the other models (producer's accuracy = 67 % to 91 %), although the user's accuracies were slightly higher in minimum and maximum, ranging from 79 % to 96 %.

Of all the species, *Bruguiera gymnorrhiza* showed the highest user's and producer's accuracies for all the data reduction options (Table 4.3, 4.4 and 4.5). Three species, including *Avicennia marina*, *Ficus trichopoda* and *Hibiscus tilliaceus*, attained some of the lowest user's accuracies (< 75 %) in the untransformed 22-band classification, as well as the PCA-RF classification, using 22 bands and 3 components. An increase in user's accuracies for these three species were observed in the PLS-RF classification of the selected 22 bands, using 8 components, resulting in 89 %, 79 % and 85 % respectively.

Table 4.5: Comparison of the prediction accuracies of partial least square components of 421 bands and 22 bands relating to plant properties used in species classification (average and standard deviations of 10 iterations).

	PLS-RF of 421 bands, 22 components		PLS-RF of 421 bands, 8 components		PLS-RF of 22 bands, 22 components		PLS-RF of 22 bands, 8 components	
OA (%)	88±4.8		83±4.0		87±4.4		84±3.6	
ACCURACY (%)	**PRODUCER**	**USER**	**PRODUCER**	**USER**	**PRODUCER**	**USER**	**PRODUCER**	**USER**
Avicennia marina	93±4.9	89±11.5	90±7.1	87±9.4	90±14.3	89±8.2	88±13.1	89±8.0
Bruguiera gymnorrhiza	90±6.4	92±3.7	93±5.9	93±5.6	90±11.6	95±4.8	91±7.8	96±4.7
Ficus sycomorus	93±10.6	90±6.3	91±11.0	83±7.6	92±7.9	87±6.2	90±9.3	84±7.2
Ficus trichopoda	84±8.1	86±7.6	77±7.1	76±9.7	83±6.8	83±9.7	82±7.1	79±11.2
Hibiscus tilliaceus	77±10.1	89±6.7	61±13.7	81±10.5	76±11.2	88±10.5	67±12.7	85±5.3
Syzygium cordatum	90±6.9	86±13.4	87±6.7	84±12.1	90±5.0	84±13.0	89±3.4	80±11.8

Table 4.6: Differences in overall accuracy for each combination of the data reduction options, using a two-sample t-test between the results of ten classification iterations.

Compared data reduction options	t	*df*	*p*
Untransformed 421b to 22b	-0.7822	17.979	0.4443
PCA+RF 421b3c to 22b	0.3647	17.49	0.7197
PLS+RF 421b8c to 22b	-0.6769	17.847	0.5071

** significant at 99 % confidence interval ($p < 0.01$); * significant at 95 % confidence interval ($p < 0.05$)

4.3. Discussion

This study investigated whether the reduction of leaf-level hyperspectral data to 22 bands, which related to plant biochemical and biophysical properties, will optimise the classification of six evergreen trees of KwaZulu-Natal, South Africa. The selected 22 untransformed bands achieved similar overall accuracies to a larger number of untransformed bands (421 bands) which included redundant bands unrelated to plant properties. Eight of the selected 22 bands were located in the visible, red edge and Mid-Infrared, whereas 14 bands were located in the SWIR. Most of the bands, particularly those in the SWIR, show a high intra-band correlation and as a result, the untransformed 22 band model is over-fitted (Figure 4.3).

The performance of PCA and PLS as data transformation methods for species classification was also compared. The average accuracies of ten iterations of the original and reduced data sets, for both the untransformed and transformed bands, were assessed in the Random Forest classification algorithm. The classification of all the 22-band models achieved similar overall accuracies compared to the original data sets. In the 22-band reduced models, however, redundancy and 'noise' were removed, the data were decorrelated and the number of components optimized. The reduced data sets are therefore for cost-effective, using only 22 bands to achieve similar accuracies, thereby optimising the classification models.

The PCA-RF classification model, where all 22 principal components were used, resulted in the highest overall accuracy of the band-reduced models (91±4 %). This was a significant increase ($p < 0.01$) of 13 % compared to the 3-component PCA-RF model. Smaller

components therefore still contributed to the classification, with the risk of overfitting the model with redundant components. The comparison of the PCA-RF and PLS-RF classification models, where 22 bands were used and the number of components optimised, showed that the PLS-RF model outperformed the PCA-RF model by 6 % ($p < 0.01$). We recommend that PLS should be used for individual species classification rather than PCA. PCA previously also showed poor performance in classification (Cheriyadat and Bruce, 2003; Tsai *et al.*, 2007).

The classification accuracies of the untransformed and optimised PCA-RF models, using the 22 selected bands, showed lower user's accuracies (< 75 %) for *Avicennia marina*, *Ficus trichopoda* and *Hibiscus tilliaceus.* These species achieved user's accuracies > 79 % however, in the optimized PLS-RF model (22 bands and 8 components). The high separability of *Bruguiera gymnorrhiza* from all the other species throughout the various data reduction options and classification models can partly be attributed to its lower concentration in plant pigments over all four seasons (Van Deventer *et al.*, 2013).

Our study was limited to leaf-level spectra of six evergreen trees, sampled in the spring season of a sub-tropical environment. The selection of the band centers for leaf structural components were based on known absorption regions which showed a high coefficient of determination of leaf spectra and nutrients for these trees (Van Deventer *et al.*, 2015b). In another species classification study, the importance of narrow spectral bands was assessed through the canopy spectra of shrubs, grasses, weeds and crop species from African savannas (Thenkabail *et al.*, 2004). The African savanna study reports an optimal number of 22 bands to achieve overall classification accuracies of > 90 %. Six of the 22 bands of the African savanna study were comparable to the 22 bands listed in our study, including those in the red edge region (700 and 760), a band related to leaf water (1245) and three bands in the SWIR (2000, 2240 and 2300). The differences for the remaining 16 bands between the two studies can be attributed to the differences in the selection approaches followed. We pre-selected band centers of known absorption features in the visible whereas bands between 800-2500 nm were selected if they showed a high coefficient of determination with foliar nutrients. In contrast, the African savanna study assessed band importance through a combined and automated selection approach, which resulted in bands from within an absorption trough to be selected, as well as band centers. In a European study of temperate tree species classification with hyperspectral image data (Fassnacht *et al.*, 2014), nine 50 nm regions were identified as important through feature selection approaches. Seven of the 22 selected bands of our work fall within the regions of the European study. Further work will be required to assess the relevance of the 22 selected bands of our study to other vegetation types and climatic regions.

In the classification of various tree species in the European study, the optimum number of bands was identified as between 15 and 20 (Fassnacht *et al.*, 2014). The classification of weeds in the African savanna study (Thenkabail *et al.*, 2004), attained overall accuracies above 90 % using between 13 and 22 bands, with marginal increase of the accuracy towards

30 bands, and reaching asymptote beyond 30 bands. Our study showed that the pre-selection of 22 bands, related to plant properties, effectively reduce hyperspectral data while optimising tree species discrimination for six evergreen trees. The importance of the 22 selected bands should be further explored to identify the plant components which contribute most to the discrimination power, and determine the optimum number of bands.

We recommend the extension of the two-step data reduction procedure, with the selection of bands which relate to plant biochemical and biophysical properties followed by a PLS-RF classification, to other deciduous and evergreen tree species, and for various seasons.

4.4. Conclusion

The most important conclusions from this Chapter include:

- Twenty-two narrow bands, which relate to known absorption regions or indices associated with biochemical and biophysical properties of plants have shown a high coefficient of determination between leaf spectra and nitrogen (Chapter 3). These bands were found to be an effective data reduction method of hyperspectral data for the classification of six evergreen tree species of a subtropical forest in South Africa.

- The transformation of highly correlated spectral bands and the classification of the species were achieved through a two-step algorithm which combines the Partial Least Square and Random Forest algorithms (PLS-RF). PLS-RF outperformed the Principal Component Analysis and Random Forest algorithm combination in species classification resulting in a significantly higher overall classification accuracy (6 %; $p < 0.01$) and increases in user accuracies.

Following the effective data reduction and classification of the six evergreen tree species for the spring season in this Chapter, the separability of the tree species remains to be assessed for the winter, summer and autumn seasons using hyperspectral data at leaf level. In addition, the hypothesis should be tested to see whether multi-seasonal information would improve the classification above a single season at hyperspectral level, as well as for multispectral sensors.

CHAPTER 5: COMPARING THE CLASSIFICATION ACCURACIES OF SIX EVERGREEN TREE SPECIES ACROSS SINGLE and MULTIPLE SEASONS FOR HYPERSPECTRAL, WORLDVIEW-2 AND RAPIDEYE SENSORS USING LEAF-LEVEL SPECTRA

This chapter is the first revision of the journal paper submitted:

Van Deventer H, Cho O, Mutanga O. Revision of first submission. Improving tree species classification across four phenological phases with multi-seasonal data and band combinations: six subtropical evergreen trees as case study. Submitted to the International Journal of Remote Sensing.

Abstract

Remote sensing offers a feasible means to monitor tree species at a regional level where species distribution and composition is affected by the impacts of global change. Furthermore, the temporal resolution of space-borne multispectral sensors offers the ability to combine phenologically important events for the optimisation of tree species classification. In this study, we determined whether multi-seasonal spectral data (winter (dormancy), spring (flowering), summer (flowering) and autumn) improved the classification of six evergreen tree species in the subtropical forest region of South Africa when compared to a single season, for hyperspectral data, WV2 and RE. Classification accuracies of the test data were assessed using a Partial Least Square Random Forest algorithm (PLS-RF). The accuracies were compared between single seasons and multi-season classification and across seasons using ANOVA and post-hoc THSD tests. The average OA of the hyperspectral data ranged from a minimum of 90±3.5 % in winter to a maximum of 92±2.7 % in summer, outperforming the WV2 and RE sensors with an average OA of between 8 and 10 % (p < 0.02, Bonferroni corrected). The classification of multiple seasons increased the average OA and decreased the number of species pair confusions for the multispectral classifications. The producer's and user's accuracies of the hyperspectral classification were > 82 % and showed no significant change using multi-season data. Multiple seasons may therefore be beneficial to multispectral sensors with ≤ 8 bands, yet remains to be tested for other species and climatic regions.

5.1. Introduction

Globally, more than 67 % of the 9 500 tree species are considered to be threatened by the International Union for Conservation of Nature's Species Survival Commission (IUCN/SCC) (IUCN, 2001; IUCN/SSC Global Tree Specialist Group, 2015). While it is estimated that approximately 13 % of forests are formally protected (FAO, 2010), an alarming rate of deforestation was observed for South America (3.3 million ha per annum) and Africa (1.6 million ha per annum) between 1990 and 2005 (FAO and JRC, 2012). The impacts of global change, particularly a rise in temperature and sea-levels as well as changes in rainfall patterns, are expected to cause a shift in species distribution, composition and functioning (Kirschbaum, 2000; Sardans and Peñuelas, 2012). A rise in temperature and decline in precipitation can, for example, result in the decline of a tree species and change in vegetation type altogether. Threatened tree species and some threatened forest types, such as mangroves, often occur in narrow range habitats which are highly fragmented (Oldfield *et al.*, 1998; Valiela *et al.*, 2001) and are therefore more difficult to map and monitor compared to general forest growth and deforestation (FAO and JRC, 2012). In order to detect losses and changes in tree species distribution and condition, tools are required to assess the status and changes across time and space in a consistent manner and at an appropriate scale.

Remote sensing is an ideal tool for the monitoring of tree species. A number of studies demonstrated that airborne hyperspectral sensors are successful in separating between tree species in mixed forest and savanna landscapes with overall accuracies above 69 % (Holmgren *et al.*, 2008; Naidoo *et al.*, 2012; Dalponte *et al.*, 2012; Fassnacht *et al.*, 2014). Hyperspectral sensors remain costly to acquire however, and offer only a limited regional extent. Space-borne multispectral sensors, in contrast, provide multitemporal regional overviews but have fewer spectral bands than the hyperspectral sensors. Very high spatial resolution multispectral sensors, such as SPOT, IKONOS and Quickbird, were found to be suitable for tree species classification because the spatial resolution matches canopy sizes (≤ 5 m) of trees, even though these sensors are limited to the four traditional bands in the blue, green, red and near-infrared (NIR) regions of the electromagnetic spectrum (Wang *et al.*, 2004). The accuracies of tree species classification using IKONOS, for example, ranged between 57 – 86 %, with producer's or user's accuracies below 50 % for some species (Wang *et al.*, 2004; Carleer and Wolff, 2004; Pu and Landry, 2012).

In 2009 two multispectral sensors, WorldView-2 (WV2) and RapidEye (RE) were launched. Both sensors match spatial resolution to tree canopy level (≤ 5 m). The sensors utilised additional bands, such as the red-edge band considered beneficial for the estimation of vegetation parameters and species classification (Mutanga and Skidmore, 2004; Cho *et al.*, 2008; Mutanga *et al.*, 2012; Adelabu *et al.*, 2013). The additional bands of these sensors resulted in an increase in the overall classification accuracy of tree species compared to using only the four traditional bands (Pu and Landry, 2012; Immitzer *et al.*, 2012; Omer *et*

al., 2015). Pu and Landry (2012), for instance, reported a 6 % increase in the overall accuracy for the sunlit canopies of seven species in the United States of America; Omer et al. (2015) reported an increase of 11 - 12 % for six tree species in a mixed forest in South Africa; and Immitzer et al. (2012) reported a 5 – 7 % increase in overall accuracy for ten tree species in Austria. The overall classification accuracy of tree species classification using WV2 exceeded 77 % (Kanniah, 2011; Cho *et al.*, 2015; Omer *et al.*, 2015). For the RapidEye sensor, the overall classification of tree species in a savanna landscape of Botswana achieved accuracies above 85 % (Adelabu *et al.*, 2013). Compared to the very high spatial resolution sensors, the WV2 and RE do appear to increase the accuracies of tree species classification. Regardless of the improvement, a number of tree species remain poorly separable (< 50 %) in the classification when using multispectral data whereas hyperspectral data appears to overcome this limitation with a wider range of spectral bands, potentially increasing the producer's and user's accuracies to above 50 % in some studies (Holmgren *et al.*, 2008; Immitzer *et al.*, 2012). The variation in classification accuracy of tree species needs to be assessed across hyperspectral and the new multispectral sensors to understand the pros and cons of using the sensors for tree species classification.

Space-borne sensors also offer the additional benefit of multitemporal data for tree species classification and monitoring. A number of studies assessed the single season in which the overall accuracy for tree species were the highest. In a temperate forest of the United States of America, a maximum overall accuracy of 76 % was attained in October (autumn) for deciduous species at the time of leaf colour changes (Key *et al.*, 2001). Similarly the overall accuracy was highest in autumn (91 %) for a mixed conifer and broadleaf forest in Sweden (Holmgren *et al.*, 2008). For 25 subtropical trees in Hong Kong, the winter seasons achieved the highest overall accuracy of 91 % with the change in leaf colour (Fung *et al.*, 2003). These studies were undertaken in temperate and subtropical climatic regions with tree species including coniferous, evergreen and deciduous species in a mixed forest, where the phenological event of leaf fall enhanced species discrimination. For evergreen tree species, leaf fall occur throughout the year and may therefore be less suitable as a phenological event for separation. Other phenological events such as seeding or flowering may offer alternative means of discrimination for evergreen tree species (Sobhan, 2007). Key *et al.* (2001) also argued that the timing of phenological events could be important in optimising tree species discrimination and that multitemporal data could optimise species classification. In separating tree species in a mixed forest, Key *et al.* (2001) combined aerial photography images from five dates between May and October using between three and four bands, achieving an overall classification accuracy of 74 % (lower than the 76 % for the autumn season) and a maximum KHAT accuracy of 0.51. A study in Germany demonstrated that the separability of seven graminoid species improved between 4 % and 7 % when multitemporal RE images, between March and October over three years, were used in a support vector machine classifier. The optimum dates were however not linked to specific phenological events, nor optimised for the least number of dates which optimise the species

classification. Changes in plant properties across phenological events or seasons result in changes of the absorption features of pigments, foliage biomass, water content and nutrients, as well as the relationship between spectra and foliar pigment or nutrient concentration (Gond *et al.*, 1999; Kokaly and Clark, 1999; Stylinski *et al.*, 2002; Nakaji *et al.*, 2006; Sobhan, 2007; Sauceda *et al.*, 2008; Panigraphy *et al.*, 2012; Dillen *et al.*, 2012; De Weirdt *et al.*, 2012; Van Deventer *et al.*, 2015b). The increased representation of these variations in plant properties through multi-season data is therefore expected to improve species discrimination when compared to a single season. For evergreen tree species, the optimal phenological event remains to be assessed, and in addition, whether multi-season data with greater representation of phenological events would improve species discrimination when compared to a single season.

The optimisation of multiple seasons for tree species classification may have a number of benefits. In regions with a high annual percentage of cloud cover (NASA, 2015), multi-season classifications may be a reasonable alternative. The tropics for instance, are known for a high diversity of tree species (Mutke and Barthlott, 2005), yet the high percentage of cloud cover during wet seasons limits species classification assessments (Asner, 2001; Ju and Roy, 2008). Despite the improvements of light detection and ranging (LiDAR) and synthetic aperture radar (SAR) in contributing to feature recognition and penetrating clouds respectively, optical data remains an important source for the classification of most features (Green *et al.*, 1998; Holmgren *et al.*, 2008; Dalponte *et al.*, 2012).

In an attempt to address some of the knowledge gaps, such as the best sensor and phenological event for optimising evergreen tree species classification, the variation in accuracy across sensors and seasons were evaluated for evergreen tree species in a subtropical environment. Six evergreen tree species were sampled in the subtropical coastal forest of the KwaZulu-Natal Province of South Africa. The classification accuracies were assessed using leaf-level data at hyperspectral scale and simulated WV2 and RE sensor scales. Accuracies were calculated for four single seasons (winter, spring, summer and autumn) and an aggregated multi-season data set. The objectives of this study were to:

(1) Investigate how leaf reflectance spectra of tree species vary across seasons for each sensor.

(2) Determine how the accuracies of the tree species classification vary between hyperspectral and multispectral sensor across the four single seasons (winter, spring, summer and autumn).

(3) Assess whether multiple seasons (the aggregation of the four single seasons into a single data set) will improve the classification of the six evergreen tree species when compared to a single season for both hyperspectral and multispectral sensors.

5.2. Methods

5.2.1. Study Area

The iSimangaliso Wetland Park (28°S, 32°30'E) is located in the KwaZulu-Natal Province of South Africa, approximately 200 km north of Durban (Figure 1; Inset *a*). The Park extends over ±218 000 Ha of land along 190 km of coastline, with vegetation and land cover categories (Figure 1; Inset *b*) consisting of natural shrubs and grassland (± 42 %), coastal and dune forests (± 17 %), wetland (± 18 %) and estuarine (± 17 %) systems as well as transformed (± 6 %) land (GeoTerraImage (GTI), 2010; Ezemvelo KZN Wildlife, 2011). The Park is listed as both a Ramsar and World Heritage Site (WHS) on grounds of the high biodiversity of fauna and flora in the region (Cowan, 1999). Owing to the large extent of wetlands and presence of dangerous animals such as hippopotami, crocodiles, rhinoceroses and the Cape buffalo (The iSimangaliso Wetland Park, 2014), safe access is limited for monitoring vegetation through fieldwork. Consequently, the Park will benefit greatly in using earth observation for vegetation assessments such as tree species monitoring at a regional scale.

Sub-tropical climate conditions prevail along a narrow ±6 km wide zone on the east coast of South Africa, with the most southern tip of mangroves recorded at about 31° south (Spalding *et al.*, 2010). The Mean Annual Precipitation (MAP) ranges from 1000 mm to 1500 mm in this coastal corridor, but decreases to below 1000 mm inland (Middleton and Bailey, 2008). In the Park, mean temperatures during summer range from 23 – 30°C, and can decrease to approximately 10°C during the winter periods (Sokolic, 2006). As a result of the climatic conditions and wetlands, critically endangered mangrove and swamp forests occur in this corridor. Other evergreen and deciduous tree species, associated with sub-tropical climate conditions, are found in the dune and coastal sandy forests in the Park.

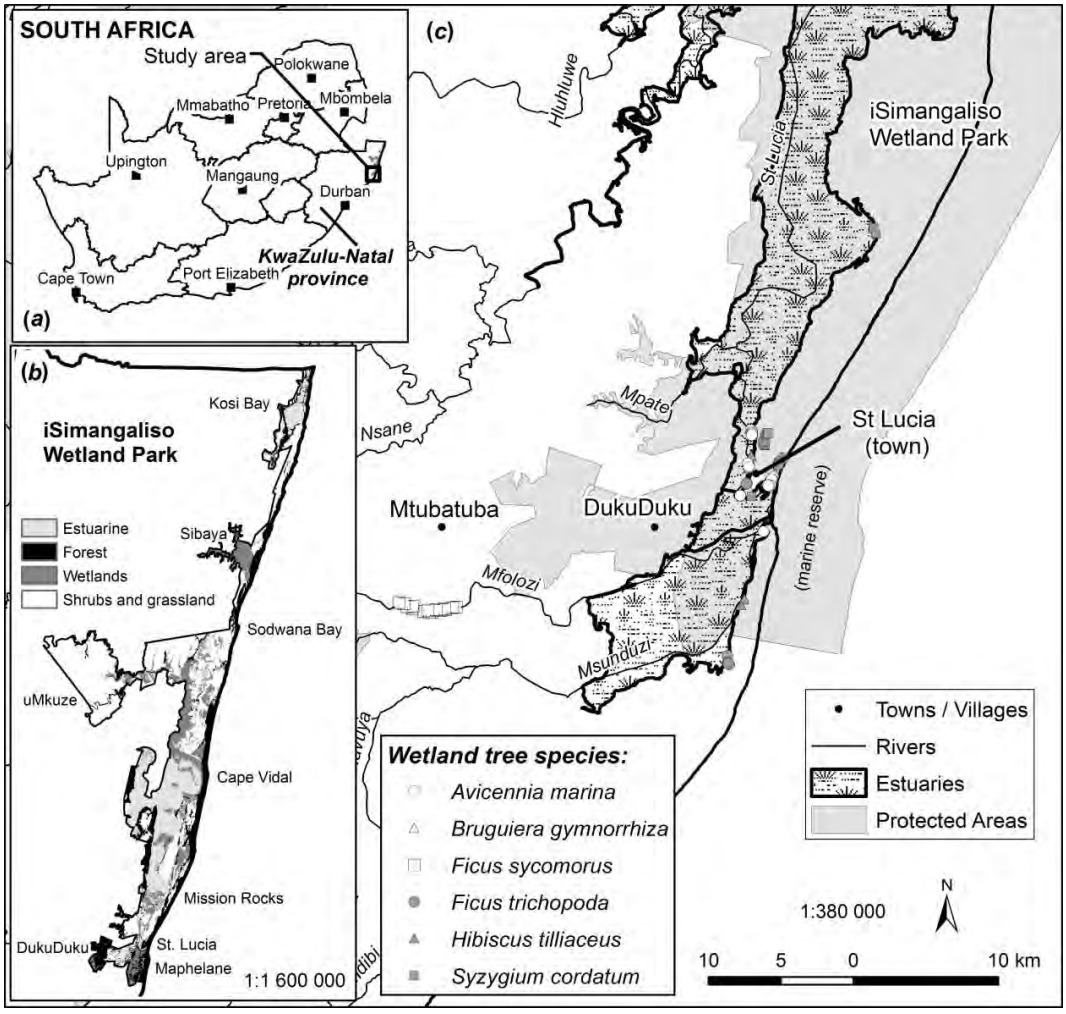

Figure 5.1: The study area is within the iSimangaliso Wetland approximately 200 km north of Durban in the KwaZulu-Natal Province of South Africa (Inset *a*). Vegetation and land cover comprises mostly of natural shrubs, grassland, forests and wetlands (Inset *b*). Six tree species were sampled along the uMsunduzi, uMfolozi and St Lucia estuarine systems (Inset *c*).

5.2.2. Sampling protocol

Six evergreen tree species (Table 5.1; Figure 5.1 Inset *c*) were sampled over four seasons (winter, spring, summer and autumn) between 2011 and 2012. The six evergreen tree species had distinctly different leaf shapes from one another (Table 5.2). Four of the six trees were in flower in both the spring and summer sampling campaigns, although the flowers of the mangroves (*Avicennia marina* and *Bruguiera gymnorrhiza*) were tiny compared to the large flowers of *Hibiscus tilliaceus* and the fluffy flowers of *Syzygium cordatum*. The fruits of the mangroves blend in with the leaves, the fruits of the figs were not large compared to the canopy sizes and were mostly carried below the leaves, but the purple fruit of *Syzygium cordatum* stood out in stark contrast to the green leaves.

Five green and fully expanded leaves were collected from across sun-exposed canopies of mature trees using a telescopic pruner, extending the reach to approximately 3.2 m. The leaves were placed in zip-lock bags in a cooled container and transported back to the laboratory.

Table 5.1: Number of tree species sampled across four seasons (number of leaves is indicated in brackets for the winter season only).

Tree species	Common name	Acronym	Trees Winter (*n* =)	Trees Spring (*n* =)	Trees Summer (*n* =)	Trees Autumn (*n* =)	Total number of trees per species (*n*=)
Avicennia marina	White mangrove	AM [2]	21(105)	21	21	21	84
Bruguiera gymnorrhiza	Black mangrove	BG [1, 2]	19(95)	19	19	19	76
Ficus sycomorus	Sycamore fig	FSYC [3]	15(75)	15	15	15	60
Ficus trichopoda	Swamp fig	FT [1, 3]	11(55)	11	11	11	44
Hibiscus tilliaceus	Lagoon hibiscus	HT [3]	30(150)	30	30	30	120
Syzygium cordatum	Waterberry	SC [3]	17(85)	17	17	17	68
Total per season:			113(564)	113	113	113	***452***

[1] - Protected tree species considered critically endangered (RSA, 1998; Mucina and Rutherford, 2006; Boon, 2010)

[2] - Internationally, population decreasing (Oldfield *et al.*, 1998; FAO, 2011)

[c] - IUCN status not assessed (Oldfield *et al.*, 1998)

5.2.3. Protocol for spectral collection

The leaf-clip device of an Analytical Spectral Device (ASD) spectroradiometer (FieldSpec Pro FR, Analytical Spectral Device, Inc, USA) was used to record a spectral measurement of the adiaxal surface of each of the five leaves within 3 to 5 hours after collection. The device is an accessory that ensures the exclusion of light interference when reflectance is recorded. The ASD covers the spectral range between 350 nm to 2500 nm with a 1.4 nm sampling interval between 350 - 1050 nm range, and a ± 2 nm between 1 050 – 2 500 nm. A white reference was taken with the white panel of the leaf clip, prior to the measurements of each tree with the black panel. Radiance was converted to reflectance against the scans of the white reference panel.

Table 5. 2: Description of leaf, flower and fruit characteristics of the six evergreen tree species (Boon, 2010). The flowering and fruit periods are indicated in brackets.

Tree species	Leaf	Flower	Fruit
Avicennia marina	Olive-green, about 12 – 40 mm in length	Small yellow-orange (Oct-Jan/May)	Grey-green, 25 mm diameter (Dec-Apr, ripe in Mar)
Bruguiera gymnorrhiza	Shiny dark to yellowish green, ± 120 mm length x 60 mm width (leaf drop is continuous)	Creamy white, 40 mm diameter (±All year)	Green leathery (not specified)
Ficus sycomorus	Green and hairy, 150 mm length x 110 mm width	-	Reddish-orange when ripe, 30 mm diameter (not specified)
Ficus trichopoda	Shiny dark green, leathery, heart-shaped, 300 mm length x 230 mm width	-	Red, 10 – 20 mm diameter (Sept – Apr)
Hibiscus tilliaceus	Olive-green heart-shaped, 150 mm diameter	Large yellow with deep reddish-purple centre which later turns coppery-apricot, 80 mm diameter (Aug - May)	Round capsule, 25 mm diameter (Sep – Jun)
Syzygium cordatum	Bluish to dark green, elliptic 100 length x 80 mm width,	Creamy-white (Aug – Mar)	Deep purple, oval ±18 x 9 mm (Oct-Jun)

5.2.4. Data preparation

For the hyperspectral data analysis, the dimensionality of the leaf reflectance data was reduced to band centers of absorption features related to plant properties. The 22 bands selected had shown a high coefficient of determination between foliar pigment or nutrient concentrations and leaf reflectance across four seasons, and were found effective in reducing and optimising the data for classification (Van Deventer *et al.*, 2015a; Van Deventer *et al.*, 2015b). The bands cover the visible to SWIR regions of the spectrum and relate to pigments (510, 680, 700, 760 nm), foliage biomass (740, 780 nm), leaf water content (860, 1240 nm) as well as proteins, starches and other nutrients (1630, 1690, 1900, 2000, 2050, 2060, 2130, 2180, 2200, 2210, 2240, 2250, 2300, 2380 nm) (Curran, 1989; Elvidge, 1990; Gao, 1996; Gitelson *et al.*, 2002; Gitelson and Merzlyak, 2004; Mutanga and Skidmore, 2004; Gitelson *et al.*, 2006; Cho *et al.*, 2007). The 22 bands proved to optimise the classification of the six tree species for the spring season compared to a large number of hyperspectral bands (Van Deventer *et al.*, 2015a). One data set was compiled for each of the four single seasons (winter, spring, summer and autumn) with each 22 variables and then aggregated into a multi-season data set with 88 variables for a multi-season classification. The 1 nm leaf-level data were resampled to the bands of the two multispectral sensors WV2 and RE (Table 5.3), using the Gaussian model (full-width half-maximum) and default spectral library information files in the Environment for Visualizing Images (ENVI) software (v.5.2, ITT Visual Information Systems, 2012-2014). The reflectance data for single seasons, with 8

variables for WV2 and 5 variables for RE, was also aggregated into multi-season data sets of 32 and 20 variables respectively.

Table 5. 3: Descriptive information of the WorldView-2 and RapidEye multispectral space-borne sensors.

Details:	WV2	RapidEye
Spatial resolution (pixel size)	2 m	5 m
Temporal resolution:	1.1 – 3.7 days	5.5 days
Bands	Coastal 400 – 450 nm	-
	Blue 450 – 510 nm	Blue 440 – 510 nm
	Green 510 – 580 nm	Green 520 – 590 nm
	Yellow 585 – 625 nm	-
	Red 630 – 690 nm	Red 630 – 685 nm
	Red-edge 705 – 745 nm	Red-edge 690 – 730 nm
	NIR1 770 -895 nm	NIR 760 – 850 nm
	NIR2 860 – 1040 nm	-
Panchromatic	Yes, 0.46 m spatial resolution	No

5.2.5. Data analysis of leaf-level data

The variation of the leaf spectra of the six tree species was compared for each sensor within a single season, listing the number of statistically significant differences per band as percentage of the total number of comparable species pairs. A parametric one-way ANalysis Of Variance (ANOVA) was used to assess differences between species for each band and each season in the R software (RStudio Inc. v. 0.98.507, 2009-2013). To account for the multiple comparisons between the six species, a post-hoc Tukey Honest Significant Difference (HSD) test was done and the alpha levels corrected for the Bonferroni effect (McDonald, 2008). The alpha level was adjusted for the 15 comparable species pairs in each band and season, resulting in an alpha level (p = 0.05/15) of $p < 0.03$ considered significant at a 95 % confidence interval.

The separability of the six tree species was subsequently assessed using an algorithm which combines the Random Forest (RF) decision-tree algorithm (Breiman, 2001) with the Partial Least Square (PLS) algorithm. RF is a non-parametric decision-tree classifier which is considered appropriate for the classification of tree species when using hyperspectral data (Naidoo *et al.*, 2012; Clark and Roberts, 2012; Dalponte *et al.*, 2012; Adelabu and Dube, 2014). Hyperspectral data are often highly correlated and not normally distributed, and requires a non-parametric classifier for optimisation in classification (Fassnacht *et al.*, 2014; Van Deventer *et al.*, 2015a). RF is furthermore effective for processing both small and large amounts of variables, because of the sampling and bootstrapping procedure at various nodes within the decision 'forest' (Prasad *et al.*, 2006; Grossmann *et al.*, 2010). Ideally, the highly correlated bands required decomposition to avoid redundancy and overfitting of the model (Pearson, 1901; Hotelling, 1933; Saeys *et al.*, 2007). The PLS method showed superior performance in transforming data for classification because the distribution of both the explanatory and response variables is considered (Wold, 1966; Wold *et al.*, 2001; Cheriyadat

and Bruce, 2003; Tsai *et al.*, 2007). The PLS-RF algorithm in the R software (RStudio Inc. v. 0.98.507, 2009-2013) combines the benefits of both PLS and RF algorithms (Boulesteix *et al.*, 2008), through first decomposing and scaling the predictor variables prior to classification. Owing to the benefits of the transformation and non-parametric classification for spectral data, the PLS-RF algorithm has been used for tree species classification in this study.

An iterative bootstrap (100 times) was used to evaluate both the optimum *ntree* per season, calculate the overall accuracy (OA) and the producer's and user's accuracies. The bootstrap included the following sequential steps:

- First the data were split into training and test data sets ensuring an equal number of leaves of each tree species are selected. The data were split into 2/3rd for the training and 1/3rd for the test data, guided by the smallest number of leaves recorded for a species in a single season (*Ficus trichopoda* = 55 leaves). This resulted in the extraction of 36 leaves of each species (totalling 216 leaves) for the training and 19 leaves of each species (totalling 114 leaves) to the test data set of single seasons (winter, spring, summer and autumn).

- Second the training data were used to build a PLS-RF decision forest and predict the species using the test data set (Boulesteix *et al.*, 2008). For the PLS regression, the maximum number of components were used for each classification, equal to the number of variables available. The *mtry* variable was left as the default (for classification it defaults to the square root of the number of variables), the *minsplit* variable was set at four, accounting for the small number of observations per species (Boulesteix *et al.*, 2008) and the number of 'trees' to build in the decision forest (*ntree*) kept at 500 to compare between the various classifications. The average of a 100 overall, producer's and user's accuracies of every *ntree* option per season was calculated.

The final results of the OA, producer's and user's accuracies of each tree species is compared between the sensors for the single seasons and multi-season classifications. The overall accuracy calculates the percentage of correctly classified trees by the total number of trees evaluated (Congalton, 1991). The producer's accuracy calculates the total number of trees that was correctly classified as a percentage of the total number of reference trees for that species, in this case 114 leaves. The producer's accuracy measures of the probability of being able to correctly classify a particular tree species (omission error). The user's accuracy, on the other hand, calculates the number of trees as a percentage of the total number of trees that were classified as a particular species (commission error), and indicates the reliability of the classification of a tree truly belonging to a particular species (Story and Congalton, 1986).

Differences between sensors were assessed using a one-way ANalysis Of Variance (ANOVA) in the R software (RStudio Inc. v. 0.98.507, 2009-2013) using the 100 recorded values of the

bootstrap. The significance of differences between sensors was assessed for both the overall accuracy as well as the producer's and user's accuracies. To account for the multiple comparisons, a post-hoc Tukey Honest Significant Difference (HSD) test was done and the alpha levels corrected for the Bonferroni effect (McDonald, 2008). Comparison between the three sensors set resulted in three comparable pairs, and therefore an adjusted alpha level (p = 0.05/3) of $p < 0.02$ was considered significant at a 95 % confidence interval. The differences between the accuracies of the single and multi-season classifications were also assessed using a one-way ANOVA and the 100 recorded values of the bootstrap. The post-hoc Tukey Honest Significant Difference (HSD) test accounted for ten comparable pairs with an adjusted alpha level (p = 0.05/10) of $p < 0.005$ to be considered significant at a 95 % confidence interval.

5.3. Results

5.3.1. Variation of spectral reflectance of tree species across seasons

The average leaf reflectance of each tree species, between 400 and 2 500 nm, was typical of vegetation across all four seasons (Figure 5.2). Across the four seasons, *Bruguiera gymnorrhiza* showed the highest reflection of all species between the visible (400 nm) and early mid-infrared (MIR; 1500 nm) region, except for the spring season where the reflectance of *Syzygium cordatum* were highest in the visible region. Between the early MIR (1500 nm) to the far MIR (2500 nm) region, *Ficus sycomorus* and *Hibiscus tilliaceus* showed higher reflectance curves of all species across the four seasons. Most of the species were highly separable (> 70 % of comparable pairs were significantly different) in the red-edge region as well as the MIR to SWIR regions for winter, spring, summer and autumn. Interestingly the bands 2130, 2180, 2200, 2210, 2240, 2250 and 2300 nm showed a 100 % separability between the six species in the summer season as well as 2240 nm in the spring season. Only five of the 22 bands had statistically significant differences between the species < 70 %, including 510 nm (winter and summer), 680 and 700 nm (all single seasons), 860 nm (spring) and 1240 nm in winter, spring and summer.

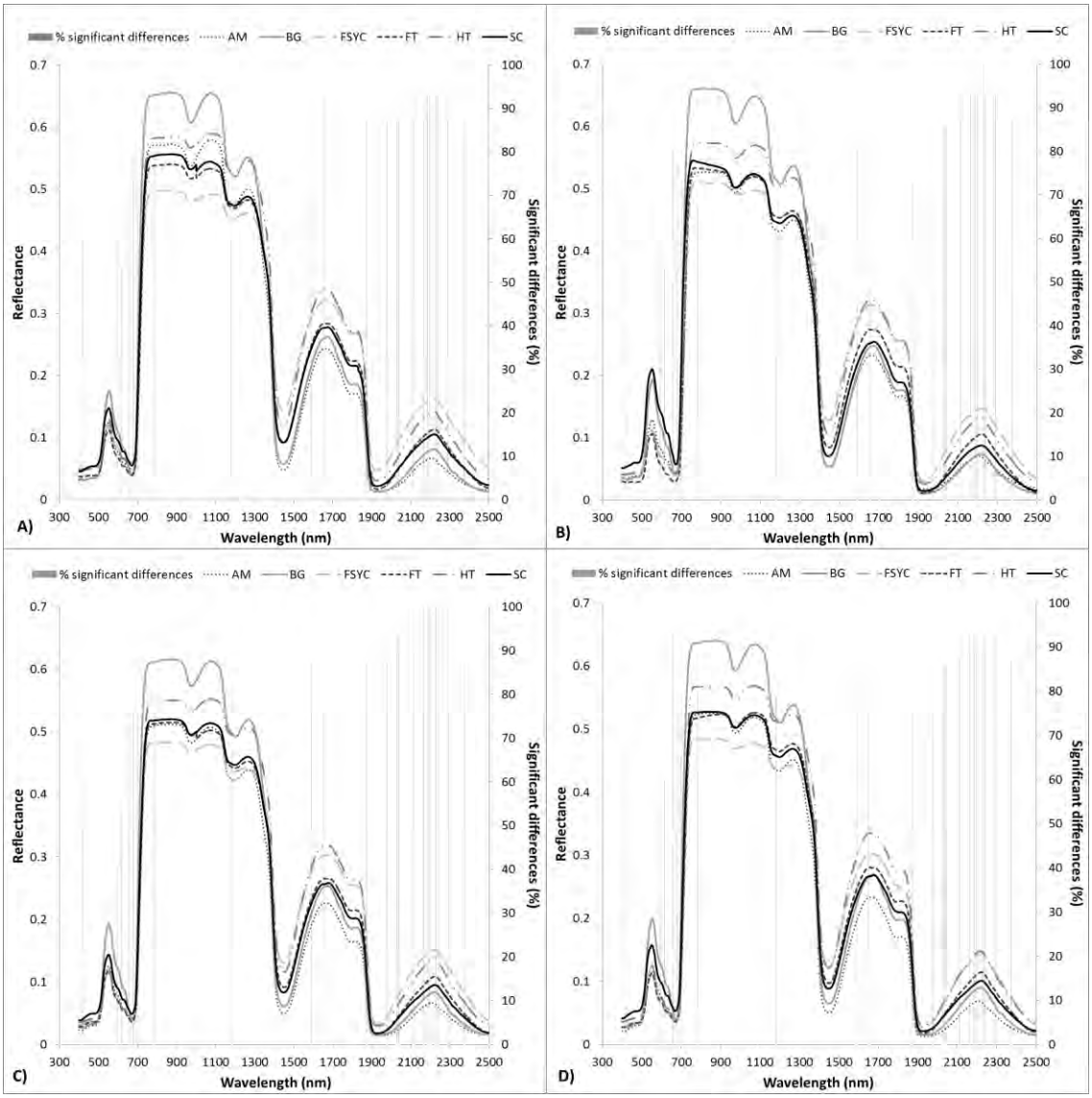

Figure 5.2: Average leaf spectra reflectance between 400 and 2 500 nm of six tree species for (A) Winter; (B) Spring; (C) Summer; (D) Autumn. The number of significant different species pairs ($p < 0.03$, Bonferroni corrected) is indicated as a percentage of the total number of comparable species pairs (15) for each of the 22 selected spectral bands related to plant properties. Tree species include AM: *Avicennia marina*; BG: *Bruguiera gymnorrhiza*; FSYC: *Ficus sycomorus*; FT: *Ficus trichopoda*; HT: *Hibiscus tilliaceus*; and SC: *Syzygium cordatum.*

The reflectance data showed a high variability in the green (band 3), red-edge (band 6), NIR1 (band 7) and NIR2 (band 8) regions for all seasons (Figure 5.3). Similar to the hyperspectral data, reflectance data for *Bruguiera gymnorrhiza* showed the highest reflection of all species in bands 3 and 6-8 across the seasons. *Syzygium cordatum* also showed an increase in reflection in the green (band 3), yellow (band 4) and red-edge (band 6) regions in spring compared to the other species. The highest percentage of separable species pairs (> 70 %) was attained in the two NIR bands (bands 7 and 8) across all seasons, as well as the coastal (band 1), blue (bands 2) and red-edge bands (band 6) in spring and autumn. The coastal band (band 1) showed a high number of separable species pairs (80 %) in the spring, summer and autumns seasons. The spring season attained the highest number of separable pairs for all the RE bands based on the parametric ANOVA analysis (> 67 % across all bands).

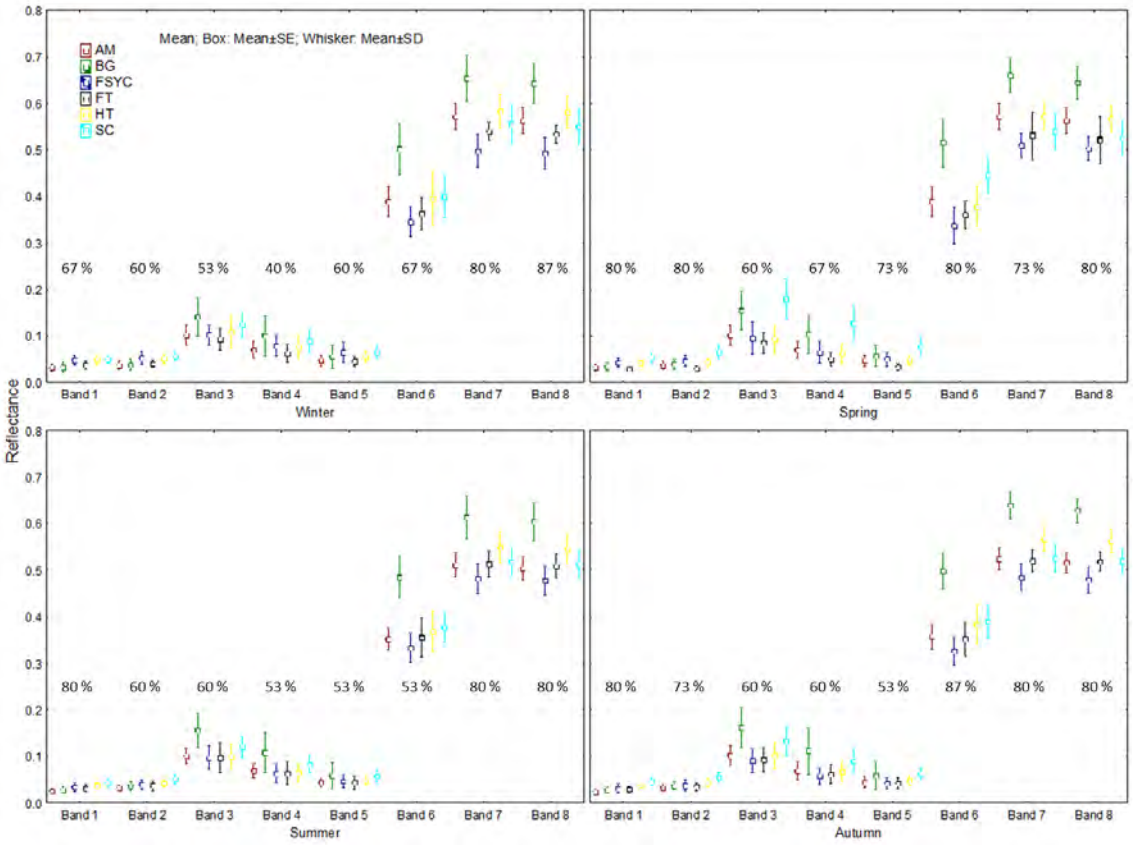

Figure 5. 3: Reflectance values of the six tree species for each band of WorldView-2 across four single seasons. The number of significant different species pairs (p < 0.03, Bonferroni corrected) is indicated as a percentage of the total number of comparable species pairs (15) for each of the bands.

For the RE sensor, the variation of species also varied more in the green (bands 2), red-edge (band 4) and NIR (band 5) regions similar to the hyperspectral and WV2 sensors (Figure 5.4). *Bruguiera gymnorrhiza* again showed the highest reflection of all species in these bands across the seasons and *Syzygium cordatum* also showed an increase in reflection in the green band in spring. The NIR band attained the highest percentage of separable species pairs across the single seasons (80 %), whereas the blue bands (band 1) in spring and autumn, and the red-edge band (band 4) in autumn also showed high separability between the species (73 %). Of all the seasons, the spring season showed the highest number of separable pairs (> 67 %) for all the RE bands based on the parametric ANOVA analysis.

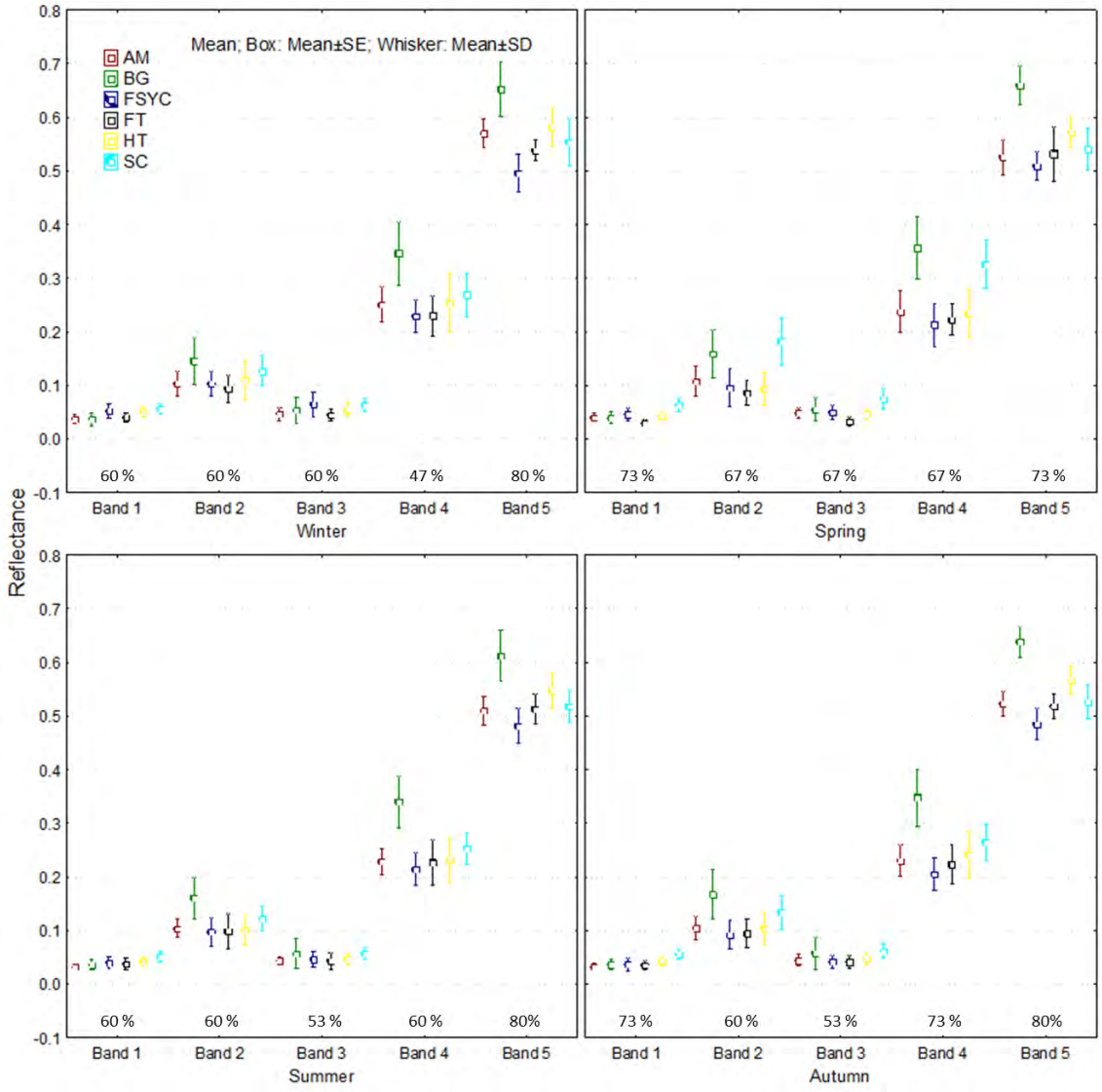

Figure 5. 4: Reflectance values of the six tree species for each band of RapidEye across four single seasons. The number of significant different species pairs ($p < 0.03$, Bonferroni corrected) is indicated as a percentage of the total number of comparable species pairs (15) for each of the bands.

5.3.2. Variation of accuracies across sensors for single seasons

The highest average OA across single seasons was attained in the summer season for the hyperspectral data classification (92,4 %) whereas the average OA of the multispectral sensors peaked in the spring season (WV2: 76 %; RE 70 %) (Table 5.4). The average OA of the hyperspectral data classification was between 90 % (winter) and 92 % (summer), compared to a range of 68 % (winter) to 76 % (spring) for WV2 and 63 (winter and summer) to 70 % (spring and autumn) for RE (Figure 5.5; Table 5.4). The hyperspectral data resulted in a significant increase in the OA classification of between 15 % (spring) to 21 % (summer) compared to the WV2 sensor, and a significant ($p < 0.02$, Bonferroni corrected) increase of 21 % (spring) to 30 % (summer) increase compared to the RE sensor (Table 5.5). The average OA of the two multispectral sensors differed between 4 % and 8.4 % across the single seasons (Table 5.5).

When comparing the average (of 100 iterations) producer's and user's accuracies across sensors, a variation in the accuracies is observed for the six tree species (Figure 5.6). The black mangrove (*Bruguiera gymnorrhiza*), for instance, showed a high separability across all sensors and seasons of above 85 % (Table 5.4). In contrast, the swamp fig (*Ficus trichopoda*) were poorly separable in winter, summer and autumn for both the multispectral sensors (ranges for WV2: 41 - 59 %; RE 36 - 50 %), however attained user's and producer's accuracies > 82 % for the hyperspectral data. The average producer's and user's accuracies for the swamp fig therefore increased significantly ($p < 0.02$, Bonferroni corrected) by between 19 - 50 % when the hyperspectral leaf-level data is used in the classification (Table 5.4; Figure 5.6; Table 5.5). An increase in average producer's and user's accuracies of more than 9 % (significant, $p < 0.02$, Bonferroni corrected) is observed for all species across all single seasons for the hyperspectral classification compared to the multispectral sensors, except the black mangrove (*Bruguiera gymnorrhiza*) and the water berry (*Syzygium cordatum*) in spring (Table 5.5; Figure 5.6).

In comparing the two multispectral sensors, WV2 showed significant ($p < 0.02$, Bonferroni corrected) higher producer's and user's accuracies for certain species (Figure 5.6; Table 5.5). The two fig species, for example, showed a significant ($p < 0.02$, Bonferroni corrected) increase of > 13 % in the producer's and user's accuracy attained from RE to WV2 (Table 5.5; Figure 5.6). The WV2 sensor also showed a significant increase in the producer's accuracies for the white mangrove (*Avicennia marina*) in spring by 23 % (Table 5.5). Other significant increases in both the producer's and user's accuracies are noted for three species, including between 6 % and 22 % for the sycamore fig (*Ficus sycomorus*) in winter, spring and summer; between 6 % and 19 % for the lagoon hybiscus (*Hibiscus tilliaceus*) in winter and summer; and between 6 % and 8 % for the water berry (*Syzygium cordatum*) in the winter season (Table 5.5; Figure 5.6).

The confusion between species in the hyperspectral classification was generally low (< 7 %), whereas the multispectral-sensor classifications resulted in confusion between species of above 10 % (Table 5.6). Between two and four species pairs showed spectral overlap for the WV2 sensor, primarily in the winter and autumn season, with a maximum percentage of confusion recorded (20 %) in the summer season. The RE classification showed confusion between two to six species pairs, mostly in winter, summer and autumn, with a maximum confusion of 23 % in the summer.

Table 5.4: Results of the classification accuracies (average of 100 iterations) of the six evergreen tree species across the four single and multi-season classifications for the (A) hyperspectral data; (B) WV2 and (C) RE sensors.

(A)	Winter		Spring		Summer		Autumn		Multi-season	
OA (%)	89.5		90.8		92.4		92.0		92.2	
STDEV	±3.5		±2.8		±2.7		±2.7		±2.9	
	PA	**UA**	**PA**	**UA**	**PA**	**UA**	**PA**	**UA**	**PA**	**UA**
AM	95.1±5.5	94.5±5.5	94.7±5.5	92.7±6.3	97.6±3.8	94.4±5.7	95.5±4.5	96.8±4.2	95.9±5.69	94.7±6.0
BG	90.4±7.2	95.0±5.1	92.3±7.1	95.9±4.5	96.1±5.1	96.0±4.5	95.4±5.2	96.4±4.4	95.3±5.4	98.3±3.1
FSYC	93.8±6.7	86.6±8.0	93.4±6.1	92.2±5.6	92.0±6.8	92.6±5.6	95.0±5.5	92.1±5.8	92.6±5.3	93.5±5.5
FT	82.7±10.8	86.2±9.2	89.7±6.6	85.5±6.3	85.7±9.3	89.5±7.1	87.3±7.4	85.1±7.6	86.3±7.8	89.0±6.6
HT	85.8±8.7	89.0±7.6	85.8±8.6	90.4±7.8	89.2±7.3	94.0±5.8	91.3±7.1	92.9±5.8	91.7±7.2	92.6±5.8
SC	89.4±8.4	86.4±7.2	88.7±7.1	88.4±5.9	93.6±5.9	88.0±7.5	87.7±8.7	89.1±6.6	91.5±7.4	85.8±8.5

(B)	Winter		Spring		Summer		Autumn		Multi-season	
OA (%)	68.2		75.9		71.0		73.6		84.4	
STDEV	±4.7		±3.7		±4.2		±4.4		±3.5	
	PA	**UA**	**PA**	**UA**	**PA**	**UA**	**PA**	**UA**	**PA**	**UA**
AM	74.8±11.7	69.1±10.0	66.8±11.7	79.6±9.3	88.6±8.7	75.3±9.5	79.4±9.8	80.1±8.3	91.1±6.8	89.7±6.5
BG	85.5±9.1	90.0±6.6	89.9±7.1	89.4±6.5	88.6±9.1	92.3±6.7	92.7±6.6	97.8±3.8	95.9±4.5	96.7±4.2
FSYC	78.1±11.9	72.8±10.8	67.8±10.7	76.9±10.2	65.5±12.3	71.2±11.6	64.7±11.4	68.8±10.2	77.6±10.5	88.1±8.1
FT	41.0±11.8	53.8±12.8	78.8±9.1	68.5±8.3	44.9±10.6	57.6±12.6	58.7±12.3	63.5±11.2	75.7±11.0	73.3±9.7
HT	63.3±12.8	60.9±10.8	66.5±12.1	70.5±10.2	69.3±12.3	69.7±9.6	66.9±11.5	71.8±9.8	77.3±10.4	81.5±8.3
SC	66.8±10.7	61.2±10.8	85.7±8.7	72.7±7.2	69.2±11.1	59.1±8.6	78.9±9.7	62.4±8.2	88.7±8.5	78.5±7.5

(C)	Winter		Spring		Summer		Autumn		Multi-season	
OA (%)	62.6		70.0		62.6		69.8		79.7	
STDEV	±4.4		±4.1		±4.3		±4.2		±4.2	
	PA	**UA**	**PA**	**UA**	**PA**	**UA**	**PA**	**UA**	**PA**	**UA**
AM	70.4±10.4	65.6±10.0	43.5±11.4	68.2±13.1	81.9±10.0	71.7±10.0	78.3±8.8	74.9±10.1	83.4±10.2	84.8±8.8
BG	85.1±9.0	86.8±8.5	92.8±7.2	88.5±7.1	87.6±7.3	90.5±6.9	92.4±7.1	96.4±5.0	94.2±5.4	96.2±4.5
FSYC	70.0±11.6	66.2±9.1	60.9±11.4	64.8±10.2	46.7±11.9	49.1±9.6	60.7±12.8	65.0±12.0	62.2±13.0	82.1±9.4
FT	45.7±13.0	48.2±10.5	70.9±12.3	63.1±10.2	35.5±10.6	43.7±15.1	40.2±12.5	50.2±13.5	78.1±9.9	67.6±8.6
HT	44.2±12.5	55.3±11.8	66.2±11.0	63.6±10.4	57.4±11.4	61.6±10.7	68.5±10.6	68.0±9.8	72.0±11.4	77.9±9.4
SC	60.5±11.2	53.0±7.9	85.7±8.7	71.0±8.8	66.7±12.3	55.9±7.9	78.6±10.3	62.7±8.0	88.1±7.8	73.4±7.3

Abbreviations of species: AM = *Avicennia marina*; BG = *Bruguiera gymnorrhiza*; FSYC = *Ficus sycomorus*; FT = *Ficus trichopoda*; HT = *Hibiscus tilliaceus;* SC = *Syzygium cordatum*. OA = Overall Accuracy, STDEV = Standard deviation of the overall accuracy, PA = producer's accuracy; UA = user's accuracy.

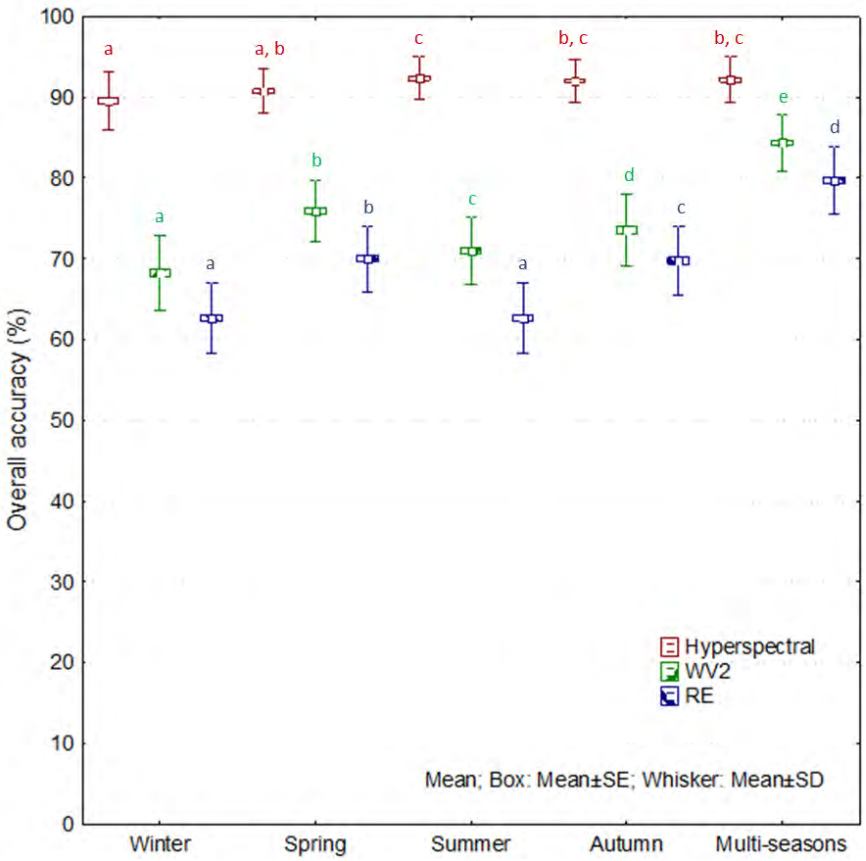

Figure 5.5: Variation of the average (of 100 iterations) overall accuracies for each sensor across single and the aggregated multi-season classification. Letters indicate statistically significant differences between seasons for each sensor ($p < 0.005$, Bonferroni corrected for ten comparable pairs).

(A)

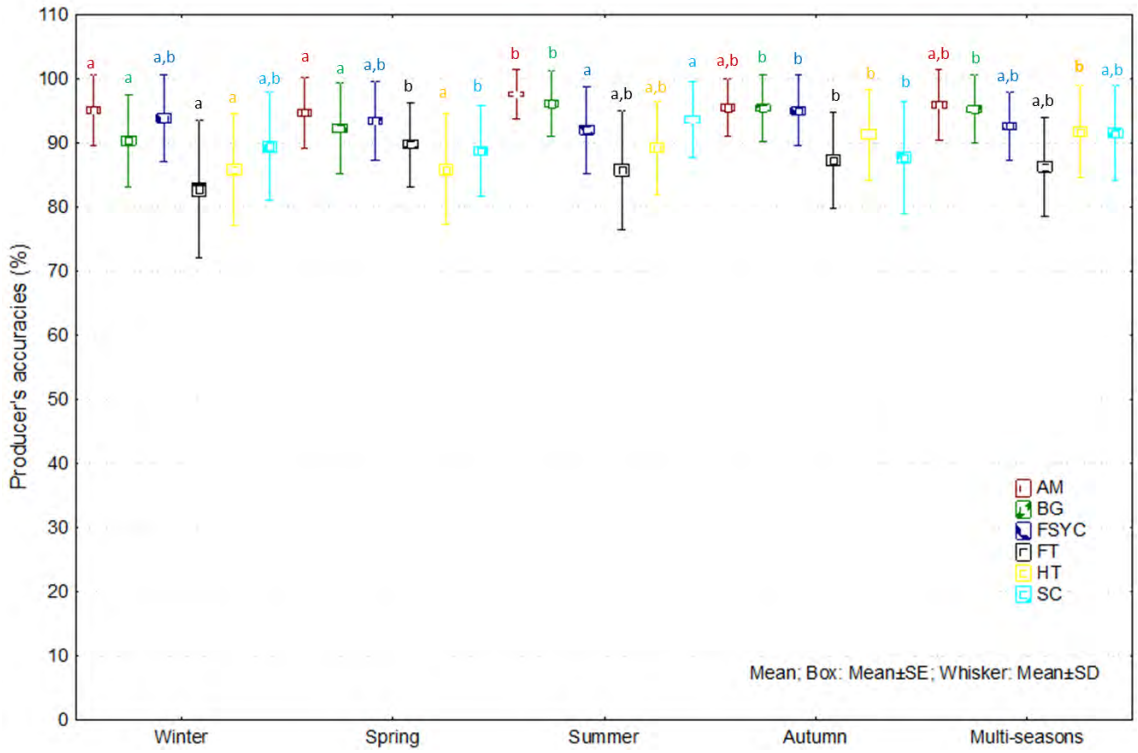
Producer's accuracies (%)
Winter
Spring
Summer
Autumn
Multi-seasons
AM
BG
FSYC
FT
HT
SC
Mean; Box: Mean±SE; Whisker: Mean±SD

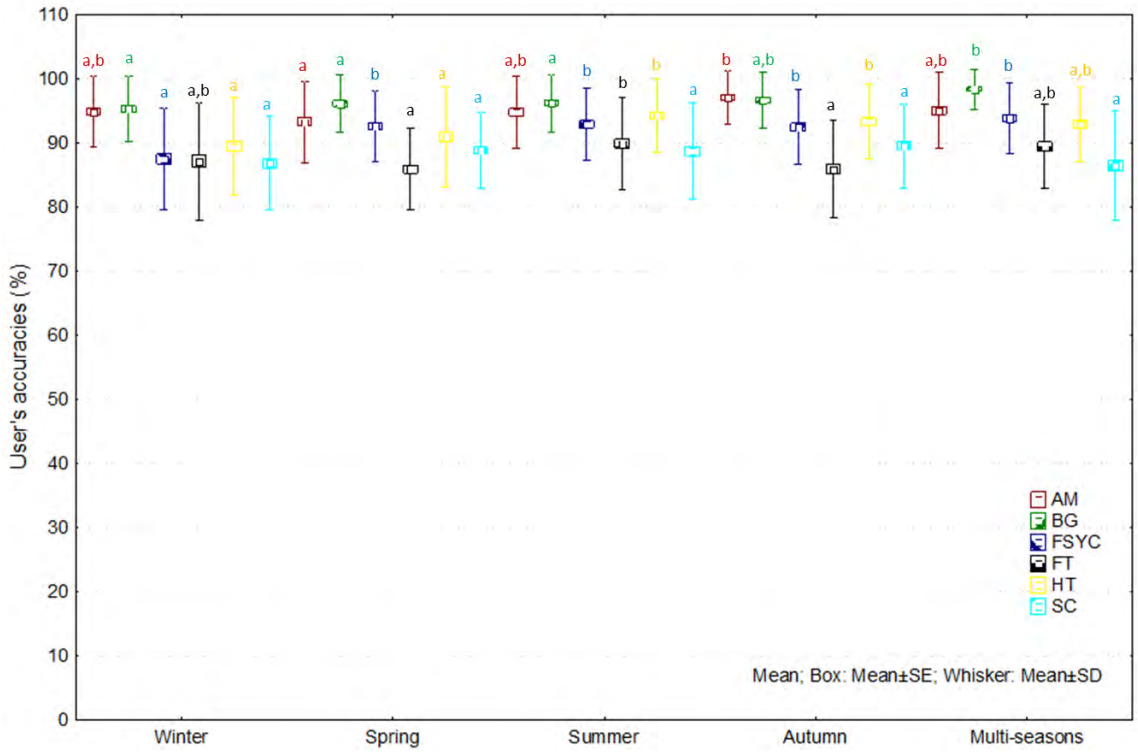
User's accuracies (%)
Winter
Spring
Summer
Autumn
Multi-seasons
AM
BG
FSYC
FT
HT
SC
Mean; Box: Mean±SE; Whisker: Mean±SD

(B)

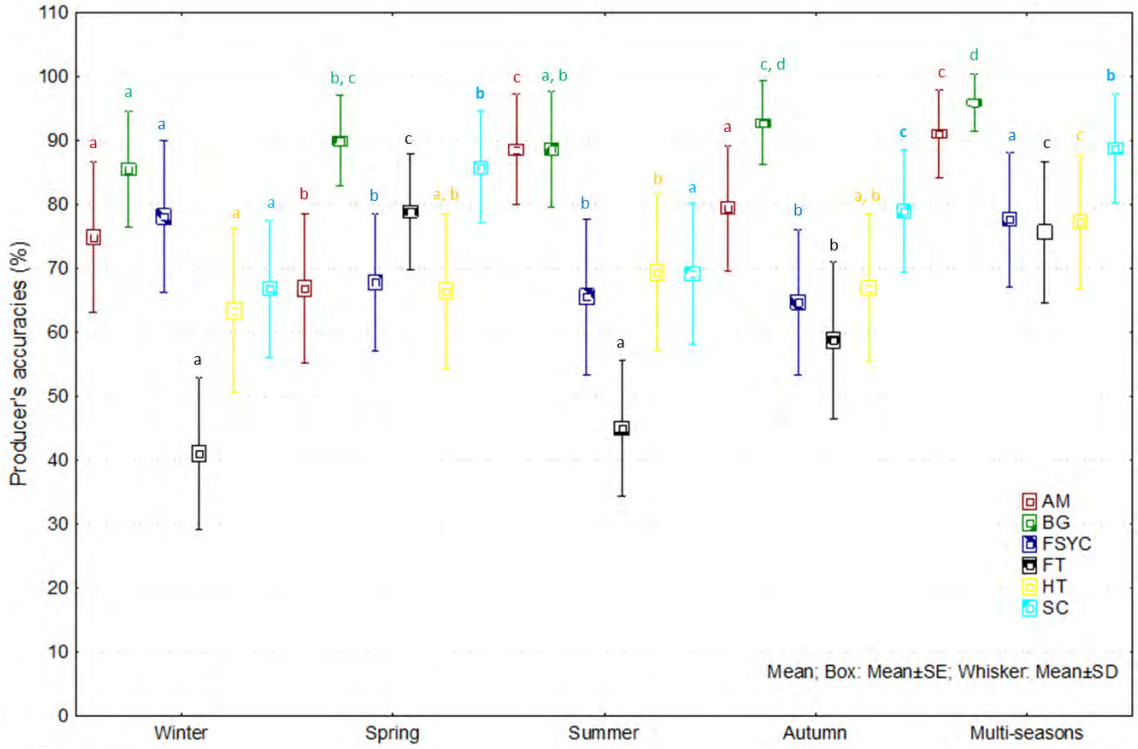
Producer's accuracies (%)
Winter
Spring
Summer
Autumn
Multi-seasons
AM
BG
FSYC
FT
HT
SC
Mean; Box: Mean±SE; Whisker: Mean±SD

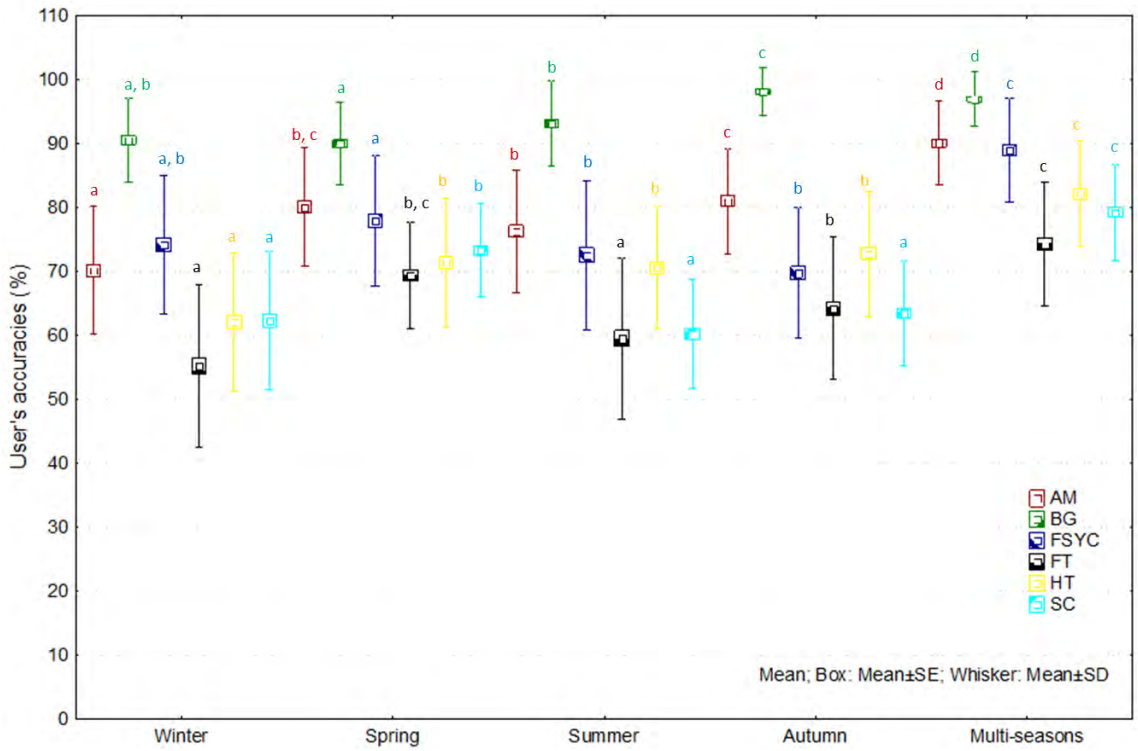
User's accuracies (%)
Winter
Spring
Summer
Autumn
Multi-seasons
AM
BG
FSYC
FT
HT
SC
Mean; Box: Mean±SE; Whisker: Mean±SD

(C)

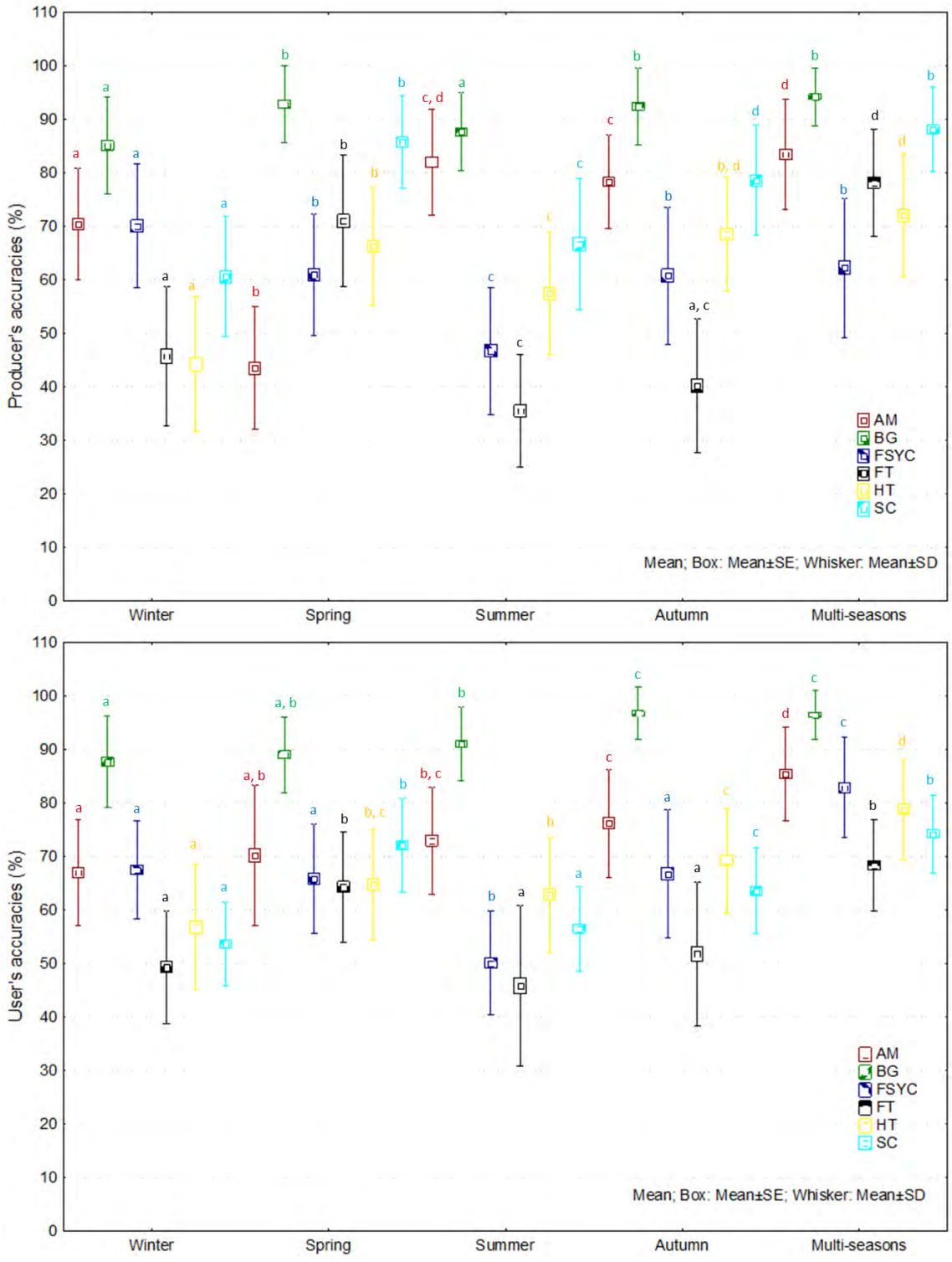

Figure 5.6: Variation of the average (of 100 iterations) producer's and user's accuracies of each of the six tree species in the winter, spring, summer, autumn and aggregated multi-season classification for (A) the hyperspectral data, (B) WV2 and (C) RE. Letters indicate statistically significant differences between seasons for each species (p < 0.005, Bonferroni corrected for ten comparable pairs).

Table 5. 5: Comparison of overall, producer's and user's accuracies (average of 100 iterations) attained by the hyperspectral, WV2 and RE multispectral sensors across the four single and multi-season classifications. Differences are calculated as from the first-mentioned to the second-mentioned sensor listed.

Seasons		Hyper-spectral to WV2	Hyper-spectral to RE	WV2 to RE		Hyper-spectral to WV2	Hyper-spectral to RE	WV2 to RE
Winter	**OA**	**-21.3 ^{s}**	**-26.9 ^{s}**	**-5.6 ^{s}**				
	AM (PA)	-20.3 ^{s}	-24.7 ^{s}	-4.4 ^{s}	AM (UA)	-25.4 ^{s}	-28.9 ^{s}	-3.5
	BG (PA)	-4.9 ^{s}	-5.3 ^{s}	-0.4	BG (UA)	-5 ^{s}	-8.2 ^{s}	-3.2 ^{s}
	FSYC (PA)	-15.7 ^{s}	-23.8 ^{s}	-8.1 ^{s}	FSYC (UA)	-13.8 ^{s}	-20.4 ^{s}	-6.6 ^{s}
	FT (PA)	-41.7 ^{s}	-37 ^{s}	-4.7 ^{s}	FT (UA)	-32.4 ^{s}	-38 ^{s}	-5.6 ^{s}
	HT (PA)	-22.5 ^{s}	-41.6 ^{s}	-19.1 ^{s}	HT (UA)	-28.1 ^{s}	-33.7 ^{s}	-5.6 ^{s}
	SC (PA)	-22.6 ^{s}	-28.9 ^{s}	-6.3 ^{s}	SC (UA)	-25.2 ^{s}	-33.4 ^{s}	-8.2 ^{s}
Spring	**OA**	**-14.9 ^{s}**	**-20.8 ^{s}**	**-5.9 ^{s}**				
	AM (PA)	-27.9 ^{s}	-51.2 ^{s}	-23.3 ^{s}	AM (UA)	-13.1 ^{s}	-24.5 ^{s}	-11.4 ^{s}
	BG (PA)	-2.4	0.5	2.9 ^{s}	BG (UA)	-6.5 ^{s}	-7.4 ^{s}	-0.9
	FSYC (PA)	-25.6 ^{s}	-32.5 ^{s}	-6.9 ^{s}	FSYC (UA)	-15.3 ^{s}	-27.4 ^{s}	-12.1 ^{s}
	FT (PA)	-10.9 ^{s}	-18.8 ^{s}	-7.9 ^{s}	FT (UA)	-17 ^{s}	-22.4 ^{s}	-5.4 ^{s}
	HT (PA)	-19.3 ^{s}	-19.6 ^{s}	-0.3	HT (UA)	-19.9 ^{s}	-26.8 ^{s}	-6.9 ^{s}
	SC (PA)	-3	-3	0	SC (UA)	-15.7 ^{s}	-17.4 ^{s}	-1.7 ^{s}
Summer	**OA**	**-21.4 ^{s}**	**-29.8 ^{s}**	**-8.4 ^{s}**				
	AM (PA)	-9 ^{s}	-15.7 ^{s}	-6.7 ^{s}	AM (UA)	-19.1 ^{s}	-22.7 ^{s}	-3.6
	BG (PA)	-7.5 ^{s}	-8.5 ^{s}	-1	BG (UA)	-3.7 ^{s}	-5.5 ^{s}	-1.8
	FSYC (PA)	-26.5 ^{s}	-45.3 ^{s}	-18.8 ^{s}	FSYC (UA)	-21.4 ^{s}	-43.5 ^{s}	-22.1 ^{s}
	FT (PA)	-40.8 ^{s}	-50.2 ^{s}	-9.4 ^{s}	FT (UA)	-31.9 ^{s}	-45.8 ^{s}	-13.9 ^{s}
	HT (PA)	-19.9 ^{s}	-31.8 ^{s}	-11.9 ^{s}	HT (UA)	-24.3 ^{s}	-32.4 ^{s}	-8.1 ^{s}
	SC (PA)	-24.4 ^{s}	-26.9 ^{s}	-2.5	SC (UA)	-28.9 ^{s}	-32.1 ^{s}	-3.2 ^{s}
Autumn	**OA**	**-18.4 ^{s}**	**-22.2 ^{s}**	**-3.8 ^{s}**				
	AM (PA)	-16.1 ^{s}	-17.2 ^{s}	-1.1	AM (UA)	-16.7 ^{s}	-21.9 ^{s}	-5.2 ^{s}
	BG (PA)	-2.7 ^{s}	-3 ^{s}	-0.3	BG (UA)	1.4	0	-1.4
	FSYC (PA)	-30.3 ^{s}	-34.3 ^{s}	-4	FSYC (UA)	-23.3 ^{s}	-27.1 ^{s}	-3.8
	FT (PA)	-28.6 ^{s}	-47.1 ^{s}	-18.5 ^{s}	FT (UA)	-21.6 ^{s}	-34.9 ^{s}	-13.3 ^{s}
	HT (PA)	-24.4 ^{s}	-22.8 ^{s}	1.6	HT (UA)	-21.1 ^{s}	-24.9 ^{s}	-3.8 ^{s}
	SC (PA)	-8.8 ^{s}	-9.1 ^{s}	-0.3	SC (UA)	-26.7 ^{s}	-26.4 ^{s}	0.3
Multi-season	**OA**	**-7.8 ^{s}**	**-12.5 ^{s}**	**-4.7 ^{s}**				
	AM (PA)	-4.9 ^{s}	-12.5 ^{s}	-7.6	AM (UA)	-5.0 ^{s}	-9.8 ^{s}	-4.9 ^{s}
	BG (PA)	0.6	-1.1	-1.7	BG (UA)	-1.6 ^{s}	-2.1	-0.5
	FSYC (PA)	-15.0 ^{s}	-30.4 ^{s}	-15.4	FSYC (UA)	-5.4 ^{s}	-11.3 ^{s}	-6.0 ^{s}
	FT (PA)	-10.6 ^{s}	-8.2 ^{s}	2.4 ^{s}	FT (UA)	-15.8 ^{s}	-21.5 ^{s}	-5.7 ^{s}
	HT (PA)	-14.4 ^{s}	-19.7 ^{s}	-5.3	HT (UA)	-11.1 ^{s}	-14.6 ^{s}	-3.5 ^{s}
	SC (PA)	-2.7 ^{s}	-3.4	-0.6	SC (UA)	-7.3 ^{s}	-12.4 ^{s}	-5.1 ^{s}

Abbreviations of tree species: AM = *Avicennia marina*; BG = *Bruguiera gymnorrhiza*; FSYC = *Ficus sycomorus*; FT = *Ficus trichopoda*; HT = *Hibiscus tilliaceus;* SC = *Syzygium cordatum*. OA = overall accuracy; PA = producer's accuracy; UA = user's accuracy.

^{s} – significant, Bonferroni corrected $p = 0.02$ for 3 comparable pairs; values rounded to 1 decimal.

Table 5. 6: Number of comparable species pairs of a total of 15 that result in classification confusion of more than 10 % for the producer's and user's accuracies (average of 100 iterations) per season and sensor. For each pair the range in confusion is given as a percentage of the total number of leaves of the producer's or user's accuracies.

	Winter		Spring		Summer		Autumn		Multi-season	
	PA	UA	PA	UA	PA	UA	PA	UA	PA	UA
Hyper-spectral	(<6)	(<7)	(<5)	(<5)	(<7)	(<4)	(<6)	(<7)	(<5)	(<5)
WV2	3 pairs (10–15)	4 pairs (12–19)	4 pairs (10–13)	(<9)	3 pairs (10–15)	2 pairs (13, 20)	4 pairs (10–18)	3 pairs (10–15)	1 pair (11)	1 pair (11)
RE	5 pairs (10–25)	5 pairs (10–19)	4 pairs (14–18)	2 pairs (10, 14)	5 pairs (13–19)	6 pairs (11–23)	5 pairs (13–15)	3 pairs (13–20)	2 pairs (14, 16)	2 pairs (10, 11)

PA = producer's accuracy; UA = user's accuracy.

5.3.2. Comparison of accuracies between single seasons and multi-season classifications

The use of the multi-season data for tree species classification resulted in a significant ($p < 0.005$, Bonferroni corrected) higher average OA of the multispectral sensors (Table 5.4; Figure 5.5). For WV2 the multi-season data resulted in an increase of 8.5 % and for RE an increase of 9.7 % compared to the highest average OA attained in a single season. The multi-season classification of the hyperspectral data, however, resulted in no significant increase in average OA. Similarly, the multi-season classification using the hyperspectral data showed no significant increase in producer's or user's accuracies of any of the tree species (Table 5.4; Figure 5.6). Multi-season data of WV2 however, showed a significant ($p < 0.005$, Bonferroni corrected) increase of between 5 – 11 % in the user's accuracies of four species (*Avicennia marina*, *Ficus sycomorus*, *Hibiscus tilliaceus* and *Syzygium cordatum*) compared to the highest user's accuracies achieved in a single season (Table 5.4; Figure 5.6). The producer's accuracy of *Hibiscus tilliaceus* also increased by 8 % (significant at $p < 0.005$, Bonferroni corrected) when multi-season WV2 data are used in the classification. Multi-season RE data resulted in a significant increase of the producer's accuracy of *Ficus trichopoda* of 7.2 %, and the user's accuracies of three species, *Avicennia marina*, *Ficus sycomorus*, *Hibiscus tilliaceus,* by 3, 16 and 10 % respectively (Table 5.4; Figure 5.6). The number of species pairs that were confused in the classification has reduced from the single seasons of more than two species pairs to one species pair in the multi-season classification of WV2. The classification of RE showed a decrease in spectrally overlapping species pairs from between two and six in the single seasons to two species pairs in the multi-season classification.

5.3. Discussion

This study demonstrated that the selection of 22 narrow hyperspectral bands, which are related to plant properties, achieved the highest classification accuracies (OA > 90 %; user's accuracies > 86 %) for six evergreen tree species in a subtropical forest of the KwaZulu-Natal Province, South Africa over four seasons (winter, spring, summer and autumn) compared to multispectral WV2 and RE sensors. The hyperspectral data showed a significant increase in accuracy of between 15 – 21 % compared to the WV2 sensor, and 21 % to 30 % compared to the RE for the OA of the tree species classification. The OAs of the multispectral sensors in this study were therefore lower than reported where WV2 was used for tree species classification of five mangroves in Malaysia (OA > 80 %) but comparable to six, mostly evergreen dryland tree species (OA 75 – 77 %) of the DukuDuku Forest in the west of the study area (Kanniah, 2011; Omer *et al.*, 2015). The OA for tree species classification in Botswana with RE were also higher than attained in this study (Adelabu *et al.*, 2013). The differences between the OA accuracies attained between the sensors were limited to leaf-level data analysis and to the simulation of the reflectance at multispectral sensor level. Further work is required to assess the accuracies at canopy scales and for other species and climatic regions too.

To our knowledge, this study is the first to report the classification accuracies between hyperspectral to multispectral, particularly for evergreen tree species only. The spectral variation of species was sampled across a number of phenological events including the dormant (winter) and flowering periods (spring and summer) for evergreen tree species. For evergreen tree species, the flowering period seems to be the ideal phenological event for species separability, compared to the leaf fall in mixed and deciduous forests (Key *et al.*, 2001; Fung *et al.*, 2003; Holmgren *et al.*, 2008). Sobhan (2007) also found the flowering period ideal for the separation of shrub species in Italy, however it has not yet been confirmed for evergreen tree species as an ideal phenological event for classification to our knowledge.

The results showed that the average OA of the hyperspectral data ranged from a minimum of 90 % (winter) to a maximum of 92 % (summer) whereas the multispectral WV2 sensor resulted in average OA from 68 % (winter) to 75 % (spring) and RE from 63 % (winter/summer) to 70 % (spring) for single seasons. The classification results showed different trends in a comparative study of subtropical tree species across four seasons in Hong Kong, China (Fung *et al.*, 2003), where the autumn season recorded the highest OA (81 %) and the summer season showed the lowest OA (69 %). Interestingly, sampling for both studies was done on the same months (April, July, October and January) with corresponding average annual rainfall and temperature ranges (Hong Kong Observatory, 2003; Van Deventer *et al.*, 2015b) and some comparable tree species (*Ficus* spp. and *Hibiscus tilliaceus*). Even though the studies show a high level of similarities, distinct differences can be seen in phenological patterns of the tree species. The variation in accuracies of tree

species classification across phenological phases for these two subtropical studies, highlight the paucity of knowledge on season-specific models for tree species classification for other subtropical and different climatic regions.

Interestingly, the tree species with the highest number of spectral overlap with other species and the lowest producer's and user's accuracies was the swamp fig (*Ficus trichopoda*), a species with no flowers and inconspicuous fruits under the canopy. In contrast, the black mangrove (*Bruguiera gymnorrhiza)* remained highly separable from all species across all three sensors, probably owing to the significantly lower amounts of foliar carotenoids and chlorophyll concentrations (Van Deventer *et al.*, 2013). In this study the separability of six evergreen wetland trees only was assessed, whereas a large number of evergreen and deciduous dryland species also occur within close proximity (10 – 15 km) which may increase the spectral overlap when combined at a regional level (Omer *et al.*, 2015; Cho *et al.*, 2015).

Using multi-season data for tree species classification significantly improved the overall accuracy attained by the multispectral sensors by between 8 % and 10 % compared to the single seasons, however no statistically significant differences were found between the multi-season and single season classification of the hyperspectral data. The species classification also resulted in fewer cases of confusion between tree species, when multi-season data from WV2 and RE were used. The results suggest, as in the case with the four-band aerial photography data of Key *et al.* (2001), that multispectral sensor with ≤ 8 bands may benefit from multi-season data, however, hyperspectral sensors with a bands representing a diverse number of plant properties, may require only a single optimal season for tree species classification. In this regard, the choice is dependent on cost and extent of the region. For this study, as an example, the use of WV2 data across four single seasons would have resulted in more than double the cost compared to RE imagery across four single seasons, whereas the OA of WV2 was ± 5 % more than that of RE. A scaled approach for regional monitoring of tree species may therefore start with the assessment of vegetation types at regional scale with RE, and WV2 or hyperspectral data for particular areas of interest or concern.

This study contributes to the knowledge of multitemporal and multi-season classification of individual tree species, although further work is required to assess whether the optimal temporal scale can be achieved through fewer seasons to reduce the cost of imagery and field campaigns. The hyperspectral data were optimised for species classification through reducing the bands to 22 related to plant properties (Van Deventer *et al.*, 2015a). A robust selection of spectral bands for the optimisation of tree species classification across climatic zones, remains to be determined (Martin *et al.*, 1998; Fung *et al.*, 2003). The PLS-RF classification in this study considered all components and an *ntree* of 500, although further optimisation could be done using fewer components and *ntree*'s in the PLS-RF classification algorithm. The PLS-RF method was found well suited for the classification of the tree species

as it transform the correlated bands with a PLS regression, prior to the classification in RF. This thesis is the first to apply this method from the medical field to tree species classification (Boulesteix *et al.*, 2008).

5.5. Conclusion

Understanding the impact of phenological variation on tree species classification is essential for the monitoring of evergreen tree species and narrow-range forest types. This study demonstrates the advantage of an optimised hyperspectral data set in comparison to that of multispectral WV2 and RE for the classification of six evergreen tree species over four seasons for a subtropical forest in the KwaZulu-Natal Province in South Africa.

The key results of this chapter include:

- The selection of twenty-two narrow bands from leaf-reflectance data resulted in the highest classification accuracies for the six evergreen tree species, compared to leaf-level spectra resampled to multispectral sensors RapidEye and WorldView-2.
- The multispectral sensors showed a significant increase (8 – 10 %) in the OA and less confusion between tree species when multi-seasonal data is used. No significant increase in accuracies was noted for the hyperspectral leaf-level classification when multi-season data were used in the classification. More research is required on the temporal optimisation of tree species classification for other species and climatic regions.
- The flowering period were found to be the ideal phenological event for species classification of the evergreen tree species.

The separability between the six tree species remains to be assessed at image level. A number of factors influence the ability of remote sensing at image level to discriminate between tree species, including where multitude of influences affect the classification accuracy, including wetland environment and canopy architecture and size of canopy.

CHAPTER 6: MULTI-SEASON RAPIDEYE IMAGERY IMPROVE THE CLASSIFICATION OF WETLAND VEGETATION TYPES AS COMPARED TO A SINGLE SEASON IMAGERY FOR EVERGREEN FORESTED WETLANDS IN KWAZULU-NATAL, SOUTH AFRICA

Abstract

Remote sensing is considered a valuable tool for monitoring the impacts of global change on tree species composition, condition and distribution. The ability to separate tree species in wetland environments, remains challenging though, and therefore the multispectral sensor RapidEye was evaluated for its capability in (i) mapping isolated tree canopies and closed-canopy forests in wetland environments; and (ii) whether multiple phenological events across four seasons would increase the classification accuracy of wetland tree species as compared to a single season imagery. RapidEye images were obtained for four seasons (winter, spring, summer and autumn) between 2011 and 2012 for a subtropical forest region of South Africa. The separability of the canopy spectra of nine tree species and associated vegetation types was assessed for each season using the Partial Least Square Random Forest algorithm (PLS-RF). The classification accuracies of a number of multi-seasonal stacked images were also calculated and compared to the single seasons, using ANOVA and post-hoc THSD tests. The optimum single and multi-season classifications were used to predict the tree species and associated vegetation maps for the study area using the random forest model.

RapidEye showed successful classifications for tree species with larger canopies, dense leaves, and broad vegetation type class but was unsuccessful for smaller canopies or less densely leaved or smaller canopies of isolated wetlands trees. The classification accuracies were highest in spring (overall accuracy of 80±2.9 %) and summer (overall accuracy of 80±3.1 %), compared to the winter (overall accuracy of 66±3.1 %). The classification accuracies using multiple seasons increased the overall and user's accuracies significantly and reduced the number and percentage of overlap between species. The summer season and an aggregation of the autumn, winter and spring seasons resulted in the two optimum classifications (multi-season overall accuracy = 86±3.1 %) and was therefore used to predict the tree species and vegetation types of the study area.

6.1. Introduction

Global change is expected to cause changes in the species distribution of vegetation (Walther *et al.*, 2002; Campoy *et al.*, 2011; Sardans and Peñuelas, 2012). Remote sensing has been proven a successful tool for tree species discrimination at space-borne level, particularly since the launch of the WorldView-2 (WV2) and RapidEye (RE) multispectral sensors in 2009. These sensors offer a spatial resolution matching tree canopy sizes (≤ 5 m) with additional bands in addition to the traditional spectral bands (blue, green, red and NIR). As a result, both sensors have been used successfully in mapping dominant tree species in mixed forests and discriminating between coniferous, evergreen and deciduous tree species with overall accuracies > 63 % (Immitzer *et al.*, 2012; Pu and Landry, 2012; Adelabu *et al.*, 2013; Cho *et al.*, 2015; Omer *et al.*, 2015). Although the additional bands of these sensors showed improvements in comparison to very high spatial multispectral sensors for tree species classification, some authors still report confusion in user's accuracies between certain tree species (Immitzer *et al.*, 2012). It remains to be assessed whether such overlaps are limited to certain species or geographic regions.

The ability to classify tree species using multispectral images is influenced by, amongst other factors, the canopy size and architecture of tree species. Densely foliated and closed-canopy forests are easier to detect and classify compared to isolated canopies since a large portion of background reflection from water, soil or other vegetation types is reduced (Gao, 2010; Adelabu and Dube, 2014). Isolated canopies, on the other hand, can be easily detected if the canopy diameter exceeds the size of an image pixel to ensure that background reflection of other objects is excluded. Yet canopy sizes of isolated trees vary between growth phases and species and therefore the suitability of a sensor should be assessed for a study area according to the size of canopies of the tree species. The reflectance measured at canopy level may include reflectance from exposed foliage and branches, inflorescences and the shadow of the upper leaves (Cho *et al.*, 2008). The background influence from below the canopy also contributes to the reflectance in less densely foliated canopies. Although many of the factors mentioned above impact tree species classification in dryland areas, the background influence of water in wetlands area is particularly problematic, as it reduces the reflectance from other objects (Hardisky *et al.*, 1986; Adam *et al.*, 2010). Closed-canopy forests, mostly mangrove tree species, in wetland environments were successfully classified with multispectral imagery (Kanniah, 2011), however the ability of multispectral imagery to separate between a diverse number and sizes of isolated and closed-canopy forests, remains to be assessed in wetland environments.

The identification of multiple key phenological events for optimising species discrimination was proposed by Key *et al.* (2001) as a means of maximising classification accuracies. In the previous chapter the average overall and user's accuracies of six evergreen tree species increased when leaf-level data, resampled to the bands of multispectral WorldView-2 (WV2) and RapidEye (RE) band centres, from multiple seasons were used in the classification. The

validity of the hypothesis remains to be assessed at image scale where spectral signatures are less pure as a result of atmospheric conditions, environmental background and fluctuating water levels.

This chapter therefore aims to assess the capability of RapidEye imagery in (i) mapping isolated tree canopies and closed-canopy forests in wetlands; and (ii) whether multiple phenological events across four seasons increase the classification accuracy of wetland tree species as compared to a single season.

6.2. Methods

6.2.1. Study area

The study area is located within the iSimangaliso Wetland Park (28°S, 32°30'E), a formal protected area, in the KwaZulu-Natal Province of South Africa (Figure 6.1). The study area extends from the Maphelane node in the south to Catalina Bay in the north, and from the DukuDuku Forest in the west to the coastline in the east. The Park is listed as both a Ramsar and World Heritage Site (WHS) on grounds of its unique faunal and floral diversity as well as the unique number of wetland types in the Park (Cowan, 1999). The climate is subtropical with seasonal variation in rainfall of between a low of 45 mm (10-year average minimum in April) to a high of 155 mm (10-year average maximum in December) (Figure 6.2).

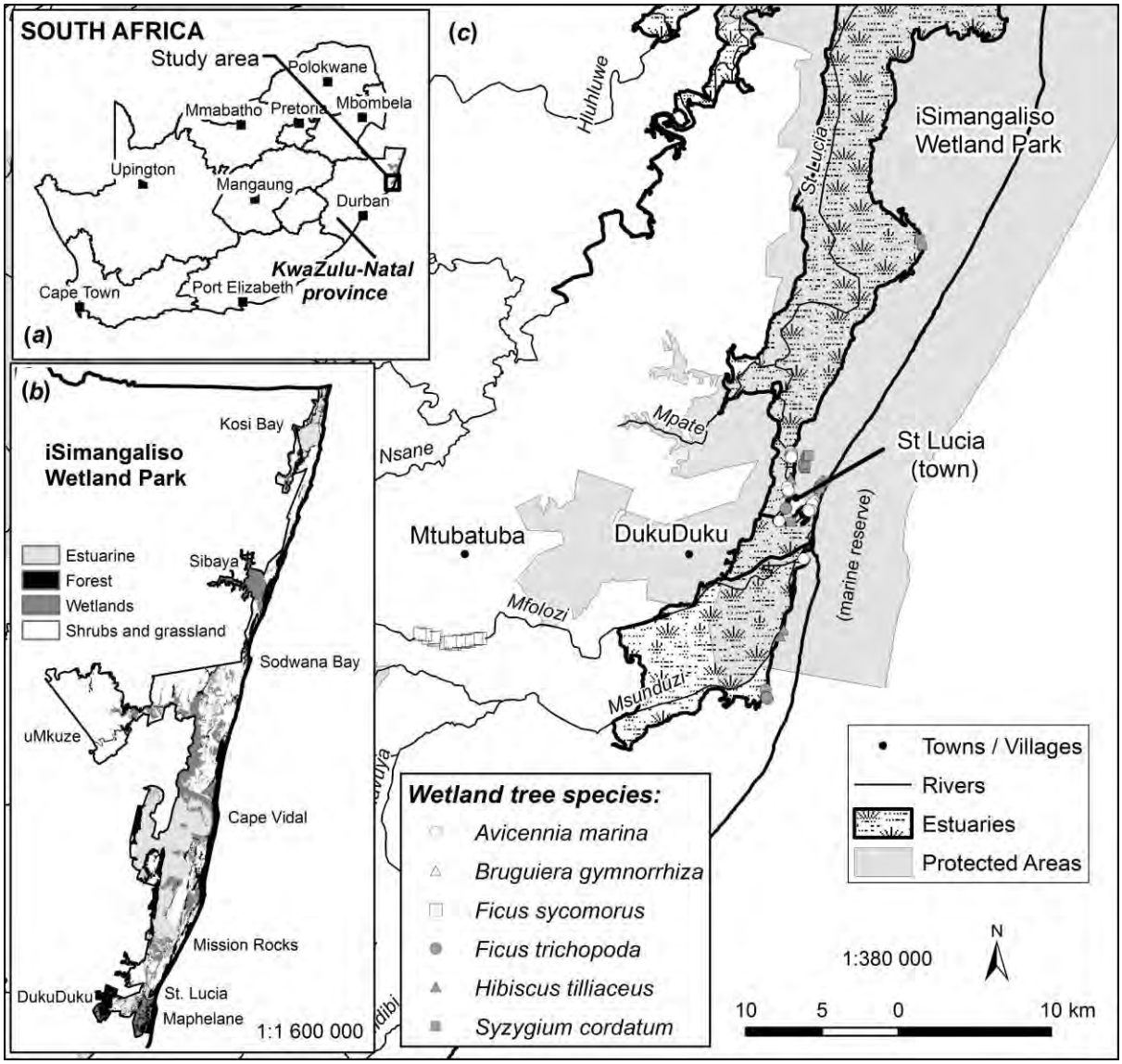

Figure 6.1: The study area is located in the KwaZulu-Natal Province of South Africa (A). Vegetation types in the iSimangaliso Wetland Park range from forest, estuarine, wetland and other natural ecosystem types (B). Sampling locations of six evergreen wetland tree species in study area ranged from the uMsunduzi River in the south, to the wetlands east of St Lucia town and Catalina Bay in the north (C).

The location of six evergreen trees species, including *Avicennia marina* (White Mangrove), *Bruguiera gymnorrhiza* (Black Mangrove), *Ficus sycomorus* subspecies *sycomorus* (Sycamore fig), *Ficus trichopoda* (Swamp fig), *Hibiscus tilliaceus* (Lagoon hibiscus) and *Syzygium cordatum* (Water berry) were identified during fieldwork campaigns between 2011 and 2012 (Table 6.1). Additional tree species and associated vegetation types in the vicinity of the wetland and estuarine ecosystems were also identified, including *Acrostichum aureum L.* (Mangrove fern), *Phragmites australis / mauritanus* (Reeds) and seasonal wetlands dominated by graminoids. A number of dryland vegetation types were also included to assess separability with the wetland tree species, including *Acacia kosiensis* (Dune sweet thorn), the coastal lowland and East Coast Dune and Lowland Forests (Table 6.1).

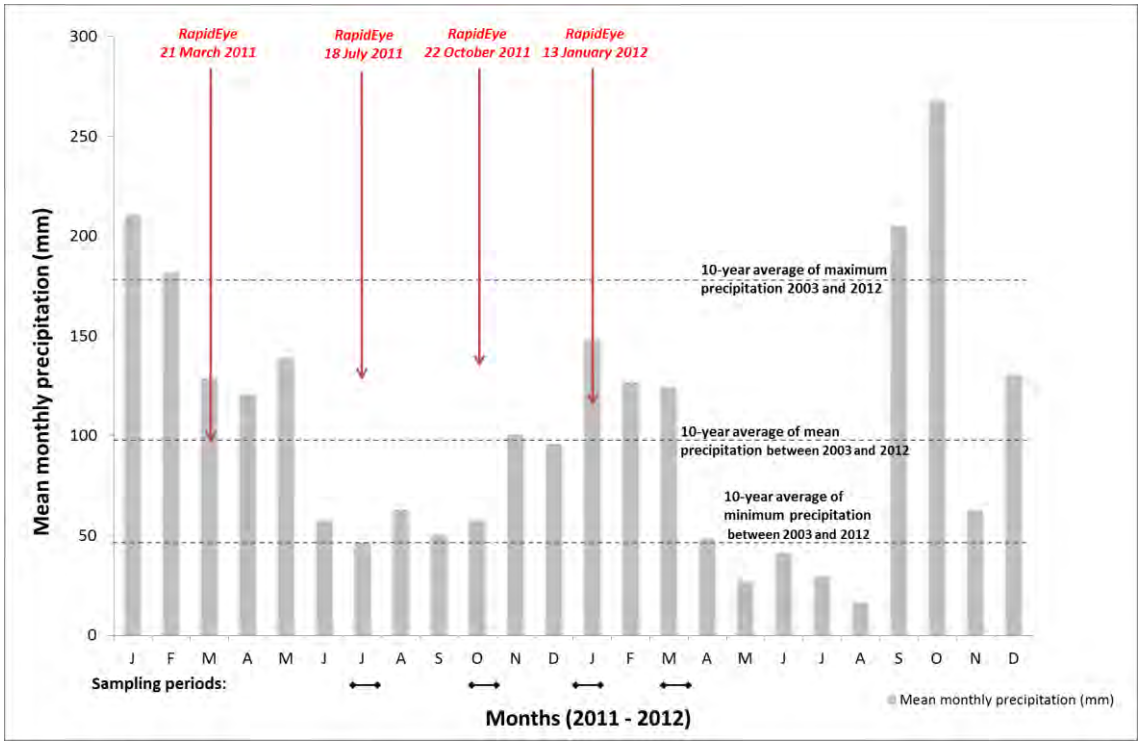

Figure 6.2: Average annual rainfall between January 2011 and December 2012 for the study area (Harris *et al.*, 2013).

Table 6.1: Wetland tree species and associated vegetation type in the St Lucia and Maphelane nodes of the iSimangaliso Wetland Park, KwaZulu-Natal.

Indicator tree species, (common name), & acronymn	Associated vegetation type and community	Description of vegetation community	Number of ROIs (and pixels) per season
Acacia kosiensis (Dune sweet thorn) AK	Terrestrial ecosystems: pioneering coastal dune forests Vegetation type FOz 7 Northern coastal forest*	Occurs as a pioneer tree on sandy coastal soils in the coastal corridor of KwaZulu-Natal, South Africa either as isolated trees or dense closed canopy stands (Boon, 2010; Van Wyk and Van Wyk, 2013). Individual tree canopies measured ±15 m in diameter and stands ±50 m**. The South African species has been renamed to *Senegalia kosiensis* in 2013.	60 (240)
Acrostichum aureum L. (Mangrove fern) AA	Estuarine ecosystems. Mangrove wetlands dominated by fern *Acrostichum aureum L.* Vegetation type FOa 3 Mangrove Forest*	The mangrove fern was found predominantly with *Bruguiera gymnorrhiza* in the Mfabeni wetland located north of the estuary mouth. The closed canopy fern wetland measured approximately 50 m in latitudinal diameter**.	50 (200)
Avicennia marina (White Mangrove) and *Bruguiera gymnorrhiza*	Estuarine ecosystems: Mangrove forests community. Vegetation type FOa 3 Mangrove	Predominantly closed canopy with forest diameter up to 10 m in latitudinal cross-section**.	90 (360)

(Black Mangrove) MF (Mangrove forests)	Forest*		
Coastal lowland forest LF (Lowland forest)	Terrestrial ecosystems. Vegetation type Northern Coastal Forest (FOz 7): KwaZulu-Natal Coastal Forests : DukuDuku Moist Coastal Lowlands Forest*	Closed-canopy forest including i.a. *Albizia adianthifolia* and *Strychnos* spp. (Cho *et al.*, 2015)	50 (69 434)
East Coast Dune Forest DF (Dune forest)	Terrestrial ecosystems. Vegetation type Northern Coastal Forest (FOz 7): KwaZulu-Natal Coastal Forests : East Coast Dune Forest	Closed-canopy forest with species similar to the coastal lowland forest.	50 (57 363)
Ficus sycomorus subspecies *sycomorus* (Sycamore fig) FSYC	Freshwater ecosystems. Vegetation type FOa 1 Lowveld Riverine Forest*	Trees along the sugarcane farm roads were approximately 20 – 30 m in diameter.	11***
Ficus trichopoda (Swamp fig) FT	Freshwater ecosystems. Swamp forests community. Vegetation type FOa 2 Swamp Forest*	Individual canopies measured >7 m in diameter whereas the closed-canopy stands were > 300 m in diameter in the study area**.	50 (3 775)
Hibiscus tilliaceus (Lagoon hibiscus) HT	Estuarine ecosystems. Vegetation type FOa 3 Mangrove Forest*	Isolated canopies measured ± 10 m in diameter and clumps >10 m in diameter**.	50 (200)
Phragmites australis / mauritanus (Reeds) PA	Estuarine and freshwater ecosystems. Macrophyte community. Vegetation type AZa 7 Subtropical Alluvial Vegetation: Alluvial Wetlands: Subtropical Alluvial Vegetation: Lowveld Floodplain Grasslands: Tall Reed Wetland*	Closed, through spectral background reflectance remains a problem between circular arrangements of leaves on canopy. The latitudinal diameter ranged between 5 and 200 m** along the Narrows.	70 (280)
Seasonal wetlands SW	Freshwater ecosystems. Vegetation type AZa 7 Subtropical Alluvial Vegetation: Alluvial Wetlands: Subtropical Alluvial Vegetation: Lowveld Floodplain Grasslands: Short Grass/ Sedge Wetlands*	Seasonal wetlands with predominant species including *Imperata cylindrica, Juncus kraussii* and *Schoenoplectus scirpoides* (Rautenbach, 2015)	50 (7 692)
Syzygium cordatum (Water berry) SC	Freshwater ecosystems. Savanna-grassland community. Vegetation type CB 1 Maputaland Coastal Belt*	The vegetation type consists of 'irregular dunes with generally open vegetation and *Syzygium cordatum* dotted predominantly on the dunes' (Scott-Shaw and Escott, 2011:15). Canopies measured on average ≤ 15 m**.	0 – unable to find pure pixels on RapidEye images

** Vegetation types were identified from (Scott-Shaw and Escott, 2011).*

*** Average canopy diameter was measured for at least 10 canopies in the study area from 20 cm colour orthophotography provided by (DRDLR NGI, 2014).*

***** an insufficient number of samples were identified on RapidEye and therefore the species was omitted from the analyses.

6.2.2. Image acquisition and preprocessing

RapidEye images covering the study area were obtained from Blackbridge Pty Ltd (http://www.blackbridge.com/) for the autumn, winter and spring of 2011 and the summer of 2012 (Table 6.2). RapidEye provides five spectral bands between 440 and 850 nm, including the blue (440-510 nm), green (520-590 nm), red (630-685 nm), red-edge (690-730 nm) and near-infrared (760-850 nm) bands. ATCOR 2 software (ReSe applications Pty Ltd, http://www.rese.ch) was used to calibrate to top-of-atmosphere reflectance using sensor and solar inclination and azimuth angles (Table 6.2) (Richter and Schläpfer, 2015). Spectra for water, vegetation and soil were used as input parameters and related to reference spectra in ATCOR. The images were provided as Level 3A which include radiometric, sensor and geometric corrections, with 5 m spatial resolution, in the Universal Transverse Mercator Zone 36 South coordinate system. The World Geodetic System 1984 was used for the spheroid and datum.

A minimum of 50 regions of interests (ROIs) per species or vegetation type were captured in ENVI 5.2 (Exelis Visual Information Solutions Pty Ltd, 2014; http://www.exelisvis.com), ensuring representation across all four seasons. Each ROI consists of a minimum of 4 pixels (Table 6.1). An insufficient number of ROIs for *Ficus sycomorus sycomorus* (Sycamore fig) and a lack of pure pixels of the canopies of *Syzygium cordatum* (Water berry) resulted in these two species being omitted from further analysis. A total number of n = 520 ROIs was captured for the study area for each season and the average spectra extracted for each ROI. A fifth data set was created through aggregating the individual seasons into one multi-season data set where the bands were separated per season, e.g. Band 1 autumn and Band 1 winter were listed as separate variables.

Table 6.2: Sensor and solar angle and azimuth as well as visibility for the RapidEye images across the four seasons

Section of study area	Northern					Southern				
	Sensor		Solar			Sensor		Solar		
RE date of acquisition (and season).	inclination	azimuth	zenith	azimuth	Visibility	inclination	azimuth	zenith	azimuth	Visibility
21 March 2011 (Autumn) *Maritime fall/spring**	5.4°	99.0°	32.3°	31.5°	40.0 km	4.9°	99.0°	32.5°	31.3°	54.0 km
18 July 2011 (Winter) *Midlat winter**	11.2°	99.5°	51.7°	19.5°	47.5 km	10.7°	99.4°	51.9°	19.4°	50.0 km
22 October 2011 (Spring) *Maritime fall/spring**	16.8°	279.7°	18.6°	24.2°	100 km	17.3°	279.6°	18.8°	23.9°	40.0 km
13 January 2012 (Summer) *Midlat summer**	16.6°	277.7°	13.3°	63.1°	100 km	17.0°	277.6°	13.4°	62.2°	36.8 km

** Atmospheric condition algorithm selected in ATCOR2.*

6.2.3. Analysis of variation of spectral reflectance data across seasons

The variation of the average canopy spectra of the tree species and associated vegetation types species was compared across the single seasons, listing the number of statistically significant differences per band as percentage of the total number of comparable pairs. A parametric one-way ANalysis Of Variance (ANOVA) was used to assess differences between species or vegetation types for each band and each season in the R software (RStudio Inc. v. 0.98.507, 2009-2013). To account for the multiple comparisons between the species or types, a post-hoc Tukey Honest Significant Difference (HSD) test was done and the alpha levels corrected for the Bonferroni effect (McDonald, 2008). The alpha level was adjusted for the 36 comparable pairs in each band and season, resulting in an alpha level ($p = 0.05/36$) of $p < 0.001$ considered significant at a 95 % confidence interval.

6.2.4. Accuracy assessment of species and vegetation type classification

The ability to separate the six wetland tree species and the associated vegetation types from the other species and vegetation types was assessed through an algorithm which combines a Partial Least Square (PLS) dimension reduction algorithm with a non-parametric decision-tree algorithm, Random Forest (RF) (Breiman, 2001; Boulesteix *et al.*, 2008). PLS regression has shown to yield high performance accuracy for classification (Wold, 1966;

Wold *et al.*, 2001; Cheriyadat and Bruce, 2003; Tsai *et al.*, 2007). In the PLS-RF script, a PLS regression scales the predictor variables prior to a bootstrap RF classification (Boulesteix *et al.*, 2008). The PLS-RF algorithm in the R software (RStudio Inc. v. 0.98.507, 2009-2013) was used to assess the classification accuracies between the nine vegetation types for the single season and for every combination of multi-season imagery. The classification results were therefore assessed for ten sets of every two-seasonal pairs, four sets of three-seasonal pairs and a set in which all four seasons were aggregated. The settings of the PLS-RF script were set to calculate as *ntree* = 500, the *mtry* variable was left as the default (single seasons: √5 = 2; multi-season: √20 = 4;), the number of components was set to maximum, while the *minsplit* variable was set at four, accounting for the small number of observations per species (Boulesteix *et al.*, 2008).

The average spectra of the ROIs were repetitively split into training and test data followed by classification in a 100-iteration bootstrap of the PLS-RF algorithm. In every iteration, the average spectra of 33 ROIs ($2/3^{rd}$) was randomly sampled from each class (total n = 297) for the training data set and 17 ($1/3^{rd}$) for the test data set (total n = 153). The overall accuracy (OA) and individual producer's and user's accuracies were recorded for the 100 iterations of the test data. The average OA and individual accuracies of the test data are reported for each individual season and the multi-season classifications.

Statistically significant differences between the OA and user's class accuracies of the test data of the single seasons were assessed using a one-way ANOVA in the R software (RStudio Inc. v. 0.98.507, 2009-2013). The post-hoc Tukey HSD test was used to assess difference between the four single seasons classifications, which comprised of ten comparable pairs, resulting in an adjusted alpha level (p = 0.05/10) of $p < 0.005$ considered significant at a 95 % confidence interval for single seasons. Thereafter, an ANOVA was used to assess differences between four of the classification results, one from the single, two-seasons, three-seasons and the multi-season classifications, where the average OA reached the maximum, the user's accuracies achieved a maximum for the majority of the tree species, and the number of species pairs confused was minimal. The alpha level of the six pairs of seasonal classifications was adjusted in a Tukey HSD test (p = 0.05/6) to $p < 0.008$ considered significant at a 95 % confidence interval.

6.2.5. Classification of nine vegetation types using the RapidEye image(s)

Two classifications, one from the single seasons and one from the multiple seasons, were selected for the classification of the RapidEye images. The classifications were selected where the average overall and user's accuracy was the highest and a minimal number of species pairs overlapped. The tree species and associated vegetation types for the study area were predicted using the random forest algorithm from the ModelMap package in R

Studio with a training data set of 33 ROIs per class (n = 297). The average spectra of the selected ROIs of the training data were used for model prediction in ModelMap, while the default values of *ntree* = 500 and the optimisation of the *mtry* variable, based on the Out-of-bag (OOB) error, were used. The accuracy of the predicted map was assessed in ENVI v.5.2 using an equal number (four) of pixels of each of the 17 ROIs per class of the test data set (*n* = 612 pixels, 68 per class). The OA, producer's and user's accuracies reported for each classification and the maps were investigated to compare the results for the whole of and selected sites in the study area.

6.3. Results

6.3.1. Variation of spectral reflectance data of vegetation types across seasons

The nine vegetation types showed a large variation in reflectance data for the NIR band of RapidEye across autumn, winter, spring and summer (Figure 6.3). The classes showed a high percentage of separability (> 69 %) across all seasons. Band 3 in autumn resulted in the highest number of separable pairs (89 %) in autumn.

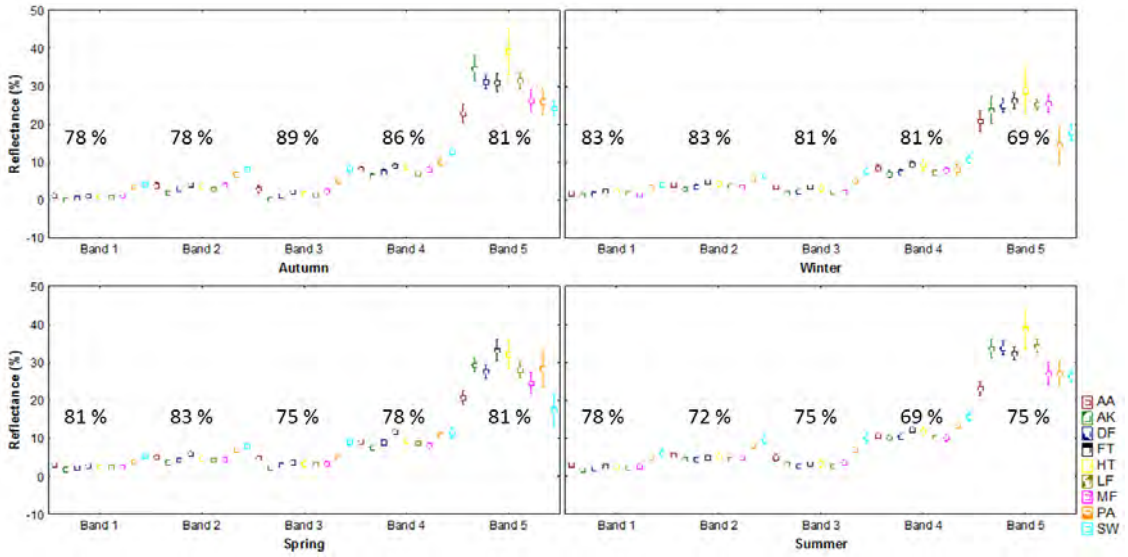

Figure 6.3: Reflectance values of the nine vegetation types for each band of RapidEye across four single seasons. The number of significant different species pairs (p < 0.001, Bonferroni corrected) is indicated as a percentage of the total number of comparable species pairs (36) for each of the bands.

6.3.2. Classification accuracies for the four and multiple seasons

The average OA accuracy (of 100 iterations) of the nine vegetation types was ± 80 % in the autumn, spring and summer, and 14 % higher (significantly $p < 0.008$, Bonferroni corrected) compared to winter (Table 6.3). The tree species and vegetation types were poorly separable in winter, with three classes (AK, DF and MF) resulting in average producer's and user's accuracies below 60 %. HT also had a low average producer's accuracy of 38 % in

winter. The average producer's and user's accuracies of these classes showed a significant (p < 0.008, Bonferroni corrected) increase of ≥ 10 % from winter to the autumn, spring and summer seasons. The minimum average producer's and user's accuracies peaked in the summer to 64±11.7 % (MF) and 69±10.9 % (DF) respectively. The classification results of the summer also showed the smallest number of intra-class confusion of > 10 %.

Table 6.3. Results of the classification accuracies of the 9 vegetation types across (A) the four single seasons and (B) the two, three and four multi-seasonal classifications.

(A)	Autumn		Winter		Spring		Summer	
Overall	78.8		66.2		80.0		79.5	
OA	±3.4		±3.1		±2.9		±3.1	
Accuracy	**PA**	**UA**	**PA**	**UA**	**PA**	**UA**	**PA**	**UA**
AA	78.8±3.4	68.6±8.2	84.5±8.6	71.0±8.4	86.9±7.7	86.9±7.9	88.6±8.6	85.7±7.3
AK	78.6±13.0	94.9±6.1	48.3±12.1	59.9±11.0	86.1±7.5	80.6±7.9	76.9±10.8	84.9±8.8
DF	73.8±10.2	82.5±10.5	51.2±11.2	43.9±8.8	68.7±12.6	69.0±9.3	65.6±11.9	69.4±10.9
FT	72.5±10.9	72.4±9.0	82.8±7.8	68.7±9.4	95.0±6.1	93.2±6.5	96.5±5.1	83.9±8.5
HT	86.4±11.0	76.4±10.4	38.3±10.6	75.7±14.9	66.1±10.4	73.5±9.6	69.6±11.7	77.6±9.4
LF	78.8±9.0	82.8±9.5	78.9±9.4	66.8±9.0	72.4±10.2	71.1±10.2	76.9±9.4	71.1±10.7
MF	50.9±11.2	63.8±12.2	34.5±13.7	41.4±13.2	52.4±11.7	67.9±12.3	63.8±11.7	76.9±9.6
PA	92.3±7.2	86.4±8.3	85.3±8.9	84.2±8.7	93.3±5.8	85.7±8.0	85.5±10.0	84.5±8.3
SW	97.1±4.2	91.6±6.6	91.6±6.9	93.9±5.9	99.2±2.0	94.6±5.2	91.8±6.7	88.5±7.4
Confusion	1	3	7	5	3	2	1	2

PA = producer's accuracy; UA = user's accuracy. Abbreviations: AA = *Acrostichum aureum* L. (Mangrove fern); AK = *Acacia kosiensis* (Dune sweet thorn); DF = East Coast Dune Forest; FT = *Ficus trichopoda* (Swamp fig); HT = *Hibiscus tilliaceus* (Lagoon hibiscus); LF = Coastal lowland forest; MF = Mangrove forests; PA = *Phragmites australis / mauritanus* (Reeds); SW = seasonal wetlands. Confusion = number of species pairs showing > 10 % confusion in the error matrix.

Across the autumn, spring and summer seasons, the mangrove forests (MF) showed the lowest separability of all the classes, with average producer's accuracies between 51 % and 64 %, average producer's accuracies < 70 % in autumn (Table 6.3) and class confusion of ±13.6 with the mangrove fern (AA) (Table 6.4). The mangrove forest (MF) and fern classes (AA) also showed a high percentage of overlap (> 10 %) in the autumn and spring season (results not shown here). The average producer's accuracies of other tree species in the autumn, spring and summer seasons ranged from 66 % to 92 % and average user's accuracies between 69 % and 95 %. The macrophyte (PA) and seasonal wetlands (SW) were highly separable from the tree classes with average producer's and user's accuracies > 85 % over autumn, spring and summer and the seasonal wetlands could be particularly well classified (> 92 %) in autumn and spring (Table 6.3). Tree species showed confusion between classes of > 10 % in all the single seasons, although the macrophytes (PA) and seasonal wetlands (SW) also showed a class confusion of > 10 % in the summer season that was not observed in the autumn, winter and spring seasons (Table 6.4).

Table 6.4: Confusion matrix showing the producer and user's accuracies of nine vegetation types for the summer season (average of 100 iterations).

	AA	AK	DF	FT	HT	LF	MF	PA	SW
AA	88.6	0.0	0.0	0.0	0.7	0.0	13.6	0.0	0.0
AK	0.1	76.9	5.8	0.0	7.3	0.0	1.9	0.0	0.0
DF	0.0	7.5	65.6	2.9	7.1	9.0	4.3	0.0	0.0
FT	0.9	0.0	1.5	96.5	1.5	6.2	5.1	1.4	0.0
HT	0.0	4.8	5.2	0.6	69.6	6.5	3.4	1.4	0.0
LF	0.0	5.9	19.9	0.0	4.9	76.9	2.4	0.0	0.0
MF	6.8	4.6	1.7	0.1	6.2	0.4	63.8	0.0	0.0
PA	3.6	0.2	0.4	0.0	1.4	0.1	2.8	85.5	7.6
SW	0.0	0.0	0.0	0.0	1.5	0.0	0.0	11.3	91.8

OA = overall accuracy (%); Stdev = standard deviation. Abbreviations: AA = *Acrostichum aureum* L. (Mangrove fern); AK = *Acacia kosiensis* (Dune sweet thorn); DF = East Coast Dune Forest; FT = *Ficus trichopoda* (Swamp fig); HT = *Hibiscus tilleaceus* (Lagoon hibiscus); LF = Coastal lowland forest; MF = Mangrove forests; PA = *Phragmites australis / mauritanus* (Reeds); SW = seasonal wetlands.

The results of the classification using multiple seasons showed a general increase in average OA of between 0 % (winter-summer) and 6 % (autumn-winter-spring) compared to the maximum average OA achieved in the single seasons (Table 6.4). The aggregation of the autumn and spring seasons showed a maximum average OA (85±2.6 %) of the two-season combinations, whereas the autumn, winter and spring season combination achieved a maximum average OA (86±3.1 %) of all the three-season classifications. The classification accuracy of the aggregation of all four seasons resulted in an average OA of 86±2.8 %, similar to the OA of the multi-season classification of autumn-winter-spring. The lowest user's accuracy recorded for the four-seasons classification was 80±8.8 % for DF, whereas the autumn-winter-spring classification's lowest user's accuracy was 81±92 % for LF (Table 6.5). The autumn-winter-spring classification also showed less classes from the user's accuracy with a confusion of > 10 % compared to the four-season classification, and therefore the autumn-winter-spring classification was selected as the optimum classification model from all the multi-season classifications (Table 6.6).

Table 6. 5: Average overall, producer's and user's accuracies (of 100 iterations) for multi-season classifications of four seasons for the nine vegetation types.

		Autumn Winter	Autumn Spring	Autumn Summer	Winter Spring	Winter Summer	Spring Summer	Autumn Winter Spring	Autumn Winter Summer	Autumn Spring Summer	Winter Spring Summer	Autumn, Winter, Spring, Summer
Overall accuracy (%) ± Standard deviation		83.7±3.2	85.3±2.6	84.6±2.7	83.6±3.2	79.9±3.6	81.7±2.8	86.4±3.1	85.4±3.1	86.4±2.9	83.1±3.1	86.0±2.8
Producer's accuracies (%)	AA	84.1±9.6	89.9±6.7	89.5±10.0	91.7±6.4	84.6±9.9	93.2±6.0	91.6±6.8	88.8±8.3	87.9±8.9	87.9±8.8	86.2±9.1
	AK	86.8±8.5	80.1±9.4	87.6±8.0	78.8±11.4	73.6±12.3	77.4±10.8	80.8±8.8	82.8±10.1	91.4±7.3	78.6±10.8	85.5±8.6
	DF	75.8±11.3	83.1±10.3	82.9±11.5	76.0±10.6	50.6±13.2	64.9±13.1	83.2±10.6	75.8±10.4	84.7±8.4	69.2±13.8	79.4±12.1
	FT	85.1±9.4	92.8±7.8	97.4±3.5	97.4±4.1	98.8±3.0	94.3±6.8	95.0±7.0	98.4±3.4	96.6±5.3	96.5±6.0	97.6±4.1
	HT	71.0±11.1	82.5±8.9	72.2±11.5	67.9±10.9	71.5±9.5	67.5±10.0	75.9±11.4	70.6±11.9	70.6±10.7	68.1±10.6	69.1±11.5
	LF	85.3±8.0	81.8±11.0	86.2±9.4	79.9±9.0	80.4±7.6	79.6±8.0	82.2±9.6	89.7±9.1	85.7±9.9	83.6±8.5	88.1±7.7
	MF	78.5±10.2	64.0±12.0	57.8±12.7	71.6±11.9	73.8±11.5	67.2±10.7	78.6±11.0	77.6±10.0	68.8±11.4	76.8±10.7	79.5±10.3
	PA	90.1±9.7	93.9±5.8	91.6±9.2	89.1±7.5	91.8±9.5	93.4±6.8	90.1±9.1	88.1±9.6	92.8±7.5	88.1±9.2	89.1±7.8
	SW	96.6±4.4	100.0±0.0	96.4±4.7	100.0±0.0	94.0±6.7	97.9±3.1	100.0±0.0	96.8±4.9	99.3±2.1	99.5±2.2	99.9±0.8
	Confusion	2	2	1	1	2	3	2	2	2	1	1
User's accuracies (%)	AA	81.8±7.6	84.1±7.9	78.8±8.0	81.4±8.8	82.2±8.2	87.3±5.9	84.1±8.2	83.2±7.7	85.4±8.8	88.0±7.5	89.1±7.3
	AK	90.5±6.6	95.2±5.7	89.9±6.7	85.2±9.2	75.9±10.1	83.1±9.6	89.2±7.4	87.0±9.5	90.1±6.8	83.5±10.3	88.4±8.0
	DF	76.0±8.3	77.1±9.2	78.0±9.5	76.4±8.8	69.7±13.9	66.6±9.9	82.4±8.2	79.9±10.3	77.1±10.3	73.9±10.6	80.4±8.8
	FT	74.9±9.2	77.1±9.2	83.8±7.5	91.0±6.9	74.8±8.2	92.3±6.4	87.5±7.7	81.8±8.2	90.2±6.7	91.8±5.6	86.2±9.0
	HT	82.8±9.1	78.7±8.7	88.3±8.8	84.0±9.2	84.1±8.8	78.4±10.6	83.5±9.8	90.3±8.0	86.8±9.7	84.5±9.1	88.9±8.0
	LF	86.7±7.2	86.8±8.9	85.9±8.6	77.2±9.7	76.4±9.6	70.3±9.6	81.1±9.2	87.0±7.9	86.5±7.3	73.9±8.7	82.5±9.3
	MF	83.8±9.0	88.9±8.5	84.8±11.3	79.6±9.1	80.3±11.3	82.0±9.3	89.3±7.6	86.3±8.5	84.4±8.8	83.1±9.9	83.5±9.5
	PA	89.2±7.1	88.2±7.7	88.2±7.3	92.1±7.2	88.5±7.8	89.2±6.4	90.8±6.7	89.9±6.5	89.2±8.2	86.1±9.1	88.2±8.3
	SW	94.4±7.1	93.5±5.8	92.7±7.4	91.6±6.1	94.2±7.1	92.8±6.7	95.7±5.5	91.0±7.2	94.2±6.2	90.2±6.5	94.1±6.1
	Confusion	2	0	0	2	4	1	1	3	2	1	2

Abbreviations: AA = *Acrostichum aureum* L. (Mangrove fern); AK = *Acacia kosiensis* (Dune sweet thorn); DF = East Coast Dune Forest; FT = *Ficus trichopoda* (Swamp fig); HT = *Hibiscus tilliaceus* (Lagoon hibiscus); LF = Coastal lowland forest; MF = Mangrove forests; PA = *Phragmites australis / mauritanus* (Reeds); SW = seasonal wetlands. Confusion = number of species pairs showing > 10 % confusion in the error matrix.

Table 6.6: Confusion matrix showing the producer and user's accuracies of nine vegetation types for the optimum multi-season classification (average of 100 iterations), including the autumn, winter and spring seasons.

	AA	AK	DF	FT	HT	LF	MF	PA	SW
AA	91.6	4.9	0.4	0.2	0.5	0.1	9.7	0.1	0.0
AK	0.2	80.8	0.6	0.0	9.1	0.9	0.0	0.0	0.0
DF	0.0	2.4	83.2	1.2	0.6	12.4	1.2	0.0	0.0
FT	0.2	2.4	0.8	95.0	5.3	0.0	2.9	1.4	0.0
HT	0.0	2.3	2.1	2.6	75.9	3.8	2.7	2.7	0.0
LF	0.0	4.3	12.3	0.9	2.0	82.2	0.3	0.4	0.0
MF	7.7	0.5	0.5	0.1	0.9	0.0	78.6	0.2	0.0
PA	0.4	1.7	0.0	0.0	5.0	0.0	2.5	90.1	0.0
SW	0.0	0.0	0.0	0.0	0.0	0.0	0.0	4.8	100.0

Abbreviations: AA = *Acrostichum aureum* L. (Mangrove fern); AK = *Acacia kosiensis* (Dune sweet thorn); DF = East Coast Dune Forest; FT = *Ficus trichopoda* (Swamp fig); HT = *Hibiscus tilleaceus* (Lagoon hibiscus); LF = Coastal lowland forest; MF = Mangrove forests; PA = *Phragmites australis / mauritanus* (Reeds); SW = seasonal wetlands.

In comparing the average OA of the classification results of the optimum classification from the single, two-season, three-season and four-season classifications, the summer classification was significantly lower ($p < 0.05$, Bonferroni corrected) compared to the multi-optimum season classifications (Figure 6.4).

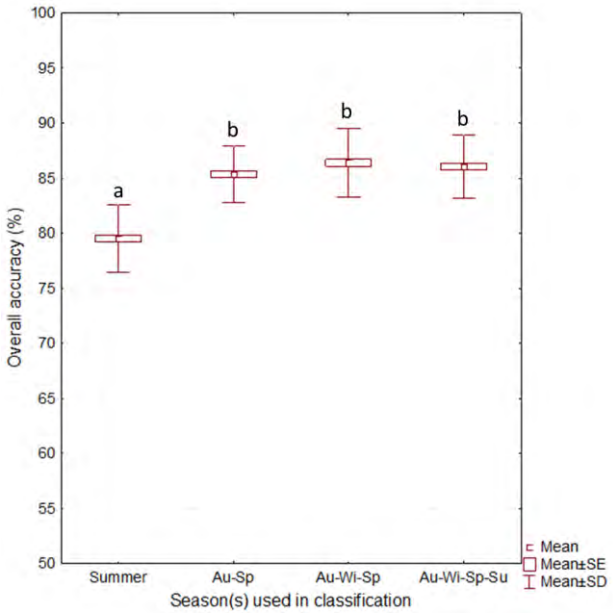

Figure 6. 4: Variation of the average OA (of 100 iterations) of four classification options. Letters above the boxplots indicate statistically significant differences ($p < 0.008$, Bonferroni corrected).

Six of the nine tree species or associated vegetation types showed a significant ($p < 0.05$, Bonferroni corrected) increase in user's accuracies when multi-season classifications were used, including AK (4 – 10 %), DF (8 - 13 %), LF (10 - 16 %), MF (7 – 12 %), PA (4 – 6 %) and SW (5 – 7 %) (Figure 6.5). In contrast, AA and FT showed no significant increase when multiple seasons were used for classification, except for an increase of 3 % for AA (significant, $p < 0.05$, Bonferroni corrected) when all four seasons are aggregated. HT showed a significant increase in user's accuracy of 6 % and 11 % when three and four seasons were aggregated, respectively.

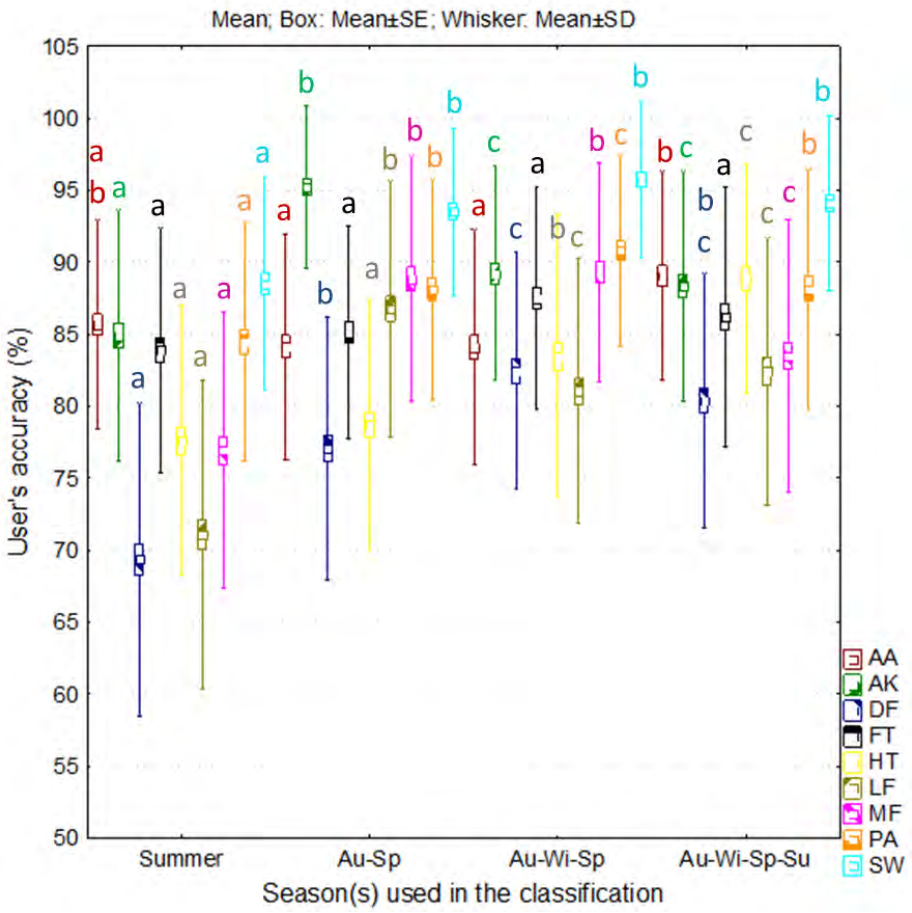

Figure 6. 5: Variation of the average user's accuracies (of 100 iterations) of four classification options. Letters above the boxplots indicate statistically significant differences ($p < 0.008$, Bonferroni corrected).

6.3.3. Predicting vegetation types for the study area

The OA of the predicted map for the multi-season was 11 % higher compared to the OA of the predicted map for summer (Table 6.7). The summer map was able to predict AA, FT, PA and SW with user's accuracies > 86 %. Five of the nine classes resulted in poor predictions in summer with user's accuracies below 70 %, including AK, DF, HT, LF and MF. These classes show a classification confusion of up to 40 % with one another (Table 6.8). The multi-season prediction resulted in fewer classes with a user's accuracy < 70 %. The lowest user's accuracies of the multi-season predicted map were recorded for DF (59 %) and HT (56 %). The user's accuracies increased in the multi-season predicted map, compared to the summer map, for a number of tree species or associated vegetation types when the multi-season were used in the prediction, including 7 % for FT and between 15 % and 30 % for AK, DF, LF and MF (Table 6.7). Fewer class pairs were also confused with the multi-season classification with the class pair HT and LF peaking at 29 % (Table 6.8).

Table 6. 7: Overall, producer's and user's accuracies for the best classification results of the (A) single season and (B) multiple seasons.

Classification:	Summer		Autumn-Winter-Spring	
Overall accuracy (%)	69.8±26.6		78.8±23.4	
	PA	**UA**	**PA**	**UA**
AA	79.4	85.7	95.6	82.3
AK	66.2	64.3	92.6	79.7
DF	41.2	38.9	58.8	58.8
FT	75.0	86.4	79.4	93.1
HT	75.0	55.4	83.8	56.4
LF	11.8	30.8	25.0	70.8
MF	70.6	50.5	82.4	80.0
PA	95.6	95.6	95.6	95.6
SW	95.6	97.0	95.6	100.0
Confusion	7	5	2	3

PA = producer's accuracy; UA = user's accuracy. Abbreviations: AA = *Acrostichum aureum* L. (Mangrove fern); AK = *Acacia kosiensis* (Dune sweet thorn); DF = East Coast Dune Forest; FT = *Ficus trichopoda* (Swamp fig); HT = *Hibiscus tilliaceus* (Lagoon hibiscus); LF = Coastal lowland forest; MF = Mangrove forests; PA = *Phragmites australis / mauritanus* (Reeds); SW = seasonal wetlands. Confusion = number of species pairs showing > 10 % confusion in the error matrix.

Table 6. 8: Confusion matrix showing in percentage the producer and user's accuracies of nine vegetation types for the (A) summer and (B) multi-season classifications.

(A)	AA	AK	DF	FT	HT	LF	MF	PA	SW
AA	79.4	0.0	0.0	0.0	0.0	0.0	20.6	0.0	0.0
AK	0.0	66.2	11.8	0.0	16.2	1.5	4.4	0.0	0.0
DF	0.0	29.4	41.2	1.5	4.4	11.8	11.8	0.0	0.0
FT	0.0	0.0	0.0	75.0	4.4	5.9	14.7	0.0	0.0
HT	2.9	1.5	13.2	2.9	75.0	4.4	0.0	0.0	0.0
LF	0.0	4.4	38.2	5.9	22.1	11.8	17.7	0.0	0.0
MF	8.8	1.5	1.5	1.5	13.2	2.9	70.6	0.0	0.0
PA	1.5	0.0	0.0	0.0	0.0	0.0	0.0	95.6	2.9
SW	0.0	0.0	0.0	0.0	0.0	0.0	0.0	4.4	95.6

(B)	AA	AK	DF	FT	HT	LF	MF	PA	SW
AA	95.6	0.0	0.0	0.0	0.0	0.0	4.4	0.0	0.0
AK	0.0	92.7	7.4	0.0	0.0	0.0	0.0	0.0	0.0
DF	1.5	11.8	58.8	0.0	8.8	7.4	11.8	0.0	0.0
FT	2.9	0.0	0.0	79.4	17.7	0.0	0.0	0.0	0.0
HT	0.0	4.4	4.4	4.4	83.8	2.9	0.0	0.0	0.0
LF	5.9	7.4	26.5	1.5	29.4	25.0	4.4	0.0	0.0
MF	5.9	0.0	2.9	0.0	8.8	0.0	82.4	0.0	0.0
PA	4.4	0.0	0.0	0.0	0.0	0.0	0.0	95.6	0.0
SW	0.0	0.0	0.0	0.0	0.0	0.0	0.0	4.4	95.6

Abbreviations: AA = *Acrostichum aureum* L. (Mangrove fern); AK = *Acacia kosiensis* (Dune sweet thorn); DF = East Coast Dune Forest; FT = *Ficus trichopoda* (Swamp fig); HT = *Hibiscus tilleaceus* (Lagoon hibiscus); LF = Coastal lowland forest; MF = Mangrove forests; PA = *Phragmites australis / mauritanus* (Reeds); SW = seasonal wetlands.

The mangrove ferns (AA) and wetlands (MF) are found to be closely associated with one another on the predicted map of the vegetation types using the summer RapidEye image along the estuarine systems as well as in the DukuDuku Forest, the eucalypt plantations and

the sugarcane farms (Figure 6.7A). The location of *Acacia kosiensis* (AK), dune (DF) and lowland (LF) forests were predicted on the dunes as well as in the DukuDuku Forest. In the area north and south of the St Lucia Estuary clusters of AK occur as closed-canopy pioneering stands. A large cluster of *Ficus trichpoda* (FT) was predicted in the summer image to be located in the uMfolozi River Swamp, with a smaller number of pixels distributed in the dune and lowland forests. The prediction of Lagoon hibiscus (HT) resulted in areas on the river floodplain north of the uMfolozi River Swamp, and areas between the sugarcane and eucalypt plantations to be classified as HT. Macrophyte vegetation fringes the estuarine systems as well as the uMfolozi River Swamp and both sides of the Narrows.

In comparison to the map predicted from the summer RapidEye images, the prediction from the multi-season images resulted in a reduction of the extent of mangrove wetlands, while the user's accuracy increased by 29 % for the mangroves (MF) and a reduction in class confusion with other forest types (Figure 6.7B). The clusters *of Acacia kosiensis* (AK) appear denser on the multi-season image, compared to the summer image, although the species are also interspersed in the dune (DF) and lowland (LF) forests. The dune forest (DF) dominates the coastal dunes north and south of the estuary mouths, although also occur in smaller patches on the coastal plain and in the DukuDuku Forest. The DukuDuku Forest consists of predicted classes AK, DF, LF and MF, but with less dominance of the DF compared to the predicted map of summer. The multi-season prediction further shows a larger extent of *Ficus trichpoda* (FT) in the uMfolozi River swamp, extending westward into the DukuDuku village and as far west as Lake Futululu, south-west of the DukuDuku Forest. In the multi-season prediction the Lagoon hibiscus (HT) is less prevalent across the study area, compared to the summer image prediction. A larger extent of the study areas was predicted as macrophytes (PA) and seasonal wetlands (SW) in the multi-season image, compared to the summer prediction, dominating the coastal plain.

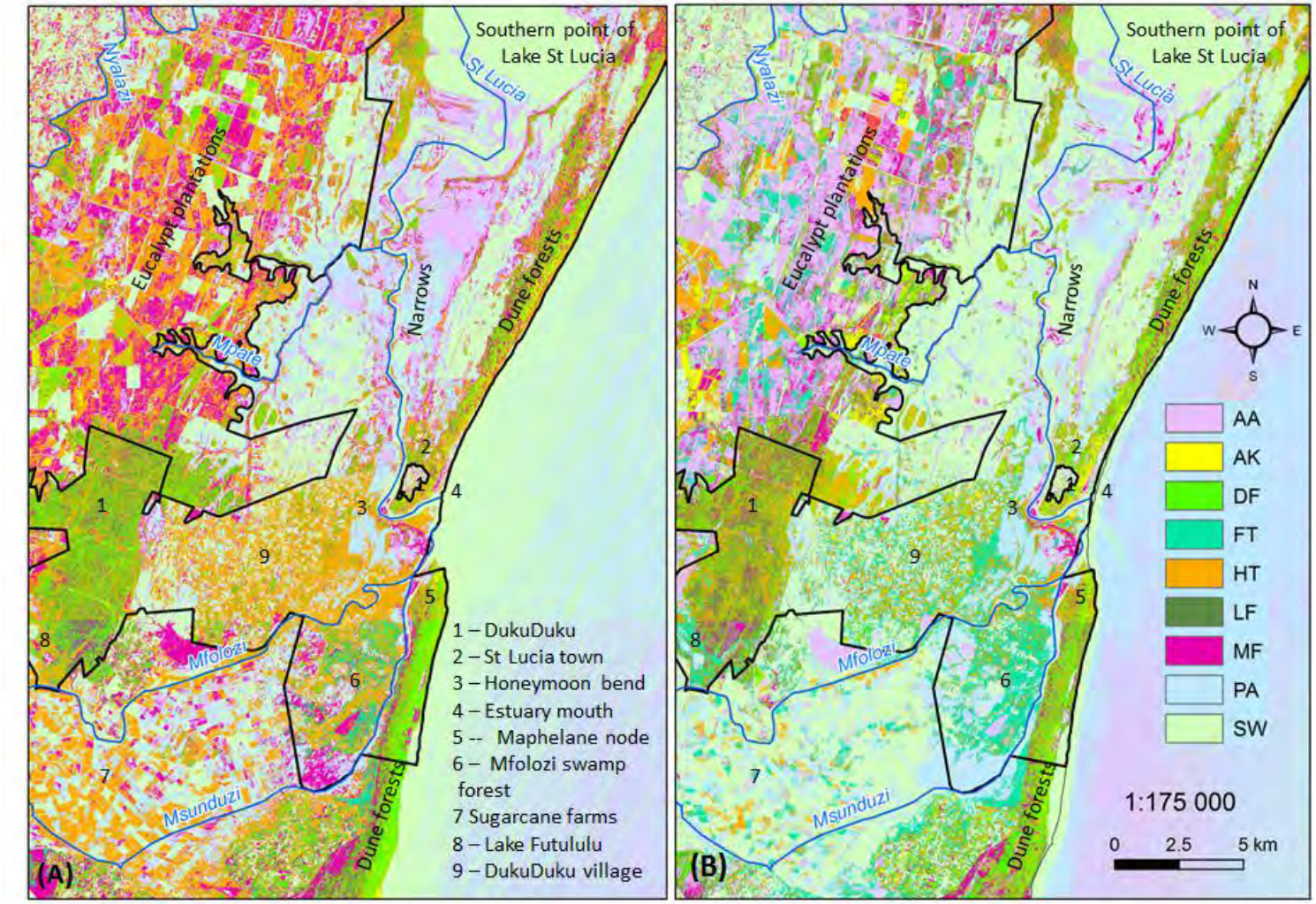

Figure 6.6: Predicted tree species or associated vegetation types using the (A) summer image of RE and (B) the multi-season RE images (autumn-winter-spring). The black outline show the boundary of the iSimangaliso Wetland Park; the blue lines the 1:500 000 rivers.

6.4. Discussion

RapidEye imagery was successful in the classification of broad vegetation types and closed-canopy forest wetlands in the St Lucia and Maphelane nodes of the iSimangaliso Wetland Park in KwaZulu-Natal, South Africa. The average overall accuracy (average of 100 random forest classifications) for four single seasons (autumn, winter, spring and summer) ranged from the lowest in winter (66±3.1 %) to the highest in spring (80±2.9 %). The summer season optimised the separability of classes with the producer's accuracies between 64±11.7 % and 97±5.1 % and user's accuracies ranging from 69±10.9 % to 89±7.4 %. The resultant accuracies were comparable to other dryland tree species classification studies using RapidEye and WorldView-2, even though the tree species in this study occur in wetland and estuarine environments (Immitzer *et al.*, 2012; Pu and Landry, 2012; Adelabu *et al.*, 2013; Cho *et al.*, 2015; Omer *et al.*, 2015). Regardless of the success with the closed-canopy classes, pure isolated canopies of tree species were difficult to identify on the RapidEye images. Canopies of *Ficus sycomorus* (FSYC), *Hibiscus tilliaceus* (HT) and *Syzygium cordatum* (SC) were difficult to separate visually from adjacent vegetation reflectance on the RapidEye imagery. HT and SC were also too small in diameter to obtain pure pixels not influenced by adjacent cover. FSYC and HT had canopy architecture that was not densely leaved, and hence the influence of background reflectance from other vegetation reduces the ability to obtain pure signatures. Obtaining regions of interest for individual canopies consistently across seasons was further compromised by parallax errors resulting from different sensor angles across the four seasons. Although the user's accuracies were high, the extent of certain classes predicted from the summer image, appeared to be over predicted in parts of the study area (Appendix 1). RapidEye imagery with a 5 m spatial resolution was therefore found unsuitable for mapping isolated tree canopies, but is suitable for broader vegetation groups and closed-canopy forests. WorldView-2 imagery with a higher spatial resolution of 2 m would likely improve the mapping of FSYC, HT and SC for this area.

Three of the four single seasons resulted in significantly higher overall classification accuracies > 79 % (autumn, spring and summer), compared to the winter season of 66±3.1 %. The use of multi-season data, however, resulted in significantly higher accuracies compared to the single season data for the nine vegetation types in the study area. The aggregation of autumn and spring showed an increase of 5.8 % compared to the highest overall accuracy of the single seasons (summer OA = 79.5 %), whereas the aggregation of autumn, winter and spring showed a significant increase of 6 % compared to the summer classification. The aggregation of all four seasons showed no significant difference compared to the aggregation of two or three seasons. Multiple seasons also resulted in significant increases of user accuracies of classes for the majority of the vegetation types and a reduction in the percentage of class overlaps when compared to the single seasons, however the improvement was mostly noticed for the four forest types which showed a

high overlap, including AK, DF, LF and MF, and to a lesser degree for the macrophytes (PA) and seasonal wetlands (SW). The predicted map resulting from the multi-season RE imagery seemed closer to the true extent of the vegetation distribution (evaluated for known areas – Appendix 1). Further validation of the prediction will be required across the area to determine true accuracy. The benefit of using multi-season data and the improvement in accuracies should be compared to the increase in cost of using multiple images, and may likely vary with species and across geographic regions.

Class confusion between dryland forest types was expected, such as *Acacia kosiensis* (AK) with the dune (DF) and lowland forests (LF) as both dune and lowland forests is host to AK and many other similar tree species (Scott-Shaw and Escott, 2011). It is likely that elevation could be used to separate the two classes, although further work is required to assess whether the dominant tree species of the dune forest significantly differ from those identified for the DukuDuku Forest. The dominant *Albizia adiathifolia* and *Strychnos* species of the DukuDuku Forest (Cho *et al.*, 2015) were predicted in this study primarily as dune and lowland forest, but also mangroves (MF) and Lagoon hibiscus (HT), the latter owing to the spectral influence of grass in the Lagoon hibiscus class. The canopy reflectance of the mangrove forests appeared to overlap with a number of species in the dune and lowland forest, possibly the *Strychnos* species, as well as known clusters of *Casuarina equisetifolia*, the eucalypt plantations (*Eucalyptus grandis*) and even areas dominated by sedges and other wetland plants around Honeymoon Bend and the Mfabeni wetland. The extent of the incorrect prediction is reduced in the predicted map of the multi-season classification, compared to the prediction of the summer RE image, and although the results compare well with previous work (Nondoda, 2012; Lück-Vogel *et al.*, Submitted), further refinement will be required to reduce areas of incorrect predictions. Similarly the prediction of the swamp forests compared well to the work of Nondoda (2012) and Lück-Vogel *et al.* (submitted), although confusion with other *Ficus* species may be prevalent across the study area. The macrophyte (PA) and seasonal wetland (SW) classes were highly separable from the tree species classes and appeared to be well predicted across the study area, however further validation will be required around the Mfolozi River Swamp and along the Narrows where access is difficult. The vegetation classification offers improved understanding of the distribution of vegetation types compared to the land cover classification of the province (Ezemvelo KZN Wildlife, 2011). Further description of selected areas is provided in Appendix 1.

The improvement of the tree species of this study, based on the classification accuracies and extent in the predicted maps, can be expected with the increase in spatial resolution and number of bands. WorldView-2 data at 2 m spatial resolution with a coastal and yellow band should be tested to assess the capability of multispectral data to classify tree species using spectral reflectance values. In addition LiDAR data and expert knowledge can contribute to an improved prediction of the location of species. Mangroves and hibiscus, for

instance, have a limited range and are mostly associated with the estuarine systems, and the prediction can therefore be limited to known habitat ranges. Further improvements to our work may also include the optimisation of the *ntree* and *mtry* variables where the PLS-RF classification assessed the separability of the canopy spectra, as well as the comparison of the PLS-RF and random forest algorithms with one another. Although it was the original intent of this study to do so, the PLS-RF was not optimised for image classification and a memory limit of 80 Gb was insufficient for the script to run. The results of the study are lastly limited to the selected tree species and vegetation types of the study area and remain to be assessed for other species and climatic regions too.

6.5. Conclusion

The ability of RapidEye imagery was evaluated for the classification of tree species in wetland and estuarine environments in the iSimangaliso Wetland Park, KwaZulu-Natal, South Africa. RapidEye imagery at 5 m spatial resolution with 5 bands was successful in separating broad vegetation types or tree species with closed-canopy forest structures although the classification of species with canopies < 10 m diameter or sparse leaves was unsuccessful. The use of multiple seasons increased the classification accuracy significantly compared the single season with the highest classification accuracies.

Acknowledgements

I would like to thank Dr Melanie Lück-Vogel for teaching me how to do atmospheric correction in ATCOR2.

CHAPTER 7: DISCUSSION

7.1. Introduction

Remote sensing is a valuable tool for monitoring the changes in forest species composition and tree species distribution at frequent intervals and regional scale. The multiple threats to coastal swamp and mangrove forests make it imperative that particular attention should be paid to these areas. Quite often ground surveys in these areas are difficult owing to inundation and in some instances access is impeded due to the presence of dangerous animals. Remote sensing offers an alternative to ground survey, particularly in swamp and mangrove forests, as well as other forested wetlands where it is necessary to predict and monitor species composition and distribution.

The separability of tree species is based on the premise that one or more of the foliar biochemical or biophysical parameters are different and that differences vary across phenological phases. Leaf fall has, for example, been identified as an important phenological event to discriminate between a number of deciduous species (Key *et al.*, 2001). For evergreen tree species, phenological events may be less pronounced or inconspicuous compared to deciduous species. Therefore a larger number of plant properties would be needed to enhance differences between evergreen tree species in remote sensing, and most likely more bands than those in the visible range where leaf colour is observed.

Hyperspectral remote sensing makes it possible to quantify a number of plant properties through narrow absorption features located between 350 nm and 2 500 nm of the electromagnetic spectrum. The cost of hyperspectral images is however too high for monitoring tree species over time and at regional extent. Multispectral sensors, on the other hand, offer more affordable images which make it possible to revisit areas at regional scale more frequently. Several of the multispectral sensors (i.e. SPOT, IKONOS and Quickbird) offer spatial resolutions matching the extents of tree canopy diameters. The number of and spectral resolution of the bands of multispectral sensors are not conducive to the detection and monitoring of multiple plant properties since they are spectrally too broad for the quantification of the narrow absorption features, and cover predominantly the visible and near-infrared spectra. A large number of narrow absorption features in the short-wave infrared, related to plant nutrients, are therefore not covered by these sensors.

The introduction of the red-edge band in the multispectral sensors RapidEye and WV2 offered new possibilities for improved tree species classification. The red-edge band was found to be effective for predicting plant nitrogen, foliage biomass while also improving species discrimination (Mutanga and Skidmore, 2004; Cho *et al.*, 2008; Mutanga *et al.*, 2012; Adelabu *et al.*, 2013). A number of studies showed promising results when using these sensors in nutrient prediction at broad regional level (Ramoelo *et al.*, 2012; Ullah *et al.*,

2012; Clevers and Gitelson, 2013; Ramoelo *et al.*, 2013; Cho *et al.*, 2013), as well as distinguishing between a number of deciduous and evergreen tree species (Immitzer *et al.*, 2012; Pu and Landry, 2012; Adelabu *et al.*, 2013; Cho *et al.*, 2015; Omer *et al.*, 2015). Class overlap remains a problem where multispectral sensors were used to classify tree species, and to a lesser degree the same problem was found with the use of hyperspectral sensors. The use of images from multiple dates has shown an improvement of species discrimination and a reduction of error for deciduous tree species in America (Key *et al*., 2001) and grassland habitats in Germany (Shuster *et al*., 2015). Key *et al*. (2001) postulated that images from multiple phenological phases could improve species discrimination when compared to a single snapshot in time. The variation in plant properties may be more pronounced across a variety of phenological phases compared to a single phenological event. The hypothesis remains to be assessed across a number of phenological phases, including dormancy, leaf development, flowering and the end of the growth season, particularly for evergreen tree species.

There are still a number of challenges associated with the use of remote sensing for tree species discrimination. While hyperspectral data may offer a better representation of plant properties in narrow absorption bands, the multitude of correlated bands requires effective data reduction and transformation methods to extract the most important bands for species discrimination. The influence of atmospheric conditions, the background reflectance from soil and other vegetation, and the reduction of reflectance from vegetation in wetland environments influence the ability to separate species using images from multispectral space-borne sensors. Pixels are often not a pure reflection of the reflectance of tree species but a mixture of reflectance from twigs, shadows cast by upper leaves and adjacent land cover where the tree canopy is not densely leaved or match the spatial resolution of the image.

The primary aim of this thesis was to assess whether multiple seasons, with representation of multiple phenological events, would improve the separability of tree species when compared to a single phenological event. At the same time, some of the limitations to remote sensing of hyperspectral and multispectral sensor are also addressed in this study. The hypothesis has therefore been formulated as follows:

> H0: multi-season information of evergreen wetland tree species is not unique and does not improve species discrimination when compared to a single season's information
>
> Ha: multi-season information of evergreen wetland tree species is unique and improves species discrimination when compared to a single season's information

Four objectives have been formulated in testing the hypothesis:

- Assess whether tree species are unique in foliar biochemical concentrations over multiple seasons.
- Ascertain which bands are the most important across phenological phases for species discrimination.
- Determine whether leaf reflectance spectra of multiple seasons will improve the species classification compared to a single season.
- Assess whether image stacks of multiple seasons will improve species discrimination when compared to a single season.

7.2. Are the seasonal profiles of tree species unique in terms of their foliar biochemical concentrations over multiple seasons?

In general, the foliar biochemical results showed that the foliar pigments (carotenoids and chlorophyll) of the six evergreen tree species varied little over winter, spring, summer and autumn. For five of the six tree species the variation in foliar pigments was not different across the four seasons, except for *Syzygium cordatum*, which showed significantly (p < 0.05, Bonferroni corrected) lower pigment concentrations in spring compared to the other three seasons. In contrast to the foliar pigments, a high variability was observed for foliar nitrogen across the four seasons. In winter the highest mean and lowest variability were observed for foliar nitrogen, while a decrease in mean foliar nitrogen was observed during the growth seasons (spring, summer and autumn) while the coefficient of variance increased. Three species, *Bruguiera gymnorrhiza*, *Ficus trichopoda* and *Syzygium cordatum*, contributed to the significantly (p < 0.05, Bonferroni corrected) higher mean nitrogen concentration in winter, compared to the other three seasons. The latter two species also showed a significant reduction in foliar nitrogen from spring to autumn. Foliar phosphorus concentrations showed little variation over the four seasons but it increased slightly from spring to summer, while it decreased from summer to autumn. *Ficus trichopoda* showed significantly higher foliar phosphorus concentration in spring compared to summer, while the average concentration in spring for *Syzygium cordatum* was significantly higher compared to winter, summer and autumn. The results contribute to a better understanding of the seasonal variation in foliar biochemicals of evergreen tree species in subtropical regions globally and are the first reported for South Africa.

The fact that foliar pigments vary little across seasons for most of these evergreen tree species, support the notion that the basic processing mechanism of photosynthesis is similar at foliar biochemical level for most of the species. On the other hand, the high variability of foliar nitrogen in the growth season suggests that there are differences between species in nitrogen remobilisation and partitioning for different plant parts during these seasons.

The six evergreen tree species had more significantly (p < 0.05, Bonferroni corrected) different comparable pairs for foliar pigments (67 %) and nitrogen (73 %) in the spring season, compared to the other three seasons. A higher number of significantly different pairs was observed for foliar nitrogen in summer (67 %) and autumn (60 %), compared to the foliar pigments and phosphorus. Species were in fact poorly separable using foliar phosphorus only, where < 53 % was significantly different across all four seasons. It is therefore more likely that species will be more separable by means of their foliar proteins and starches related to nitrogen rather than their foliar pigments. The findings support the importance of the SWIR bands for tree species classification (Martin *et al.*, 1998; Huber *et al.*, 2008; Immitzer *et al.*, 2012).

7.3. Most important bands for tree species classification across seasons

The most important spectral bands for the classification of the six evergreen tree species were determined through the relationship between leaf reflectance spectra and foliar nutrient (nitrogen and phosphorus) concentration across the four seasons. Twenty-four spectral bands, which are associated with known absorption features of plant properties, were initially selected where the coefficient of determination (R^2) between leaf spectra and nutrient concentration were high across all four seasons for both foliar nitrogen and phosphorus. These include absorption regions for pigments (500, 510, 670, 680, 700 and 760 nm), foliage biomass (740 nm and 780 nm), leaf water content (860 nm and 1240 nm), as well as for starch, lignin, tannins, pectin, protein and cellulose (1630, 1690, 1900, 2000, 2050, 2060, 2130, 2180, 2200, 2210, 2240, 2250, 2300 and 2380 nm).

The relationship between foliar nutrients and leaf spectra varied for both nitrogen and phosphorus, contributing to an improved understanding of this relationship for evergreen tree species in subtropical forests. Foliar nitrogen showed a higher coefficient of determination across the selected bands and four seasons (maximum average R^2 = 0.8), compared to foliar phosphorus (maximum average R^2 = 0.38). The most important bands for predicting foliar nitrogen were associated with protein, cellulose, lignins, tannins and pectin bands in the SWIR and to a lesser degree, the foliage biomass in the red-edge region (Figure 7.1). The spectral bands which resulted in the highest coefficients of determination for phosphorus were also located in the SWIR and associated with lignin, waxes, protein and nitrogen. The spectral band combination 2130 nm and 2240 nm yielded the highest coefficient of determination between leaf spectra and foliar nitrogen across all four seasons, followed by 2180 nm and 2210 nm, then 1630 nm and 1690 nm and lastly foliage biomass bands 740 nm and 780 nm (Figure 7.1).

The poor relationship between leaf spectra and foliar nutrient concentration during winter can be ascribed to the fact that nutrients are stored in older leaves of evergreen tree species during the dormancy period. The increased relationship between leaf reflectance

and nutrient concentration during the spring, summer and autumn seasons, on the other hand, reflects the dynamic nature of nutrient partitioning and relocation to other plant parts during the growth season. The error in predicting nutrients from leaf spectra is lowest for individual seasons, however increase when models from one season is applied to another. The red-edge region, often used as a surrogate for predicting leaf nitrogen, was found to be accurate in predicting leaf nitrogen only in the winter, whereas the SWIR bands outperformed the red-edge band during the spring, summer and autumn seasons. The SWIR bands are therefore crucial to the decoupling of chlorophyll and other co-variants of nitrogen from foliar nitrogen. Considering that the foliar biochemical analysis also indicated less significantly different species pairs for foliar pigments than for foliar nitrogen, it therefore becomes less likely that the red-edge band in RapidEye and WorldView-2 would be sufficient in decoupling pigments and nutrients for the improvement of tree species classification.

Table 7. 1: Maximum linear regression coefficient of determination (R^2), extracted from a matrix showing the relationship between selected nutrient concentrations and spectra for band regions known to relate to leaf features, listed per season and nutrient.

Foliar nutrient	VI Band combination •	Associated parameter	Winter	Spring	Summer	Autumn	*Average*
N	2130, 2240	Protein	0.09*	0.80*	0.77*	0.71*	*0.59*
	2180, 2210	Protein & cellulose	0.06*	0.60*	0.63*	0.59*	*0.47*
	1630, 1690	Lignin, tannins, pectin & protein	0.06*	0.66*	0.47*	0.33*	*0.38*
	740, 780	Foliage biomass	0.08*	0.62*	0.49*	0.49*	*0.42*
P	2050, 2380	Lignin, waxes, protein & nitrogen	0.28*	0.24*	0.09*	0.38*	*0.25*
	2060, 2380	Protein, nitrogen & lignin	0.20*	0.25*	0.13*	0.36*	*0.24*

• Two-band combinations yielding high correlations were extracted from regions known to be related to pigments (Gitelson *et al.*, 2002; Gitelson and Merzlyak, 2004; Gitelson *et al.*, 2006); foliage biomass (Mutanga and Skidmore, 2004; Cho *et al.*, 2007); leaf water content (Gao, 1996); proteins & starches (Curran, 1989); waxes & protein/enzyme *D*-ribulose 1-5-diphosphate carboxylase@2050, tannic acid@1660, lignin, pectins & protein/enzyme *D*-ribulose 1-5-diphosphate carboxylase@1680, lignin@2380 (Elvidge, 1990).

* –significant ($p < 0.01$)

The twenty-two spectral bands, associated with plant properties and which showed a high coefficient of determination between leaf spectra and foliar nitrogen, were found to be an effective method for data reduction of the hyperspectral data of the six evergreen tree species. The classification of the six tree species showed optimum results where the hyperspectral data were reduced to the 22 bands followed by PLS transformation, which removes the correlation between the bands, the reduction of the number of components used and a RF decision-tree algorithm for the classification. The average overall accuracy of ten iterations of the classification for spring was 84±3.6 % with the lowest user accuracy at 79±11.2 % for *Ficus trichopoda*. In comparison an optimised PCA-RF classification had an overall accuracy of 78±5 % with the lowest user's accuracy at 69±12.2 % for *Ficus sycomorus*.

The classification of the six evergreen tree species using 1 nm leaf spectra reduced to 22 selected bands and a 100 iteration of the PLS-RF in R Studio, resulted in average overall accuracies > 90 % (Table 7.2). In comparison, the classification of the leaf reflectance data, resampled to the bands of the multispectral sensors WorldView-2 and RapidEye, showed lower overall and user's accuracies. Using the most important spectral bands at hyperspectral scale therefore result in a significant higher overall accuracy of between 15 % and 29 % across the four seasons compared to the bands of the multispectral sensors.

Table 7. 2: Classification results of leaf and canopy reflectance data across four seasons using the PLS-RF algorithm. The average overall accuracy and standard deviation of 100 iterations are showed with the lowest user's accuracy of the tree species for leaf-level data and vegetation types for canopy-level data.

	Winter	Spring	Summer	Autumn
Leaf reflectance for 22 bands at hyperspectral scale.	90±3.5 (FT 86±9.2)	91±2.8 (FT 86±6.3)	92±2.7 (SC 88±7.5)	92±2.7 (FT 85±7.6)
Leaf reflectance resampled to WV2 bands.	68±4.7 (FT 54±12.8)	76±3.7 (FT 69±8.3)	71±4.2 (FT 58±12.6)	74±4.4 (SC 62±8.2)
Leaf reflectance resampled to RE bands.	63±4.4 (FT 48±10.5)	70±4.1 (FT 63±10.2)	63±4.3 (FT 44±15.1)	70±4.2 (FT 50±13.5)

Acronyms: FT = *Ficus trichopoda*; SC = *Syzygium cordatum*.

The robustness of the 22 most important hyperspectral bands identified for the classification of the six evergreen tree species should however be assessed for other tree species and climatic zones. In the Introduction it was postulated that the red-edge band of RapidEye and WorldView-2 would possibly contribute to improved condition monitoring and classification of tree species. Yet the results of this study indicate that an increase of the number of bands, particularly those in the SWIR, as well as narrow spectral band ranges are likely to contribute to significant increases in classification accuracies of tree species.

7.4. Would multiple seasons improve tree species classification?

The aggregation of foliar biochemical data from all four seasons increased the number of significantly different species pairs for foliar carotenoids (from 67 % to 73 %) and phosphorus (from 53 % to 60 %), it did not increase the maximum significant different species pairs attained for chlorophyll and nitrogen in spring (67 % and 73 % respectively). The analysis emphasized the importance of nitrogen for species discrimination, but provided only a narrow view on the widely complex molecules associated with nitrogen and which may vary between species more than the total foliar nitrogen concentration. Using leaf spectra from multiple seasons to predict foliar nitrogen also showed a slight decrease in the error of prediction for spring, although no major changes were seen for summer and autumn, while the error increased between 4 % and 7 % for the winter season. The

prediction of foliar phosphorus decreased in prediction error when data from multiple seasons were used similar to the foliar biochemical results.

The overall, producer's and user's accuracy of the classification results using the most important 22 hyperspectral bands for six tree species showed no statistically significant differences between the multi-season data and accuracies attained in summer and autumn. The use of the multi-season data for the two multispectral sensors resulted in a significant ($p < 0.005$, Bonferroni corrected) increases in the average overall accuracies of 8.5 % for WorldView-2 and 9.7 % for RapidEye. The increase in producer's and user's accuracies from the single seasons with the highest accuracies to the multi-season classification varied according to species. The multi-season classifications also decreased the number of species pairs which overlapped as well as the percentage of overlap between species pairs. This study is the first to compare the classification accuracies of six evergreen tree species using leaf-level data from single and multiple seasons at both hyperspectral and multispectral sensor scales. The improvements found in the classification for multispectral sensors remains to be assessed for other species and climatic zones to assess the validity of these findings.

The identification of three of the six tree species was problematic on RapidEye images. *Bruguiera gymnorrhiza* has narrow canopies of about 2 m in diameter and often grows underneath closed-canopy stands of *Avicennia marina*. Pixel impurity prohibited the identification of canopies of *Syzygium cordatum* while an insufficient number of known locations of *Ficus sycomorus* limited the classification of this species at image level. The remaining tree species *Avicennia marina*, *Ficus trichopoda* and *Hibiscus tilliaceus* were therefore mapped at image level, as well as a number of predominant vegetation types in the study area. Closed-canopy stands of *Avicennia marina* were mapped, although with the likeliness of hosting *Bruguiera gymnorrhiza* underneath the forest canopy. *Ficus trichopoda* often occur as large canopies forming dense swamp forests, leaving *Hibiscus tilliaceus* as the only species occurring as isolated canopies or clusters of trees. In the end nine vegetation types were used for classification, of which three were predominantly associated with the original six evergreen tree species, with the addition of *Bruguiera gymnorrhiza* co-occurring with *Avicennia marina.*

The average overall accuracy (of 100 iterations) increased in general when canopy reflectance data from multiple seasons were used for the classification of the nine vegetation types compared to the single season with optimal performance (summer average OA = 80±3.1 %). The aggregation of the autumn and spring seasons showed a significant ($p < 0.05$, Bonferroni corrected) increase of 5 % whereas the aggregation of autumn, winter and spring seasons, as well as all four seasons separately, increased the average overall accuracy significantly by 6 %. An increase in the user's accuracies of some vegetation types was observed, as well as a reduction in the number of and percentage of class overlaps, which is similar to what was observed when multiple season data for the

classification of the leaf reflectance data of the six tree species using were used. The prediction of the nine vegetation types (using the randomForest algorithm in ModelMap of R Studio) for the RapidEye image stack of autumn, winter and spring also resulted in higher overall accuracies and the user's accuracies of species which showed class overlaps, such as *Acacia kosiensis* clusters as well as dune, lowland and mangrove forests. The extent of the classes on the predicted map was also closer to the true extent compared to the prediction of the vegetation types using the summer RapidEye image.

Class confusion between certain species and vegetation types remains a problem in the multi-season classifications. Further refinement of the models may reduce this overlap. For example, the PLS-RF algorithm was not optimised for image classification and was unable to run the prediction on a single image, regardless of extending the memory size limit to 80 Gb. The randomForest algorithm was therefore used to predict the vegetation types for the study. The randomForest algorithm does not remove the correlation between bands through a transformation process, as is the case with the PLS-RF algorithm. Further optimisation of the algorithm can be done through assessing optimal values of *ntree* and *mtry*. It is however possible that further increases in classification accuracies with multispectral sensors may only be possible where the number of bands across the electromagnetic spectrum is increased and the range of the bands reduced and the spatial resolution increased. WorldView-2 with eight bands and 2 m spatial resolution would therefore be a suitable sensor to further assess for improved classification accuracies using multiple seasons. The benefit of the increase in overall and user's accuracies, as well as the accuracy of the prediction, should be weighed against the increase cost of using multi-season imagery.

7.5. Conclusion

The study provides new understanding of the seasonal variation of foliar biochemicals of six evergreen tree species in the subtropical forests in the KwaZulu-Natal Province of South Africa. The majority of the species showed no significant seasonal variation in foliar pigments across the four seasons (winter, spring, summer and autumn), however, more statistically significant differences were seen in foliar nitrogen and less in foliar phosphorus. Differences were species specific. The null hypothesis was therefore only partly true for foliar pigments, at the same time the alternative hypothesis was partly true, in that these six evergreen tree species showed some statistically significant differences across the four seasons. Seasonally unique profiles of foliar chemicals are therefore species specific. The number of foliar chemicals was however limited to two pigments and two nutrients. Should more foliar biochemical have been analysed, particularly compounds of foliar nitrogen, more subtle differences between species may have been emphasized.

In addition, the study contributes to our knowledge of the varying relationship between leaf spectra and foliar nutrients across seasons for these evergreen tree species in subtropical forests. The coefficient of determination was highest between foliar nitrogen and leaf spectra during spring, summer and autumn, although low in winter. The seasons associated with flowering for the six tree species, were therefore more useful for the prediction of foliar nitrogen, compared to the dormant season, even though evergreen tree species are known to store nutrients in older leaves. The coefficient of determination was inadequate to predict foliar phosphorus. Foliar nitrogen showed a high coefficient of determination (R^2 > 0.71) between leaf spectra and foliar concentration during the spring, summer and autumn seasons for narrow bands associated with absorption features of proteins compared to the red-edge region. Season-specific prediction models were found to be more accurate in predicting foliar nitrogen than prediction models where data from all seasons were used. The SWIR region is important for the improved prediction of foliar nitrogen of these tree species and the decoupling of foliar nitrogen from the chlorophyll red-edge. The results support the previous evidence that the SWIR region is important for species discrimination.

Twenty-two narrow bands, known to be associated with plant properties, were found to be effective for data reduction of the hyperspectral data. The PLS-RF algorithm effectively removed correlation and classified the tree species with an increase in the average overall and user's accuracies compared to the PCA-RF algorithm. The PLS-RF algorithm was useful for the classification of leaf and canopy spectra, however was unable to predict species for an image, as it is not yet optimised for image classification.

Multi-seasonal data improved tree species classification for multispectral sensors with a few bands. The classification, in which multi-season leaf spectra or canopy data from RadpiEye was used, resulted in higher overall and user's accuracies when compared to the single-season classifications. In contrast, the use of multi-season data for the classification of leaf spectra with 22 narrow bands, showed no statistically significant differences compared to the classification results of the single season in which the highest overall accuracy of all single seasons had been obtained. It remains to be determined whether multi-seasonal data will also increase the overall and user's accuracies of tree species classification if other multispectral sensors with more spectral bands than RapidEye (5 bands), such as WorldView-2 with eight bands, are used. The value of an increased classification accuracy should however be measured against the increase of cost when using images from multiple seasons. In this regard, the alternative hypothesis was proved true in part in that multi-season information improve species discrimination.

REFERENCES

Adam E, Mutanga O, 2009. Spectral discrimination of papyrus vegetation (*Cyperus papyrus L.*) in swamp wetlands using field spectrometry. *ISPRS Journal of Photogrammetry and Remote Sensing* **64**: 612-620. DOI: 10.1016/j.isprsjprs.2009.04.004.

Adam E, Mutanga O, and Rugege D, 2010. Multispectral and hyperspectral remote sensing for identification and mapping of wetland vegetation: a review. *Wetlands Ecology and Management* **18**: 281-296.

Adams ML, Philpot WD, and Norvell WA, 1999. Yellowness index: an application of spectral second derivatives to estimate chlorosis of leaves in stressed vegetation. *International Journal of Remote Sensing* **20**: 3663-3675.

Adelabu S, Dube T, 2014. Employing ground and satellite-based QuickBird data and random forest to discriminate five tree species in a Southern African woodland. *Geocarto International* **30**: 457-471.

Adelabu S, Mutanga O, Adam E, and Cho MA, 2013. Exploiting machine learning algorithms for tree species classification in a semiarid woodland using RapidEye image. *Journal of Applied Remote Sensing* **7**: 1-13.

Alongi DM, 2002. Present state and future of the world's mangrove forests. *Environmental Conservation* **29**: 331-349.

Artigas FJ, Yang JS, 2006. Spectral discrimination of marsh vegetation types in the New Jersey Meadowlands, USA. *Wetlands* **26,** 1: 271-277.

Asner GP, 1998. Biophysical and Biochemical Sources of Variability in Canopy Reflectance. *Remote Sensing of Environment* **64**: 234-253. DOI: 10.1016/S0034-4257(98)00014-5.

Asner GP, 2001. Cloud cover in Landsat observations of the Brazilian Amazon. *International Journal of Remote Sensing* **22**: 3855-3862.

Asner GP, Martin RE, Ford AJ, Metcalfe DJ, and Liddell MJ, 2009. Leaf chemical and spectral diversity in Australian tropical forests. *Ecological Applications* **19**, 1: 236-253.

Barnard E, Cho MA, Debba P, Mathieu R, Wessels R, Van Heerden C, Van der Walt C, and Asner GA, 2010. Optimizing tree species classification in hyperspectral images. Pages 33-38. In: Nicolls F (Ed.). *Twenty-first annual symposium of the pattern recognition association of South Africa.* Available online at: *http://www.prasa.org/proceedings/2010/* [14 January 2016]. Stellenbosch, South Africa: PRASA.

Barta C, Loreto F, 2006. The relationship between the methyl-erythritol phosphate pathway leading to emission of volatile isoprenoids and abscisic acid content in leaves. *American Society of Plant Biologists* **141**: 1676-1683.

Bartlett DS, Klemas V, 1980. Quantitative assessment of tidal wetlands using remote sensing. *Environmental Management* **4**: 337-345.

Bate GC, Whitfield AK, and Forbes AT, 2010. *A review of studies on the Mfolozi estuary and associated flood plain, with emphasis on information required by management for future reconnection of the river to the St Lucia system.* Water Research Commission (WRC) Report No. KV 255/10, pp. 264. Pretoria, South Africa: Water Research Commission (WRC).

Bell DT, Ward SC, 1984. Seasonal changes in foliar macronutrients (N, P, K, Ca and Mg) in *Eucalyptus saligna* Sm. and *E. wandoo* Blakely growing in rehabilitated bauxite mine soils of the Darling Range, Western Australia. *Plant and Soil* **81**: 377-388.

Belluco E, Camuffo M, Ferrari S, Modenese L, Silvestri S, Marani A, and Marani M, 2006. Mapping salt-marsh vegetation by multispectral and hyperspectral remote sensing. *Remote Sensing of Environment* **105**: 54-67.

Blackburn GA, 1998a. Spectral indices for estimating photosynthetic pigment concentrations: a test using senescent tree leaves. *International Journal of Remote Sensing* **19**, 4: 657-675.

Blackburn GA, 1998b. Quantifying Chlorophylls and Carotenoids at Leaf and Canopy Scales: An Evaluation of Some Hyperspectral Approaches. *Remote Sensing of Environment* **66**: 273-285. DOI: 10.1016/S0034-4257(98)00059-5.

Blackburn GA, 1999. Relationships between Spectral Reflectance and Pigment Concentrations in Stacks of Deciduous Broadleaves. *Remote Sensing of Environment* **70**: 224-237. DOI: 10.1016/S0034-4257(99)00048-6.

Boon R, 2010. *Pooley's trees of eastern South Africa.* South Africa: Fauna and Flora Publication Trust.

Booth BBB, Jones CD, Collins M, Totterdell IJ, Cox PM, Sitch S, Huntingford C, Betts RA, Harris GR, and Lloyd J, 2012. High sensitivity of future global warming to land carbon cycle processes. *Environmental Research Letters* **7**: 024002-8.

Boulesteix AL, Porzelius C, and Daumer M, 2008. Microarray-based classification and clinical predictors: on combined classifiers and additional predictive value. *Bioinformatics* **24**: 1698-1706.

Breiman L, 2001. Random Forests. *Machine Learning* **45**: 5-32.

Cai Z, Schnitzer SA, and Bongers F, 2009. Seasonal differences in leaf-level physiology give lianas a competitive advantage over trees in a tropical seasonal forest. *Oecologia* **161**: 25-33.

Campoy JA, Ruiz D, and Egea J, 2011. Dormancy in temperate fruit trees in a global warming context: A review. *Scientia Horticulturae* **130**: 357-372.

Carleer A, Wolff E, 2004. Exploitation of very high resolution satellite data for tree species identification. *Photogrammetric Engineering and Remote Sensing* **70**: 135-140.

Carlson KM, Asner GP, Hughes RF, Ostertag R, and Martin RE, 2007. Hyperspectral remote sensing of canopy biodiversity in a Hawaiian Lowland Rainforest. *Ecosystems* **10**: 536-549.

Carter GA, 1994. Ratios of leaf reflectances in narrow wavebands as indicators of plant stress. *International Journal of Remote Sensing* **15**: 697-703.

Chapin FS,III, Kedrowski RA, 1983. Seasonal Changes in Nitrogen and Phosphorus Fractions and Autumn Retranslocation in Evergreen and Deciduous Taiga Trees. *Ecology* **64**: 376-391.

Chappelle EW, Kim MS, and McMurtrey III JE, 1992. Ratio Analysis of Reflectance Spectra (RARS): An Algorithm for the Remote Estimation of the concentrations of Chlorophyll *a*, Chlorophyll *b*, and Carotenoids in Soybean Leaves. *Remote Sensing of Environment* **39**: 239-247.

Chaturvedi RK, Raghubanshi AS, and Singh JS, 2011. Leaf attributes and tree growth in a tropical dry forest. *Journal of Vegetation Science* **22**: DOI: 917-931. 10.1111/j.1654-1103.2011.01299.x.

Chen C, Liaw A, and Breiman L, 2004. *Using random forest to learn imbalanced data.* Berkeley, United States of America: Department of Statistics, University of California.

Cherbuy B, Joffre R, Gillon D, and Rambal S, 2001. Internal remobilization of carbohydrates, lipids, nitrogen and phosphorus in the Mediterranean evergreen oak *Quercus ilex*. *Tree Physiology* **21**: DOI: 9-17. 10.1093/treephys/21.1.9.

Cheriyadat A, Bruce LM, 2003. Why Principal Component Analysis is not an Appropriate Feature Extraction Method for Hyperspectral Data. *Proceedings of the 2003 IEEE International Geoscience and Remote Sensing Symposium* **6**: 3420-3422.

Cho MA, Debba P, Mathieu R, Naidoo L, Van Aardt J, and Asner GP, 2010a. Improving discrimination of savanna tree species through a multiple-endmember spectral angle mapper approach: canopy-level analysis. *IEEE Transactions - Geoscience and Remote Sensing Society* **48**: 4133-4142.

Cho MA, Malahlela O, and Ramoelo A, 2015. Assessing the utility WorldView-2 imagery for tree species mapping in South Africa subtropical humid forest and the conservation implications: DukuDuku forest patch as a case study. *International Journal of Applied Earth Observation and Geoinformation* **38**: 349-357.

Cho MA, Ramoelo A, Debba P, Mutanga O, Mathieu R, Van Deventer H, and Ndlovu N, 2013. Assessing the effects of subtropical forest fragmentation on leaf nitrogen distribution using remote sensing data. *Landscape Ecology* **28**: 1479-1491.

Cho MA, Sobhan I, and Skidmore, Andrew K. and De Leeuw J, 2008. Discriminating species using hyperspectral indices at leaf and canopy scales. *The International Archives of the Photogrammetry, Remote Sensing and Spatial Information Sciences. Vol. XXXVII. Part B7. Beijing.* Available online at: http://www.isprs.org/proceedings/XXXVII/congress/7_pdf/3_WG-VII-3/28.pdf [14 January 2016].

Cho MA, Skidmore AK, 2006. A new technique for extracting the red edge position from hyperspectral data: The linear extrapolation method. *Remote Sensing of Environment* **101**: DOI: 181-193. 10.1016/j.rse.2005.12.011.

Cho MA, Skidmore AK, and Sobhan I, 2009. Mapping beech (*Fagus sylvatica L.*) forest structure with airborne hyperspectral imagery. *International Journal of Applied Earth Observation and Geoinformation* **11**: DOI: 201-211. 10.1016/j.jag.2009.01.006.

Cho MA, Skidmore A, Corsi F, van Wieren SE, and Sobhan I, 2007. Estimation of green grass/herb biomass from airborne hyperspectral imagery using spectral indices and partial least squares regression. *International Journal of Applied Earth Observation and Geoinformation* **9**: DOI: 414-424. 10.1016/j.jag.2007.02.001.

Cho MA, Van Aardt J, Main R, and Majeke B, 2010b. Evaluating variations of physiology-based hyperspectral features along a soil water gradient in a *Eucalyptus grandis* plantation. *International Journal of Remote Sensing* **31**: 3143-3159.

Clark ML, Roberts DA, 2012. Species-level differences in hyperspectral metrics among tropical rainforest trees as determined by a tree-based classifier. *Remote Sensing* **4**: 1820-1855.

Clark ML, Roberts DA, and Clark DB, 2005. Hyperspectral discrimination of tropical rain forest tree species at leaf to crown scales. *Remote Sensing of Environment* **96**: 375-398. 10.1016/j.rse.2005.03.009.

Clevers JGPW, Gitelson AA, 2013. Remote estimation of crop and grass chlorophyll and nitrogen content using red-edge bands on Sentinel-2 and -3. *International Journal of Applied Earth Observation and Geoinformation* **23**: 344-351.

Cochrane MA, 2000. Using vegetation reflectance variability for species level classification of hyperspectral data. *International Journal of Remote Sensing* **21**: 2075-2087.

Collins W, 1978. Remote Sensing of Crop Type and Maturity. *Engineering* **44**: 43-55.

Congalton RG, 1991. A review of assessing the accuracy of classifications of remotely sensed data. *Remote Sensing of Environment* **37**: 35-46.

Cooke JEK, Weih M, 2005. Nitrogen storage and seasonal nitrogen cycling in Populus: bridging molecular physiology and ecophysiology. *The New Phytologist* **167**: 19-30.

Cowan GI, 1999. The St Lucia System. Available online at: http://hdl.handle.net/1834/460[18 February 2013].

Crooks S, Herr D, Tamelander J, Laffoley D, and Vandever J, 2011. *Mitigating climate change through restoration and management of coastal wetlands and near-shore marine ecosystems: Challenges and opportunities.* Washington, D.C., United States of America: Environment Department Paper 121, World Bank.

Curran PJ, 1989. Remote Sensing of Foliar Chemistry. *Remote Sensing of Environment* **30**: 271-278.

Curran PJ, 2001. Imaging spectrometry for ecological applications. *International Journal of Applied Earth Observation and Geoinformation* **3**: 305-312. DOI: 10.1016/S0303-2434(01)85037-6.

Curran PJ, Dungan JL, and Peterson DL, 2001. Estimating the foliar biochemical concentration of leaves with reflectance spectrometry: Testing the Kokaly and Clark methodologies. *Remote Sensing of Environment* **76**: DOI: 349-359. 10.1016/S0034-4257(01)00182-1.

Dalponte M, Bruzonne L, and Gianelle D, 2012. Tree species classification in the Southern Alps based on the fusion of very high geometrical resolution multispectral/hyperspectral images and LiDAR data. *Remote Sensing of Environment* **123**: 258-270.

Dash J, Curran PJ, 2004. The MERIS terrestrial chlorophyll index. *International Journal of Remote Sensing* **25**: 5403-5413. DOI: 10.1080/0143116042000274015.

Datt B, 1998. Remote Sensing of Chlorophyll *a*, Chlorophyll *b*, Chlorophyll *a*+*b*, and Total Carotenoid Content in Eucalyptus Leaves. *Remote Sensing of Environment* **66**: 111-121. DOI: 10.1016/S0034-4257(98)00046-7.

Datt B, 1999. Visible/near infrared reflectance and chlorophyll content in Eucalyptus leaves. *International Journal of Remote Sensing* **20**: 2741-2759. DOI: 10.1080/014311699211778.

De Weirdt M, Verbeeck H, Maignan F, Peylin P, Poulter B, Bonal D, Ciais P, and Steppe K, 2012. Seasonal leaf dynamics for tropical evergreen forests in a process-based global ecosystem model. *Geoscientific Model Development* **5**: 1091-1108.

Dillen SY, de Beeck MO, Hufkens K, Buonanduci M, and Phillips NG, 2012. Seasonal patterns of foliar reflectance in relation to photosynthetic capacity and color index in two co-occurring tree species, *Quercus rubra* and *Betula papyrifera*. *Agricultural and Forest Meteorology* **160**: 60-68.

Drake BG, Gonzalez-Meler MA, 1997. More efficient plants: A consequence of rising atmospheric CO_2? *Annual Review of Plant Physiology and Plant Molecular Biology* **48**: 609-639.

DRDLR NGI, 2014. South Africa 50cm colour imagery from 2008 to 2012. Cape Town, South Africa: DRDLR NGI.

Dudeni N, Debba P, Cho MA, and Mathieu R, 2009. Spectral band discrimination for species observed from hyperspectral remote sensing. *Hyperspectral Image and Signal Processing: Evolution in Remote Sensing. WHISPERS'09,* pp. 1-4.

Elvidge CD, 1990. Visible and near infrared reflectance characteristics of dry plant materials. *International Journal of Remote Sensing* **11**: 1775-1795. DOI: 10.1080/01431169008955129.

Evans JR, 1989. Photosynthesis and Nitrogen Relationships in Leaves of C_3 Plants. *Oecologia* **78**: 9-19.

Ezemvelo KZN Wildlife, 2011. *KwaZulu-Natal Land Cover 2008 V1.1.* Unpublished GIS Coverage [Clp_KZN_2008_LC_V1_1_grid_w31.zip], Biodiversity Conservation Planning Division, Ezemvelo KZN Wildlife, P. O. Box 13053, Cascades, Pietermaritzburg, 3202. bgis.sanbi.org/kznlandcover/project.asp [31 October 2013].

FAO, 2010. Global Forest Resources Assessment 2010. Main Report. FAO Forestry Paper **163**: 1-378. Available online at: http://www.fao.org/forestry/fra/fra2010/en/ [14 January 2016].

FAO, 2011. FAO Forestry Paper 153: The world's mangroves 1980 – 2005. A thematic study prepared in the framework of the Global Forest Resources Assessment 2005. Available online at: ftp://ftp.fao.org/docrep/fao/010/a1427e/a1427e00.pdf [13 June 2011].

FAO and JRC, 2012. *Global forest land-use change 1990–2005.* Available online at: http://foris.fao.org/static/data/fra2010/FP169En.pdf [14 January 2016].

Fassnacht FE, Neumann C, Förster M, Buddenbaum H, Ghosh A, Clasen A, Joshi PK, and Koch B, 2014. Comparison of feature reduction algorithms for classifying tree species with hyperspectral data on three central European test sites. *IEEE Journal of Selected Topics in Applied Earth Observations and Remote Sensing* **7**: 2547-2561.

Ferwerda JG, Skidmore AK, and Mutanga O, 2005. Nitrogen detection with hyperspectral normalized ratio indices across multiple plant species. *International Journal of Remote Sensing* **26**: 4083-4095. DOI: 10.1080/01431160500181044.

Fife DN, Nambiar EKS, and Saur E, 2008. Retranslocation of foliar nutrients in evergreen tree species planted in a Mediterranean environment. *Tree Physiology* **28**: 187-196.

Flores-de-Santiago F, Kovacs JM, and Flores-Verdugo F, 2012. Seasonal changes in leaf chlorophyll *a* content and morphology in a sub-tropical mangrove forest of the Mexican Pacific. *Marine Ecology Progress Series* **444**: 57-68.

Flores-de-Santiago F, Kovacs JM, and Flores-Verdugo F, 2013. The influence of seasonality in estimating mangrove leaf chlorophyll-*a* content from hyperspectral data. *Wetlands Ecological Management* **21**: 193-207.

Franco AC, Bustamante M, Caldas LS, Goldstein G, Meinzer FC, Kozovits AR, Rundel P, and Coradin VTR, 2005. Leaf functional traits of Neotropical savanna trees in relation to seasonal water deficit. *Trees* **19**: 326-335.

Fung T, Ma HFY, and Siu WL, 2003. Band selection using hyperspectral data of subtropical tree species. *Geocarto International* **18**: 3-11.

Gamon JA, Serrano L, and Surfus JS, 1997. The Photochemical Reflectance Index: An Optical Indicator of Photosynthetic Radiation Use Efficiency across Species, Functional Types, and Nutrient Levels. *Oecologia* **112**: 492-501.

Gamon JA, Surfus JS, 1999. Assessing leaf pigment content and activity with a reflectometer. *New Phytologist* **143**: 105-117.

Gao B, 1996. NDWI - A normalised difference water index for remote sensing of vegetation liquid water from space. *Remote Sensing of Environment* **58**: 257-266.

Gao J, 2010. A hybrid method toward accurate mapping of mangroves in a marginal habitat from SPOT multispectral data. *International Journal of Remote Sensing* **19**: 1887-1899.

Garcia-Plazaola J, Faria T, Abadia J, Abadia A, Chaves MM, and Pereira JS, 1997. Seasonal changes in xanthophyll composition and photosynthesis of cork oak (*Quercus suber* L.) leaves under Mediterranean climate. *Journal of Experimental Botany* **48**, 314: 1667-1674.

Garrity SR, Eitel JUH, and Vierling LA, 2011. Disentangling the relationships between plant pigments and the photochemical reflectance index reveals a new approach for remote estimation of carotenoid content. *Remote Sensing of Environment* **115**: 628-635. DOI: 10.1016/j.rse.2010.10.007.

Gaston KJ, 2000. Global patterns in biodiversity. *Nature* **205**: 220-227.

GeoTerraImage (GTI), 2010. *2008 KZN province land-cover mapping (from SPOT5 satellite imagery circa 2008): Data users report and meta data (version 1.0).* Pretoria: GTI.

Gitelson AA, Gritz † Y, and Merzlyak MN, 2003. Relationships between leaf chlorophyll content and spectral reflectance and algorithms for non-destructive chlorophyll assessment in higher plant leaves. *Journal of Plant Physiology* **160**: 271-282. DOI: 10.1078/0176-1617-00887.

Gitelson AA, Keydan GP, and Merzlyak MN, 2006. Three-band model for noninvasive estimation of chlorophyll, carotenoids and anthocyanin contents in higher plant leaves. *Papers in Natural Resources*: 1-5.

Gitelson A, Merzlyak MN, 1994. Quantitative estimation of chlorophyll-*a* using reflectance spectra: Experiments with autumn chestnut and maple leaves. *Journal of Photochemistry and Photobiology B: Biology* **22**: 247-252. DOI: 10.1016/1011-1344(93)06963-4.

Gitelson AA, Merzlyak MN, 2004. Non-destructive assessment of chlorophyll, carotenoid and anthocyanin content in higher plant leaves: Principles and Algorithms. *Papers in Natural Resources*: 77-94.

Gitelson AA, Zur Y, Chivkunova OB, and Merzlyak MN, 2002. Assessing carotenoid content in plant leaves with reflectance spectroscopy. *Photochemistry and Photobiology* **75**: 272-281.

Gond V, De Pury DGG, Veroustraete F, and Ceulemans R, 1999. Seasonal variations in leaf area index, leaf chlorophyll, and water content; scaling-up to estimate fAPAR and carbon balance in a multilayer, multispecies temperate forest. *Tree Physiology* **19**: 673-679.

Green AA, Berman M, Switzer P, and Craig MD, 1988. A transformation for ordering multispectral data in terms of image quality with implications for noise removal. *IEEE Transactions - Geoscience and Remote Sensing* **26**: 65-74.

Green EP, Clark CD, Mumby PJ, Edwards AJ, and Ellis AC, 1998. Remote sensing techniques for mangrove mapping. *International Journal of Remote Sensing* **19**: 935-956.

Grossmann E, Ohmann J, Kagan J, May H, and Gregory M, 2010. Mapping ecological systems with a random forest model: tradeoffs between errors and bias. *GAP Analysis Bulletin* **17**: 16-22.

Hardisky MA, Gross MF, and Klemas V, 1986. Remote sensing of coastal wetlands. *Bioscience* **36**: 453-460.

Harris I, Jones PD, Osborn TJ, and Lister DH, 2013. Updated high-resolution grids of monthly climatic observations - the CRU TS3.10 Dataset. *International Journal of Climatology* **34**: 623-642. DOI: 10.1002/joc.3711.

Heywood VH, Watson RT, 1996. *Global Biodiversity Assessment*. United Nations Environment Programme. Cambridge, United Kingdom: Cambridge University Press.

Hilker T, Gitelson A, Coops NC, Hall FG, and Black TA, 2011. Tracking plant physiological properties from multi-angular tower-based remote sensing, *Oecologia* **165**, 4: 865-876.

Holmgren J, Persson A, and Söderman U, 2008. Species identification of individual trees by combining high resolution LiDAR data with multi-spectral images. *International Journal of Remote Sensing* **29**: 1537-1552.

Hong Kong Observatory, 2003. Monthly climatological normals for Hong Kong. Available online at: http://www.hko.gov.hk/cis/normal/1971_2000/normals_e.htm [18 March 2015].

Horneck DA, Miller RO, 1998. Determination of total nitrogen in plant tissue. Pages 81-83. In: Kalra YP (Ed.). *Handbook of reference methods for plant analysis.* Boca Raton: CRC Press.

Hotelling H, 1933. Analysis of a complex of statistical variables into principal components. *Journal of Educational Psychology* **24**: 417-441 & 498-520.

Huang Z, Turner BJ, Dury SJ, Wallis IR, and Foley WJ, 2004. Estimating foliage nitrogen concentration from HYMAP data using continuum removal analysis. *Remote Sensing of Environment* **93**: 18-29.

Huber S, Kneubühler M, Psomas A, Itten K, and Zimmermann NE, 2008. Estimating foliar biochemistry from hyperspectral data in mixed forest canopy. *Forest Ecology and Management* **256**: 491-501.

Hughes GF, 1968. On the mean accuracy of statistical pattern recognizers. *IEEE Transactions on Information Theory* **14**: 55-63.

Immitzer M, Atzberger C, and Koukal T, 2012. Tree species classification with Random Forest using very high spatial resolution 8-band WorldView-2 satellite data. *Remote Sensing* **4**: 2661-2693.

Intergovernmental Panel on Climate Change (IPCC), 2007. *Climate Change 2007: Synthesis Report. Contributions of Working Groups I, II and III to the Fourth Assessment Report of the Intergovernmental Panel on Climate Change.* Core Writing Team, Pachauri, R.K. and Reisinger, A. Geneva, Switzerland: IPCC.

Isaac RA, Johnson WC, 1998. Elemental determination by inductively coupled plasma. Pages 165-170. In: Kalra YP (Ed.). *Handbook of reference methods for plant analysis.* Boca Raton: CRC Press.

ITT Visual Information Systems. 2012-2014. Environment for Visualizing Images (ENVI) software v.4.8 and 5.2.

IUCN, 2001. *2001 IUCN red list categories and criteria available at http://www.iucnredlist.org/technical-documents/categories-and-criteria/2001-categories-criteria.* Gland, Switzerland: IUCN.

IUCN/SSC Global Tree Specialist Group, 2015. *Global Trees Campaign*. Available online at: http://globaltrees.org/threatened-trees/red-list/ [9 March 2015].

Jacquemoud S, Ustin SL, Verdebout J, Schmuck G, Andreoli G, and Hosgood B, 1996. Estimating leaf biochemistry using the PROSPECT leaf optical properties model. *Remote Sensing of Environment* **56**: 194-202.

Johnson LF, 2001. Nitrogen influence on fresh-leaf NIR spectra. *Remote Sensing of Environment* **78**: 314-320.

Jones TG, Coops NC, and Sharma T, 2010. Assessing the utility of airborne hyperspectral and LiDAR data for species distribution mapping in the coastal Pacific Northwest, Canada. *Remote Sensing of Environment* **114**: 2841-2852.

Jordan CF. 1985. Nutrient Cycling in Tropical Forest Ecosystems. Chichester, United Kingdom: John Wiley & Sons.

Ju J, Roy DP, 2008. The availability of cloud-free Landsat ETM+ data over the conterminous United States and globally. *Remote Sensing of Environment* **112**: 1196-1211.

Kanniah KD, 2011. *WorldView-2 remote sensing data for tropical mangrove species classification.* Research report submitted to DigitalGlobe Incorporated, USA for the WorldView-2 8-bands Research Challenge. Available online at: *http://www.mdpi.com/2072-4292/7/11/14360/htm* [14 January 2016].

Key T, Warner TA, McGraw JB, and Fajvan MA, 2001. A Comparison of Multispectral and Multitemporal Information in High Spatial Resolution Imagery for Classification of Individual Tree Species in a Temperate Hardwood Forest. *Remote Sensing of Environment* **75**: 100-112. DOI: 10.1016/S0034-4257(00)00159-0.

Kirschbaum MUF, 2000. Forest growth and species distribution in a changing climate. *Tree Physiology* **20**: 309-322.

Knox NM, Skidmore AK, Prins HHT, Asner GP, van der Werff HMA, De Boer WF, Van der Waal C, De Knegt HJ, Kohi EM, Slotow R, and Grant RC, 2011. Dry season mapping of savanna forage quality, using the hyperspectral Carnegie Airborne Observatory sensor. *Remote Sensing of Environment* **115**: 1478-1488. DOI: 10.1016/j.rse.2011.02.007.

Knyazikhin Y, Schull MA, Stenberg P, Mõttus M, Rautiainen M, Yang Y, Marshak A, Carmona PL, Kaufmann RK, Lewis P, Disney MI, Vanderbilt V, Davis AB, Baret F, Jacquemoud S, Lyapustin A, and Myneni RB, 2012. Hyperspectral remote sensing of foliar nitrogen content. *The Proceedings of the National Academy of Sciences of the United States of America* E185-E192.

Kokaly RF, 2001. Investigating a Physical Basis for Spectroscopic Estimates of Leaf Nitrogen Concentration. *Remote Sensing of Environment* **75**: 153-161.

Kokaly RF, Asner GP, Ollinger SV, Martin ME, and Wessman CA, 2009. Characterizing canopy biochemistry from imaging spectroscopy and its application to ecosystem studies. *Remote Sensing of Environment* **113**, Supplement 1: S78-S91.

Kokaly RF, Clark RN, 1999. Spectroscopic Determination of Leaf Biochemistry Using Band-Depth Analysis of Absorption Features and Stepwise Multiple Linear Regression. *Remote Sensing of Environment* **67**: 267-287.

Kooistra L, Salas EAL, Clevers JGPW, Wehrens R, Leuven RSEW, Nienhuis PH, and Buydens LMC, 2004. Exploring field vegetation reflectance as an indicator of soil contamination in river floodplains. *Environmental Pollution* **127**: 281-290. DOI: 10.1016/S0269-7491(03)00266-5.

Kumar L, Schmidt KS, Dury S, and Skidmore AK, 2001. Imaging spectroscopy and vegetation science. In: Van der Meer FD, and De Jong SM (Eds.). *Image spectroscopy.* Dordrecht: Kluver Academic Publishers.

Laba M, Tsai F, Ogurcak D, Smith S, and Richmond ME, 2005. Field determination of optimal dates for the discrimination of invasive wetland plant species using derivative spectral analysis, *Photogrammetric Engineering and Remote Sensing* **71**, 5: 603-611.

Lal CB, Annapurna C, Raghubanshi AS, and Singh JS, 2001. Foliar demand and resource economy of nutrients in dry tropical forest species. *Journal of Vegetation Science* **12**: 5-14.

Landgrebe D, 1997. *On information extraction principles for hyperspectral data: A white paper.* West Lafayette, United States of America: Purdue University: School Electrical and Computer Engineering.

Lewandowska M, Jarvis PG, 1977. Changes in Chlorophyll and Carotenoid Content, Specific Leaf Area and Dry Weight Fraction in Sitka Spruce, in Response to Shading and Season. *New Phytologist*: 247-256. DOI: 10.2307/2433777.

Liaw A, Weiner M, 2008. randomForest: Breiman and Cutler's Random Forests for Classification and Regression. *http://CRAN. R-project. org/ package=randomForest.,* RStudio, Inc. v. 0.98.507 © 2009-2013.

Lichtenthaler HK, Buschmann C, 2001. Chlorophylls and carotenoids: Measurement and characterization by UV-VIS spectroscopy. *Current protocols in food analytical chemistry.* Hoboken, N.J: John Wiley & Sons, Inc.

Lieth H, 1974. *Phenology and seasonality modeling.* Berlin- New York: Springer-Verlag.

Lin Y, Liu X, Zhang H, Fan H, and Lin G, 2010. Nutrient conservation strategies of a mangrove species *Rhizophora stylosa* under nutrient limitation. *Plant Soil* **326**: 469-479.

Lu E, Liu Y, and Yen C, 2007. Dynamics of foliar nutrients in major species of a broadleaf forest in the Fushan Experimental Forest, Northeastern Taiwan. *Taiwan Journal of Forest Science* **22**: 307-319.

Lück-Vogel M, Mbolambi C, Rautenbach K, Adams J, and Van Niekerk L, Submitted. Vegetation mapping in the St Lucia estuary using very high resolution multispectral imagery and LiDAR. *African Journal of Botany*.

Lukac M, Calfapietra C, Lagomarsino A, and Loreto F, 2010. Global climate change and tree nutrition: effects of elevated CO_2 and temperature. *Tree Physiology* **30**: 1209-1220.

Maccioni A, Agati G, and Mazzinghi P, 2001. New vegetation indices for remote measurement of chlorophylls based on leaf directional reflectance spectra. *Journal of Photochemistry and Photobiology B: Biology* **61**: 52-61. DOI: 10.1016/S1011-1344(01)00145-2.

Mafuratidze P. 2010. Discriminating wetland vegetation species in an African savanna using hyperspectral data. M.Sc thesis. Pietermaritzburg, South Africa: University of KwaZulu-Natal.

Main R, Cho MA, Mathieu R, O'Kennedy M, Ramoelo A, and Koch S, 2011. An investigation into robust spectral indices for leaf chlorophyll estimation. *ISPRS Journal of Photogrammetry and Remote Sensing* **66**: 751-761.

Manevski K, Manakos I, Petropoulos GP, and Kalaitzidis C, 2011. Discrimination of common Mediterranean plant species using field spectroradiometry. *International Journal of Applied Earth Observation and Geoinformation* **13**: 922-933. DOI: 10.1016/j.jag.2011.07.001.

Martin ME, Newman SD, Aber JD, and Congalton RG, 1998. Determining forest species composition using high spectral resolution remote sensing data. *Remote Sensing of Environment* **65**: 249-254.

McDonald JH, 2008. *Handbook of biological statistics.* Maryland, USA: Sparky House Publishing.

Middleton BJ, Bailey AK, 2008. *Water Resources of South Africa, 2005 Study (WR2005) and Book of Maps*. WRC Research Reports No.TT381/08 & TT382/08. Pretoria, South Africa: Water Research Commission (WRC).

Millard P, Grelet G, 2010. Nitrogen storage and remobilization by trees: ecophysiological relevance in a changing world. *Tree Physiology* **30**: 1083-1095.

Miller JR, Hare EW, and Wu J, 1990. Quantitative Characterization of the Vegetation Red Edge Reflectance 1. An Inverted-Gaussian Reflectance Model. *International Journal of Remote Sensing* **11**: 1755-1773.

Mucina L, Rutherford MC, 2006. *The vegetation of South Africa, Lesotho and Swaziland.* Pretoria, South Africa: South African National Biodiversity Institute (Strelizia).

Mumby PJ, Green EP, Edwards AJ, and Clark CD, 1999. The cost-effectiveness of remote sensing for tropical coastal resources assessment and management. *Journal of Environmental Management* **55**: 157-166.

Mutanga O, Adam E, and Cho MA, 2012. High density biomass estimation for wetland vegetation using WorldView-2 imagery and random forest regression algorithm. *International Journal of Applied Earth Observation and Geoinformation* **18**: 399-406. DOI: 10.1016/j.jag.2012.03.012.

Mutanga O, Kumar L, 2007. Estimating and mapping grass phosphorus concentration in an African savanna using hyperspectral image data. *International Journal of Remote Sensing* **28**: 4897-4911. DOI: 10.1080/01431160701253253.

Mutanga O, Skidmore AK, 2004. Narrow band vegetation indices overcome the saturation problem in biomass estimation. *International Journal of Remote Sensing* **19**: 3999-4014.

Mutanga O, Skidmore AK, 2007. Red edge shift and biochemical content in grass canopies. *ISPRS Journal of Photogrammetry and Remote Sensing* **62**: 34-42.

Mutke J, Barthlott W, 2005. Patterns of vascular plant diversity at continental to global scales. *Biologiske Skrifter Kongelige Danske Videnskaberbes Selskab* **55**: 521-531.

Naidoo L, Cho MA, Mathieu R, and Asner G, 2012. Classification of savanna tree species, in the Greater Kruger National Park region, by integrating hyperspectral and LiDAR data in a Random Forest data mining environment. *ISPRS Journal of Photogrammetry and Remote Sensing* **69**: 167-179. DOI: 10.1016/j.isprsjprs.2012.03.005.

Nakaji T, Oguma H, and Fujinuma Y, 2006. Seasonal changes in the relationship between photochemical reflectance index and photosynthetic light use efficiency of Japanese larch needles. *International Journal of Remote Sensing* **27**: 493-509. DOI: 10.1080/01431160500329528.

NASA, 2015. *International Satellite Cloud Climatology Project. Cloud Analysis: Seasonal Variations of Cloud and Surface Properties.* Available online at: http://isccp.giss.nasa.gov/climanal3.html [6 March 2015].

Niinements U, Tamm U, 2005. Species differences in timing of leaf fall and foliage chemistry modify nutrient resorption efficiency in deciduous temperate forest stands. *Tree Physiology* **25**: 1001-1014.

Nondoda SP. 2012. *Macrophyte distribution and responses to drought in the St. Lucia Estuary.* M.Sc. thesis. Port Elizabeth, South Africa: Nelson Mandela Metropolitan University.

Nondoda S, Adams J, Bate G, and Taylor R, 2011. An assessment of the microalgae and macrophytes of the Msunsuzi estuary. Pages 138-154. In: Bate GC, Whitfield AK, and Forbes AT (Eds.). *A review of studies on the Mfolozi estuary and associated flood plain, with emphasis on information required by management for future reconnection of the river to the St Lucia system.* WRC report no. KV255/10. Pretoria, South Africa: Water Research Commission (WRC).

Oldfield S, Lusty C, and MacKinven A, 1998. *The world list of threatened trees.* Available online at: *https://Archive.org/stream/worldlistofthrea98oldf#page/6/mode/2up.* Cambridge, United Kingdom: WCMC, IUCN.

Ollinger SV, Reich PB, Frolking S, Lepine LC, Hollinger DY, and Richardson AD, 2013. Nitrogen cycling, forest canopy reflectance and emergent properties of ecosystems. *The Proceedings of the National Academy of Sciences of the United States of America* **110**: E2437.

Ollinger SV, Richardson AD, Martin ME, Hollinger DY, Frolking SE, Reich PB, Plourde LC, Katul GG, Munger JW, Oren R, Smith M-, Paw U KT, Bolstad PV, Cook BD, Day MC, Martin TA, Monson RK, and Schmid HP, 2008. Canopy nitrogen, carbon assimilation, and albedo in temperate and boreal forests: Functional relations and potential climate feedbacks. *The Proceedings of the National Academy of Sciences of the United States of America* **105**: 19336-19341.

Ollis DJ, Snaddon CD, Job NM, and Mbona N, 2013. *Classification System for wetlands and other aquatic ecosystems in South Africa. User Manual: Inland Systems.* SANBI Biodiversity Series 22. Pretoria, South Africa: South African National Biodiversity Institute.

Omer G, Mutanga O, Abdel-Rahman EM, and Adam E, 2015. Performance of Support Vector Machines and Artificial Neural Network for mapping endangered tree species using WorldView-2 data in DukuDuku Forest, South Africa. *IEEE Journal of Selected Topics in Applied Earth Observation and Remote Sensing* **99**: 1-16.

Panigraphy S, Kumar T, and Manjunath KR, 2012. Hyperspectral leaf signature as an added dimension for species discrimination: case study of four tropical mangroves. *Wetlands Ecology and Management* **20**: 101-110.

Partridge TC, Dollar ESJ, Moolman J, and Dollar LH, 2010. The geomorphic provinces of South Africa, Lesotho and Swaziland: A physiographic subdivision for earth and environmental scientists. *Transactions of the Royal Society of South Africa* **65**: 1-47.

Pearson K, 1901. On lines and planes of closest fit to systems of points in space. *Philosophical Magazine* **2**: 559-572.

Peerbhay KY, Mutanga O, and Ismail R, 2014. Investigating the capability of few strategically placed WorldView-2 multispectral bands to discriminate forest species in KwaZulu-Natal, South Africa. *IEEE Journal in Selected Topics in Applied Earth Observation and Remote Sensing* **7**: 307-316.

Penuelas J, Baret F, and Filella I, 1995. Semiempirical Indexes to Assess Carotenoids Chlorophyll-*a* Ratio from Leaf Spectral Reflectance, *Photosynthetica* **31**, 2: 221-230.

Posa MRC, Wijedasa LS, and Corlett RT, 2011. Biodiversity and conservation of tropical peat swamp forests. *BioScience* **61**: 49-57.

Prasad AM, Iverson LR, and Liaw A, 2006. Newer classification and regression tree techniques: bagging and Random Forest for ecological prediction. *Ecosystems* **9**: 181-199.

Pu R, Landry S, 2012. A comparative analysis of high spatial resolution IKONOS and WorldView-2 imagery for mapping urban tree species. *Remote Sensing of Environment* **124**: 516-533. DOI: 10.1016/j.rse.2012.06.011.

Ramoelo A, Skidmore AK, Cho MA, Schlerf M, Mathieu R, and Heitkönig IMA, 2012. Regional estimation of savanna grass nitrogen using the red-edge band of the spaceborne RapidEye sensor. *International Journal of Applied Earth Observation and Geoinformation* **19**: 151-162.

Ramoelo A, Skidmore AK, Schlerf M, Heitkönig IMA, Mathieu R, and Cho MA, 2013. Savanna grass nitrogen to phosphorous ratio estimation using field spectroscopy and the potential for estimation with imaging spectroscopy. *International Journal of Applied Earth Observation and Geoinformation* **23**: 334-343.

Ramoelo A, Skidmore AK, Schlerf M, Mathieu R, and Heitkönig IMA, 2011. Water-removed spectra increase the retrieval accuracy when estimating savanna grass nitrogen and phosphorus concentrations. *ISPRS Journal of Photogrammetry and Remote Sensing* **66**: 408-417.

Rautenbach K. 2015. *Present state of macrophytes and responses to management scenarios at the St Lucia and Mfolozi estuaries.* M.Sc thesis. Port Elizabeth, South Africa: Nelson Mandela Metropolitan University.

Rebelo LM, Finlayson CM, and Nagabhatla N, 2009. Remote sensing and GIS for wetland inventory, mapping and change analysis. *Journal of Environmental Management* **90**: 2144-2153.

Reef R, Feller IC, and Lovelock CE, 2010. Nutrition of mangroves. *Tree Physiology* **30**: 1148-1160. DOI: 10.1093/treephys/tpq048.

Reich PB, Oleksyn J, 2004. Global patterns of plant leaf N and P in relation to temperature and latitude. *Proceedings of the National Academy of Sciences of the United States of America* **101**: 11001-11006. DOI: 10.1073/pnas.0403588101.

Republic of South Africa (RSA), 1998. *National Forest Act, Act no. 84 of 1998.* Available online at: http://www.dwaf.gov.za/Documents/Forestry/Tact84.pdf [14 June 2011].

Republic of South Africa (RSA), 2008. *National Environmental Management: Integrated Coastal Management Act (No. 24 of 2008).* Available online at: http://www.polity.org.za/article/national-environmental-management-integrated-coastal-management-act-no-24-of-2008-2009-02-26 [20 August 2014].

Richardson AD, Keenan TF, Migliavacca M, Ryu Y, Sonnentag O, and Toomey M, 2013. Climate change, phenology, and phenological control of vegetation feedbacks to the climate system. *Agricultural and Forest Meteorology* **169**: 156-173.

Richter R, Schläpfer D. 2015. A*tmospheric / Topographic Correction for Satellite Imagery - ATCOR-2/3 User Guide, Version 9.0.0, June 2015*. Available online at http://www.rese.ch/[6 July 2015]. ReSe Applications SchläpferWil, Switzerland.

Rouse J, Haas R, Schell J, and Deering D, 1973. Monitoring Vegetation Systems in the Great Plains with ERTS. *Third ERTS Symposium, United States of America, National Aeronautics and Space Administration (NASA) SP-351 I*: 309-317.

Sabaté S, Sala A, and Gracia CA, 1995. Nutrient content in *Quercus ilex* canopies: Seasonal and spatial variation within a catchment. *Plant and Soil* **168-169**: 297-304.

Saeys Y, Inza I, and Larrañaga P, 2007. A review of feature selection techniques in bioinformatics. *Bioinformatics* **23**: 2507-2517.

Sardans J, Peñuelas J, 2012. The Role of plants in the effects of global change on nutrient availability and stoichiometry in the plant-soil system. *Plant Physiology* **160**: 1741-1761.

Sauceda JIU, Rodriguez HG, Lozano RGR, Silva IC, and Meza MVG, 2008. Seasonal Trends of Chlorophylls *a* and *b* and Carotenoids in Native Trees and Shrubs of Northeastern Mexico. *Journal of Biological Sciences* **8**: 258-267.

Schlerf M, Atzberger C, Hill J, Buddenbaum H, Werner W, and Schüler G, 2010. Retrieval of chlorophyll and nitrogen in Norway spruce (*Picea abies L. Karst*.) using imaging spectroscopy. *International Journal of Applied Earth Observation and Geoinformation* **12**: 17-26.

Schmidt KS, Skidmore AK, 2003. Spectral discrimination of vegetation types in a coastal wetland. *Remote Sensing of Environment* **85**, 1: 92-108.

Scott-Shaw R, Escott BJ, 2011. *KwaZulu-Natal Provincial Pre-Transformation Vegetation Type Map - 2011.* Unpublished GIS Coverage [kznveg05v2_011_wll.zip], Biodiversity Conservation Planning Division, Ezemvelo KZN Wildlife, PO Box 13053, Cascades, Pietermaritzburg, 3202, South Africa. Available online at: http://www.bgis.sanbi.org/KZN/project.asp [10 June 2014].

Seppälä R, Buck A, and Katila P, 2009. *Adaptation of Forests and People to Climate Change. A Global Assessment Report.* IUFRO World Series Volume 22. Helsinki, Finland: International Union for Forest Research Organisations (IUFRO).

Sharma BM, 1983. Mineral content of leaves of some common tropical forest trees and their associated soils in Ibadan, Nigeria. *Canadian Journal of Forest Research* **4**: 556-562.

Shuster C, Schmidt T, Conrad C, Kleinschmidt B, and Förster M, 2015. Grassland habitat mapping by intra-annual time series analysis - Comparison of RapidEye and TerraSAR-X satellite data. *International Journal of Applied Earth Observation and Geoinformation* **34**: 25-34.

Sims DA, Gamon JA, 2002. Relationships between leaf pigment content and spectral reflectance across a wide range of species, leaf structures and developmental stages. *Remote Sensing of Environment* **81**: 337-354. DOI: 10.1016/S0034-4257(02)00010-X.

Skidmore AK, Ferwerda JG, Mutanga O, Van Wieren SE, Peel M, Grant RC, Prins HHT, Balcik FB, and Venus V, 2010. Forage quality of savannas — Simultaneously mapping foliar protein and polyphenols for trees and grass using hyperspectral imagery. *Remote Sensing of Environment* **114**: 64-72.

Sluiter R, Pebesma EJ, 2010. Comparing techniques for vegetation classification using multi- and hyperspectral images and ancillary environmental data. *International Journal of Remote Sensing* **31**: 6143-6161.

Smith M, Ollinger SV, Martin ME, Aber JD, Hallett RA, and Goodale CL, 2002. Direct estimation of aboveground forest productivity through hyperspectral remote sensing of canopy nitrogen. *Ecological Applications* **12**: 1286-1302.

Sobhan I, 2007. Species discrimination from a hyperspectral perspective. Ph.D dissertation. Wageningen, Netherlands: Wageningen University.

Sokolic F. 2006. The use of satellite remote sensing to determine the spatial and temporal distribution of surface water on the Eastern Shores of Lake St Lucia. M.Sc. thesis. Durban, South Africa: University of KwaZulu-Natal.

Spalding M, Kaunuma M, and Collins L, 2010. *World atlas of mangroves. A collaborative project of ITTO, ISME, FAO, UNEP-WCMC, UNESCO-MAB, UNU-INWEH and TNC.* London, United Kingdom: Earthscan.

Story M, Congalton R, 1986. Accuracy assessment: a user's perspective. *Photogrammetric Engineering and Remote Sensing* **52**: 397-399.

Strobl C, Hothorn T, and Zeileis A, 2009. P*arty on! A new, conditional variable importance measure for Random Forest available in the party package.* Technical Report Number 050. Available online at: http://www.stat.uni-muenchen.de. Munich, Germany: University of Munich.

Stylinski CD, Gamon JA, and Oechel WC, 2002. Seasonal patterns of reflectance indices, carotenoid pigments and photosynthesis of evergreen chaparral species, *Oecologia* **131**, 3: 366-374.

Taylor R, 2011. The St Lucia-Mfolozi connection: A historical perspective. Pages 2-21. In: Bate GC, Whitfield AK, and Forbes AT (Eds.). *A review of studies on the Mfolozi estuary and associated flood plain, with emphasis on information required by management for future reconnection of the river to the St Lucia system.* WRC project no. KV 255/10. Pretoria, South Africa: Water Research Commission (WRC).

The iSimangaliso Wetland Park, 2014. *The iSimangaliso Wetland Park.* Available online at: http://isimangaliso.com/ [4 March 2015].

Thenkabail PS, Enclona EA, Ashton MS, and Van Der Meer B, 2004. Accuracy assessments of hyperspectral waveband performance for vegetation analysis applications. *Remote Sensing of Environment* **91**: 354-376. DOI: 10.1016/j.rse.2004.03.013.

Tillé Y, Matei A, 2014. *Stratified sampling in R Package 'sampling'.* Available online at: http://cran. r-project. org/web/packages/sampling/sampling.pdf*,* 2.6, RStudio, Inc. v. 0.98.507 © 2009-2013.

Townsend PA, Foster JR, Chastain RA, Jr., and Currie WS, 2003. Application of imaging spectroscopy to mapping canopy nitrogen in the forest of the central Appalachian Mountains using Hyperion and AVIRIS. *IEEE Transactions on Geoscience and Remote Sensing* **41**: 1347 - 1354.

Tsai F, Lin E-, and Yoshino K, 2007. Spectrally segmented principal component analysis of hyperspectral imagery for mapping invasive plant species. *International Journal of Remote Sensing* **28**: 1023-1039.

Tu YK, Kellet M, Clerehugh V, and Gilthorpe MS, 2005. Problems of correlations between explanatory variables in multiple regression analysis in the dental literature. *British Dental Journal* **199**: 457-461.

Tucker CJ, 1979. Red and photographic infrared linear combinations for monitoring vegetation. *Remote Sensing of Environment* **8**: 127-150. DOI: 10.1016/0034-4257(79)90013-0.

Turner W, Spector S, Gardiner N, Fladeland M, Sterling E, and Steininger M, 2003. Remote sensing for biodiversity science and conservation. *Trends in Ecology and Evolution* **18**: 306-314.

Ullah S, Si Y, Schlerf M, Skidmore AK, Shafique M, and Iqbal IA, 2012. Estimation of grassland biomass and nitrogen using MERIS data. *International Journal of Applied Earth Observation and Geoinformation* **19**: 196-204.

United States Department of Energy (US DOE), 2012. *Research Priorities for Tropical Ecosystems Under Climate Change Workshop Report.* US Department of Energy Office of Science, DOE/SC-0153. Compiled by Chambers J, Fisher R, Hall J, Norby R and Wofsy S.

Vaiphasa C, Ongsomwang S, Vaiphasa T, and Skidmore AK, 2005. Tropical mangrove species discrimination using hyperspectral data: A laboratory study. *Estuarine, Coastal and Shelf Science* **65**: 371-379. DOI: 10.1016/j.ecss.2005.06.014.

Valiela I, Bowen JL, and York JK, 2001. Mangrove Forests: One of the world's threatened major tropical environments. *Bioscience* **51**: 807-815.

Van Aardt J, Wynne RH, 2001. Spectral separability among six southern tree species. *Photogrammetric Engineering and Remote Sensing Journal* **67**: 1367-1375.

Van Deventer H, Cho MA, and Mutanga O, 2013. Do seasonal profiles of foliar pigments improve species discrimination of evergreen coastal tree species in KwaZulu-Natal, South Africa? Pages 1-12. *Conference proceedings of the 35th international symposium on remote sensing of environment (ISRSE).* Beijing, China: ISRSE, pp. 1-12.

Van Deventer H, Cho MA, Mutanga O, Naidoo L, and Dudeni-Tlhone N, 2015a. Reducing leaf-level hyperspectral data to 22 components of biochemical and biophysical bands optimises tree species discrimination. *IEEE Journal of Selected Topics in Applied Earth Observation and Remote Sensing* **8, 6:** 3161-3171.

Van Deventer H, Cho MA, Mutanga O, and Ramoelo A, 2015b. Capability of models to predict leaf N and P across four seasons for six subtropical forest evergreen trees. *ISPRS Journal of Photogrammetry and Remote Sensing* **101**: 209-220.

Van Heerden IL, 2011. Management concepts for the Mfolozi flats and estuary as a component of the management of the iSimangaliso Wetland Park. Pages 45-63. In: Bate GC, Whitfield AK, and Forbes AT (Eds.). *A review of studies on the Mfolozi estuary and associated flood plain, with emphasis on information required by management for future reconnection*

of the river to the St Lucia system. WRC report no. KV255/10. Pretoria, South Africa: Water Research Commission (WRC).

Van Niekerk L, Turpie JK, 2012. National Biodiversity Assessment 2011: Technical Report. Volume 3: Estuary Component. *Council for Scientific & Industrial Research (CSIR),* CSIR/NRE/ECOS/ER/2011/0045/B. Available online at: http://www.bgis.sanbi.org/NBA/project.asp. [14 January 2016].

Van Wyk B, Van Wyk P, 2013. *Veldgids tot bome van Suider-Afrika.* Kaapstad, Suid-Afrika: Struik Nature.

Vogelmann JE, Rock BN, and Moss DM, 1993. Red edge spectral measurements from sugar maple leaves. *International Journal of Remote Sensing* **14**: 1563-1575. DOI: 10.1080/01431169308953986.

Walther G, Post E, Convey P, Menzel A, Parmesan C, Beebee TJC, Fromentin J, Hoegh-Guldberg H, and Bairlein F, 2002. Ecological responses to recent climate change. *Nature* **416**: 389-395.

Wang L, Sousa WP, Gong P, and Biging GS, 2004. Comparison of IKONOS and QuickBird images for mapping mangrove species on the Caribbean coast of Panama. *Remote Sensing of Environment* **91**: 432-440. DOI: 10.1016/j.rse.2004.04.005.

Wold H, 1966. Estimation of principal components and related models by iterative least squares. In: Krishnaiah PR (Ed.). *Multivariate analysis.* New York, USA: Academic Press.

Wold S, Sjöström M, and Eriksson L, 2001. PLS-regression: a basic tool of chemometrics. *Chemometrics and Intelligent Laboratory Systems* **58**: 109-130.

Wu C, Niu Z, Tang Q, and Huang W, 2008. Estimating chlorophyll content from hyperspectral vegetation indices: Modeling and validation. *Agricultural and Forest Meteorology* **148**: 1230-1241. DOI: 10.1016/j.agrformet.2008.03.005.

Yasamura Y, Ishida A, 2011. Temporal variation in leaf nitrogen partitioning of broad-leaved evergreen tree, *Quercus myrsinaefolia*. *Journal of Plant Research* **124**: 115-123.

Yoder BJ, Pettigrew-Crosby RE, 1995. Predicting nitrogen and chlorophyll content and concentrations from reflectance spectra (400–2500 nm) at leaf and canopy scales. *Remote Sensing of Environment* **53**: 199-211.

Zhang Y, Chen JM, and Thomas SC, 2007. Retrieving seasonal variation in chlorophyll content of overstory and understory sugar maple leaves from leaf-level hyperspectral data. *Canadian Journal of Remote Sensing* **33**: 406-415.

Zhou L, Kaufmann RK, Tian Y, Myneni RB, and Tucker CJ, 2003. Relation between interannual variations in satellite measures of northern forest greenness and climate between 1982 and 1999. *Journal of Geophysical Research* **108**: 1-11.

APPENDIX 1: COMPARISONS BETWEEN PREDICTED VEGETATION TYPE MAPS FOR SUMMER AND THE MULTI-SEASON CLASSIFICATIONS.

This Appendix offers a more detailed discussion on the prediction of vegetation types resulting from Chapter 6. The predicted vegetation types from the summer and multi-season RapidEye imagery are considered for various locations in the study area and in some instances compared to the KZN land cover classification of 2008. A number of images are shown for each location in the subsections below, including (A) an RGB composite (Bands 3-2-1) of the RapidEye image for the summer of (January) 2012; (B) an RGB composite (Bands 3-2-1) of the WorldView-2 image for the summer of (December) 2010; (C) an RGB composite of the 20 cm colour orthophotos taken during a LiDAR campaign of autumn 2013; (D) the KZN land cover classification with classes listed in Figure A1.1; (E) the predicted vegetation types from the summer RapidEye images and (F) the predicted vegetation type classes from the selected multiple seasons of RapidEye images.

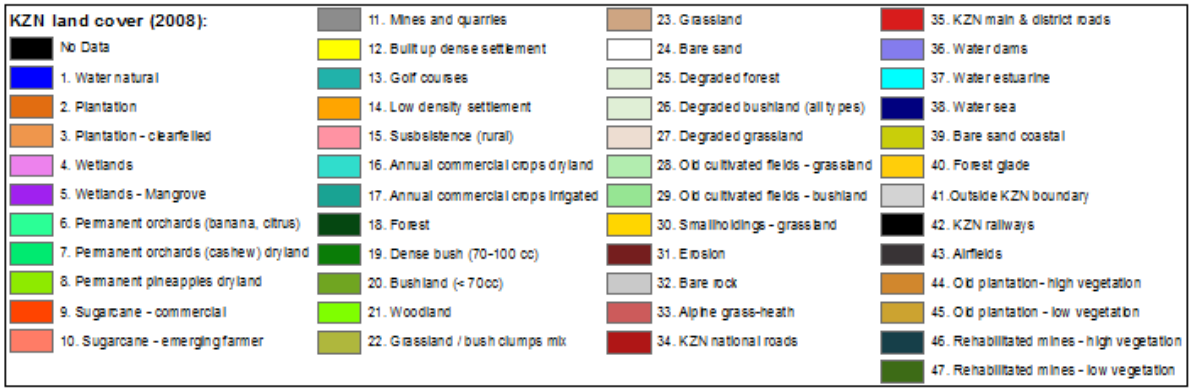

Figure A1. 1: Land cover categories of the KwaZulu-Natal land cover data set (Ezemvelo KZN Wildlife, 2011).

1. Bridge over the Narrows on the way to St Lucia

The vegetation types located at point 1 in Figure A1.2(A) consist mainly of macrophytes *Juncus kraussi* and *Phragmites australis* in the channel (Narrows), with predominantly *Hibiscus tilliaceus* and *Avicennia marina* west of the macrophytes. Figure A1.2 shows a section of the vegetation south of point 1. All three satellite images, including RapidEye (A), WorldView-2 (B) and the 20 cm colour orthophotography (C), show that the macrophytes and trees are clearly discernible, increasing in separability from A to C. The KZN classification (D) correctly indicates the mangrove forest at point 1, though identifies the macrophytes as degraded bushland or degraded forest. The predictions from RapidEye images better identifies the macrophyte vegetation zone and the *Hibiscus tilliaceus* along the channel. The predicted vegetation types from the summer RapidEye image (E) shows the mangrove forest to the west of point 1 as a mixture of dryland, lowland, *Acacia kosiensis* and *Hibiscus*

tilleaceus, whereas the multi-season image resulted in a pure-mangrove forest stand. Further validation of this cluster is required to assess the accuracy of the prediction. The patch in the forest may be a degraded path or where *Bruguiera gymnorrhiza* forms the top canopy rather than *Avicennia marina* as is the case in Figure A1.4.

Point 2 (Figure A1.2-A) is a marsh consisting predominantly of *Phragmites australis.* In the KZN land cover data (Figure A1.2 D) it is mainly classified as grassland, while the predicted vegetation types (E – F) showed it as a mixture of *Phragmites australis* and mangrove fern wetland (AA – associated with *Acrostichum auereum*). The predicted vegetation types of the multi-season RapidEye (F) better identifies this area as being dominated by *Phragmites australis* while the remaining patches of mangrove fern wetland may have resulted from the spectral overlap with muddy areas, yet should be validated with field surveys.

The extent of *Phragmites australis* and *Hibiscus tilleaceus* at the entrance to the boat yard at point 3 (Figure A1.5-A) is better predicted with the multi-season RapidEye images (F) compared to the summer image (E), and improves on the vegetation types of the KZN land cover data (D).

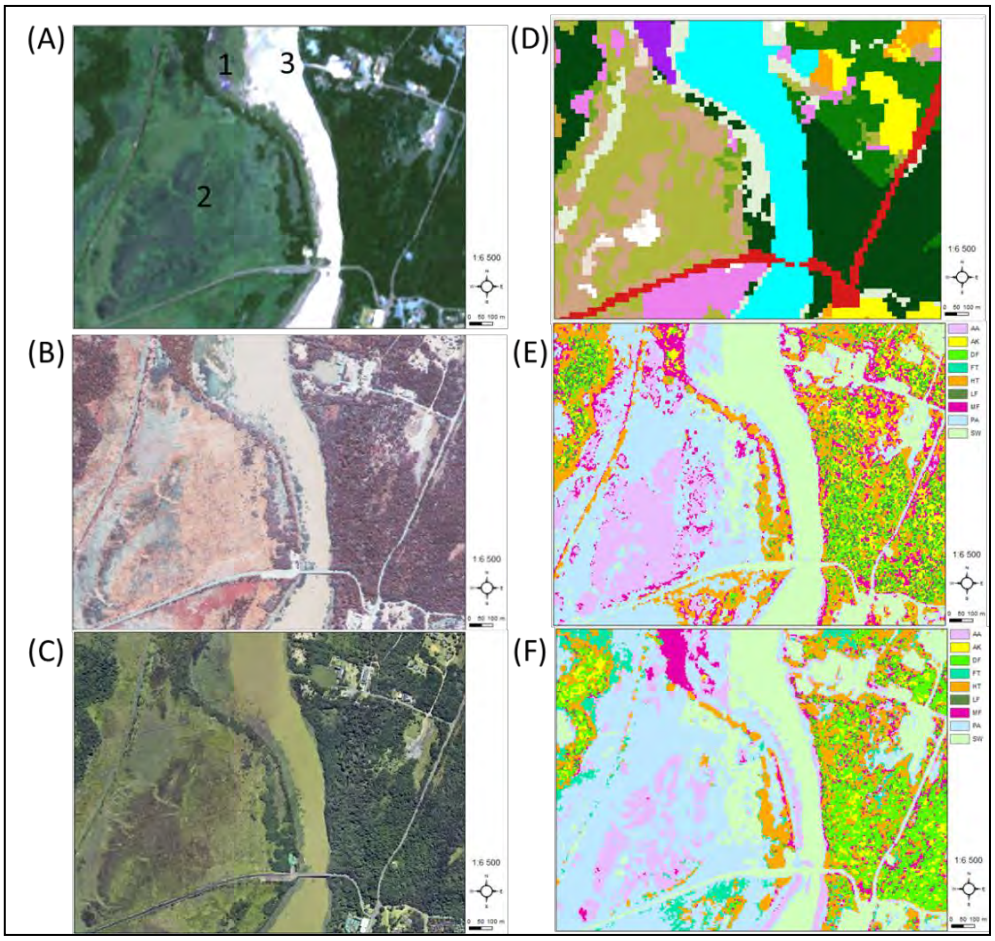

Figure A1. 2: Maps of the St Lucia bridge over the narrows showing RGB composites of satellite imagery of (A) RapidEye January 2012, (B) WorldView-2 imagery December 2010 and (C) 20 cm colour orthophotos taken in the autumn of 2013; (D) the KZN 2008 land cover classes; (E) the predicted vegetation types from the summer RapidEye images and (F) the predicted vegetation types of the multi-season RapidEye images.

Figure A1. 3: Photograph taken in April 2011, facing in a westerly direction near point 1. Photo by H. van Deventer

Figure A1. 4: Mangrove forests consisting of *Avicennia marina* dominating the canopy and *Bruguiera gymnorrhiza* in the undercanopy. Photo taken April 2011 by H. van Deventer.

Figure A1. 5: View of the boatyard, facing an easterly direction. Photo taken April 2011 by H. van Deventer.

2. Honeymoon Bend

Expert knowledge would be required to verify the vegetation types of points 1 and 2, for the example of Honeymoon bend (Figure A1.6-A). These areas were not accessible through commercial boat trips, and therefore it is unclear whether the vegetation at point 1 is truly macrophytes, or *Potamogeton perfoliatus*. The prediction from the multi-season RapidEye incorrectly predicts the vegetation at point 1 as mangrove forests, while the prediction from the summer RapidEye image are more correct as it classifies them as seasonal wetlands, which include a range of graminoids. The vegetation on the island at point 2 is classified as predominantly mangrove forests, similar to the visual interpretation of Rautenbach (2015) and the classified WorldView-2 image of Lück-Vogel *et al.* (Submitted). The predicted extent of the mangroves and reeds appear close to the true extent of these vegetation types at point 3, where a number of sites were visited during field surveys.

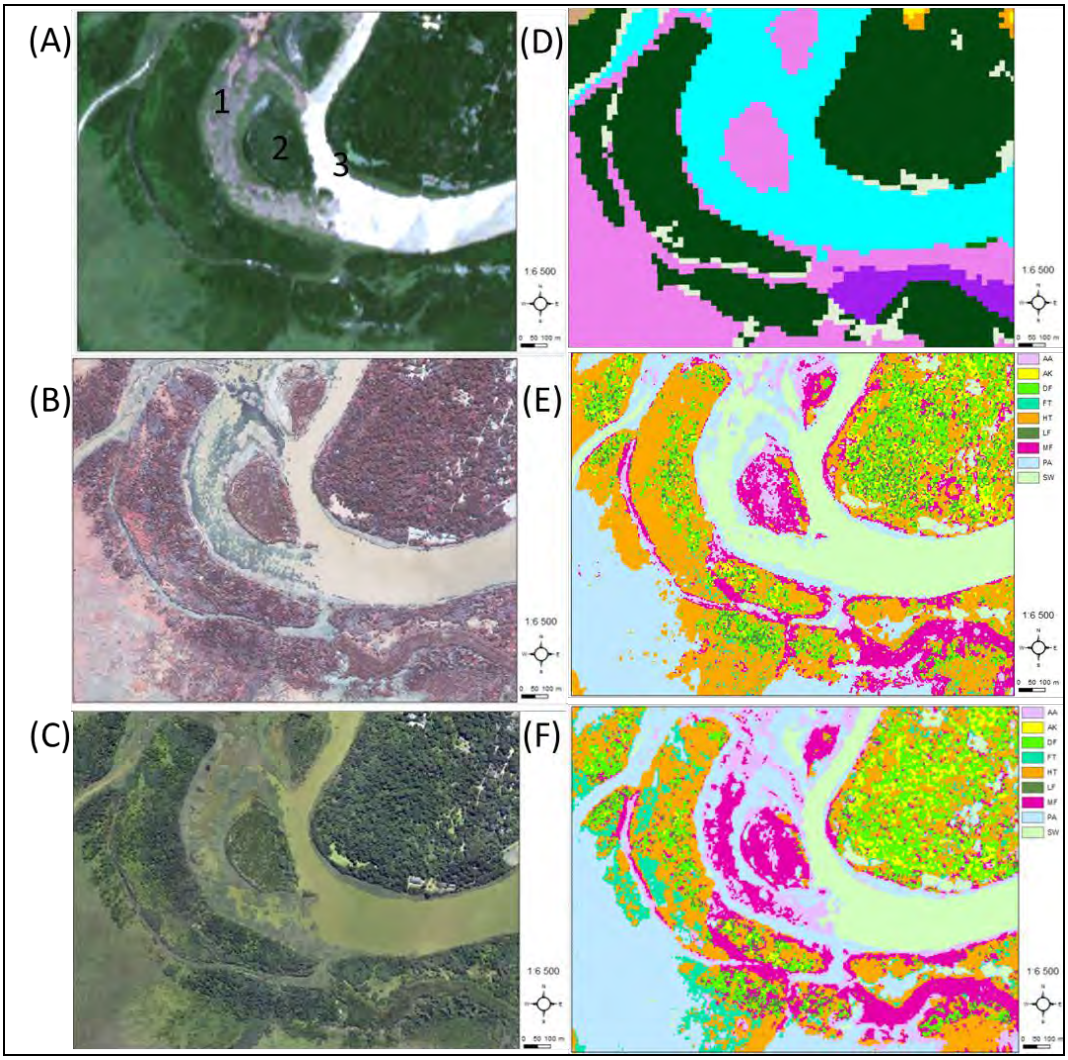

Figure A1. 6: Maps of Honeymoon bend showing RGB composites of satellite imagery of (A) RapidEye January 2012, (B) WorldView-2 imagery December 2010 and (C) 20 cm colour orthophotos taken in the autumn of 2013; (D) the KZN 2008 land cover classes; (E) the predicted vegetation types from the summer RapidEye images and (F) the predicted vegetation types of the multi-season RapidEye images.

3. Estuary Mouth

The vegetation types of the wetland at point 1 in Figure A1.7(B) should be verified through field surveys. In the predicted map of vegetation types using the summer RapidEye image (E), the area is predicted to be dominated by *Hibiscus tilliaceus*, while *Ficus trichopoda* appears to dominate the area in the predicted map where the multi-season RapidEye images were used (F).

RapidEye (E and F) were able to detect the patch of *Phragmites australis* at point 2 as well as the mangrove forest at 3. The shallow muddy water at 4 was however incorrectly classified as mangrove wetland in the prediction where multi-season images were used (F).

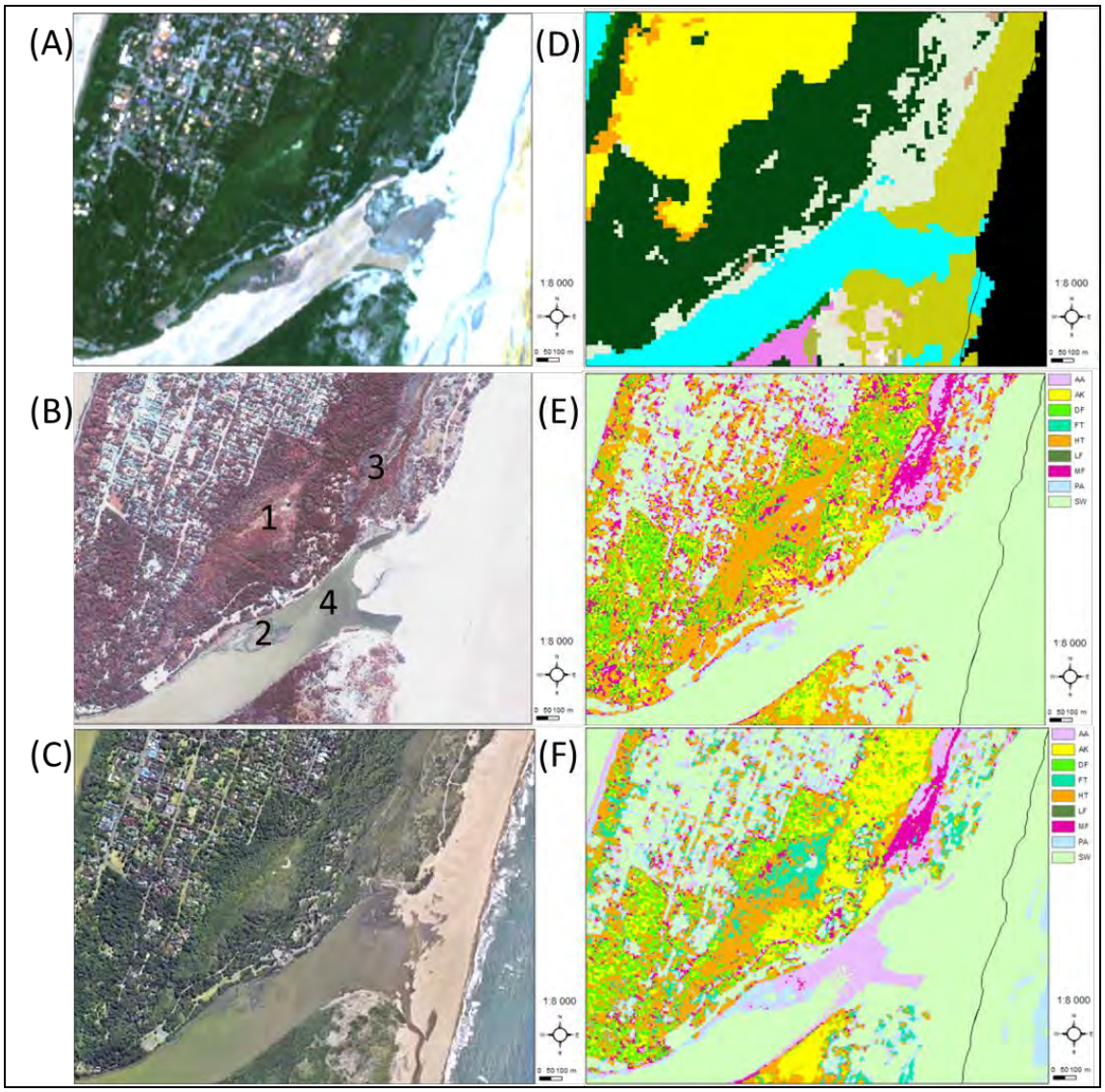

Figure A1. 7: Maps of the St Lucia estuary mouth showing RGB composites of satellite imagery of (A) RapidEye January 2012, (B) WorldView-2 imagery December 2010 and (C) 20 cm colour orthophotos taken in the autumn of 2013; (D) the KZN 2008 land cover classes; (E) the predicted vegetation types from the summer RapidEye images and (F) the predicted vegetation types of the multi-season RapidEye images.

4. Maphelane node

As discussed in Chapter 6 of the main thesis, the prediction of *Hibiscus tilliaceus* from RapidEye is suspected to overlap spectrally with another vegetation type and hence its full extent appears to be over predicted. The predictions of the summer and multi-season RapidEye images, for example, show a large extent of *Hibiscus tilliaceus* at point 1 as well as south of the uMfolozi River (northly channel in Figure A1.8-B) and along the sand dunes on the coast side. The multi-season image resulted in a larger extent of *Ficus trichopoda* at point 1 (F), compared to the prediction of the summer RapidEye image (E).

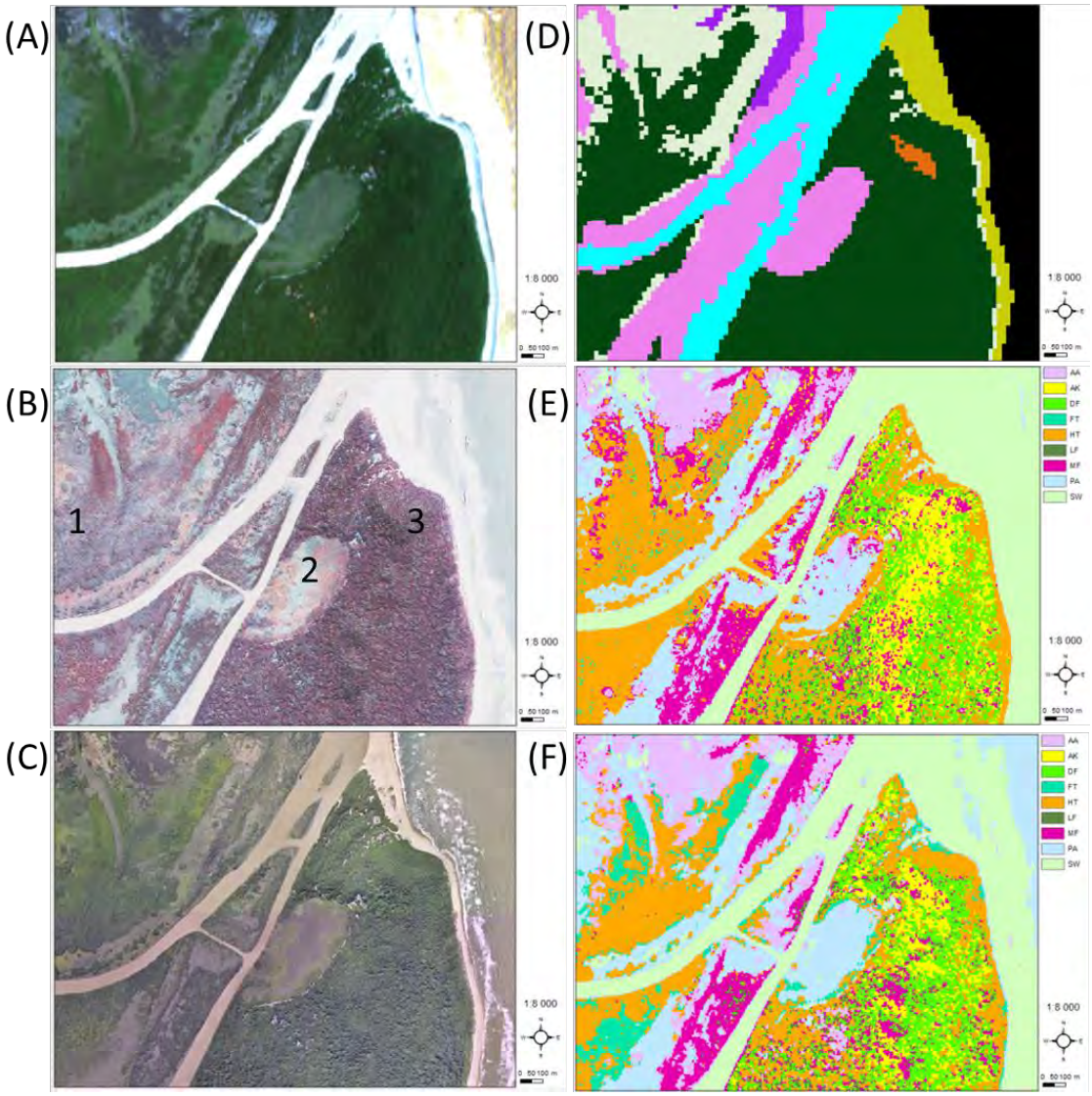

Figure A1. 8: Maps of the Maphelane node showing RGB composites of satellite imagery of (A) RapidEye January 2012, (B) WorldView-2 imagery December 2010 and (C) 20 cm colour orthophoto's taken in the autumn of 2013; (D) the KZN 2008 land cover classes; (E) the predicted vegetation types from the summer RapidEye images and (F) the predicted vegetation types of the multi-season RapidEye images.

For the wetland at point 2, the summer RapidEye image (E) predicted the occurrence of mangrove forests for parts of the wetland while the multi-season RapidEye image predicted *Ficus trichopoda* on the edges of the wetland. The wetland is dominated primarily by *Phragmites australis / mauritanus* and *Cyperus papyrus* with a more diverse number of shrub and tree species on the fringe (Figure A1.9). In this case the prediction from the multi-season RapidEye images appears closer to the true extent of the vegetation, though the fringe vegetation requires further refinement.

The prediction of the dune vegetation at point 3 requires further validation. Both the predictions from the summer and multi-season RapidEye images resulted in the expected mixture of dune forests (DF) and *Acacia kosiensis* (AK), though spectral confusion of mangrove forests with another species is suspected, as well as an over prediction of *Hibiscus tilliaceus*.

Figure A1. 9: View over the wetland at the Maphelane node of the iSimangaliso Wetland Park. The photo was taken in October 2011 by H. van Deventer facing a southerly direction. The wetland is appears to be predominantly *Phragmites australis/mauritanus* and *Cyperus papyrus*. The dune forests (DF) are visible in the background.

5. Lake Futululu and the DukuDuku Forest

Three wetlands are shown to the west, north-east and south-east of the DukuDuku Forest in Figure A1.10(B). The Futululu wetland at point 1 has a longitudinal extent of ± 7 km from north to south and is located to the west of the DukuDuku Forest. The wetland is dominated by *Cyperus papyrus*. The summer image of RapidEye (E) incorrectly predicted a dominance of *Hibiscus tilliaceus* and mangrove forests for the wetland, whereas the prediction of the multi-season RapidEye images resulted in the prediction of *Ficus trichopoda* in the north and south, with mangrove fern wetlands (AA – associated with *Acrostichum auereum*) predicted for the centre. Further refinement of the spectral overlap between the *Acrostichum auereum* and *Cyperus papyrus* will be required, while validation of the vegetation type and biomass at the northern and southern tips will resolve uncertainty.

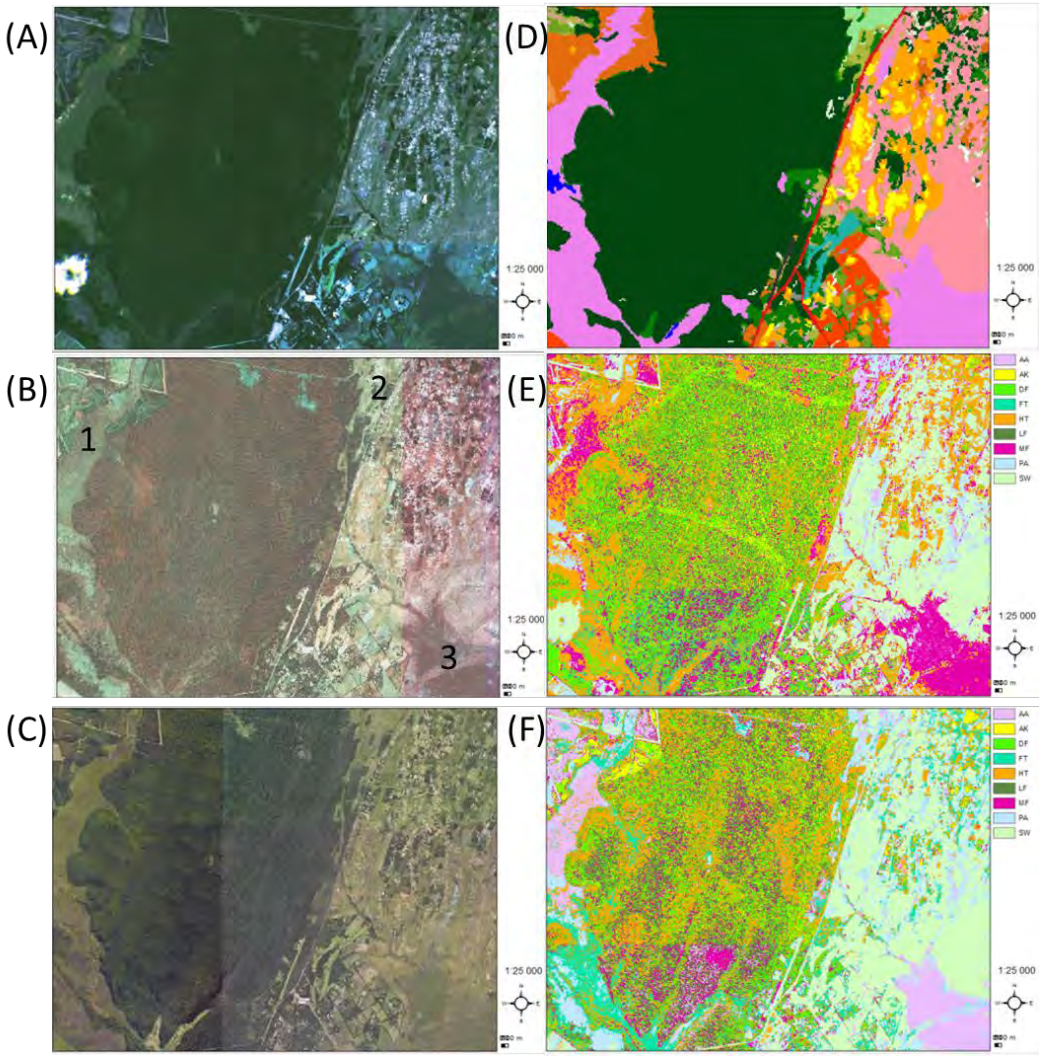

Figure A1. 10: Maps of the wetlands surrounding the DukuDuku Forest showing RGB composites of satellite imagery of (A) RapidEye January 2012, (B) WorldView-2 imagery December 2010 and (C) 20 cm colour orthophoto's taken in the autumn of 2013; (D) the KZN 2008 land cover classes; (E) the predicted vegetation types from the summer RapidEye images and (F) the predicted vegetation types of the multi-season RapidEye images.

The wetland at point 2, north-east of the DukuDuku Forest, consists predominantly of grasses. The vegetation types from the multi-season RapidEye images (F) were closest in predicting the vegetation types of the wetland compared to the types predicted from the summer RapidEye images (E).

The wetland to the south-east of the DukuDuku Forest at point 3, similar to the Futululu wetland, showed a spectral overlap with mangrove fern wetlands (AA – associated with *Acrostichum auereum*) when the multi-season RapidEye images were used for predicting the vegetation types. The predicted mangrove forests resulting from the summer RapidEye images (E) are clearly incorrect, though the vegetation type should be verified through field surveying.

6. East of the Narrows

A variety of seasonal wetlands occurs to the east of the Narrows (Figure A1.11), and consists mainly of graminoid species (Figures A1.12 and A1.13). In general the vegetation types predicted from the RapidEye images (E – F) aptly show macrophyte (PA - *Phragmites australis*) or graminoid (SW – seasonal wetlands) for these areas. Mangrove forests are however incorrectly predicted to occur between these wetlands which may be a result of spectral overlap with other tree species. At point 1 (Figure A1.11-C) the prevalence of mangrove forest should be validated. At point 2 the prediction of *Hibiscus tilliaceus* is more likely to be a variety of species forming the swamp forest along the Mfabeni stream.

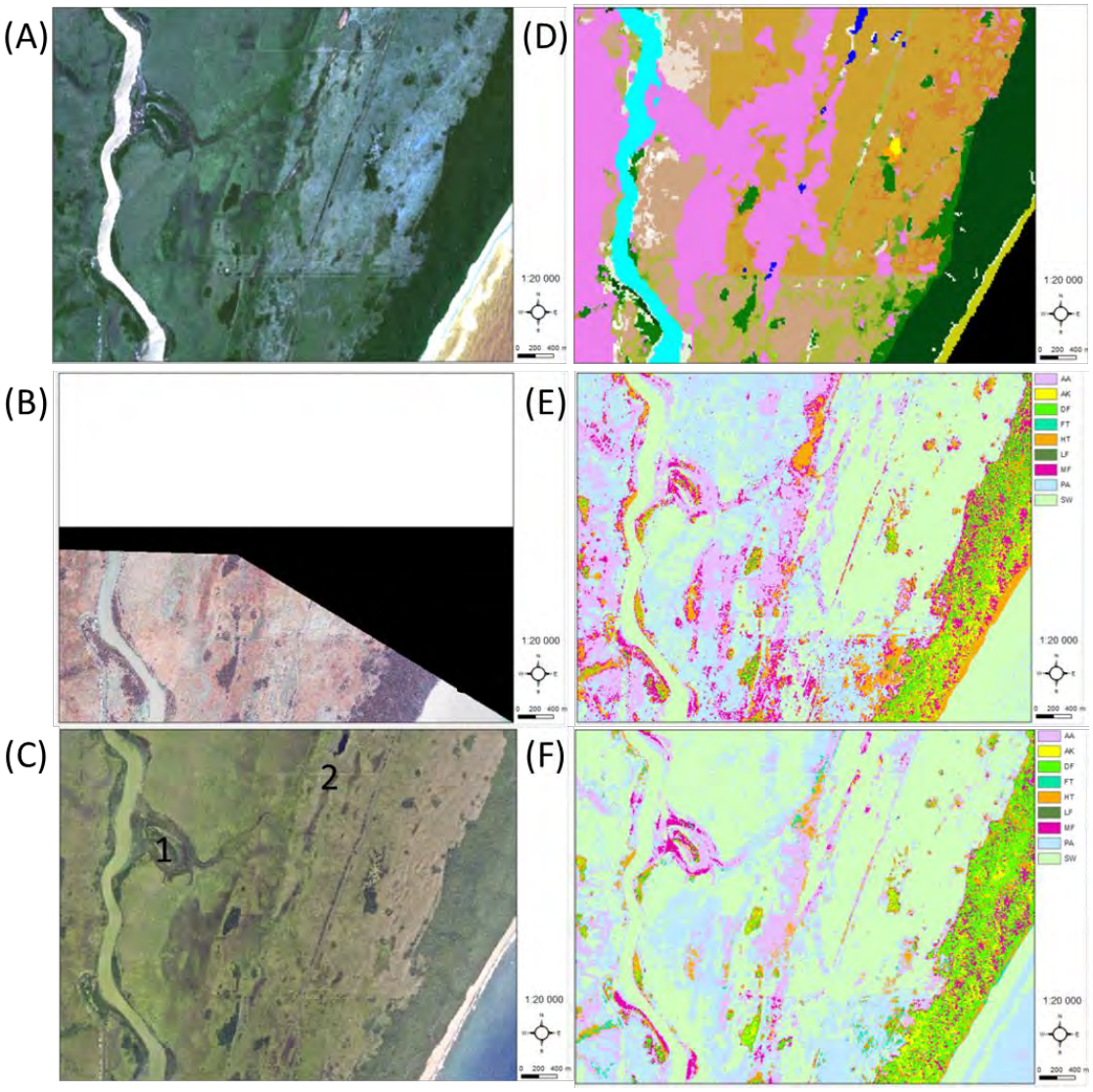

Figure A1. 11: Maps of the wetlands to the east of the Narrows showing RGB composites of satellite imagery of (A) RapidEye January 2012, (B) WorldView-2 imagery December 2010 and (C) 20 cm colour orthophoto's taken in the autumn of 2013; (D) the KZN 2008 land cover classes; (E) the predicted vegetation types from the summer RapidEye images and (F) the predicted vegetation types of the multi-season RapidEye images.

Figure A1. 12: Photo of a seasonal wetland dominated by ferns. The wetland is situated to the east of the Narrows *en route* from the Benghazi gate to Cape Vidal. Photo taken by H. van Deventer April 2011.

Figure A1. 13: Photo of a seasonal wetland dominated by water and *Juncus kraussi*. The wetland is situated to the east of the Narrows *en route* from the Benghazi gate to Cape Vidal. Photo taken by H. van Deventer April 2011.